MECHANISTIC STUDIES ON PALLADIUM-CATALYZED COUPLING REACTIONS

BY

BRADLEY PATRICK CARROW

DISSERTATION

Submitted in partial fulfillment of the requirements
for the degree of Doctor of Philosophy in Chemistry
in the Graduate College of the
University of Illinois at Urbana-Champaign, 2011

Urbana, Illinois

Doctoral Committee:

Professor John F. Hartwig, Chair
Professor Scott E. Denmark
Professor Gregory S. Girolami
Professor Jeffrey S. Moore

Abstract

A series of mechanistic studies reported here has revealed fundamental information about the individual steps of palladium-catalyzed coupling reactions. In one case, the oxidative addition of PhX (X = I, Br, Cl) to the complexes $Pd(P^tBu_3)_2$ (**1**), Pd(1-$AdP^tBu_2)_2$(**2**), $Pd(CyP^tBu_2)_2$ (**3**), and $Pd(PCy_3)_2$ (**4**) (1-Ad = 1-adamantyl, Cy = cyclohexyl) was studied to determine the effect of steric properties on the coordination number of the species that undergoes oxidative addition and to determine whether the type of halide affects the identity of this species. The kinetic data imply that the number of phosphines coordinated to the complex that reacts in the irreversible step of the oxidative addition process for complexes **1**−**4** depends more on the halide than on the steric properties of the ligands. The rate-limiting step of the oxidative addition of PhI occurred with $L_2Pd(0)$ in all cases, as determined by the lack of dependence of k_{obs} on [P^tBu_3], [1-AdP^tBu_2], or [CyP^tBu_2] and the inverse dependence of the rate constant on [PCy_3] when the reaction was initiated with $Pd(PCy_3)_3$. The irreversible step of the oxidative addition of PhCl occurred with a monophosphine species in each case, as signaled by an inverse dependence of the rate constant on the concentration of ligand. The irreversible step of the oxidative addition of PhBr occurred with a bisphosphine species, as signaled by the zeroth-order or small dependence of the rate constant on the concentration of phosphine. Thus, the additions of the less reactive chloroarenes occur through lower-coordinate intermediates than additions of the more reactive haloarenes.

An unusual autocatalytic mechanism for oxidative addition of bromobenzene to $Pd(P^tBu_3)_2$ was also observed when reactions were run in the absence of strong base.

Studies on the effect of various additives showed that the degree of rate acceleration followed the trend: $(P^tBu_3)Pd(Ph)(Br) \approx (HP^tBu_3)Br < [(P^tBu_3)Pd(\mu\text{-}Br)]_2 < (P^tBu_3)_2Pd(H)(Br)$. Studies on the reactions of $Pd(P^tBu_3)_2$ in the presence of $(P^tBu_3)_2Pd(H)(Br)$ showed that the concentration of $(P^tBu_3)_2Pd(H)(Br)$ decreased only after the Pd(0) complex had been consumed. These data indicated that the catalyst in this process is $(P^tBu_3)_2Pd(H)(Br)$. Thermal decomposition of the three-coordinate oxidative addition product $(P^tBu_3)Pd(Ar)(Br)$ during the reaction of $Pd(P^tBu_3)_2$ and bromoarenes ultimately leads to formation of $(P^tBu_3)_2Pd(H)(Br)$. Parallel reactions of bromobenzene with $(P^tBu_3)_2Pd(H)(Br)$ and $Pd(P^tBu_3)_2$ showed that the bromoarenes reacted considerably faster with the Pd(II) species than with the Pd(0) species. We therefore propose a catalytic cycle for oxidative addition in which $PBu^t_3 \cdot HBr$ reacts with the Pd(0) species to form $(P^tBu_3)_2Pd(H)(Br)$, and $(P^tBu_3)_2Pd(H)(Br)$ reacts with the bromoarene, possibly though the anionic species $[HP^tBu_3^+][(P^tBu_3)Pd(Br)^-]$, to form $[Pd(P^tBu_3)(Ar)(Br)]$.

In a separate study, the isolation and reactivity of a series of "ligandless," anionic arylpalladium complexes of the general structure $[Pd(Ar)Br_2]_2^{2-}$ were conducted. These anionic complexes insert olefins at room temperature, and these fast insertions indicate that the anionic complexes are kinetically competent to be intermediates in Heck−Mizoroki reactions conducted under "ligandless" conditions (lacking added dative ligand). Kinetic studies showed that the anionic complexes insert olefins much faster than the corresponding neutral, P(*t*-Bu)$_3$-ligated complexes. Addition of halide to the reaction of the neutral complex $(^tBu_3P)Pd(Ar)(Br)$ and styrene led to a significant rate acceleration, suggesting that the anionic complex forms rapidly and reversibly in situ

from the neutral species prior to migratory insertion. These data, along with studies on the regioselectivity for reaction of aryl halides with butyl vinyl ether in the presence of the different starting catalysts, are consistent with the intermediacy of the same anionic, arylpalladium intermediates in Heck reactions catalyzed by palladium complexes containing bulky trialkylphosphine ligands as in reactions conducted under ligandless conditions.

Lastly, a systematic study of the stoichiometric reactions of isolated arylpalladium hydroxo and halide complexes with arylboronic acids and aryltrihydroxyborates was conducted to evaluate the relative rates of the two reaction pathways commonly proposed to account for transmetallation in the Suzuki-Miyaura reaction. Based on the relative populations of the palladium and organoboron species generated under conditions common for the catalytic process and the observed rate constants for the stoichiometric reactions between the two classes of reaction components, we conclude that the reaction of a palladium hydroxo complex with boronic acid, not the reaction of a palladium halide complex with trihydroxyborate, accounts for transmetallation in catalytic Suzuki-Miyaura reactions conducted with weak base and aqueous solvent mixtures.

To My Grandparents Ralph and Nathalee Froeschle

Acknowledgements

I owe a great deal of thanks to a number of people who have supported me during my life and academic career. Foremost, my family has been an unfaltering source of love and encouragement. It would be hard for anyone to waiver in their endeavors with the knowledge that they always have such a wonderful family to lift them up in their difficult times. Anything good in me came from them. Of course, anything bad I learned somewhere else.

I'm also grateful for the mentoring of Professor John F. Hartwig through the years of my thesis research. It's difficult to put into words how much I have matured and learned while a member of the Hartwig group. It is equally difficult to describe my awe and gratefulness for the endless offerings of knowledge and insightful suggestions from Prof. Hartwig. Not only has my knowledge of organometallic chemistry been expanded tremendously, but the development of my understanding of how to plan, execute, and critically evaluate chemical research is something that will no doubt be the foundation for success in my professional career.

To my thesis committee members: Prof. Scott E. Denmark, Prof. Gregory S. Girolami, and Prof. Jeffrey S. Moore, I thank you for your advice but also for your encouragement to strive to achieve during my graduate career. I owe a special thanks to Professor Scott E. Denmark who offered not only lab space and resources to me before the Hartwig group relocated from Yale University, but also all the intellectual activities afforded to members of the Denmark group during that time. I'm also grateful to others that have mentored and encouraged me through portions of my academic career. My

interest in pursuing a career in science was undoubtedly inspired and encouraged by Mrs. Elaine Rees both through her infectious passion for science and her generous efforts in supporting many extracurricular scientific activities. Also, Prof. Thomas Schuman, Prof. Harvest Collier, Prof. Peter Beak, and Prof. Toh-Ming Lu, I thank all of you for your advice, support, and enthusiasm.

Of course in the day to day, I have also been fortunate to work with a number of colleagues that have also become good friends. The past and present members of the Hartwig group are amazing scientists. To spend so many days around people who are ambitious, motivated, and enthusiastic is humbling. I hope to have assimilated some of those attributes by proximity. Dr. Levi Stanley, thank you for all our discussions of chemistry and enjoying takeout (by necessity) as much as I do. I wish we had more occasions to hit the links, but I had fun all the times we were able to get out. To Russell Smith, who was a friend inside and outside of lab, I am so glad we had an occasion to meet during my time spent in the Denmark group. I also had great fun on our occasions to hit the links, and of course the many outings to the racquetball courts. I am endlessly surprised how many epiphanies and good ideas come from casual discussions of science with friends. To that end, I thank all those colleagues with which I have interacted during my years at Illinois.

Table of Contents

Chapter 1. Overview of Mechanistic Studies on Cross-Coupling Reactions Catalyzed by Palladium Complexes Containing Bulky, Electron-Rich Phosphine Ligands

---

1.1 Introduction

The development of transition metal-catalyzed cross-coupling reactions,[1-3] which form carbon-carbon and carbon-heteroatom bonds, is arguably one of the most important contributions to synthetic organic chemistry over the last half-century. This broad class of methods has become an indispensable tool for the synthesis of small and macromolecular architectures relevant to medicinal chemistry, natural products chemistry, industrial-scale synthesis, and materials science. The mildness of the reaction conditions is typically compatible with a breadth of sensitive functional groups,[4] and the regioselectivity is often superior to traditional methods for the formation of multiply-substituted arenes.

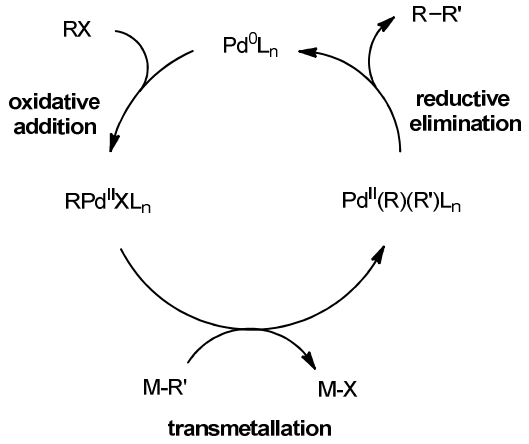

Scheme 1. Catalytic Cycle of Cross-Coupling Reactions

The general catalytic cycle of palladium-catalyzed cross-coupling has changed little since the seminal reports of these transformations (Scheme 1). Catalysis takes place first

by oxidative addition of a C-X bond (X = I, Br, Cl, OSO_2R) to a palladium (0) complex, transmetallation transfers a second covalent ligand from an appropriate main group organometallic reagent, and C-C or C-X (X = N, O, S) bond-forming reductive elimination furnishes the organic product and regenerates a Pd(0) intermediate. The types of organometallic agents used for cross-coupling reactions are typically categorized by name reactions (Scheme 2), including organo-tin, boron, silicon, zinc (also zirconium and aluminum), and magnesium compounds.

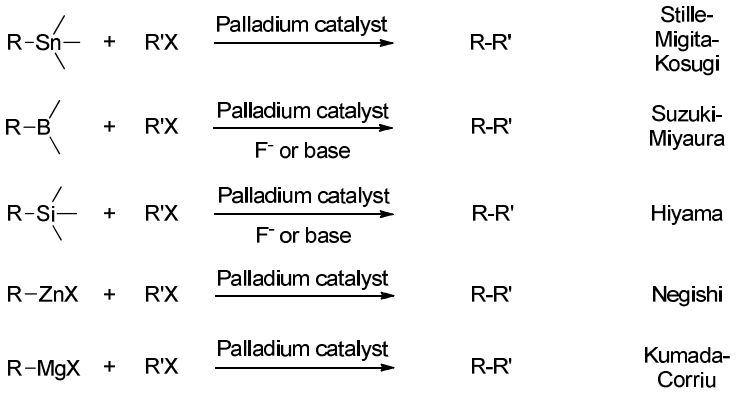

Scheme 2. Classes of Cross-Coupling Reactions

Additionally, coupling reactions of haloarenes with olefins to form substituted alkenes (Mizoroki-Heck) or with terminal alkynes to form internal alkynes (Sonogashira) are typically associated with cross-coupling reactions (Scheme 3). More recently, coupling reactions of electrophiles with heteroatom nucleophiles such as amines (Buchwald-Hartwig), alcohols, and thiols to form substituted amines, ethers, and sulfides have been developed (Scheme 3). These C-X bond-forming reactions are also commonly referred to as cross-coupling reactions because they share some mechanistic similarities to C-C bond-forming cross-coupling reactions.

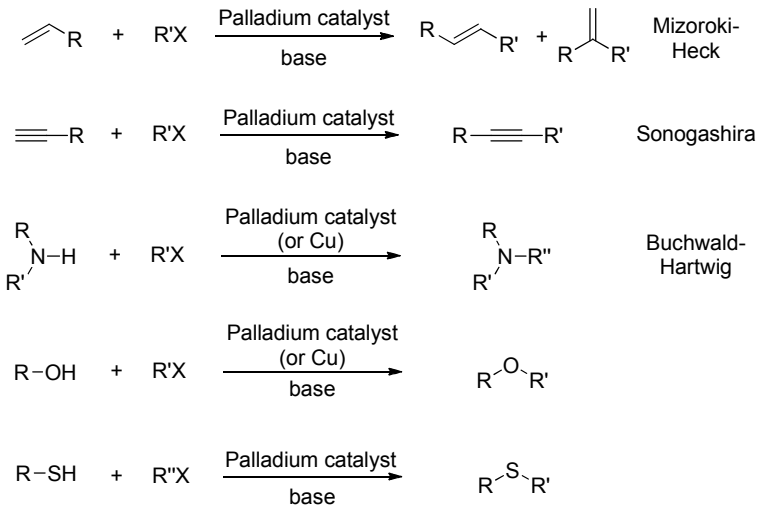

Scheme 3. Reactions Associated with Cross-Coupling Reactions

The structure of palladium catalysts for cross-coupling reactions has evolved concomitantly with the design of new ancillary ligands that afford enhanced catalytic activity. Most often these ancillary ligands are aryl- and alkylphosphines, although *N*-heterocyclic carbene (NHC) ligands are commonly used as well. The influence of the steric and electronic properties of the ancillary ligands on the reactivity of the resulting palladium complexes is surveyed in the subsequent sections. When possible, emphasis is placed on studies of complexes ligated by bulky phosphine ligands that form some of the most active catalysts to date for the coupling reactions of a range of coupling partners.

1.2 Oxidative Addition

1.2.1 Introduction

Oxidative addition of the C-X bond of aryl halides and sulfonates to a palladium(0) complex is the first step of all cross-coupling reactions, and consequently many studies of the mechanism of this reaction have been conducted.[1,5] Studies of the mechanism of

oxidative addition of haloarenes to palladium(0) complexes ligated by PPh_3 and bidentate phosphines revealed several guiding principles that have led to the development of catalysts that are more active towards oxidative addition of less reactive carbon electrophiles.

Oxidative additions of iodo and bromoarenes to $Pd(PPh_3)_4$ have been established to occur by generation of the PdL_2 species by reversible dissociation of phosphine.[6-7] Studies of oxidative addition of chloroarenes to palladium complexes ligated by bidentate phosphines have concluded that the reactive palladium complex is also a PdL_2 species.[8] Additionally, PdL_2 complexes of bidentate phosphines generally undergo oxidative addition faster than PdL_2 complexes ligated by monophosphines, which exist in a linear geometry. The phosphine ligands for PdL_2 species containing bidentate ligands are forced into a *cis* orientation, which causes the frontier orbitals that interact with the electrophile to be more accessible than for PdL_2 complexes of monophosphines that have a linear geometry.

1.2.2 Phosphine Ligands that Promote Reactions of Chloroarenes

With regards to substrates for cross-coupling reactions, chloroarenes are less reactive than bromo- and iodoarenes because they undergo oxidative addition more slowly. In fact, traditional palladium catalysts for cross-coupling reactions such as $Pd(PPh_3)_4$ are ineffective to promote couplings of chloroarenes because the rate of oxidative addition is prohibitively slow in the absence of activating substituents. The dramatic increase in activity of palladium complexes ligated by bulky alkylphosphine ligands over complexes

ligated by arylphosphines for cross-coupling reactions of historically difficult or unreactive substrates such as chloroarenes is intriguing. Studies that have begun to uncover the origins of this marked increase in activity are described below.

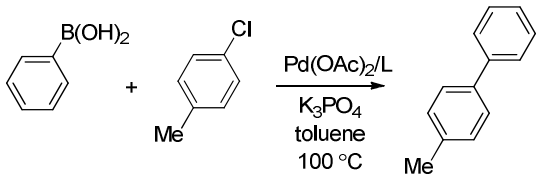

% [Pd]	L =	yield
0.1	PPh_3	5%
0.1	(*o*-biphenyl)PCy_2	93%
0.01	P(*t*-Bu)$_3$	92%
0.005	BuP(1-Ad)$_2$	94%

Scheme 4. Comparison of Ligand Identity on Yield of Biaryl

In 1998, Fu reported that the coupling of unactivated chloroarenes and arylboronic acids catalyzed by the combination of a Pd(0) precatalyst and either of the bulky, electron-rich phosphines P(*t*-Bu)$_3$ and PCy_3 (Cy=cyclohexyl) furnished biaryls in good yield (Scheme 4).[9] At nearly the same time Buchwald reported Suzuki-Miyaura couplings of a range of electron-neutral and electron-rich chloroarenes with arylboronic acids catalyzed by palladium complexes ligated by bulky, electron-rich dialkylbiarylphosphines.[10-11] Both Fu and Buchwald subsequently reported that tailoring of the ligand structure or base/activator allows for *room temperature* couplings of chloroarenes that only a few years prior were considered poor substrates even at elevated temperatures.[12-13] Beller also reported at about the same time that the combination of di-1-adamanyl-*n*-butylphosphine (cataCXium® A) and a palladium precatalyst promoted Suzuki-Miyaura couplings of non-activated and deactivated chloroarenes with high turnover numbers.[14] Following these early reports, a flurry of interest in developing

catalysts containing bulky, electron-rich phosphines, and related *N*-heterocyclic carbene ligands,[15-16] has resulted in myriad methods for cross-coupling reactions of chloroarenes and chloroheteroarenes with various organometallic reagents.[17-18]

1.2.3 Origin of the High Reactivity of Palladium Complexes of Bulky Phosphines Towards Oxidative Addition Reactions

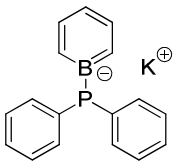

Figure 1. Potassium 1-(diphenylphosphido)boratabenzene (DPB).

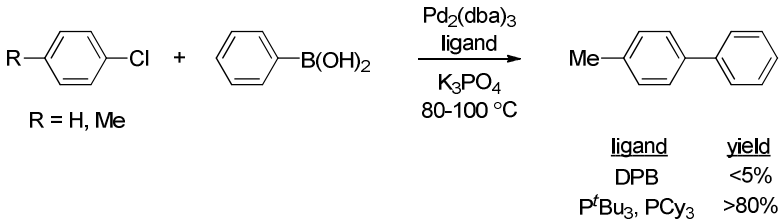

Scheme 5. Comparison of Ligand Identity on Yield of Biaryl

Studies aimed at understanding the factors that enhance the activity of catalysts with ligands that are more bulky and electron-rich than PPh_3 were underway concurrently with the methods development mentioned above. Fu reported the synthesis of an anionic analogue of PPh_3 (Fig 1), which was subsequently investigated as a catalyst for the Suzuki-Miyaura coupling of unactivated chloroarenes.[19-20] Because oxidative additions to metal complexes tend to be faster when electron-density at the metal center is increased,[1] the authors hypothesized that the combination of a Pd(0) precatalyst and the more electron-rich 1-(diphenylphosphido)boratabenzene (DPB) would accelerate the oxidative

addition of chloroarenes compared to complexes of PPh_3. However, the Suzuki-Miyaura reaction of 4-chlorotoluene and phenylboronic acid catalyzed by $Pd_2(dba)_3$ and DPB resulted in very low yield of 4-methylbiphenyl (Scheme 5). The observation that DPB, which is isosteric with PPh_3, forms ineffective catalysts for the cross-coupling of unactivated chloroarenes but complexes with bulkier ligands such as P(*t*-Bu)$_3$ and PCy_3 are effective suggests that factors other the electron-density at the metal complex also play a significant role in enhancing catalytic activity.

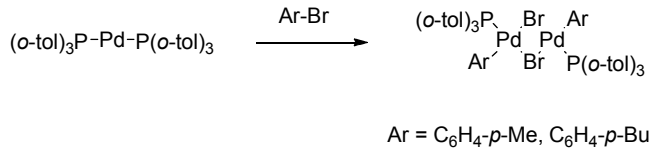

Scheme 6. Synthesis of [Pd{P(*o*-tol)$_3$}(C$_6$H$_4$-*p*-R)(μ-Br)]$_2$ (R = Me, Bu)

Following early reports of the amination of aryl bromides catalyzed by palladium complexes of the bulky ligand P(*o*-tol)$_3$,[21-23] Hartwig et al. investigated the intermediates involved in the catalytic cycle of these reactions. Of particular note was the identification and isolation of the oxidative addition product of an aryl bromide with palladium complexes ligated by P(*o*-tol)$_3$, which exist in the solid state and in solution as halide-bridged dimers containing only a single phosphine (Scheme 6).[22] The three-coordinate dimer was an important discovery since three-coordinate monomers have been implicated in reductive elimination reactions,[24-25] and transmetallation would be expected to be faster from a three-coordinate, monophosphine complex than for a coordinatively saturated, bisphosphine complex.

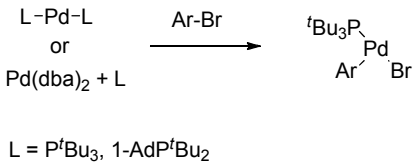

Scheme 7. Preparation of T-shaped Complexes

More recently monomeric, three-coordinate aryl halide complexes LPd(Ar)(X) ligated by P(*t*-Bu)$_3$ and 1-AdP^tBu_2 (Ad=adamantyl) were also reported by Hartwig (Scheme 7).[26-27] These bulky alkylphosphines, which are more sterically-encumbered compared to PPh_3 and P(*o*-tol)$_3$, form three-coordinate palladium complexes of T-shaped geometry. Single crystal X-ray diffraction and computational studies indicate the complexes are stabilized by a weak agostic interaction from the *tert*-butyl group of the phosphine. However, more recently isolated T-shaped complexes containing an amido ligand instead of a halide are also T-shaped but do not appear to be stabilized by an agostic interaction.[28] Thus, the products of oxidative additions to palladium complexes containing bulky phosphine ligands form products that are ligated by a single phosphine unlike complexes ligated by less bulky ligands such as PPh_3 or bidentate bisphosphine ligands. Following these reports, studies of the oxidative addition of haloarenes to complexes of bulky phosphine ligands began to probe whether the mechanisms for reactions involving these species are also distinct compared to complexes of PPh_3.

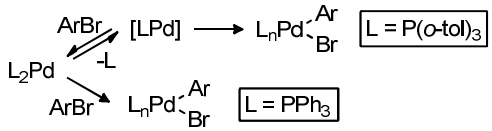

Scheme 8: Mechanisms for Oxidative Addition

Hartwig described the identification and subsequent isolation of a stable, 14-electron complex Pd[P(*o*-tol)$_3$]$_2$,[22,29] and the mechanism of oxidative addition of bromoarenes to this complex was studied concurrently.[30] A series of kinetic experiments for the oxidative addition of bromoarenes to Pd[P(*o*-tol)$_3$]$_2$ revealed an inverse dependence of the rate on the concentration of added ligand, indicating that oxidative addition proceeds by initial dissociation of phosphine. These data are consistent with a dissociative mechanism involving a 12-electron, mono-ligated species Pd-L (Scheme 8), not by direct reaction with the PdL_2 species, as was previously determined for reactions of Pd(PPh$_3$)$_4$ with iodo- and bromoarenes.[6] The bulkiness of the P(*o*-tol)$_3$ ligand is proposed to disfavor direct reaction of haloarene with the PdL_2 complex, but the steric bulk can promote dissociation of phosphine from the PdL_2 species to generate a small concentration of the 12-electron PdL species. The high reactivity of the PdL species is likely due to better access of the incoming electrophile to the frontier orbitals of the metal, an effect similar to that observed for faster oxidative additions to bent PdL_2 species compared to PdL_2 species of linear geometry (vide supra). Thus, the steric bulk of the ancillary ligands appears to be a very important factor for promoting fast oxidative addition reactions.

Other qualitative studies have implicated monoligated Pd(0) intermediates in cross-coupling reactions of chloroarenes. Fu reports that 1:1 ratio of a Pd(0) precatalyst to P(*t*-Bu)$_3$ generates the most active catalyst for Suzuki[31] and Heck[32] reactions of bromo- and chloroarenes. Hartwig also reported a similar effect for α-arylation[33] and amination reactions[34-35] of bromo- and chloroarenes. Buchwald has also implicated mono-ligated

intermediates in cross-coupling reactions with catalysts containing dialkylbiarylphosphines.[36]

1.2.4 Effect of Ionic Additives on the Rate of Oxidative Addition

Ionic additives have also been shown to impact the rates of oxidative addition reactions relevant to a number of cross-coupling reactions. The interactions of anions with palladium complexes ligated by PPh_3 during oxidative addition reactions has been extensively reported by Amatore and Jutand.[37] More recently, similar phenomena have been observed for reactions catalyzed by complexes containing bulky alkylphosphine ligands. A anion-induced pathway for oxidative addition has been described by Hartwig et al. for the amination of chloroarenes catalyzed by $Pd(P^tBu_3)_2$.[38-39] The authors report that two concurrent mechanisms for oxidative addition are operative for the reaction of secondary benzylamines with chloroarenes catalyzed by $Pd(P^tBu_3)_2$ (Scheme 9). The first is a pathway that involves the generation of the neutral monoligated species $Pd(P^tBu_3)$, while the second concurrent pathway involves generation of an anionic species $[(^tBu_3P)PdX]^-$ (X = halide or alkoxide).

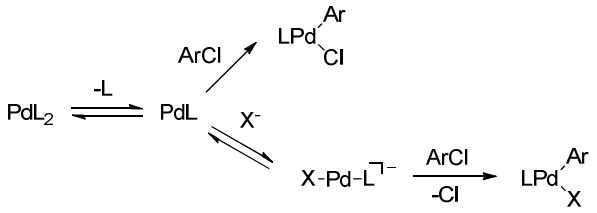

Scheme 9. Mechanisms of Oxidative Addition in the Presence of Anions

The relative contribution of the anionic pathway appears to be dependent on the softness and steric bulk of the anion. Chloride ions do not accelerate the rate of the

anionic pathway, but bromide ions have a marked accelerating effect. Likewise, the added base can accelerate the anionic pathway for oxidative addition in the order 2,4,6-tri-*tert*-butylphenoxide > O^tBu^- >> $OCEt_3^-$. The lack of acceleration of added $OCEt_3^-$ is attributed to the presumed low binding affinity of this very sterically hindered base. Previous mechanistic studies of aminations catalyzed by complexes containing bidentate phosphines were clearly zeroth-order in the concentration of similar bases, indicating that aminations conducted with $Pd(P^tBu_3)_2$ are mechanistically distinct.[40]

Oxidative additions of arenesulfonates to palladium complexes ligated by bidentate and monophosphines also exhibit acceleration in the presence of ionic additives. Reactions of $Pd[P(o\text{-tol})_3]_2$ with phenyltrifluoromethansulfonate (PhOTf) occurred considerably faster in the presence of tetraalkylammonium chloride and bromide salts, forming $[Pd\{P(o\text{-tol})_3\}(Ph)(\mu\text{-X}]_2$ (X = Cl, Br) as the organometallic product. Reactions of $Pd[P(o\text{-tol})_3]_2$ and PhOTf conducted in the presence of a fixed concentration of $N(octyl)_4Br$ and with or without additional NBu_4PF_6 were also conducted. The reaction with added NBu_4PF_6 was not faster than in the absence of the weakly coordinating ions, indicating that the acceleration of the rate by added bromide was not simply a polarity effect of the medium.

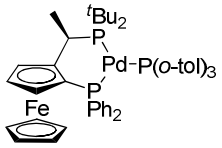

Figure 2. Pd(PPF-*t*-Bu)[($P(o\text{-tol})_3$].

In contrast to reaction of palladium complexes of the bulky monophosphine $P(o\text{-tol})_3$, reactions of palladium complexes of bulky, electron-rich bidentate Josiphos ligands (Fig

2) with arenesulfonates exhibit a different effect of ionic additives. Oxidative addition of phenyl *p*-toluenesulfonate (PhOTs) to the Josiphos complex Pd(PPF-*t*-Bu)[(P(*o*-tol)$_3$] was accelerated in the presence of tetralkylammonium salts. However, reactions conducted with the weakly coordinating salt NBu_4PF_6 were about twice as fast as reactions conducted in the presence of the same concentration of NBu_4Br, which contrasts the trend observed for additions of aryl triflates to Pd[P(*o*-tol)$_3$]$_2$. These kinetic data indicate that oxidative additions of arenesulfonates to complexes ligated by Josiphos ligands occurred by a mechanism that is faster in more polar medium, not by coordination of the anion to the Pd(0) complex. Such an effect has rarely been observed for oxidative addition reactions of aryl electrophiles.[41]

1.2.5 Correlation of Mechanisms of Oxidative Addition to the Properties of the Metal Complex and Electrophile

Empirical studies of the mechanism of oxidative addition of haloarenes to palladium complexes ligated by bulky alkylphosphines are few. Additionally, differing conclusions about the mechanism and factors that affect the mechanism for oxidative addition have emerged. Brown and Jutand reported that the mechanism of oxidative addition of aryl iodides and aryl triflates to PdL_2 (L = PCy_3, $PCy_2{}^tBu$, PCy^tBu_2, and P^tBu_3) is affected by the steric properties of the ligand.[42] They concluded that oxidative additions of complexes with the bulkier PCy^tBu_2 and P^tBu_3 occur by initial dissociation of ligand and reaction through a monoligated species, similar to Pd[P(*o*-tol)$_3$]$_2$.[30] On the other hand,

complexes ligated by the less bulky PCy_3 and $PCy_2{}^tBu$ occur by reaction of the PdL_2 species in the first irreversible step.

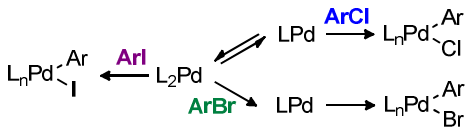

Scheme 10. Mechanisms of Oxidative Addition of Haloarenes

Hartwig and Barrios-Landeros subsequently conducted a study of oxidative addition of iodo-, bromo-, and chloroarenes to $Pd(QPhos)_2$ (QPhos = 1,2,3,4,5-pentaphenyl-1′-(di-*tert*-butylphosphino)ferrocene).[43] These kinetic studies concluded that oxidative addition to the three classes of haloarenes occurs by three distinct mechanisms (Scheme 10). Oxidative addition of chloroarenes occurs by reversible dissociation of phosphine followed by rate-limiting oxidative addition to a mono-ligated species. Oxidative addition of bromoarenes occurs by rate-limiting dissociation of phosphine. Oxidative addition of iodoarenes occurs by associative displacement of phosphine by iodoarene, which is to say that the rate-limiting step involves a bisphosphine palladium species. The reports of Hartwig and of Brown and Jutand draw differing conclusions about the factors that control the mechanism of oxidative addition. In one case the identity of the halide and in the other case the steric properties of the ligand are proposed to control the mechanism of oxidative addition. However, it remains unclear to what extent the steric properties of the ligand or the identity of the halide impact the mechanism of oxidative addition across a range of ligand steric properties and a range of haloarene substrates.

1.3 Reductive Elimination

1.3.1 Introduction

Reductive elimination of two covalent ligands from a metal complex is the elementary step of palladium-catalyzed cross-coupling reactions that forms the new bond in the resulting organic product.[1-3] While this transformation is concerted and often a rapid reaction for $C(sp^2)$-$C(sp^2)$ bond formation, more recently developed coupling reactions that involve $C(sp^3)$-$C(sp^3)$, $C(sp^2)$-N, $C(sp^2)$-O, and $C(sp^2)$-S bond formation may proceed by other mechanisms.[24,44-46] Furthermore, reductive elimination is the microscopic reverse of oxidative addition, which might lead one to conclude that the factors that lead to faster oxidative addition reactions for complexes of bulky, electron-rich ligands would in turn decelerate reductive elimination reactions. It is difficult to predict whether the steric or electronic properties of these types of ligands affect the rate of reductive elimination more because such processes tends to be accelerated by ancillary ligands that are more sterically hindered,[47] but are decelerated for ancillary ligands that are more electron-donating.[48] Studies of the mechanisms of reductive elimination of C-C and C-X (X = N, O, S) bonds in palladium complexes ligated by bulky phosphine ligands are described in this section.

Several important trends for the reductive elimination to form C-C bonds have been revealed in previous studies of palladium complexes containing bidentate phosphines and monophosphines that are similar in size to PPh_3. First, reductive elimination is faster from three-coordinate palladium complexes than from four-coordinate complexes. [45,49-50] The rates of reductive elimination reactions of palladium complexes with two

monophosphines occur with an inverse dependence on the concentration of added phosphine indicating that such reactions proceed through a three-coordinate intermediate by reversible loss of one phosphine.[24,44] Additionally, reductive eliminations from complexes with bidentate phosphines generally occur more slowly than analogous complexes ligated by two monophosphines because the former cannot readily dissociate phosphine to generate three-coordinate intermediates.[22,51-52]

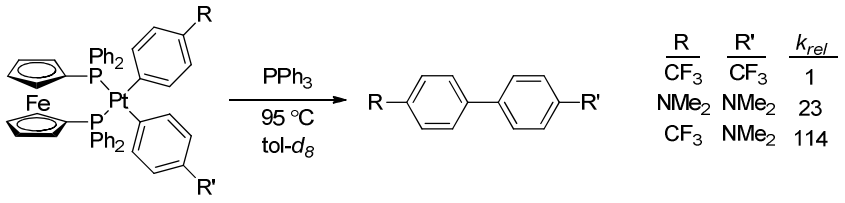

Scheme 11. Reductive Elimination of Biaryls from Platinum Complexes

Electronic effects of the reacting ligands can have a significant impact on the rate of reductive elimination. Reductive elimination of biaryls from platinum complexes ligated by 1,1'-bis(diphenylphosphine)ferrocene (DPPF) occurred faster if both aryl ligands contained electron-donating substituents than when the aryl ligands contained electron-withdrawing substituents.[53] Furthermore, when there is a large discrepancy between the electronic properties of the two reacting aryl ligands, then the rate of reductive elimination is faster still (Scheme 11).

Finally, reductive eliminations of aryl amido, thiolato, and alkoxo palladium complexes ligated by bidentate phosphines have been extensively studied. In brief, reductive eliminations to form C-N, C-S, and C-O bonds are accelerated for more electron-poor carbon-based ligands and more electron-rich amido, thiolato, or alkoxo ligands.[46,54] The magnitude of the effect of the electronic properties of the aryl ligand on

the rate of reductive elimination depends on the identity of the second reacting ligand and follows the general trend: C-C < C-S < C-N < C-O. Whether similar or different trends in electronic effects also occur during reduction elimination reactions from palladium complexes ligated by bulky, electron-rich phosphine ligands has been the subject of several recent studies (vide infra).

1.3.2 Reductive Elimination of C-C Bonds

Pioneering studies by Hartwig to develop palladium-catalyzed α-arylations of carbonyl compounds and nitriles has led to a number of important observations about reduction eliminations of $C(sp^2)$-$C(sp^3)$ bonds with electron-withdrawing substituents at the α-position of the $C(sp^3)$ ligand, which have been reviewed.[55] Relevant to this discussion, significant enhancement of the rate of catalytic α-arylation reactions have been observed when reactions are conducted with palladium complexes containing bulky alkylphosphine ligands. In the context of α-arylation reactions, perhaps the most striking effect of this class of ligands is on the rates of reductive elimination reactions of isolated arylpalladium malonate complexes.

Arylpalladium malonate complexes containing bidentate and monophosphines were prepared and structurally characterized.[56] Complexes of monophosphines formed stable η^2 O,O'-bound structures upon exchange of halide for malonate anion, and bidentate phosphine complexes were η^1 C-bound upon exchange of halide for malonate (Scheme 12). Because malonates form η^2 complexes in monophosphine complexes, access to three-coordinate intermediates prior to reductive elimination is difficult. In addition, the

presence of two electron-withdrawing groups at the more electron-rich sp^3-carbon ligand undergoing reductive elimination would also be expected to slow the rate. Not surprisingly, reductive elimination of α-arylated product upon thermolysis of these complexes was slow, even though palladium complexes containing these phosphine ligands and enolate ligands with less electron-withdrawing substituents have been observed to undergo facile reductive elimination under similar conditions.[50] However, reductive elimination of arylpalladium malonate ligated by the bulky alkylphosphine FcP^tBu_2 occurred in high yield and at lower temperatures than complexes of PPh_3 or those ligated by bidendate phosphines (Scheme 12). The faster reductive elimination from complexes of FcP^tBu_2 over those ligated by PPh_3 or DPPE is attributed to the increased steric bulk of the alkylphosphine in the three-coordinate intermediate.

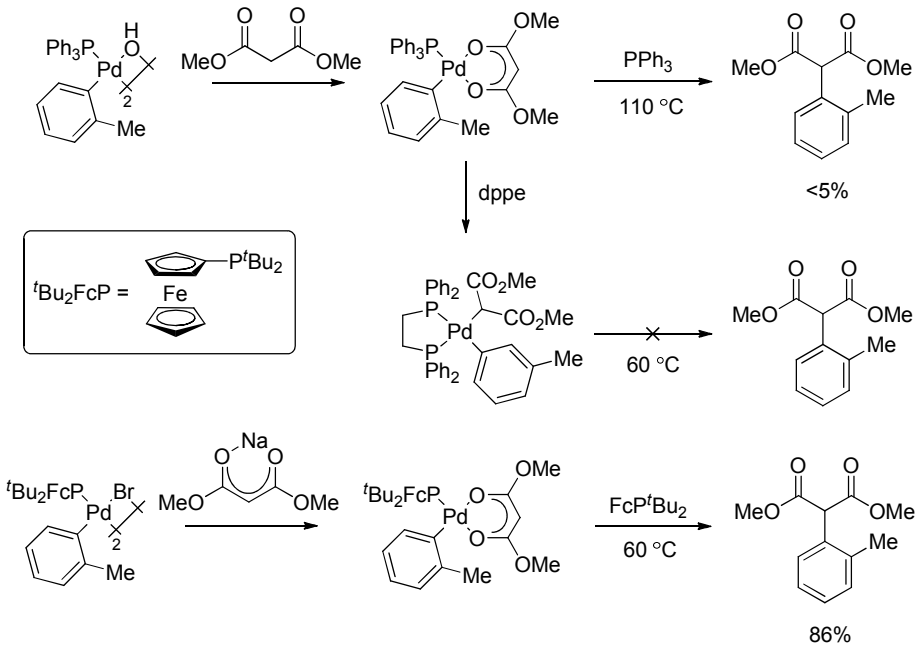

Scheme 12. Preparation and Reductive Elimination of Palladium-Malonate Complexes

1.3.3 Reductive Elimination of C-N Bonds

Buchwald-Hartwig amination reactions catalyzed by palladium complexes with bulky, electron-rich ligands such as P(*t*-Bu)$_3$ or dialkylbiarylphosphines are rapid even at low reaction temperatures, often proceeding at room temperature.[10,57] For these processes to be successful, C-N reductive elimination must also be rapid. Previous studies of reductive eliminations of anilido and alkylamido complexes ligated by PPh_3 and bidentate phosphines revealed several important trends.[25,52] First, reductive elimination of arylpalladium amido complexes of PPh_3 occurred through three-coordinate intermediates. Second, reductive eliminations of alkylamido ligands were faster than anilido ligands, and secondary anilido ligands undergo reductive elimination more slowly than primary anilido ligands.

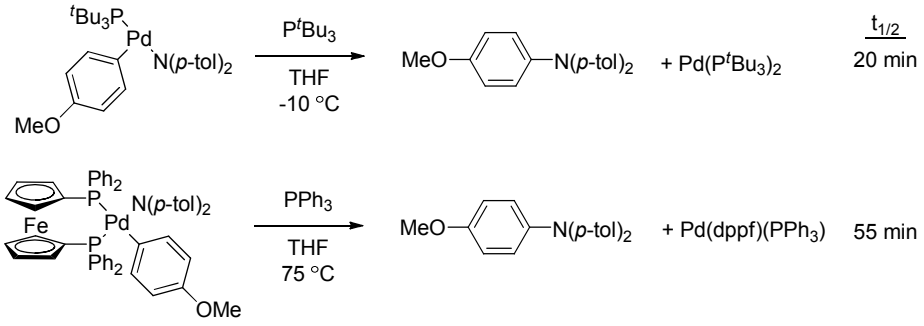

Scheme 13. Reductive Eliminations from Arylpalladium Amide Complexes

Hartwig and Yamashita recently reported the first examples of monomeric three-coordinate arylpalladium amido palladium complexes and subsequently studied the reductive elimination of arylamines from these complexes.[28] Reactions of amides with three-coordinate arylpalladium halide complexes LPd(Ar)(Br) (L = P^{t}Bu$_3$, Ph$_5$FcP^{t}Bu$_2$ (QPhos), and FcP^{t}Bu$_2$)[58] formed the corresponding three-coordinate arylpalladium amido

complexes, which were stable at room temperature if the aryl and amido ligands were deactivated towards reductive elimination (substituted with electron-rich and electron-poor substituents, respectively). These complexes underwent reductive elimination to form arylamines upon thermolysis. The yield of the organic product increased for complexes substituted with the more sterically bulky phosphine (P^tBu_3 > QPhos, FcP^tBu_2). If the aryl and amido ligands were not substituted with deactivating substituents, the corresponding arylpalladium amido complex ($(^tBu_3P)Pd(Ar)(NAr'_2)$) was only stable at low temperature. In fact, $(^tBu_3P)Pd(C_6H_4\text{-}p\text{-}OMe)(N(p\text{-}tol)_2)$ underwent reductive elimination at -10 °C with a half-life of 20 min and formed the corresponding triarylamine in 91% yield (Scheme 13). The rate of this reaction was much faster than the reductive elimination of the analogous complex ligated by DPPF, which occurred with a longer half-life of 55 min at a much higher temperature (75 °C). Thus, once again the reductive elimination from three-coordinate complexes is shown to be much faster than four-coordinate complexes that cannot readily dissociate phosphine, and these three-coordinate amido complexes ligated by bulky phosphines also undergo faster reductive eliminations than analogues ligated by less bulky arylphosphines.

1.3.4 Reductive Elimination of C-S Bonds

Palladium catalysts of bulky bidentate ligands (i.e. 1,1'-bis(di-*iso*-propylphosphino)ferrocene {Josiphos}) form the most active catalysts for the formation of aryl thioethers by cross-coupling.[59] Accordingly, studies of reductive eliminations that form C-S bonds have focused on complexes ligated by bidentate phosphines,[60-61] and

there are no reports of reductive eliminations from arylpalladium thiolato complexes ligated by bulky monophosphine ligands.[46] As such, discussions of reductive eliminations to form thioethers are not discussed further here.

1.3.5 Reductive Elimination of C-O Bonds

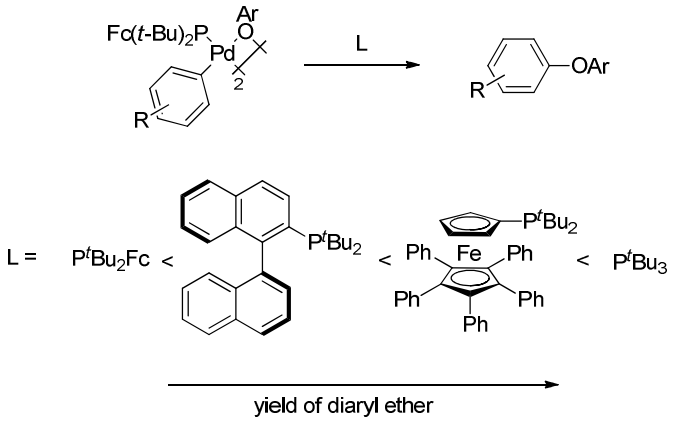

Scheme 14. Effect of Ligand Identity on C-O Reductive Elimination

The development of catalysts that promote etherification of aryl halides has been challenging, with progress lagging most other types of cross-coupling reactions. The turnover-limiting step in these reactions is believed to be C-O reductive elimination, and fundamental studies of this process indicate reductive eliminations that form ethers are difficult.[46] Recently Hartwig found that the yields of diaryl ether by reductive elimination from isolated arylpalladium aryloxo complexes can be significantly increased by the addition of bulky alkylphosphine ligands (Scheme 14).[47] The yield of diaryl ether was highest in the presence of the most sterically bulky ligand, which was rationalized by acceleration of reductive elimination to an extent that out-competes the rate of non-productive decomposition of the starting complex.

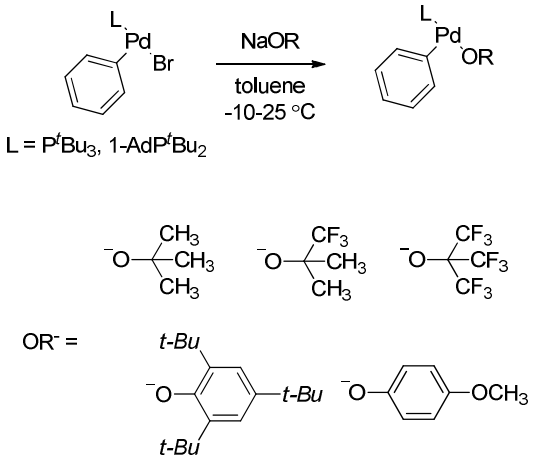

Scheme 15. Preparation of T-shaped Arylpalladium Alkoxo and Aryloxo Complexes

Further evidence of the influence of bulky, electron-rich phosphines to promote faster C-O reductive elimination subsequently came from studies of the first isolated monomeric, T-shaped arylpalladium alkoxides and aryloxides.[62] The formation of three-coordinate alkoxo palladium complexes LPd(Ar)(OR) (L = P(*t*-Bu)$_3$, 1-AdP^{t}Bu$_2$; R = *p*-anisyl, 2,4,6-(*t*-Bu)$_3$C$_6$H$_4$, *t*-Bu, C(CH$_3$)$_2$(CF$_3$), C(CF$_3$)$_3$) occurs by reaction of the corresponding aryl halide complex with alkoxo or aryloxo salts (Scheme 15). Thermolysis of these complexes at 10-70 °C afforded good yields of the aryl ether products, with the exception of (1-AdP^{t}Bu)Pd(Ph)(O{2,4,6-(*t*-Bu)C$_6$H$_4$}) which decomposed to form biphenyl and (^{t}Bu$_3$P)Pd(Ph)(OC(CF$_3$)$_3$) which did not react because of the strong electron-withdrawing groups of the alkoxide. Most impressively, (^{t}Bu$_3$P)Pd(Ph)(O^{t}Bu) could not be isolated because of rapid reductive elimination to form aryl ether product in high yield at or below ambient temperature. The electron-rich and sterically bulky *tert*-butoxide ligand is presumed to account for the much higher reactivity of (^{t}Bu$_3$P)Pd(Ph)(O^{t}Bu) compared to analogous complexes with aryloxides or

fluorinated *tert*-butoxides. However, reductive elimination of (^{t}Bu$_3$P)Pd(Ph)(O^{t}Bu) occurred over the same period of time as that of (^{t}Bu$_3$P)Pd(C$_6$H$_4$-*p*-OMe)(N(*p*-tol)$_2$) but at a reaction temperature of 30 °C and -10 °C, respectively. Thus, even though reductive elimination of aryl ethers from aryl alkoxo palladium complexes is greatly accelerated by bulky ancillary ligands, C-N reductive eliminations of analogous aryl amido complexes are considerably faster.

The results of these studies indicate that the steric properties of the ancillary ligand have a considerable accelerating effect on the rate of reductive elimination of C-O bonds even though such ancillary ligands tend to be stronger donors than arylphosphines. In general, the steric bulk of alkylphosphine ligands appears to override the electronic properties of the ligand with respect to the rate of reductive elimination reactions. As a result, palladium complexes ligated by bulky alkylphosphines exhibit characteristics that are favorable both for oxidative addition and reductive elimination reactions even though one might expect opposite effects on the rates of these two elementary steps of cross-coupling reactions.

1.4 Transmetallation

1.4.1 Introduction

Of the three elementary steps of cross-coupling reactions, transmetallation of a covalent ligand to palladium from a main group organometallic reagent is the least understood. Several classes of organometallic reagents (i.e. Mg, Zn, B, Si, Sn) are known to undergo this transformation, and their mechanisms can vary among the classes of reagents, the identity of the organic moieties, or even the reaction solvent and temperature.[63] Mechanistic studies of these processes published to date have solidified some aspects of the transmetallation sequence for the Stille, Suzuki, and Hiyama reactions. However, details of transmetallation with other organometallic reagents are essentially unknown even today (i.e. Kumada-Corriu coupling). Additionally, mechanistic studies of transmetallation for palladium complexes ligated by recently developed bulky phosphine ligands are few. Some important aspects of the current understanding of transmetallation are described in this section, with emphasis on studies that involve palladium complexes of bulky monophosphines that form some of the most active catalysts for cross-coupling reactions.

1.4.2 Transmetallation of Organozinc and Organomagnesium Compounds

The palladium or nickel-catalyzed reactions of organozinc and magnesium reagents with arene and alkene electrophiles constitute some of the earliest examples of cross-coupling reactions.[64] However, the transmetallation of these reagents to late metal complexes is the least understood of the cross-coupling reactions. Two recent reports by

Espinet et al. have begun to probe the transmetallation sequence of organozinc reagents to arylpalladium complexes.[65-67] DFT calculations suggest that the transfer of the organic ligand occurs through a four-centered transition state (Fig 3). Though transmetallation reactions are often thought to be irreversible, Espinet proposes that transmetallation of organozinc reagents is a reversible process.[65] A reversible transmetallation step has implications for homo-coupling, which has been observed in some Negishi couplings. Unfortunately, studies on the mechanism of transmetallation for systems containing bulky alkylphosphines have not been reported to date even though such complexes function as highly-active catalysts for this transformation.[68-69]

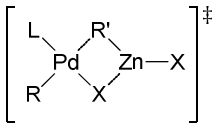

Figure 3. Proposed Transition State for the Transmetallation of an Organic Moiety from Zinc to Palladium.

1.4.3 Transmetallation of Organostannanes

The most studied reaction with regard to the transmetallation sequence is the Stille coupling involving the transfer of alkyl, alkenyl, aryl, or heteroaryl stannanes.[70] The transfer of the organic moiety from tin to palladium has been proposed to proceed through cyclic or open transition states (Fig 4) and by associative or dissociative ligand substitution, and these mechanisms depend on the substituents of the organic moiety, the solvent, the halide/psuedohalide on palladium, or a combination of these factors. The

conditions that promote the cyclic or open pathway have been explored by a number of studies.

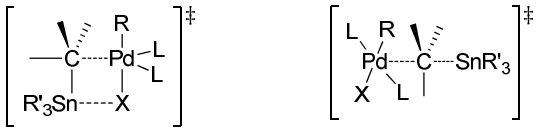

Figure 4. Proposed Transition States for the Transmetallation of an Alkyl Ligand from Tin to Palladium by a Cyclic (left) or Open (right) S_E2 Pathway.

Reactions of alkylstannanes that possess a chiral, non-racemic stereogenic center alpha to tin should give retention of configuration in the resulting organic product if transmetallation proceeds by the cyclic pathway, since reductive elimination is also thought to proceed by retention of configuration.[71] Conversely, transmetallation by an open pathway should proceed with inversion of configuration in the resulting organic product. Reactions in non-polar solvents tend to promote transmetallation by a cyclic S_E2 transition state, as evidenced by retention of configuration,[72-73] and polar solvents promote transmetallation by an open S_E2 pathway as evidenced by inversion of configuration in the product.[74] The presence of heteroatoms adjacent to the *ipso*-carbon of the organotin reagent may also influence the mechanism of transfer towards a cyclic pathway.[72-73] Palladium complexes with weakly coordinating anions (i.e. OTf) are also biased towards an open pathway for transmetallation because the anionic ligand, which is involved in the cyclic pathway, readily dissociates to form a cationic intermediate.[75]

Additional factors that accelerate the rate of transmetallation of organotin reagents have been documented. First, transmetallation occurs faster with three-coordinate complexes than four-coordinate complexes.[76] Reactions of four-coordinate complexes are

faster when the ancillary ligands more readily dissociate (i.e. $AsPh_3 > P(2\text{-furyl})_3 > PPh_3$) to form three-coordinate intermediates.[77-78] Second, organostannanes that contain an internal Lewis base undergo transmetallation faster than similar reagents lacking such a moiety.[79] This effect is attributed to coordination of the internal Lewis base to tin, which generates a more nucleophilic stannate. Finally, added external base can also accelerate transmetallation by coordination to tin to generate pentavalent intermediates, of which flouride is particularly effective.[80] The positive effective of fluoride, akin to effects observed in Hiyama couplings of organosilicon reagents,[81] was a contributing factor to the first high-yielding Stille coupling of bromoarenes at room temperature, and chloroarenes catalyzed by palladium complexes of $P(t\text{-Bu})_3$.[82-83]

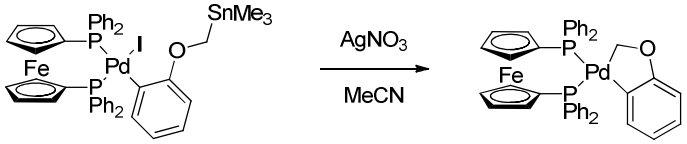

Scheme 16. Palladacycle Formation from Intramolecular Transmetallation

Stoichiometric studies of the reactions of isolated palladium complexes with orgnaostannanes have provided important information about the transmetallation sequence. Cotter concluded from low temperature reactions of cationic palladium-pincer complexes and heteroarylstannanes that transmetallation is a reversible process, similar to organozinc compounds (vide supra), and transmetallation is initiated by initial formation of a π-complex for unsaturated organostannanes.[84] Echavarren has also prepared a series of arylpalladium complexes containing alkyltin substituents. Thermolysis of these complexes led to the intramolecular transmetallation of the organostannane to generate stable palladadcycles.[85-86] These studies provided evidence that transmetallation occurs

by an open pathway because the reactions proceeded only after initial abstraction of the palladium-bound halide by silver(I) salt (Scheme 16).

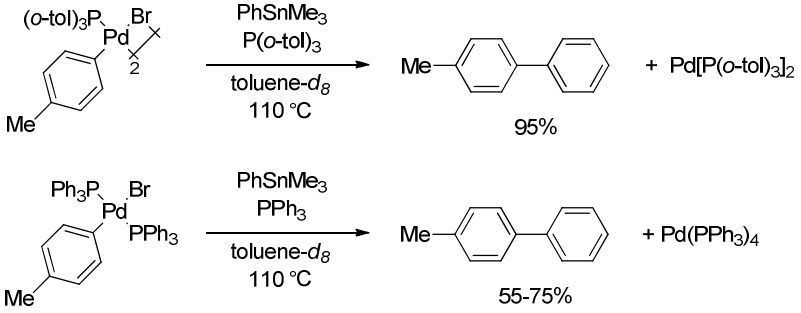

Scheme 17. Biaryl Formation from Transmetallation and Reductive Elimination

Stoichiometric reactions of tin reagents with palladium complexes ligated by bulky phosphines have been reported by Hartwig.[76] The combination of the three-coordinate dimer $[Pd\{P(o\text{-tol})_3\}(C_6H_4\text{-}p\text{-}CH_3)(\mu\text{-}Br)]_2$ and Me_3SnPh formed 4-methylbiphenyl from the combination of transmetallation and reductive elimination (Scheme 17). The rate of this reaction occurred with a half-order dependence on the concentration of palladium dimer and a zeroth-order dependence on the concentration of added phosphine, which is indicative of a mechanism involving a three-coordinate intermediate by dissociation of the dimeric starting complex. The same study found that transmetallation to complexes ligated by PPh_3 also proceed through three-coordinate intermediates, as evidenced by an observed inverse first-order dependence of the reaction rate on the concentration of added phosphine. These data are also consistent with transmetallation of organostannanes to palladium via a three-coordinate intermediate. Addition of Me_3SnBr did not retard the rate of the reaction of $[Pd\{P(o\text{-tol})_3\}(C_6H_4\text{-}p\text{-}CH_3)(\mu\text{-}Br)]_2$ and Me_3SnPh, indicating that transmetallation to palladium complexes of $P(o\text{-tol})_3$ is irreversible.[87] However reactions

of $(Ph_3P)_2Pd(Ar)(Br)$ with Me_3SnPh or Me_3Sn^tBu did appear to be reversible. Data reported by Cotter[84] for transmetallation of organostannanes and Espinet[65] for transmetallation of organozinc reagents also suggest that transmetallation of organostannanes is reversible. However, it is difficult to compare these reports by Cotter, Espinet and Hartwig since they concern reactions with different organometallic reagents and with palladium complexes ligated by different ancillary ligands.

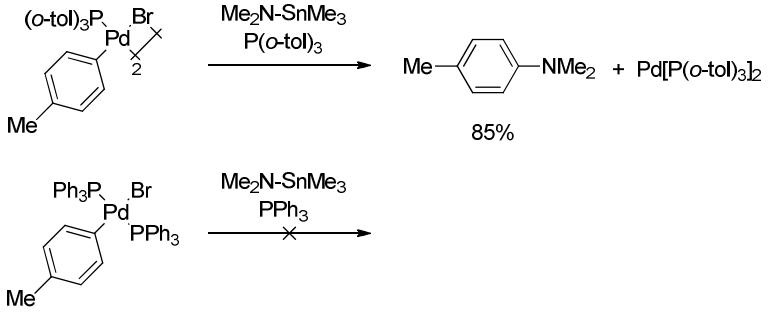

Scheme 18. Formation of Arylamine from Transmetallation and Reductive Elimination

The transmetallation of tin-amides to palladium complexes ligated by P(*o*-tol)$_3$ has also been studied.[76] Because of the slow transmetallation of these stannanes, differences in the reactivity among palladium complexes ligated by different monophosphines could be observed. While reaction of Me_3SnNMe_2 with an arylpalladium complex ligated by P(*o*-tol)$_3$ underwent transmetallation and reductive elimination to form *N,N*-dimethyltoluidine in 85% yield, no reaction was observed for the related complex ligated by PPh_3 (Scheme 18). These data indicate that the transmetallation step of cross-coupling reactions can also be positively affected by the properties of bulky monophosphine ligands, in addition to the positive effects described above for the rates of oxidative addition and reductive elimination reactions.

1.4.4 Transmetallation of Organoboron Compounds

Unlike organostannanes, organoboronic acids that are typical reagents for Suzuki-Miyaura reactions do not undergo transmetallation in the absence of a nucleophilic additive, such as base or fluoride. The general hypothesis of the role of base in the Suzuki-Miyaura reaction is to enhance the electron density of the *ipso*-carbon through coordination to boron creating an anionic boron-ate adduct. The organometallic reagent is thus rendered more reactive as a nucleophile by the action of the added base. However, conclusions from computational and empirical studies of the mechanism of transmetallation step in Suzuki-Miyaura have been unable to reach consensus.

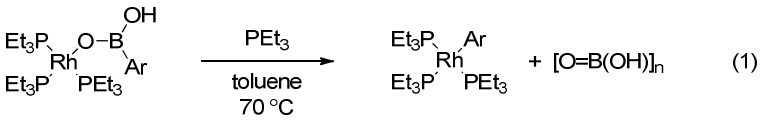

(1)

Several stoichiometric studies of reactions of organoboron compounds with metal complexes to generate metal aryl products have been reported, but the mechanism of transfer of the organic moiety from boron to the metal is not revealed in these studies.[88-91] Hartwig has reported the isolation of a late metal boronate complex.[92] The rhodium-boronate complex underwent thermally-induced intramolecular transfer of an aryl group from boron to rhodium by β-elimination (Eq 1). Note that the organoboron species is not coordinated by a base in these stoichiometric reactions even though transfer of the aryl group from boron to rhodium does occur. Although this stoichiometric reaction is directly related to transmetallation in rhodium-catalyzed Michael additions of arylboronic acids to conjugated carbonyl compounds, analogous boronate compounds of group 10 metals that are proposed intermediates in Suzuki-Miyaura reactions have not been reported.

Additionally, studies of transmetallation of organoboron compounds to palladium complexes ligated by bulky alkylphosphines that generate the most active catalysts for the Suzuki-Miyaura reaction are rare.[93]

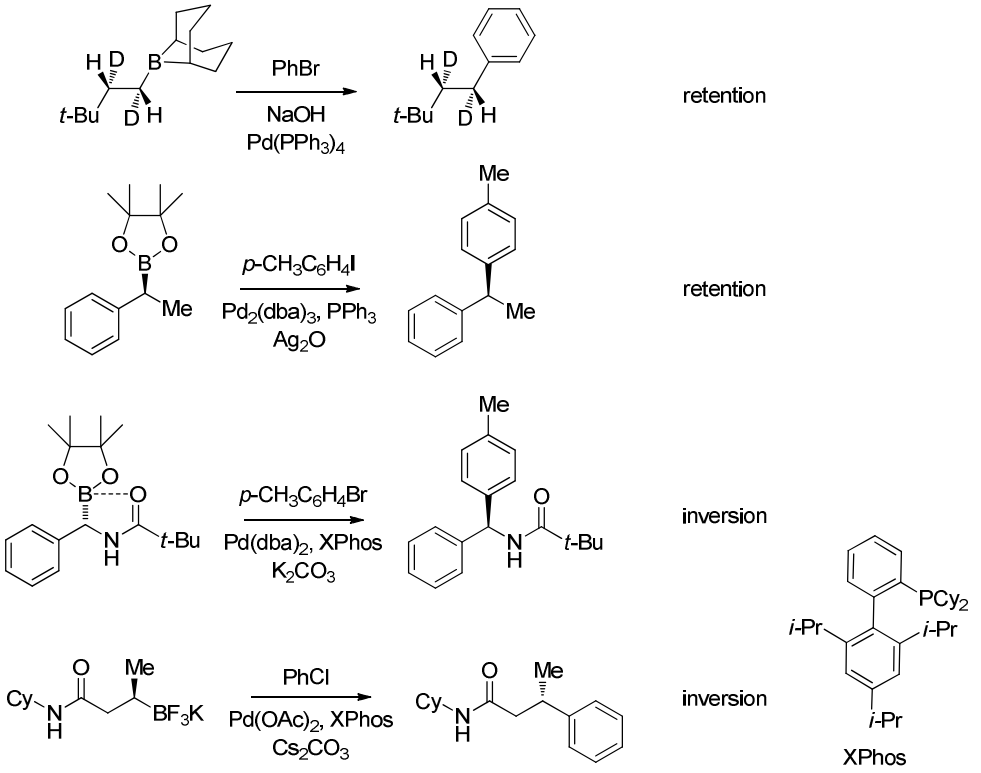

Scheme 19. Suzuki-Miyaura Reactions of Alkylboron Compounds

Suzuki-Miyaura reactions of chiral, non-racemic alkylboron reagents have been employed as stereochemical probes to distinguish between cyclic and open pathways for transmetallation of organoboron compounds.[94-97] Polar substituents appended to the alkyl group of the organoboron appear to play a significant role as to whether retention of configuration is observed. The presence of polar functional groups that can form five or six-membered rings upon coordination to boron appear to promote inversion of configuration, whereas organoboron reagents that lack these coordinating groups couple

with retention of configuration (Scheme 19). Explanations for this effect are speculative, but implicate intramolecular coordination of the heteroatom substituent to boron that could prevent binding of the organoboron substrate to palladium. Binding of the organoboron reagent to palladium prior to transfer of the organic moiety is thought to be involved in the cyclic pathway but not for the open pathway (Fig 5).

Figure 5. Potential Transition States for the Transmetallation of an Alkyl Ligand from Boron to Palladium by a Cyclic (left) or Open (right) S_E2 Pathway.

The origin of effect of the ligand on the stereochemical consequences of transmetallation is not clear because reactions that were conducted with catalysts ligated by PPh_3 were paired with the organoboron compounds lacking coordinating substituents, and reactions that were conducted with catalysts ligated by bulky alkylphosphines were only paired with organoboron compounds that did contain coordinating groups. Combinations of these catalysts with the other class of chiral organoboron compounds have not been performed to determine the possible influence of ancillary ligands on the stereochemical outcome of transmetallation.

1.4.5 Transmetallation of Organosilicon Compounds

Transmetallation of organosilicon reagents to palladium is believed to require the generation of pentavalent silicon intermediates in order to enhance the reactivity of the C-Si bond prior to transfer, because these reagents possesses the smallest difference in

electronegativity of the classes of organometallic reagents used in cross-coupling reactions. Traditionally, Hiyama couplings are run in the presence of fluoride as the requisite nucleophilic activator.[98] Denmark et al. have reported a thorough study of the fluoride-promoted cross-coupling of alkenylsilanols, in which the intermediacy of a hydrogen-bonded complex of fluoride and silanol was identified by NMR spectroscopic and kinetic analyses as the species that undergoes turnover-limiting transmetallation.[99] Stereochemical analysis of coupling reactions of chiral, non-racemic secondary benzylic silicon reagents were also conducted by Hiyama.[81] The transmetallation of these reagents during reactions with aryl triflates proceeded with retention of configuration in non-polar solvents and with inversion in polar solvent mixtures. However, the stereochemical fidelity was also affected by the reaction temperature; inversion of configuration was observed at high reaction temperatures and retention at lower temperatures. These results suggest, akin to observations of Stille couplings of chiral benzylstannanes (vide supra), that the propensity for transmetallation to proceed by cyclic or open S_E2 pathways is sensitive to the reaction conditions.

Fluoride-free cross-coupling reactions of organosilicon compounds have also been developed.[100-104] Organosilanolates are typically used as the organometallic reagent in these particular reactions, and the mechanism of these reactions has been investigated in detail. The nucleophilic silanolates are proposed to coordinate through oxygen to palladium prior to intramolecular transmetallation.[105] This mechanism is distinct from fluoride-promoted organosilicon cross-coupling reactions, which are proposed to proceed by intermolecular transmetallation of a pentavalent silicon intermediate. Studies of

transmetallation of silanolates to platinum have been reported but did not involve reactions of an isolated group 10 metal-silanolate.[106-107]

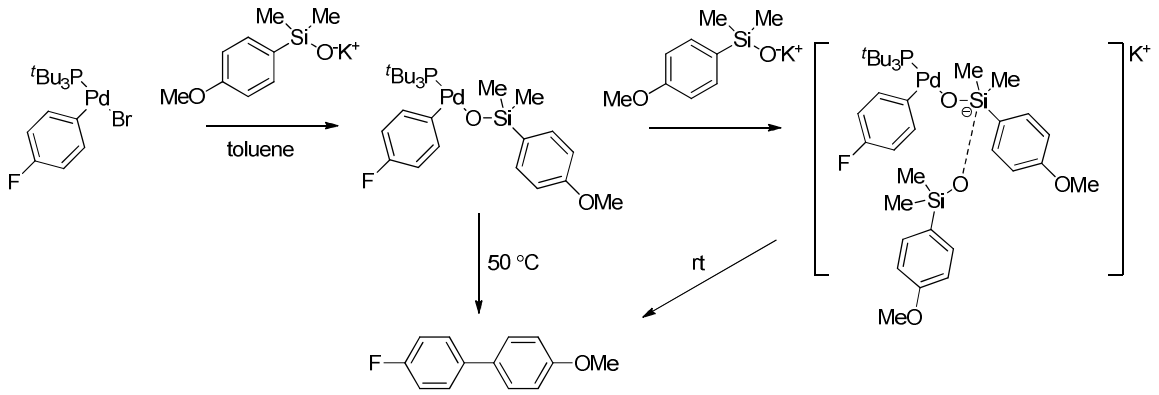

Scheme 20. Preparation and Transmetallation of an Arylpalladium Silanolate Complex

Recently, Denmark and Smith reported the first example of an isolated palladium-silanolate complex ligated by the bulky phosphine P(*t*-Bu)$_3$.[108] Stoichiometric reactions of the palladium-silanolate complex, which were generated in situ, revealed two competing pathways for intramolecular transmetallation (Scheme 20). First, a thermally-induced pathway proceeds without prior activation of silicon to a pentavalent state. [109110] Second, addition of silanolate accelerates the rate of transmetallation by nucleophilic activation of the palladium-bound silanolate. The rate of the later reaction is faster than the thermal pathway by an order of magnitude at the same temperature. Since fluoride-free organosilicon cross-coupling reactions are typically run with preformed silanolate salt that would be present in solution in a large excess relative to the concentration of the palladium catalyst, the activated pathway is proposed to account for transmetallation under catalytic conditions. Although Hartwig et al. have isolated T-shaped arylpalladium alkoxide, aryloxide, and amide complexes,[28,62] this report currently stands as the only

study of intramolecular transmetallation of a well-characterized palladium complex of T-shaped geometry.

1.5 Summary and Objectives

The studies of the fundamental steps of cross-coupling reactions outlined above have elucidated many important trends for how the steric and electronic properties of the ancillary ligands influence the resulting catalyst and affect the rates of the individual steps of the catalytic cycle. Mechanistic studies conducted to date indicate that palladium complexes ligated by bulky monophosphines are capable of accelerating each fundamental step of cross-coupling reactions relative to complexes of arylphosphines. Thus, regardless of the turnover-limiting step of a particular catalytic reaction, complexes of these bulky ligands have the capability to accelerate the turnover frequency. However, it should also be clear that many important questions remain about how these transition metal complexes cleave and form bonds. The subject of the work described in subsequent chapters focuses on studies to improve the understanding of the factors responsible for enhancing the rates of catalysis for complexes ligated by bulky alkylphosphines. The mechanistic investigations can be summarized as follows:

1) Systematic kinetic studies of oxidative additions of haloarenes to Pd^0L_2 complexes ligated by trialkylphosphines of varied steric bulk. (Chapter 2)
2) Kinetic studies of oxidative additions of bromoarenes to $Pd(P^tBu_3)_2$ in the absence of base, which occurs by an unusual autocatalytic process. (Chapter 3)

3) The isolation and characterization of anionic arylpalladium halide complexes that lack dative ligands, as well as kinetic data that implicate their intermediacy in coupling reactions catalyzed by complexes of trialkylphosphines. (Chapter 4)

4) Investigations to elucidate the palladium species that undergoes transmetallation in Suzuki-Miyaura reactions by kinetic, NMR spectroscopic, and competition experiments. (Chapter 5)

1.6 References

(1) Hartwig, J. F. *Organotransition Metal Chemistry*; University Science Books: Sausalito, California, 2010.
(2) de Meijere, A.; Diederich, F., Eds. *Metal-Catalyzed Cross-Coupling Reactions*; Wiley-VCH: Weinheim, 2004.
(3) *Handbook of Organopalladium Chemistry for Organic Synthesis*; Negishi, E.-i., Ed.; John Wiley & Sons, Inc., 2003.
(4) The exception to this functional group tolerance is Kumada-Corriu couplings that utilize Grignard reagents.
(5) Amatore, C.; Jutand, A. *J. Organomet. Chem.* **1999**, *576*, 254-278.
(6) Fauvarque, J. F.; Pfluger, F.; Troupel, M. *J. Organomet. Chem.* **1981**, *208*, 419-427.
(7) Amatore, C.; Pfluger, F. *Organometallics* **1990**, *9*, 2276-2282.
(8) Portnoy, M.; Milstein, D. *Organometallics* **1993**, *12*, 1665-1673.
(9) Littke, A. F.; Fu, G. C. *Angew. Chem., Int. Ed.* **1998**, *37*, 3387-3388.
(10) Old, D. W.; Wolfe, J. P.; Buchwald, S. L. *J. Am. Chem. Soc.* **1998**, *120*, 9722-9733.
(11) Wolfe, J. P.; Buchwald, S. L. *Angew. Chem., Int. Ed.* **1999**, *38*, 2413-2416.
(12) Littke, A. F.; Dai, C.; Fu, G. C. *J. Am. Chem. Soc.* **2000**, *122*, 4020-4028.
(13) Wolfe, J. P.; Singer, R. A.; Yang, B. H.; Buchwald, S. L. *J. Am. Chem. Soc.* **1999**, *121*, 9550-9561.
(14) Zapf, A.; Ehrentraut, A.; Beller, M. *Angew. Chem., Int. Ed.* **2000**, *39*, 4153-4155.
(15) Kantchev, E. A. B.; O'Brien, C. J.; Organ, M. G. *Angew. Chem., Int. Ed.* **2007**, *46*, 2768-2813.
(16) Marion, N.; Nolan, S. P. *Acc. Chem. Res.* **2008**, *41*, 1440-1449.
(17) Littke, A. F.; Fu, G. C. *Angew. Chem., Int. Ed.* **2002**, *41*, 4176-4211.
(18) Bedford, R. B.; Cazin, C. S. J.; Holder, D. *Coord. Chem. Rev.* **2004**, *248*, 2283-2321.
(19) Hoic, D. A.; Davis, W. M.; Fu, G. C. *J. Am. Chem. Soc.* **1996**, *118*, 8176-8177.

(20) Fu, G. C. *Acc. Chem. Res.* **2008**, *41*, 1555-1564.
(21) Kosugi, M.; Kmeyama, M.; Migata, T. *Chemistry Letters* **1983**, 927-928.
(22) Paul, F.; Patt, J.; Hartwig, J. F. *J. Am. Chem. Soc.* **1994**, *116*, 5969-5970.
(23) Guram, A. S.; Buchwald, S. L. *J. Am. Chem. Soc.* **1994**, *116*, 7901-7902.
(24) Moravskiy, A.; Stille, J. K. *J. Am. Chem. Soc.* **1981**, *103*, 4182-4186.
(25) Driver, M. S.; Hartwig, J. F. *J. Am. Chem. Soc.* **1995**, *117*, 4708-4709.
(26) Stambuli, J. P.; Bühl, M.; Hartwig, J. F. *J. Am. Chem. Soc.* **2002**, *124*, 9346-9347.
(27) Stambuli, J. P.; Incarvito, C. D.; Bühl, M.; Hartwig, J. F. *J. Am. Chem. Soc.* **2004**, *126*, 1184-1194.
(28) Yamashita, M.; Hartwig, J. F. *J. Am. Chem. Soc.* **2004**, *126*, 5344-5345.
(29) Paul, F.; Patt, J.; Hartwig, J. F. *Organometallics* **1995**, *14*, 3030-3039.
(30) Hartwig, J. F.; Paul, F. *J. Am. Chem. Soc.* **1995**, *117*, 5373-5374.
(31) Littke, A. F.; Fu, G. C. *Angew. Chem. Int. Ed.* **1999**, *37*, 3387-3388.
(32) Littke, A. F.; Fu, G. C. *J. Am. Chem. Soc.* **2001**, *123*, 6989-7000.
(33) Hama, T.; Hartwig, J. F. *Org. Lett.* **2008**, *10*, 1545-1548.
(34) Hartwig, J. F.; Kawatsura, M.; Hauck, S. I.; Shaughnessy, K. H.; Alcazar-Roman, L. M. *J. Org. Chem.* **1999**, *64*, 5575-5580.
(35) Stambuli, J. P.; Kuwano, R.; Hartwig, J. F. *Angew. Chem. Int. Ed.* **2002**, *41*, 4746-4748.
(36) Barder, T. E.; Biscoe, M. R.; Buchwald, S. L. *Organometallics* **2007**, *26*, 2183-2192.
(37) Amatore, C.; Jutand, A. *Acc. Chem. Res.* **2000**, *33*, 314-321.
(38) Alcazar-Roman, L. M.; Hartwig, J. F. *J. Am. Chem. Soc.* **2001**, *123*, 12905-12906.
(39) Shekhar, S.; Hartwig, J. F. *Organometallics* **2007**, *26*, 340-351.
(40) Alcazar-Roman, L. M.; Hartwig, J. F.; Rheingold, A. L.; Liable-Sands, L. M.; Guzei, I. A. *J. Am. Chem. Soc.* **2000**, *122*, 4618-4630.
(41) Sørensen, H. S.; Larsen, J.; Rasmussen, B. S.; Laursen, B.; Hansen, S. G.; Skrydstrup, T.; Amatore, C.; Jutand, A. *Organometallics* **2002**, *21*, 5243-5253.
(42) Galardon, E.; Ramdeehul, S.; Brown, J. M.; Cowley, A.; Hii, K. K.; Jutand, A. *Angew. Chem., Int. Ed.* **2002**, *41*, 1760-1763.
(43) Barrios-Landeros, F.; Hartwig, J. F. *J. Am. Chem. Soc.* **2005**, *127*, 6944-6945.
(44) Loar, M. K.; Stille, J. K. *J. Am. Chem. Soc.* **1981**, *103*, 4174-4181.
(45) Widenhoefer, R. A.; Buchwald, S. L. *J. Am. Chem. Soc.* **1998**, *120*, 6504-6511.
(46) Hartwig, J. F. *Acc. Chem. Res.* **1998**, *31*, 852-860.
(47) Mann, G.; Shelby, Q.; Roy, A. H.; Hartwig, J. F. *Organometallics* **2003**, *22*, 2775-2789.
(48) Low, J. J.; Goddard, W. A. *J. Am. Chem. Soc.* **1986**, *108*, 6115-6128.
(49) Tatsumi, K.; Hoffmann, R.; Yamamoto, A.; Stille, J. K. *Bull. Chem. Soc. Jpn.* **1981**, *54*, 1857-1867.
(50) Culkin, D. A.; Hartwig, J. F. *Organometallics* **2004**, *23*, 3398-3416.
(51) Louie, J.; Paul, F.; Hartwig, J. F. *Organometallics* **1996**, *15*, 2794-2805.
(52) Driver, M. S.; Hartwig, J. F. *J. Am. Chem. Soc.* **1997**, *119*, 8232-8245.
(53) Shekhar, S.; Hartwig, J. F. *J. Am. Chem. Soc.* **2004**, *126*, 13016-13027.
(54) Hartwig, J. F. *Inorg. Chem.* **2007**, *46*, 1936-1947.

(55) Culkin, D. A.; Hartwig, J. F. *Acc. Chem. Res.* **2003**, *36*, 234-245.
(56) Wolkowski, J. P.; Hartwig, J. F. *Angew. Chem., Int. Ed.* **2002**, *41*, 4289-4291.
(57) Hartwig, J. F.; Kawatsura, M.; Hauck, S. I.; Shaughnessy, K. H.; Alcazar-Roman, L. M. *J. Org. Chem.* **1999**, *64*, 5575-5580.
(58) Arylhalide complexes of FcP^tBu_2 are dimeric.
(59) Alvaro, E.; Hartwig, J. F. *J. Am. Chem. Soc.* **2009**, *131*, 7858-7868.
(60) Baranano, D.; Hartwig, J. F. *J. Am. Chem. Soc.* **1995**, *117*, 2937-2938.
(61) Mann, G.; Baranano, D.; Hartwig, J. F.; Rheingold, A. L.; Guzei, I. A. *J. Am. Chem. Soc.* **1998**, *120*, 9205-9219.
(62) Stambuli, J. P.; Weng, Z.; Incarvito, C. D.; Hartwig, J. F. *Angew. Chem., Int. Ed.* **2007**, *46*, 7674-7677.
(63) The transfer of amides, alkoxides, and thiolates (or alternatively amines, alcohols, and thiols in the presence of base) to palladium is not included here since these processes technically do not involve a main group organometallic reagent, though the catalytic transformations that couple haloarenes and these substrates are often classified as cross-coupling reactions.
(64) Negishi, E.-I. *J. Organomet. Chem.* **2002**, *653*, 34-40.
(65) Casares, J. A.; Espinet, P.; Fuentes, B.; Salas, G. *J. Am. Chem. Soc.* **2007**, *129*, 3508-3509.
(66) Fuentes, B.; García-Melchor, M.; Lledós, A.; Maseras, F.; Casares, J. A.; Ujaque, G.; Espinet, P. *Chem. Eur. J.* **2010**, *16*, 8596-8599.
(67) Liu, Q.; Lan, Y.; Liu, J.; Li, G.; Wu, Y.-D.; Lei, A. *J. Am. Chem. Soc.* **2009**, *131*, 10201-10210.
(68) Dai, C.; Fu, G. C. *J. Am. Chem. Soc.* **2001**, *123*, 2719-2724.
(69) Han, C.; Buchwald, S. L. *J. Am. Chem. Soc.* **2009**, *131*, 7532-7533.
(70) Espinet, P.; Echavarren, A. M. *Angew. Chem. Int. Ed.* **2004**, *43*, 4704-4734.
(71) Milstein, D.; Stille, J. K. *J. Am. Chem. Soc.* **1979**, *101*, 4981-4991.
(72) Ye, J.; Bhatt, R. K.; Falck, J. R. *J. Am. Chem. Soc.* **1994**, *116*, 1-5.
(73) Ye, J.; Bhatt, R. K.; Falck, J. R. *Tetrahedron Lett.* **1993**, *34*, 8007-8010.
(74) Labadie, J. W.; Stille, J. K. *J. Am. Chem. Soc.* **1983**, *105*, 6129-6137.
(75) Farina, V.; Roth, G. P. *Adv. Met.-Org. Chem.* **1996**, *5*, 1-53.
(76) Louie, J.; Hartwig, J. F. *J. Am. Chem. Soc.* **1995**, *117*, 11598-11599.
(77) Farina, V.; Krishnan, B. *J. Am. Chem. Soc.* **1991**, *113*, 9585-9595.
(78) Amatore, C.; Bahsoun, A. A.; Jutand, A.; Meyer, G.; Ndedi, N.; Ricard, L. *J. Am. Chem. Soc.* **2003**, *125*, 4212-4222.
(79) Vedejs, E.; Haight, A. R.; Moss, W. O. *J. Am. Chem. Soc.* **1992**, *114*, 6556-6558.
(80) Mee, S. P. H.; Lee, V.; Baldwin, J. E. *Angew. Chem., Int. Ed.* **2004**, *43*, 1132-1136.
(81) Hatanaka, Y.; Hiyama, T. *J. Am. Chem. Soc.* **1990**, *112*, 7793-7794.
(82) Littke, A. F.; Fu, G. C. *Angew. Chem., Int. Ed.* **1999**, *38*, 2411-2413.
(83) Littke, A. F.; Schwarz, L.; Fu, G. C. *J. Am. Chem. Soc.* **2002**, *124*, 6343-6348.
(84) Cotter, W. D.; Barbour, L.; McNamara, K. L.; Hechter, R.; Lachicotte, R. J. *J. Am. Chem. Soc.* **1998**, *120*, 11016-11017.

(85) Mateo, C.; Cárdenas, D. J.; Fernández-Rivas, C.; Echavarren, A. M. *Chem. Eur. J.* **1996**, *2*, 1596-1606.
(86) Cárdenas, D. J.; Mateo, C.; Echavarren, A. M. *Angew. Chem. Int. Ed. Engl.* **1995**, *33*, 2445-2447.
(87) Added Me_3SnBr did inhibit the rates of reaction of complexes ligated by PPh_3 indicating that transmetallation is reversible in this case.
(88) Nishikata, T.; Yamamoto, Y.; Miyaura, N. *Organometallics* **2004**, *23*, 4317-4324.
(89) Suzaki, Y.; Osakada, K. *Organometallics* **2006**, *25*, 3251-3258.
(90) Nishihara, Y.; Onodera, H.; Osakada, K. *Chem. Commun.* **2004**, 192-193.
(91) Simpson, R. D.; Bergman, R. G. *Organometallics* **1992**, *11*, 3980-3993.
(92) Zhao, P.; Incarvito, C. D.; Hartwig, J. F. *J. Am. Chem. Soc.* **2007**, *129*, 1876-1877.
(93) Jover, J.; Fey, N.; Purdie, M.; Lloyd-Jones, G. C.; Harvey, J. N. *J. Mol. Catal. A.: Chem.* **2010**, *324*, 39-47.
(94) Matos, K.; Soderquist, J. A. *J. Org. Chem.* **1998**, *63*, 461-470.
(95) Imao, D.; Glasspoole, B. W.; Laberge, V. r. S.; Crudden, C. M. *J. Am. Chem. Soc.* **2009**, *131*, 5024-5025.
(96) Ohmura, T.; Awano, T.; Suginome, M. *J. Am. Chem. Soc.* **2010**, *132*, 13191-13193.
(97) Sandrock, D. L.; Jean-Gérard, L.; Chen, C.-y.; Dreher, S. D.; Molander, G. A. *J. Am. Chem. Soc.* **2010**, *132*, 17108-17110.
(98) Sugiyama, A.; Ohnishi, Y.-y.; Nakaoka, M.; Nakao, Y.; Sato, H.; Sakaki, S.; Nakao, Y.; Hiyama, T. *J. Am. Chem. Soc.* **2008**, *130*, 12975-12985.
(99) Denmark, S. E.; Sweis, R. F.; Wehrli, D. *J. Am. Chem. Soc.* **2004**, *126*, 4865-4875.
(100) Denmark, S. E.; Smith, R. C.; Chang, W.-T. T.; Muhuhi, J. M. *J. Am. Chem. Soc.* **2009**, *131*, 3104-3118.
(101) Denmark, S. E.; Werner, N. S. *J. Am. Chem. Soc.* **2008**, *130*, 16382-16393.
(102) Denmark, S. E.; Butler, C. R. *J. Am. Chem. Soc.* **2008**, *130*, 3690-3704.
(103) Denmark, S. E.; Kallemeyn, J. M. *J. Am. Chem. Soc.* **2006**, *128*, 15958-15959.
(104) Denmark, S. E.; Sweis, R. F. *J. Am. Chem. Soc.* **2001**, *123*, 6439-6440.
(105) Denmark, S. E.; Sweis, R. F. *J. Am. Chem. Soc.* **2004**, *126*, 4876-4882.
(106) Fukuoka, A.; Sato, A.; Kodama, K.-Y.; Hirano, M.; Komiya, S. *Inorg. Chim. Acta* **1999**, *294*, 266-274.
(107) Mintcheva, N.; Nishihara, Y.; Mori, A.; Osakada, K. *J. Organomet. Chem.* **2001**, *629*, 61-67.
(108) Denmark, S. E.; Smith, R. C. *J. Am. Chem. Soc.* **2010**, *132*, 1243-1245.
(109) A palladium-silanolate ligated by DPPP was also reported to suffer thermally-induced transmetallation by an unactivated pathway. See Ref 110.
(110) Denmark, S. E.; Regens, C. S. *Acc. Chem. Res.* **2008**, *41*, 1486-1499.

Chapter 2. Effect of Ligand Steric Properties and Halide Identity on the Mechanism for Oxidative Addition of Haloarenes to Trialkylphosphine Pd(0) Complexes

---

2.1 Introduction

The oxidative addition of haloarenes to palladium(0) complexes is a fundamental organometallic reaction.[1] It constitutes the first step in palladium-catalyzed reactions of haloarenes, such as aromatic amination,[2-4] Heck,[5,6] Suzuki,[7-10] and Stille[11,12] couplings. Many of these oxidative additions occur to phosphine-ligated Pd(0) species. Some of the most active catalysts for these reactions involve hindered alkylphosphine ligands that form bis-phosphine complexes of Pd(0).[13-17] Because of the high activity of these catalysts, the mechanism of the oxidative addition to these bisphosphine complexes is important to determine. Moreover, it would be valuable to reveal the relationships between the reactivity of the isolated $L_2Pd(0)$ species in which L is a hindered trialkylphosphine and the Pd(0) reactive intermediates in which L is PPh_3.[18,19]

The oxidative addition of haloarenes to $L_2Pd(0)$ complexes in which L is a trialkylphosphine could occur directly to the bisphosphine starting complex to form a four-coordinate product, or it could occur to a monophosphine intermediate[20,21] that would form a three-coordinate arylpalladium halide complex[22,23] as the immediate product. Previous studies have shown that the coordination number of the palladium species that undergoes oxidative addition and the structure of the complexes produced by oxidative addition are different for reactions of complexes containing various ligands.[18,19,24-32,33,34-36]

A majority of these studies have been conducted on complexes containing monophosphine ligands.[18,19,24-29] The mechanism appears to depend on the steric and electronic properties of the ligand. For example, classic studies on the addition of ArI to $Pd(PPh_3)_4$ showed that this reaction occurs through the 14-electron intermediate $Pd(PPh_3)_2$ to produce a four-coordinate arylpalladium halide complex.[18,19] In contrast, more recent studies on the oxidative addition of PhBr to $Pd(P(o\text{-tol})_3)_2$ implied that this addition occurred to a monophosphine intermediate to form a dimeric arylpalladium bromide complex containing a single phosphine per metal center.[20] Addition of ArI to a series of trialkylphosphine palladium complexes of the general formula $Pd(Cy_nP^tBu_{3-n})_2$ (n = 0–3) has also been conducted. These authors concluded that complexes containing the bulkier phosphines (n = 0, 1) underwent addition of ArI after dissociation of ligand to form a monophosphine intermediate and that complexes containing the smaller phosphines (n = 2, 3) reacted through an associative pathway.[27] The results of studies on reactions of PPh_3 complexes in the presence of anions have also been published. For example, the 16-electron anionic $[Pd(PPh_3)_2(OAc)]^-$ generated *in situ* from $Pd(OAc)_2$ and PPh_3 is proposed to be the species that adds haloarenes when the reaction is conducted in the presence of acetate.[25,26]

Studies on oxidative addition to complexes of bidentate ligands have also been conducted. The oxidative addition of aryl bromides to [Pd(bisphosphine)$_2$] (bisphosphine = 1,1'-bis(diphenylphosphino)ferrocene (DPPF), 2,2''-bis(diphenylphosphino-1,1'-binaphthyl) (BINAP)) occurred predominantly to Pd(bisphosphine), with a second pathway appearing to involve addition to [Pd(κ^2-bidentate)(κ^1-bidentate)].[31,32] Prior

studies on the oxidative addition of ArCl to $Pd(dippp)_2$ (dippp =bis(diisopropylphosphino)propane) showed that this reaction occurred to the 14-electron Pd(dippp) intermediate to form *cis*-(dippp)Pd(Ph)(Cl) as the main product. In the presence of free phosphine, this complex equilibrates with *trans*-(κ^1-dippp)$_2$Pd(Ph)(Cl).[28]

The identity of the halide in the haloarene could affect the mechanism of oxidative addition for a given ligand. Recently, we reported in communication form that the oxidative addition of iodo-, bromo-, and chlorobenzene to the Pd(0) complexes of Q-phos (Q-phos = pentaphenylferrocenyl di-*tert*-butylphosphine) occurs with three different kinetic behaviors.[21] Addition of PhI occurred by irreversible associative displacement of a phosphine; addition of PhBr occurred by rate-limiting dissociation of phosphine; and addition of PhCl occurred by reversible dissociation of phosphine, followed by rate-limiting oxidative addition.[21]

The diversity of these results from reactions of several complexes with various haloarenes under different reaction conditions illustrates the need for a systematic study of the factors that control the coordination number of the Pd(0) species that adds the haloarene. Thus, we have conducted such a study of the oxidative addition of iodo-, bromo-, and chlorobenzene to complexes of alkyl phosphines of varied size. This study has produced data that begin to clarify the effects of the halide in the haloarene and the effects of the size of the alkyl phosphine on the reaction mechanism. In brief, the number of phosphines coordinated to the complex that reacts in the irreversible step is more dependent on the identity of the halide than on the size of the cyclohexyl, *tert*-butyl, and 1-adamantyl phosphine ligands in this study.

The oxidative addition of PhX (X = I, Br, or Cl) to PdL_2 complexes **1-4** containing the trialkylphosphines P^tBu_3, 1-AdP^tBu_2, CyP^tBu_2, and PCy_3 were studied. Scheme 21 summarizes the Pd(0) complexes **1**–**4** and their reactions to form the arylpalladium halide products **5–19**. Although kinetic studies on the oxidative addition reactions show that the mechanism depends predominantly on the identity of the halide, the identity of the reaction products depended most strongly on the steric properties of the ligand. Thus, this section that describes the reactions and characterization of the products is organized by type of ligand.

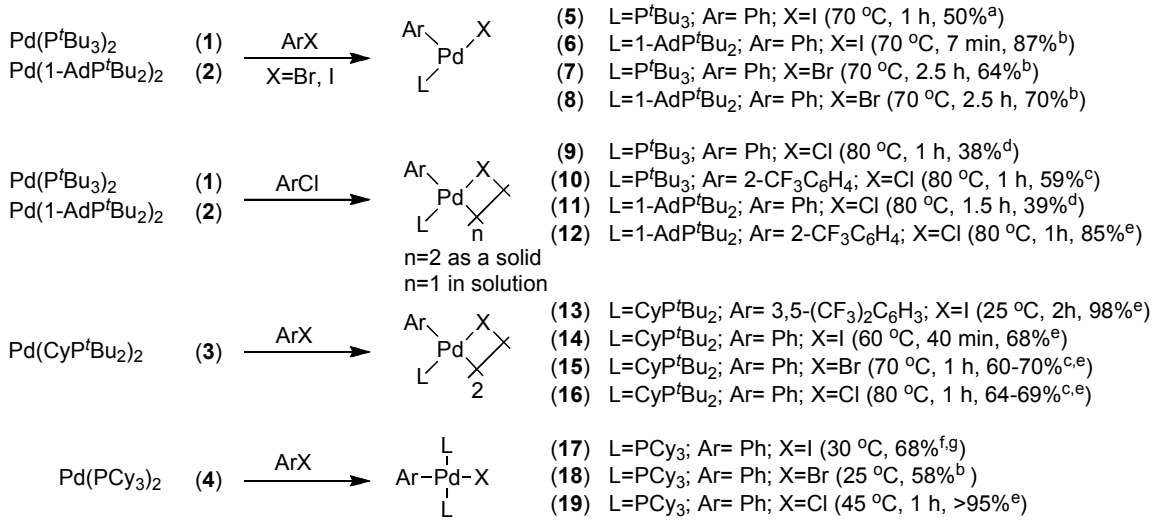

[a] see Ref. 22. [b] see Ref. 23. [c] see Supporting Information. [d] yield of product formed in situ, as determined by ^{31}P NMR spectroscopy, at 50% conversion. The yield decreased at longer reaction times. [e] yield of product formed in situ, as determined by ^{31}P NMR spectroscopy. [f] see Ref. 27. [g] see Ref. 39.

Scheme 21. Complexes formed by oxidative addition of different ArX to $L_2Pd(0)$.

2.1.1. Additions of ArX to complexes of P^tBu_3 and 1-AdP^tBu_2.

The reactions of PhI and PhBr with the Pd(0) complexes Pd(P^tBu_3)$_2$ (**1**) and Pd(1-AdP^tBu_2)$_2$ (**2**) has been shown to produce the known three-coordinate complexes **5**–**8** (Scheme 21) in 50 to 87% yield.[22,23] These complexes have been shown previously to be stabilized by a weak agostic interaction of the metal with a phosphine C–H bond positioned at the open coordination site.

In the current work, the reaction of **1** with 1-chloro-2-trifluoromethylbenzene occurred at 80 °C in 1 h to produce the stable [(P^tBu_3)Pd(2-$CF_3C_6H_4$)(Cl)]$_2$ (**10**) in 59% isolated yield (Scheme 21). Reaction of **2** with 1-chloro-2-trifluoromethylbenzene occurred at 80 °C in 1 h to produce [(1-AdP^tBu_2)Pd(2-$CF_3C_6H_4$)(Cl)]$_2$ (**12**) in 85% yield as determined by ^{31}P NMR spectroscopy. Complex **12** was isolated in 39% yield after reaction for 20 min at 100 °C and subsequent recrystallization. The reaction of **1** and **2** in neat PhCl at 80 °C formed [LPd(Ph)(Cl)]$_2$ (**9**, L = P^tBu_3 and **11**, L = 1-AdP^tBu_2), but the yield of the oxidative addition product at full conversion was low due to decomposition of the oxidative addition product. The yield of the oxidative addition products at 50% conversion was high (about 80% with respect to the amount of reacted Pd(0) species), but at higher conversions the arylpalladium halide products decayed.

Thus, phenylpalladium chloride complexes **9** and **11** were characterized after preparing them independently (Scheme 22). P^tBu_3-ligated complex **9** was isolated in 42% yield from the reaction of (Py)$_2$Pd(Ph)(Cl) (**20**) with P^tBu_3 in toluene solvent under dynamic vacuum to evaporate the liberated pyridine. 1-AdP^tBu_2-ligated **11** was isolated in 86% yield from the reaction of N(octyl)$_4$Cl with the known

(1-AdP^tBu_2)Pd(Ph)(CF_3SO_3),[37] which was obtained by the previously reported reaction of (1-AdP^tBu_2)Pd(Ph)(Br) (**8**) with AgOTf.[23]

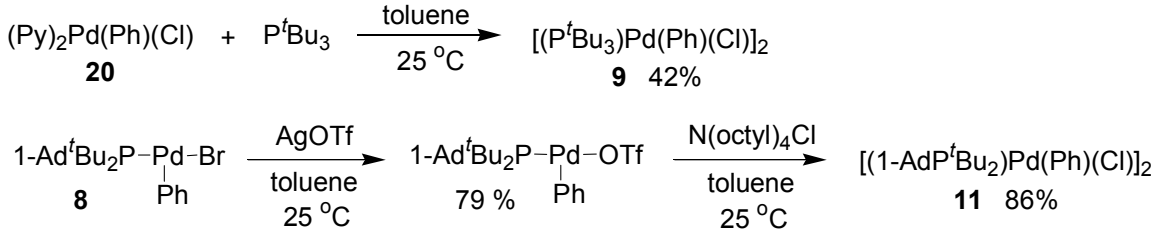

Scheme 22. Routes for the synthesis of chloride complexes [(P^tBu_3)Pd(Ph)(Cl)]$_2$ (**9**) and [(1-AdP^tBu_2)Pd(Ph)(Cl)]$_2$ (**11**).

The nuclearity of the arylpalladium chloride complexes **10** and **11** depended on the phase. Our data indicate that both complexes are dimeric in the solid state and contain two bridging chlorides but are predominantly monomeric in solution. The solid-state structures of P^tBu_3-ligated, 2-$CF_3C_6H_4$-complex **10** and 1-AdP^tBu_2-ligated, phenyl-complex **11** are shown in Figure 6. In this state, complex **10** contains two palladium atoms that are bridged nearly symmetrically by two μ^2-chloride ligands. The two aryl groups are located *anti* to each other. The Pd–Cl bond distances range from 2.39 to 2.49 Å, and the two palladium atoms are separated by 3.61 Å. The Pd coordination planes intersect at an angle of 145.6°. The structure of **11** also contains two palladium atoms that are bridged by two μ^2-chloride ligands, but the two aryl groups are *syn* to each other. In this case, the Pd–Cl(1) distances are shorter than the Pd–Cl(2) distances by about 0.1 Å, possibly caused by the steric congestion of the phosphines and the larger trans influence of the aryl groups located trans to Cl(1) than of the phosphines located trans to Cl(2). The

two palladium atoms are separated by a longer distance of 3.78 Å, and the two coordination planes intersect at an angle of 166.3°.

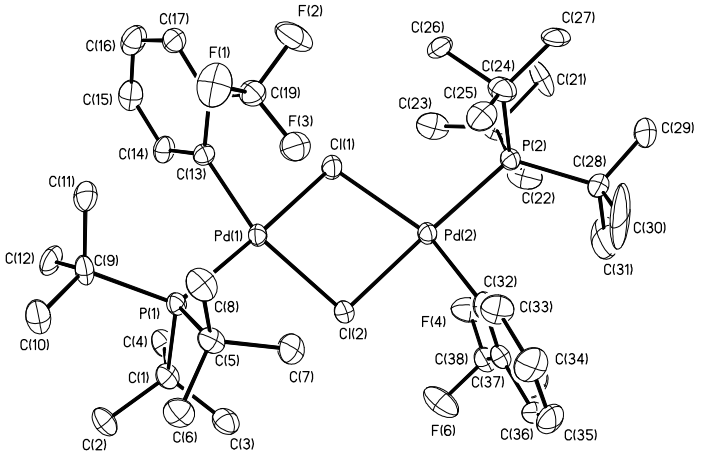

Figure 6a. ORTEP diagram of $[(P^tBu_3)Pd(2\text{-}CF_3C_6H_4)(Cl)]_2$ (**10**).

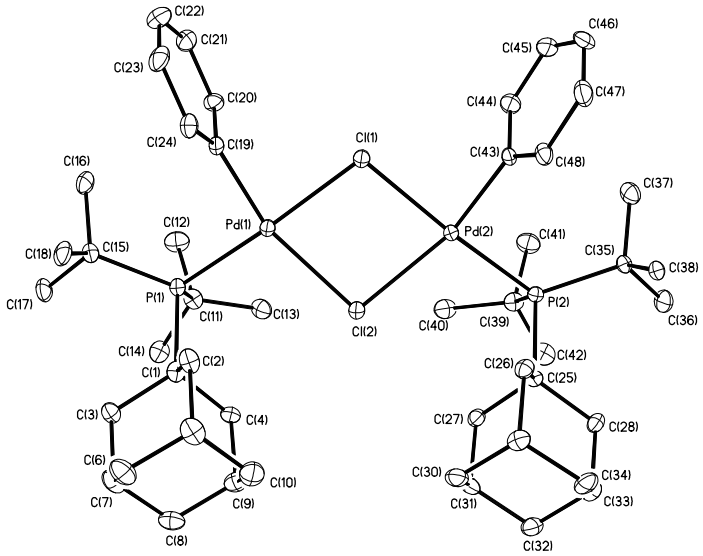

Figure 6b. ORTEP diagram of $[(1\text{-}AdP^tBu_2)Pd(Ph)(Cl)]_2$ (**11**).

Solution molecular weight and NMR spectroscopic data indicate that the tri-*tert*-alkylphosphine-ligated arylpalladium chloride complexes **9-11** are monomeric in solution. The molecular weight measurements by the Signer method[38] on the more stable complex **10**, provided measurements of 530 g/mol in THF and 505 g/mol in benzene. These values are closer to the calculated molecular weight of the monomer (489.29 g/mol) than to that of the dimer (978.29 g/mol). The ^{31}P NMR chemical shift of the arylpalladium chloride complexes **9-11** were similar, and ranged from 69–73 ppm. These chemical shifts are expected for a monomeric species, based on the chemical shifts of the monomeric arylpalladium bromide (60–65 ppm) and iodide (55–60 ppm) complexes. Thus, the spectroscopic and solution molecular weight data together provide evidence that **9** and **11** possess the same monomeric structure shown clearly for **10** in solution. The nuclearity of these species, however, do not affect our conclusions about the mechanism of oxidative addition because the steps that control a monomer-dimer equilibrium occur after the rate-limiting steps.

2.1.2. Additions of ArX to Complexes of the Less Hindered CyP^{t}Bu$_2$ and PCy$_3$.

The reactions of Pd(CyP^{t}Bu$_2$)$_2$ (**3**) with 3,5-(CF$_3$)$_2$C$_6$H$_3$I and PhI at 25 and 60 °C, respectively, produced the dimeric arylpalladium halide complexes [(CyP^{t}Bu$_2$)Pd(Ar)(I)]$_2$ (Ar = 3,5-(CF$_3$)$_2$C$_6$H$_3$, **13**; Ar = Ph, **14**)[27] in 98% and 68% yields, as determined by ^{31}P NMR spectroscopy. Complex **3** reacted with PhBr and PhCl over 1 h at 70 and 80 °C to produce the analogous bromide (**15**) and chloride (**16**) dimers in 70% and 64% yield. The complex Pd(PCy$_3$)$_2$ (**4**) reacted with PhI, PhBr, and PhCl at 25 °C to 45 °C to produce the known stable *trans* four-coordinate complexes **17**[27,39], **18**[23] and **19.**[40,41] These reactions

occurred in high yield, as determined by ^{31}P NMR spectroscopy; isolated yields depended on the solubility and crystallinity of the products.

The nuclearity of CyP^{t}Bu$_2$-ligated **15** was determined by X-ray crystallography (Figure 7) and Signer solution molecular weight analysis. In the solid state, the complex contains two bridging μ^2-bromide ligands and *syn* aryl groups. The core contains acute Br–Pd–Br angles of 82.79 and 82.53°, and the Pd coordination planes intersect at an angle of 20.7°. The Pd–Br(1) distances are longer than the Pd–Br(2) distances by about 0.1 Å, possibly because of the steric bulk the phosphines and the large trans influence of the aryl moiety.

This complex **15** appears to dissociate to predominantly a monomeric species in solution. The molecular weight in THF as determined by the Signer method was 523 g/mol. This value is close to the 491.78 molecular weight of the monomer. Considering that the nuclearity of (1-AdP^{t}Bu$_2$)-complex **10** was the same in THF and benzene by the Signer molecular weight measurement, that neither THF nor benzene coordinates to the metal center in either structure, and that the ^{31}P NMR chemical shifts in these two solvents for this class of compound have generally been nearly identical, we assert that complex **15** is predominantly monomeric in solution.

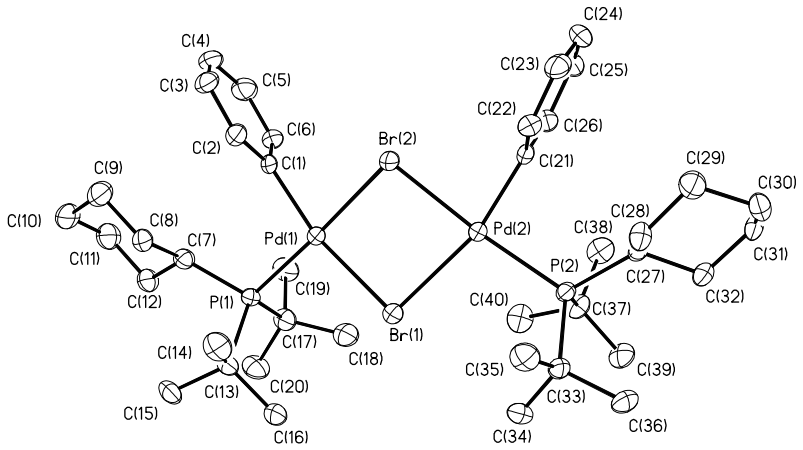

Figure 7. ORTEP of the complex $[(CyP^tBu_2)Pd(Ph)(Br)]_2$ (**15**).

2.2 Kinetic Studies

2.2.1 General Considerations

The rates of oxidative addition of PhX (X = I, Br, Cl) to $Pd(0)L_2$ complexes were measured for complexes containing the bulky trialkylphosphines P^tBu_3, 1-AdP^tBu_2, CyP^tBu_2, and PCy_3. The mechanism of the oxidative addition depended largely on the identity of the halide. For this reason, the kinetic data are presented according to the type of haloarene undergoing reaction with the palladium(0) complexes. The data on the oxidative addition of iodoarenes and chloroarenes are simplest to interpret and are presented first. Our kinetic data on these reactions are plotted as the reciprocal of the rate constants to fit with the typical linear equations corresponding to reactions occurring through a pre-equilibrium, followed by an irreversible step. The data on the additions to bromoarenes are more complex. These data were treated in several ways and suggest that the additions occur in some cases by a combination of mechanisms.

The LPd(Ph)(X) products from oxidative addition of PhBr and PhCl to $Pd(P^tBu_3)_2$ (**1**) and $Pd(1\text{-}AdP^tBu_2)_2$ (**2**) were unstable at the temperatures of oxidative addition, leading to decomposition by cyclometallation at the phosphine to form L·HX as side product. This phosphonium salt has been shown to accelerate the rate of oxidative addition of aryl bromides.[42] Because this autocatalysis has been shown to be suppressed by conducting reactions in the presence of the hindered phosphazene base *tert*-butylimino-trispyrrolidino phosphorane (**BTPP**),[42] the rate constants for oxidative addition of PhBr and PhCl to **2** were obtained on reactions containing 30 to 60 mol% of phosphazene base. Because the addition of PhI to **1** and **2** occurred at lower temperatures than those that lead to the cyclometallation process, the oxidative addition of PhI occurs with an exponential decay of the starting Pd(0) complexes without autocatalysis in the presence or absence of phosphazene base.

Before presenting data on the kinetics of oxidative addition to PCy_3 complex **4**, comments on the coordination chemistry of this Pd(0) species are warranted. Spectroscopic studies show that the combination of PCy_3 and **4** generates an equilibrium mixture of **4**, free ligand, and the trisphosphine complex $Pd(PCy_3)_3$.[43-45] The ^{31}P NMR spectra of a solution consisting of **4** and 2 equiv. of PCy_3 obtained between 20 and −40 °C contained two broad signals (δ 39 and 10 ppm) that corresponded to **4** and free PCy_3. At lower temperatures (−60 °C to −80 °C), a sharp signal for $Pd(PCy_3)_3$ at 26 ppm and a sharp signal for the remaining PCy_3 were observed. Thus, the $Pd(PCy_3)_2$ complex coordinates a third phosphine at low temperatures.

2.2.2. Kinetic Studies of the Oxidative Addition of Phenyl Iodide.

Kinetic studies were conducted on the oxidative addition of iodobenzene to Pd(0) complexes **1**–**4**. In all cases, the rate constants were measured by ^{31}P NMR spectroscopy. The rate constants for reactions of complexes **1**–**3** were obtained from the decay of the starting Pd(0) species. Because signals of PCy_3-ligated **4** were broad in the presence of added PCy_3, the rate constants for reaction of this complex were determined from the appearance of the oxidative addition product. The decay of complexes **1**–**3** and the appearance of product from reaction of **4** were clearly exponential with time, and the products were stable, except for the product ligated by P^tBu_3. Some of the arylpalladium iodide complex ligated by P^tBu_3 decomposed to form the iodo-bridged Pd(I) dimer $[(P^tBu_3)Pd(\mu\text{-}I)]_2$,[27] but this subsequent process did not affect the decay of P(t-Bu)$_3$ complex **1**. Although autocatalysis was not observed for reactions of iodoarenes, the reaction of 1-AdP^tBu_2 complex **2** with PhI was carried out in the presence of 30 mol% phosphazene to be consistent with the reactions of **2** with PhBr and with ArCl.

*2.2.2.1. Kinetic Studies of the Oxidative Addition of Iodobenzene to P^tBu_3 Complex **1**.*

The rate constants for oxidative addition of PhI to P^tBu_3-ligated **1** to produce complex **5** were measured on reactions in toluene solvent at 70 °C. A plot of these $1/k_{obs}$ vs 1/[PhI] for varied concentration of PhI is shown in Figure 8 (left) and indicates that the reaction is first-order in PhI. However, the observed rate constant did not change significantly as a function of $[P^tBu_3]$ (Figure 8, right); the average observed rate constant over the concentration range of phosphine was $k_{obs} = 1.3 \pm 0.2 \times 10^{-3}$ s^{-1}.

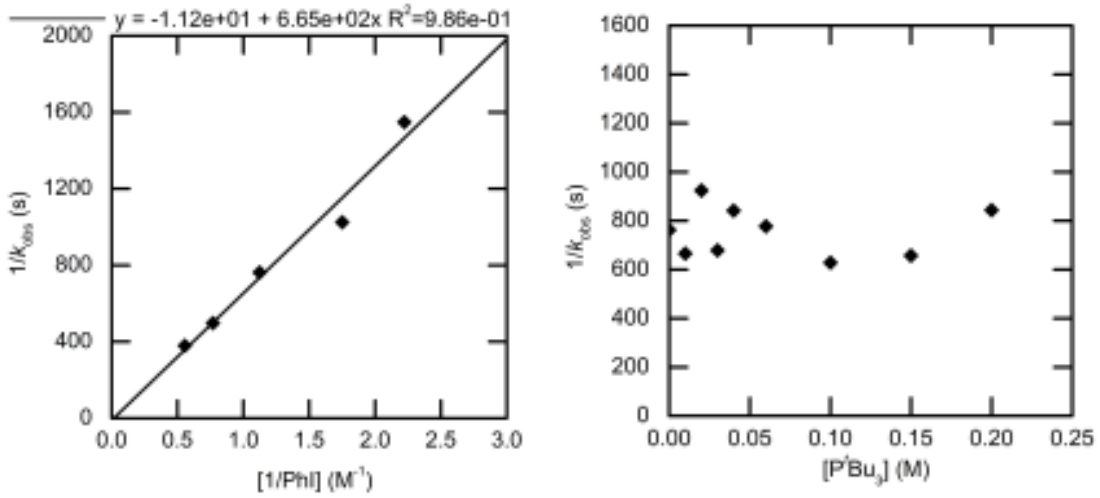

Figure 8. Dependence of the observed rate constant on the concentration of PhI (0.45–1.8 M) with no added P^tBu_3 (left) and on the concentration of P^tBu_3 (0-0.20 M) for the oxidative addition of PhI (0.90 M) (right) to $Pd(P^tBu_3)_2$ (**1**) (0.040 M) in chlorobenzene at 70 °C.

*2.2.2.2. Kinetic Studies of the Oxidative Addition of Iodobenzene to 1-AdP^tBu_2-Ligated **2**.*

The rate constants for the oxidative addition of PhI to 1-AdP^tBu_2-ligated **2** to form arylpalladium iodide complex **6** were measured in chlorobenzene at 50 °C. The orders for this reaction were similar to those for the oxidative addition of PhI to **1**. The plot of $1/k_{obs}$ vs 1/[PhI] with varied [PhI] shown in Figure 9 (left) indicates that the reaction is first order in PhI. Like the rate constants for the reaction of PhI with the P^tBu_3-ligated **1**, the rate constants for addition to **2** did not change significantly when varying [1-AdP^tBu_2] (Figure 9, right); the average observed rate constant for reactions conducted with this range of phosphine concentration was $3.4 \pm 0.4 \times 10^{-4}$ s^{-1}.

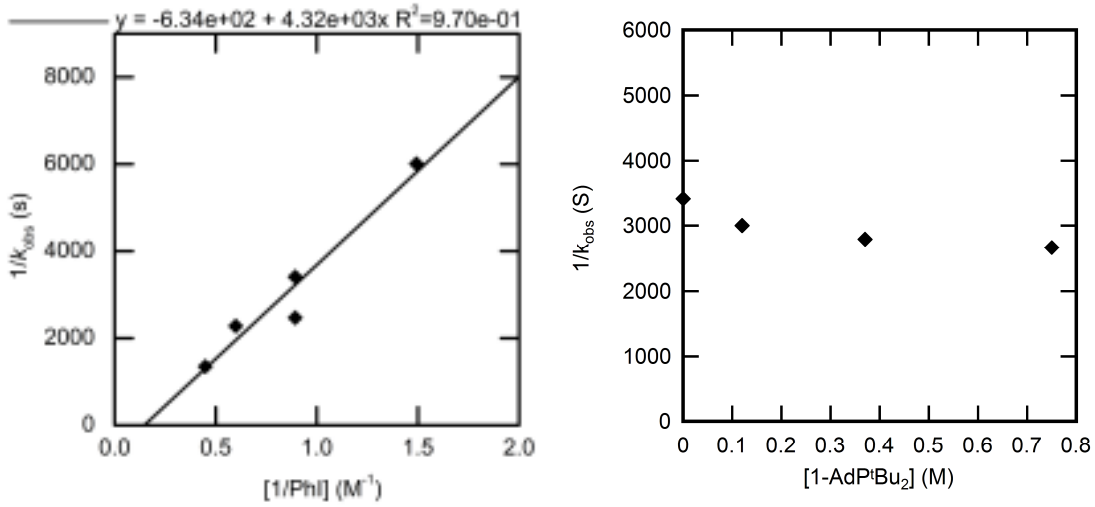

Figure 9. Dependence of the observed rate constant on the concentration of PhI (0.67–2.2 M) with no added 1-AdP^{t}Bu$_2$ (left) and on the concentration of 1-AdP^{t}Bu$_2$ (0-0.75 M) for the oxidative addition of PhI (1.1 M) (right) to Pd(1-AdP^{t}Bu$_2$)$_2$ (**2**) (0.025 M) in chlorobenzene at 50 °C.

*2.2.2.3. Kinetic Studies of Oxidative Addition of Iodoarenes to CyP^{t}Bu$_2$-Ligated **3**.*

The rate constants of the oxidative addition of PhI to CyP^{t}Bu$_2$-ligated **3** to form phenylpalladium iodide complex **14** were measured in toluene at 50 °C. A plot of $1/k_{obs}$ vs 1/[PhI] is provided in Figure 10 (left); these data show that the reaction is first order in PhI. The reaction rate did not depend significantly on the concentration of ligand, as shown in Figure 10 (right); the average observed rate constant for reactions conducted with this range of phosphine concentration was $k_{obs} = 1.1 \pm 0.1 \times 10^{-3}$ s^{-1}. These data do not agree with previously published work,[27] which stated that doubling the concentration of ligand decreased the rate of oxidative addition of 1-iodo-3,5-bistrifluoromethylbenzene by a factor of two. Thus, we investigated more closely the oxidative addition of haloarenes to CyP^{t}Bu$_2$-ligated **3**.

The rate constants for the oxidative addition of 1-iodo-3,5-bistrifluoromethylbenzene to CyP^tBu_2-ligated **3** to form arylpalladium iodide complex **13** were measured at 25 °C in benzene with concentrations [**3**] = 0.036 M, [ArI] = 0.36 M, and concentrations of [CyP^tBu_2] ranging from 0–1.8 M. These substrates and conditions are identical to those reported previously.[27] In contrast to the published data, the rate of the reaction was only slightly affected by the presence of excess ligand; the average value for k_{obs} was 6.1 ± 0.6 × 10^{-4} s^{-1}. We do not have an explanation for the difference between the previously published data and the data we report in this paper; however, the previous reactions were monitored to only two half-lives, and reactions at only two different concentrations of ligand were reported.

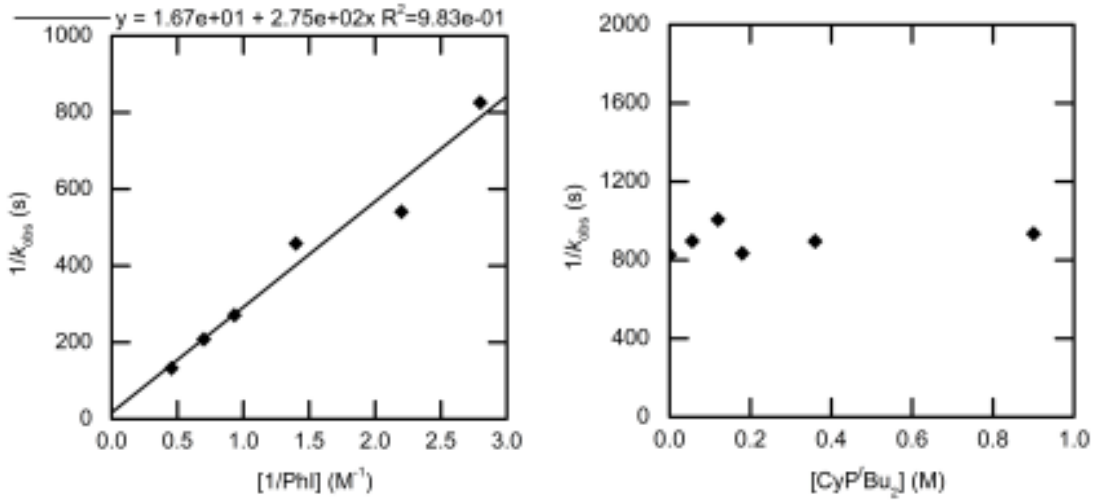

Figure 10. Dependence of the observed rate constant on the concentration of PhI (0.36–1.4 M) with no added CyP^tBu_2 in toluene at 50 °C (left) and on the concentration of CyP^tBu_2 (0-0.90 M) for the oxidative addition of PhI (0.36 M) in toluene at 50 °C to Pd(CyP^tBu_2)$_2$ (**3**) (0.036 M).

*2.2.2.4. Kinetic Studies of the Oxidative Addition of Iodobenzene to PCy_3-Ligated **4**.*

The reactions of PCy_3-ligated **4** with PhI occurred to form phenylpalladium iodide complex **17** within minutes at room temperature. Thus, kinetic data on these oxidative additions were obtained on reactions conducted at −80 °C. Three series of reactions with iodobenzene were conducted, the first with varied [PhI], the second with [PCy_3] ranging from 0.030–0.12, and the third with [PCy_3] ranging from a lower 0.61–6.1 mM.. The inverse of the rate constants for oxidative addition of PhI to the combination of **4** and PCy_3 with varied [PhI] and [PCy_3] are shown in Figure 11. These data show that the reaction is first order in PhI and inverse first order in PCy_3 when concentration of ligand is high. As noted in detail in the introduction to this section, the trisphosphine-ligated Pd(0) is the major species in the presence of more than 0.030 M added PCy_3 at −80 °C. Thus, this plot corresponds to data and rate expressions when the starting complex is the [$Pd(PCy_3)_3$] complex,[46] and the inverse order in PCy_3 indicates reversible dissociation of PCy_3 from $Pd(PCy_3)_3$ prior to carbon-halogen bond cleavage. At low concentrations of added ligand, the major species observed in solution at −80 °C is $Pd(PCy_3)_2$ (**4**). Under these conditions, the rate of the reaction was zeroth order in added ligand; the average observed rate constant was $9.8 \pm 0.1 \times 10^{-4}$ s^{-1}.

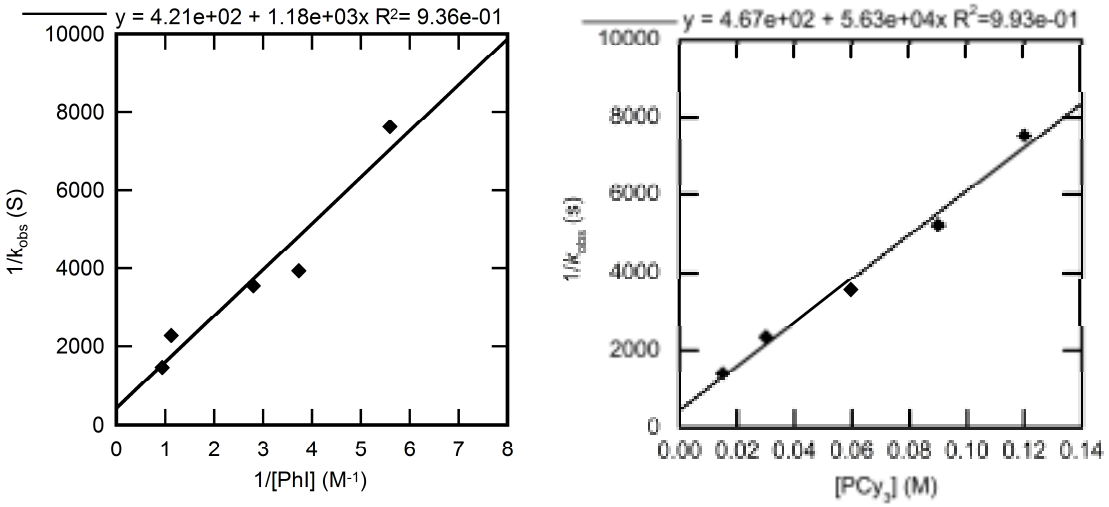

Figure 11. Dependence of the observed rate constant on the concentration of PhI (0.18–1.1 M) with [PCy_3] = 0.056 M (left) and on the concentration of PCy_3 (0.03-0.12 M) for the oxidative addition of PhI (0.36 M) (right) to $Pd(PCy_3)_3$ (**4**) (0.020 M) in toluene at −80 °C.

2.2.3. Kinetic Studies of Oxidative Addition of Chloroarenes.

Kinetic studies on the oxidative addition of chloroarene to Pd(1-AdP^tBu_2)$_2$ (**2**) were conducted with 2-$CF_3C_6H_4Cl$ because it formed a more stable arylpalladium chloride complex than did PhCl. These reactions were conducted in the presence of added phosphazene base to avoid potential autocatalysis by the side products from decomposition of the arylpalladium chloride complex. They were also conducted with higher concentrations of haloarene than the reactions of bromoarenes and iodoarenes to improve the reaction yields that are affected by product decomposition.[47] The decay of **2** was measured by ^{31}P NMR spectroscopy.

*2.2.3.1. Kinetic Studies of Oxidative Addition of 2-$CF_3C_6H_4Cl$ to 1-AdP^tBu_2-Ligated **2**.*

The rate constants for reactions of 2-$CF_3C_6H_4Cl$ with 1-AdP^tBu_2-ligated **2** to form arylpalladium chloride complex **12** were measured in toluene or neat ArCl at 100 °C in

the presence of 0.015 M (60 mol %) phosphazene base (BTPP). The decay of **2** was exponential, showing that the additions of ArCl are first order in the palladium(0) complex. The plots of $1/k_{obs}$ with varied [ArCl] and [1-AdP^{t}Bu$_2$] are shown in Figure 12. The plot of $1/k_{obs}$ vs 1/[ArCl] revealed a positive dependence of k_{obs} on chloroarene. The plot of $1/k_{obs}$ vs [1-AdP^{t}Bu$_2$] showed an inverse dependence of k_{obs} on [1-AdP^{t}Bu$_2$], although this dependence was not simply inverse first order.

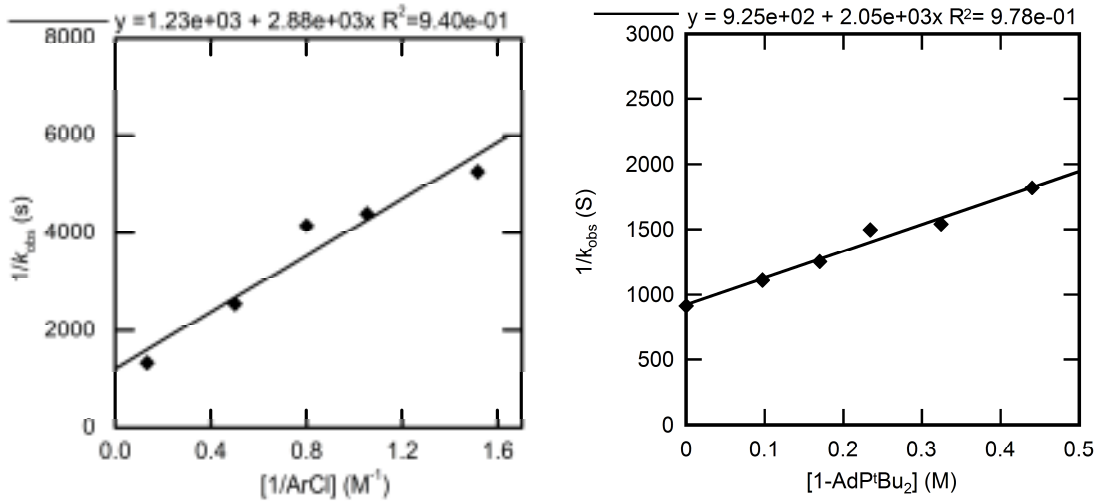

Figure 12. Dependence of the observed rate constant on the concentration of 2-$CF_3C_6H_4Cl$ (0.54–7.2 M) with [1-AdP^{t}Bu$_2$] = 0.17 M (left) and on the concentration of 1-AdP^{t}Bu$_2$ (0-0.44 M) for the oxidative addition of 2-$CF_3C_6H_4Cl$ (7.6 M) (right) to Pd(1-AdP^{t}Bu$_2$)$_2$ (**2**) (0.025 M) in toluene at 100 °C.

*2.2.3.2. Kinetic Studies of Oxidative Addition of Chlorobenzene to CyP^{t}Bu$_2$-Ligated **3**.*

The rate constants for the oxidative addition of PhCl to CyP^{t}Bu$_2$-ligated **3** to form phenylpalladium chloride complex **16** were measured in toluene at 100 °C in the absence of any added base. The plots of $1/k_{obs}$ measured with varied [PhCl] and [CyP^{t}Bu$_2$] are shown in Figure 13. The plot of $1/k_{obs}$ vs 1/[PhCl] revealed a positive dependence of k_{obs}

on chlorobenzene. The plot of $1/k_{obs}$ vs [CyP^{t}Bu$_2$] revealed an inverse dependence of k_{obs} on the concentration of ligand.

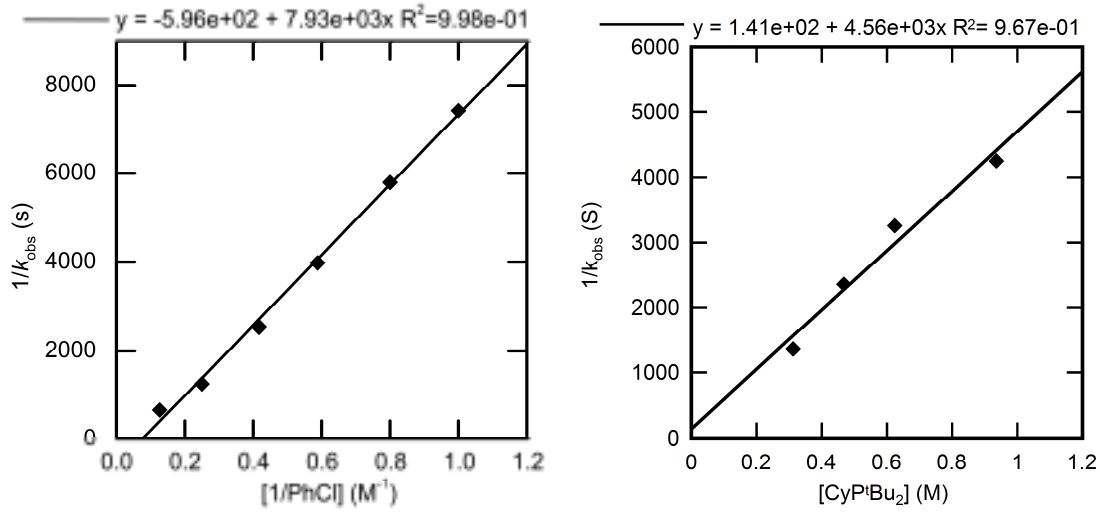

Figure 13. Dependence of the observed rate constant on the concentration of chlorobenzene (1.0–7.9 M) with [CyP^{t}Bu$_2$] = 0.32 M (left) and on the concentration of CyP^{t}Bu$_2$ (0.32-0.94 M) for the oxidative addition of chlorobenzene (5.9 M) (right) to Pd(CyP^{t}Bu$_2$)$_2$ (**3**) (0.036 M) in toluene at 100 °C.

*2.2.3.3. Kinetic Studies of Oxidative Addition of Chlorobenzene to PCy$_3$-Ligated **4**.*

The rate constants for reactions of PCy$_3$-ligated **4** with chlorobenzene to form complex **19** were measured in toluene at 70 °C. At the concentrations of [PCy$_3$] investigated and the 70 °C temperature of the reaction, the starting Pd(0) species is the two-coordinate complex **4**. The plots of $1/k_{obs}$ obtained with varied [PhCl] and [PCy$_3$] are shown in Figure 14 and are similar to the analogous plots for the additions of PhCl to 1-AdP^{t}Bu$_2$-ligated **2** and CyP^{t}Bu$_2$-ligated **3**. The plot of $1/k_{obs}$ vs 1/[PhCl] revealed a

positive dependence of k_{obs} on chloroarene; the plot of $1/k_{obs}$ vs [PCy_3] revealed an inverse dependence of k_{obs} on the concentration of ligand.

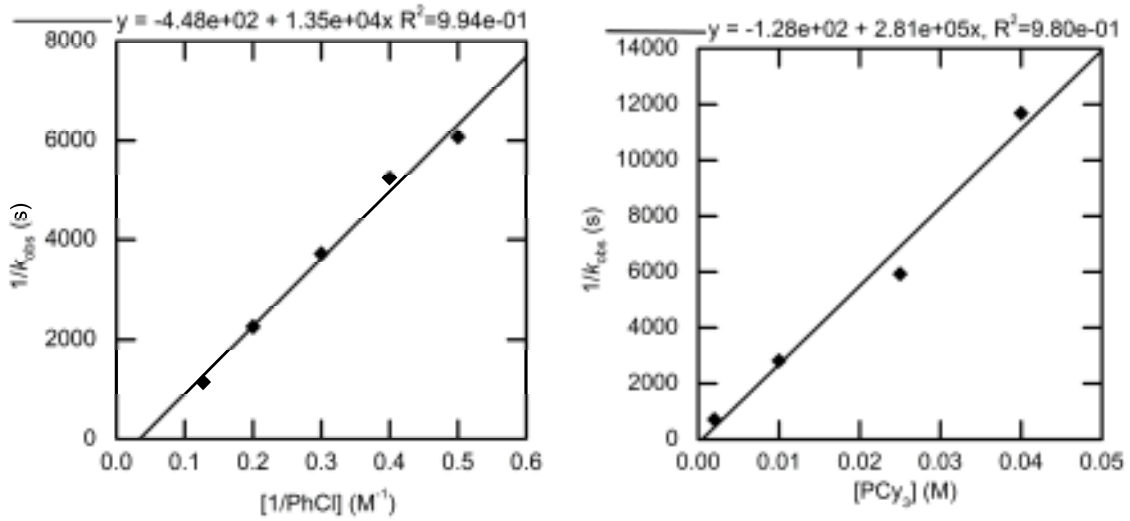

Figure 14. Dependence of the observed rate constant on the concentration of chlorobenzene (2.0–7.9 M) with [PCy_3] = 0.009 M (left) and on the concentration of PCy_3 (0.002-0.040 M) for the oxidative addition of chlorobenzene (3.9 M) (right) to $Pd(PCy_3)_2$ (**4**) (0.019 M) in toluene at 70 °C. Data for [PhCl] = 2.5, 3.3 M (left) are an average value from 2-3 runs.

2.2.4. Kinetic Studies of Oxidative Addition of Bromobenzene.

As noted in section 2.1 and in published work,[42] the arylpalladium bromide product from oxidative addition of bromobenzene to P^{t}Bu$_3$-ligated **1** is unstable at elevated temperatures for extended times and undergoes cyclometallation to generate L•HBr. To avoid the problems associated with the generation of the phosphonium salt, the rate constants for oxidative addition of PhBr to **1** and **2** were measured in the presence of phosphazene base. Moreover, we focused on the oxidative addition of PhBr to 1-AdP^{t}Bu$_2$-ligated **2** because the oxidative addition product (1-AdP^{t}Bu$_2$)Pd(Ph)(Br) (**8**)

was sufficiently stable to form in >90 % yield in the presence of the phosphazene base. In contrast, the reactions of CyP^tBu_2-ligated **3** and PCy_3-ligated **4** occurred in high yield and with an exponential decay of the Pd(0) complex in the absence of any added base. Thus, the additions of PhBr to **3** and **4** were conducted in the absence of base.

*2.2.4.1. Kinetic Studies of Oxidative Addition of Bromobenzene to 1-AdP^tBu_2-Ligated **2**.*

The reaction of PhBr with 1-AdP^tBu_2-ligated **2** to form phenylpalladium bromide complex **8** was studied at 90 °C. The reactions were conducted in the presence of 0.015 M (60 mol %) added phosphazene. A clear exponential decay of **2** was observed under these conditions. Thus, the additions of PhBr are first order in the Pd(0) complex. The kinetic data on the effect of the concentration of arene on the rate constant for oxidative addition of PhBr are plotted as k_{obs} vs [PhBr]. This plot allows us to assess the potential that two mechanisms contribute to the observed rate constant. When such a plot is linear with a y-intercept, the double reciprocal plots shown for data on the oxidative addition of ArCl and ArI are nonlinear. Conversely, when the double reciprocal plot has a clear, non-zero y-intercept, the direct plot is curved.

The plot of k_{obs} vs [PhBr] (Figure 15, left) was linear with a positive slope and non-zero intercept. Moreover, the rate constant for this oxidative addition to 1-AdP^tBu_2-ligated **2** did not depend on the concentration of ligand at high or low concentration of bromobenzene. The plot of the dependence of k_{obs} on [1-AdP^tBu_2] is shown in Figure 15 (right) and shows the observed rate constant was independent of the concentration of added ligand (average $k_{obs} = 6.2 \pm 1.2 \times 10^{-4}$ s^{-1}). The data at high concentration of PhBr contained some deviation, yet a change in [1-AdP^tBu_2] by a factor of four led to a

variation in rate by less than a factor of two. Additionally, when [PhBr] = 2.5 M and [1-AdP^{t}Bu$_2$] ranged from 0.10-0.50 M, the value of k_{obs} varied by only 10-15% (2.5 ± 0.3 × 10^{-4} s^{-1}). As described in the discussion section, these data suggest that two mechanisms for oxidative addition of bromoarenes occur simultaneously.

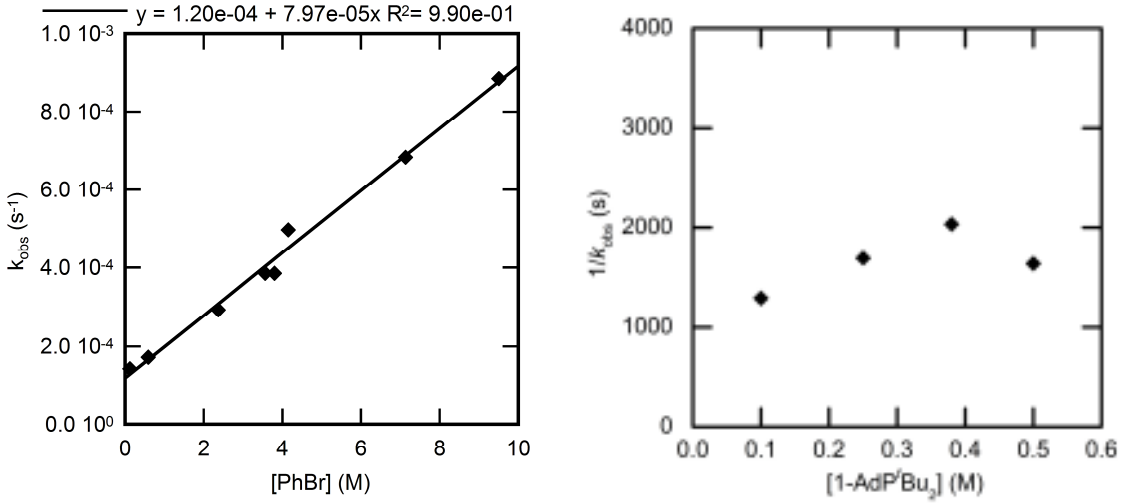

Figure 15. Dependence of the observed rate constant on the concentration of PhBr (0.12–9.5 M) with no added 1-AdP^{t}Bu$_2$ (left) and on the concentration of 1-AdP^{t}Bu$_2$ (0.10-0.50 M) for the oxidative addition of PhBr (8.5 M) (right) to Pd(1-AdP^{t}Bu$_2$)$_2$ (**2**) (0.025 M) in toluene at 90 °C.

*2.2.4.2. Kinetic Studies of Oxidative Addition of Bromobenzene to CyP^{t}Bu$_2$-Ligated **3**.*

The rate constants for the reaction of *CyP^{t}Bu$_2$-ligated* **3** with PhBr to form phenylpalladium bromide complex **15** were measured in toluene at 70 °C. The plots of these data are shown in Figure 16. The observed rate constant depended positively on the concentration of bromoarene. Again, the plot of k_{obs} vs [PhBr] contained a non-zero y-intercept. In contrast, the observed rate constant was independent of the concentration of added ligand; the average observed rate constant was 7.1 ± 0.7 × 10^{-4} s^{-1}.

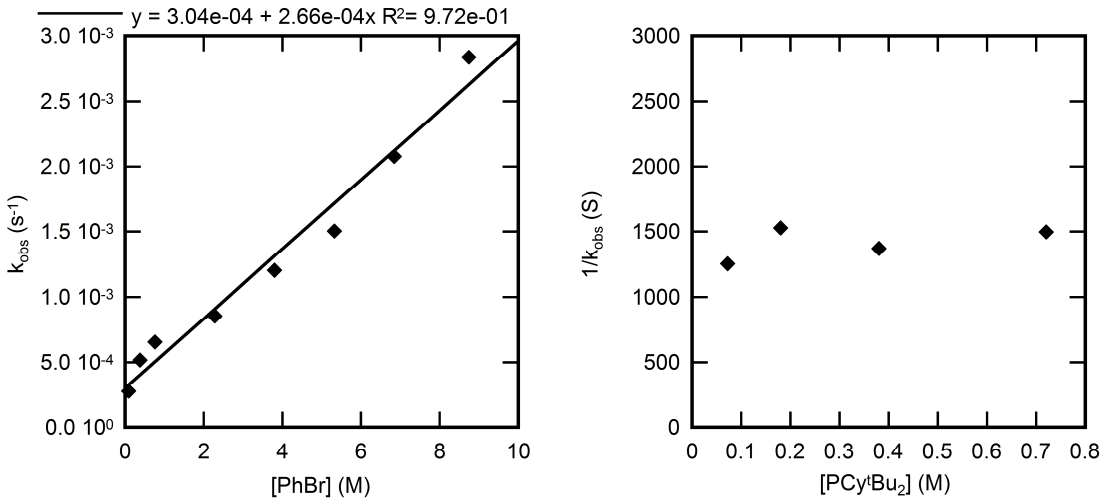

Figure 16. Dependence of the observed rate constant on the concentration of PhBr (0.09-8.7 M) with [CyP^{t}Bu$_2$] = 0.32 M (left) and on the concentration of CyP^{t}Bu$_2$ (0.07-0.72 M) for the oxidative addition of PhBr (1.5 M) (right) to Pd(CyP^{t}Bu$_2$)$_2$ (**3**) (0.036 M) in toluene at 70 °C.

*2.2.4.3. Kinetic Studies of Oxidative Addition of Bromobenzene to PCy$_3$-Ligated **4**.*

The rate constants for reactions of *PCy$_3$*-ligated **4** with bromobenzene to form arylpalladium bromide complex **18** were measured in toluene at 10 °C. The plots of these data are shown in Figure 17. These plots reveal a positive dependence of k_{obs} on [ArBr] and a nearly zeroth-order dependence on [PCy$_3$]. A change in the concentration of PCy$_3$ by a factor of six led to a decrease in rate constant by less than a factor of two.

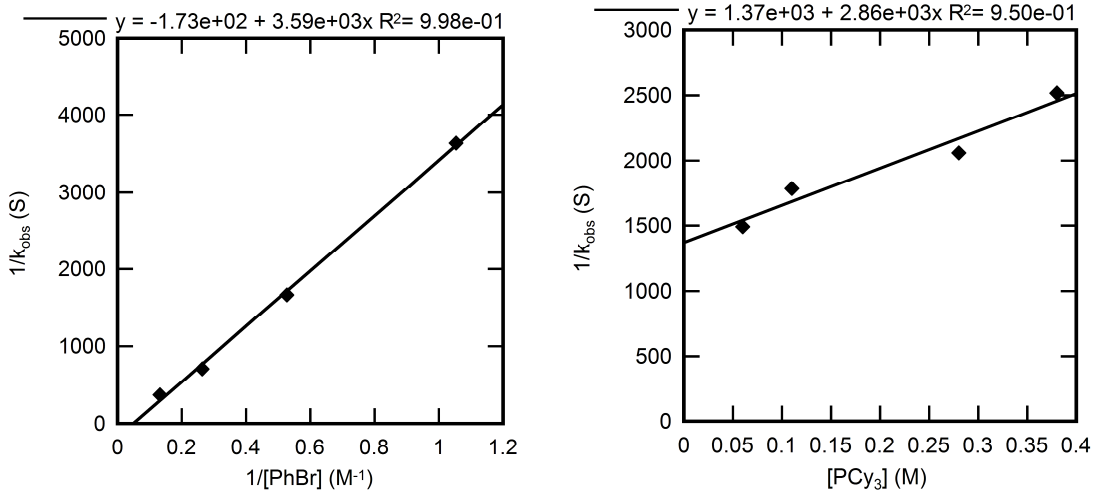

Figure 17. Dependence of the observed rate constant on the concentration of PhBr (0.95–7.6 M) with [PCy_3] = 0.19 M (left) and on the concentration of PCy_3 (0.060-0.38 M) for the oxidative addition of PhBr (1.9 M) (right) to $Pd(PCy_3)_3$ (**4**) (0.019 M) in toluene at 10 °C.

2.3 Discussion

2.3.1 Structures of the Palladium and Arylpalladium Halide Reactants and Products.

The most stable Pd(0) complexes of the bulky phosphines P^tBu_3,[48] 1-AdP^tBu_2[22] and CyP^tBu_2[27] are the bisphosphine complexes PdL_2.[49] In contrast, the most stable Pd(0) complex of PCy_3 depended on the temperature and the concentration of added PCy_3. At temperatures below −70 °C with [PCy_3] < 0.03 M, the complexes $Pd(PCy_3)_3$ and bis ligated $Pd(PCy_3)_2$ were observed by ^{31}P NMR spectroscopy.[18] At the same temperature with [PCy_3] > 0.03 M, the trisphosphine complex $Pd(PCy_3)_3$ was the only Pd(0) complex observed. At room temperature or above, the signals due to the free and coordinated ligand are broad due to exchange on the NMR time scale, but the bisphosphine complex $Pd(PCy_3)_2$ is the major Pd(0) species present.

The identities of some of the oxidative addition products have been published. The product from addition of PhX (X= Cl, Br, I) to the Pd(0) complex of PCy_3 are bisphosphine, four-coordinate species,[23,27,39-41] but the products from addition of ArX to complexes of the more hindered ligands contain a single ligand and are either dimeric with bridging halides[27] or monomeric.[22,23] Further, the structure of the arylpalladium halide complexes depended in some cases on the identity of the halide.[21] For example, the arylpalladium bromide and iodide complexes containing the ligands P^tBu_3 and 1-AdP^tBu_2 are monomeric three-coordinate complexes, while the arylpalladium chloride complexes are mainly monomers in solution and dimers in the solid state. The kinetic data analyzed in the following sections show that the reactant and product structures do not correlate with either the coordination number of the species undergoing oxidative addition or the initial product formed by oxidative addition in many cases.

2.3.2 Potential Mechanisms for Oxidative Addition.

Three possible mechanisms were considered for the oxidative addition of ArX to the palladium complexes $L_2Pd(0)$. In the first mechanism, oxidative addition would take place by direct reaction of ArX with the starting bisphosphine complex $L_2Pd(0)$ to form a four-coordinate arylpalladium halide complex. This addition would be followed in some cases by dissociation of ligand and subsequent dimerization, depending on the phosphine or haloarene used. The rate of reaction by this pathway would be first order in the concentration of haloarene and independent of the concentration of ligand (Scheme 23).

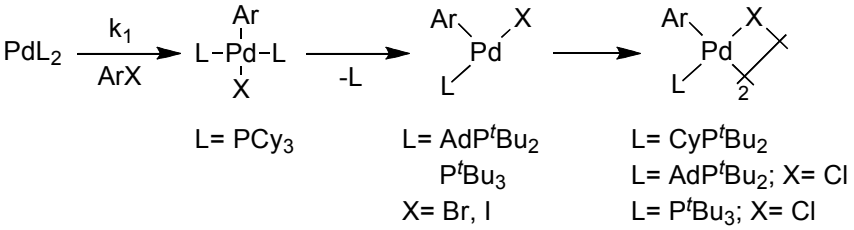

$$rate = [PdL_2]k_{obs} \qquad k_{obs} = k_1[ArX]$$

Scheme 23. Oxidative addition of ArX by direct reaction with PdL_2.[50]

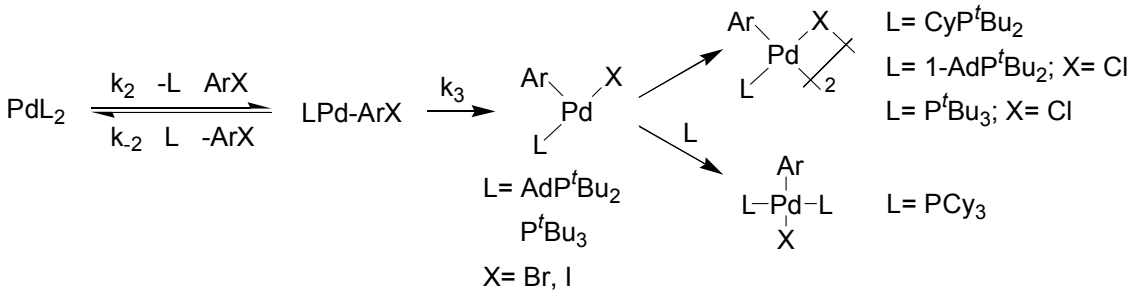

$$rate = [PdL_2]k_{obs} \qquad kobs = \frac{k_2k_3[ArX]}{k_3 + k_{-2}[L]}$$

$$1/k_{obs} = \frac{1}{k_2[ArX]} + \frac{[L]}{K_2k_3[ArX]} \qquad 1/k_{obs} = \left(\frac{1}{k_2} + \frac{[L]}{K_2k_3}\right)\frac{1}{[ArX]}$$

If $k_3 >> k_{-2}[L]$
$k_{obs} = k_2[ArX]$

Scheme 24. Oxidative addition of ArX after associative displacement of ligand from PdL_2.[50]

Alternatively, the reaction could occur by reversible or irreversible associative displacement of the phosphine in PdL_2 by the haloarene, as shown in Scheme 24. This first step would form a monophosphine intermediate coordinated by a haloarene that contains an intact C–X bond. Carbon–halogen bond cleavage would then form a three-coordinate arylpalladium halide complex. This three-coordinate complex could be the final product, or it could undergo dimerization or recoordination of ligand to form the final reaction product. If the initial associative displacement of phosphine were

reversible, then the reaction rate would depend on the concentration of both the haloarene and the ligand. If the initial associative displacement of phosphine were irreversible (k_3 >> k_{-2}[L]), then the reaction rate would depend only on the concentration of haloarene. Thus, the orders of the reaction in haloarene and ligand alone cannot distinguish between irreversible, direct carbon-halogen bond cleavage by the L_2Pd complex (Scheme 23) and irreversible displacement of ligand by the haloarene, followed by carbon-halogen bond cleavage by a monophosphine intermediate (Scheme 24). However, both mechanisms occur by reaction of the aryl halide with a bis-ligated Pd(0) species. In some cases, we were able to distinguish between these two mechanisms by the kinetic behavior of the reverse reaction.

Finally, the oxidative addition could occur by dissociation of a phosphine followed by oxidative addition of ArX to the resulting LPd intermediate to form a three-coordinate arylpalladium halide complex (Scheme 25). This dissociation of phosphine could be reversible or effectively irreversible (i.e. k_5[ArX] >> k_{-4}[L]) under the reaction conditions. If the ligand dissociation is fully reversible, then the reaction will depend on the concentration of both the haloarene and the ligand. If dissociation of ligand is effectively irreversible, then the rate of the reaction would be independent of the concentration of the haloarene and added ligand. In this case, the observed rate constant would be equal to k_4. After the addition, dimerization of the three-coordinate complex or coordination of a second ligand to form a square planar complex could occur, depending on the identity of the phosphine or the halide (Scheme 25).

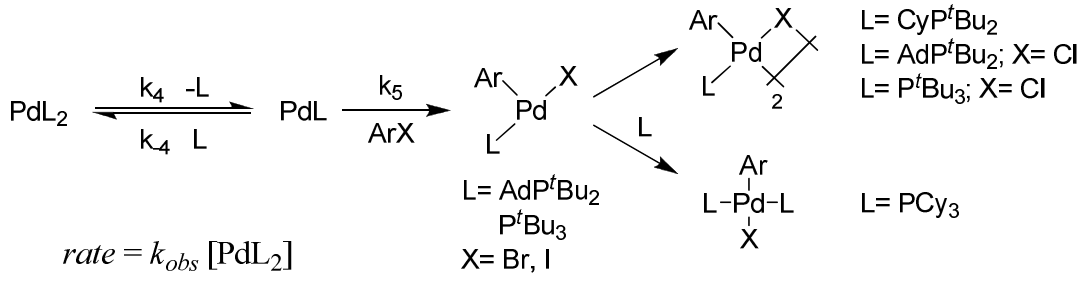

$$k_{obs} = \frac{k_4 k_5[\mathrm{ArX}]}{k_5[\mathrm{ArX}] + k_{-4}[\mathrm{L}]} \qquad 1/k_{obs} = \frac{1}{k_4} + \frac{[\mathrm{L}]}{K_4 k_5[\mathrm{ArX}]} \qquad \text{If } k_5[\mathrm{ArX}] >> k_{-4}[\mathrm{L}],\ k_{obs} = k_4$$

Scheme 25. Oxidative addition of ArX after dissociation of ligand from PdL_2.[50]

All of these mechanisms considered predict a positive dependence of k_{obs} on [ArX], which is consistent with the observations. However, the predicted differences in the dependence on [L] can be used to differentiate the mechanisms. Direct oxidative addition to PdL_2 (Scheme 23) is excluded if there is an inverse dependence of k_{obs} on [L]. Oxidative addition to PdL (Scheme 25) is excluded if there is no dependence on [L] but a positive dependence on [ArX]. Associative displacement of L by ArX (Scheme 24) is excluded if the plot of $1/k_{obs}$ vs 1/[ArX] has a significant y-intercept, but such analysis requires extremely accurate data, and we could not use this y-intercept to distinguish between the mechanisms in Schemes 24 and 25 in most cases. These predictions apply to systems in which the $L_2Pd(0)$ complex is the starting complex. The palladium complex of PCy_3 adopts an L_3Pd structure with added phosphine at low temperature. Thus, reactions under these conditions are analyzed separately. Most generally, the analysis of our data shows that the identity of the halide, rather than the identity of the ligands in this

study has a larger effect on whether the irreversible step of the mechanism involves a bisphosphine or monophosphine complex.

2.3.3. Mechanism of Oxidative Addition of Iodoarenes.

2.3.3.1. Overview.

The kinetic data for addition of iodobenzene to all four Pd(0) complexes **1–4** imply that the irreversible ("rate determining") step involves reaction of the iodoarene with a palladium complex ligated by two phosphines. The reactions of iodobenzene with complexes **1**–**3** were zeroth order in ligand and first order in iodobenzene. The reactions of iodobenzene with complex **4** depended inversely on the concentration of added ligand when the concentration of the added ligand was high, but this kinetic behavior was observed because the starting complex **4** was converted to the trisphosphine complex in the presence of this amount of added ligand.

2.3.3.2. Addition of PhI to L_2Pd Complexes 1–3 ligated by P^tBu_2, 1-AdP^tBu_2 and CyP^tBu_2.

Our kinetic data indicate that the "rate-determining" or first irreversible step of the reaction of iodobenzene with bisphosphine complexes **1** –**3** ligated by P^tBu_3, 1-AdP^tBu_2 and CyP^tBu_2 involves the starting bisphosphine species. This step can occur either by direct oxidative addition to the starting Pd(0) species shown in Scheme 23 or by irreversible displacement of the coordinated phosphine by iodoarene shown in Scheme 24 ($k_3 >> k_{-2}$[L]). Both rate equations are zeroth order in the concentration of added ligand and first order in the concentration of iodoarene. Although the two pathways cannot be

distinguished by the reaction orders of the forward process, we were able to distinguish between these two mechanisms by the kinetic behavior of the reverse reaction we studied previously, reductive elimination of iodoarene from the arylpalladium halide product.[21]

If the carbon–halogen bond cleavage during the oxidative addition process occurs directly by the PdL_2 complex (Scheme 23), then the principle of microscopic reversibility dictates that the elimination of ArI must also occur from a bisphosphine palladium complex. In this case, reductive elimination from the LPd(Ar)(I) complex would be first order in the concentration of ligand. In contrast, if carbon–halogen bond cleavage during the oxidative addition process occurs by a monophosphine species generated by associative displacement of the ligand by the iodoarene (Scheme 24), then microscopic reversibility would dictate that the elimination of ArI must occur from a monophosphine palladium complex, and reductive elimination from the LPd(Ar)(I) complex would be zeroth order in added ligand.

We previously showed that the rate of reductive elimination of 2-iodotoluene from (P^tBu_3)Pd(*o*-tol)(I) was independent of the concentration of added ligand (Scheme 26).[21] Thus, we conclude that the oxidative addition of PhI to **1** and **2** occurs by irreversible, associative displacement of a phosphine, followed by cleavage of the C–X bond by the resulting haloarene complex (Scheme 24). This mechanism is the same as that proposed for oxidative addition of iodobenzene to the Pd(0) complex ligated by the hindered ferrocenylphosphine Q-phos.[21]

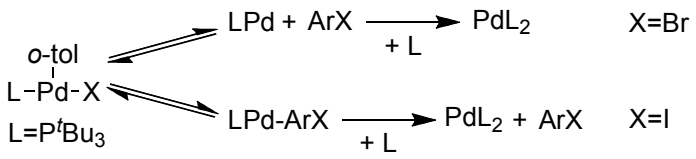

Scheme 26. Mechanisms for the reductive elimination of ArX from 3-coordinate aryl palladium(II) halide complexes.

The mechanism of reductive elimination of haloarene did not provide clear information on the mechanism of the oxidative addition of iodoarenes to CyP^{t}Bu$_2$-ligated **3** because reductive elimination of ArI from complexes ligated by CyP^{t}Bu$_2$ occurred in low yield.[51] The smaller size of the CyP^{t}Bu$_2$ ligand in complex **3** provides the potential that the oxidative addition of iodobenzene occurs directly to **3**, but the presence of a single phosphine in the product argues against this pathway. Thus, we favor a pathway involving irreversible displacement of the phosphine by the iodoarene. However, in either case, the kinetic data show that *the rate-determining step during the reaction of PhI with CyP^{t}Bu$_2$-ligated **3** involves a bisphosphine complex*. This conclusion contrasts with the dissociative mechanism deduced previously by others for reactions of CyP^{t}Bu$_2$-ligated **3** with iodoarenes.[27]

2.3.3.3. Mechanism of the Oxidative Addition of PhI to Pd(PCy$_3$)$_3$.

Because the trisphosphine complex Pd(PCy$_3$)$_3$ is the major Pd(0) complex at the −80 °C temperature of the oxidative addition process, interpretation of the kinetic data for oxidative addition of iodobenzene to the PCy$_3$-ligated Pd(0) complex is slightly different from interpretation of the data for oxidative addition of iodobenzene to the other two

complexes. Scheme 27 shows the possible mechanisms for oxidative addition of PhI to the trisphosphine species $Pd(PCy_3)_3$.

The observed inverse dependence on added ligand shows that the oxidative addition process occurs after loss of one (Path A) or two (Path B) ligands to generate $Pd(PCy_3)_2$ or $Pd(PCy_3)$, respectively. The data could not be obtained over a wide enough range of concentrations with sufficient accuracy to distinguish between an inverse first-order and an inverse second-order dependence on the concentration of added ligand that would correspond to reaction of the iodoarene with $Pd(PCy_3)_2$ and $Pd(PCy_3)$, respectively. However, we were able to distinguish between addition to $Pd(PCy_3)_2$ and addition to $Pd(PCy_3)$ by conducting the oxidative addition with low enough concentrations of added ligand at −80 °C that PdL_2 was the major species in solution. Under these conditions, the reaction was independent of the concentration of added ligand. Therefore, we conclude that the dependence on the concentration of ligand observed at high concentrations of added phosphine resulted from the reversible dissociation of one phosphine from $Pd(PCy_3)_3$ to form $Pd(PCy_3)_2$. We then conclude that $Pd(PCy_3)_2$ reacts with PhI by irreversible reaction between PhI and the bisphosphine complex. This irreversible reaction could occur by Path A in Scheme 27 involving irreversible oxidative addition to $Pd(PCy_3)_2$ or by a version of Path B in which the ArI irreversibly displaces a phosphine from $Pd(PCy_3)_2$.

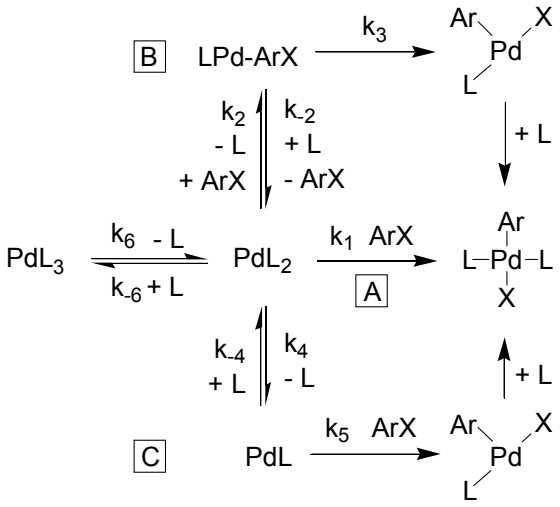

$rate = [PdL_3]k_{obs}$

A. Direct reaction to L_2Pd

$$k_{obs} = \frac{k_6 k_1[ArX]}{k_1[ArX] + k_{-6}[L]}$$

$$1/k_{obs} = \frac{1}{k_6} + \frac{[L]}{K_6 k_1[ArX]}$$

B. Associative displacement of the ligand in L_2Pd

$$k_{obs} = \frac{k_6 k_2 k_3[ArX]}{k_2 k_3[ArX] + k_3 k_{-6}[L] + k_{-6} k_{-2}[L]^2}$$

$$1/k_{obs} = \frac{1}{k_6} + \frac{[L]}{K_6 k_2[ArX]} + \frac{[L]^2}{K_6 K_2 k_3[ArX]}$$

C. Dissociation of ligand from L_2Pd

$$k_{obs} = \frac{k_6 k_4 k_5[ArX]}{k_4 k_5[ArX] + k_4 k_{-6}[ArX][L] + k_{-6} k_{-4}[L]^2}$$

$$1/k_{obs} = \frac{1}{k_6} + \frac{[L]}{K_6 k_4} + \frac{[L]^2}{K_6 K_4 k_5[ArX]}$$

Scheme 27. Possible mechanisms for the oxidative addition of ArI to PdL_3 L = PCy_3.[50]

2.4 Mechanism of Oxidative Addition of Chloroarenes

The data on the oxidative addition of chloroarenes to $Pd(0)L_2$ complexes **2**, **3** and **4** containing the ligands 1-AdP^tBu_2, CyP^tBu_2, and PCy_3 imply that the irreversible step in these processes involves a monophosphine palladium(0) complex. Each of the reactions

depended positively on the concentration of chlorobenzene and inversely on the concentration of added ligand. Thus, the number of phosphines in the complex involved in the rate-determining step for addition of chloroarenes is the same for complexes containing all the ligands studied and is different from the number of phosphines contained in the complex involved in the rate-determining step for addition of iodoarenes.

More specifically, the rate data for the addition of PhCl to the complexes **2–4** were consistent with the rate equations for the mechanisms in Schemes 24 and 25 involving reversible loss of a ligand. These rate data include linear plots of $1/k_{obs}$ vs 1/[ArCl] and $1/k_{obs}$ vs [L] for reactions of PhCl with all three Pd(0) complexes.

The pathway in Scheme 24 involves reversible associative displacement of ligand by the haloarene, and the pathway in Scheme 25 involves a reversible sequence of dissociation of ligand and association of haloarene. In principle, these two pathways can be distinguished by the y-intercepts of the plots of $1/k_{obs}$ vs 1/[ArCl] and $1/k_{obs}$ vs [L]. Reaction by either mechanism predicts that a plot of $1/k_{obs}$ vs [L] will have a non-zero y-intercept. However, the mechanism in Scheme 24 predicts that a plot of $1/k_{obs}$ vs 1/[ArCl] will lack a y-intercept, while the mechanism in Scheme 25 predicts that the same plot would have a non-zero y-intercept. Moreover, the mechanism in Scheme 25 predicts that the y-intercept of the plot of $1/k_{obs}$ vs 1/[ArCl] would be identical to the y-intercept of the plot of $1/k_{obs}$ vs [L]. For the reactions of 1-AdP^{t}Bu$_2$ complex **2**, the kinetic behavior predicted for reaction by initial dissociation of ligand was clearly observed. As shown in Figure 11, the plot of $1/k_{obs}$ vs. [L] has a clear non-zero y-intercept. Moreover, the y-intercepts of the plots of $1/k_{obs}$ vs. [L] and $1/k_{obs}$ vs. 1/[ArCl] are within experimental

error of each other (925 s and 1230 s). Finally, the values for K_4k_5 deduced from these plots (5.9 x 10^{-5} s^{-1} and 6.4 x 10^{-5} s^{-1}) are within experimental error of each other. We could not distinguish between these two mechanisms as confidently for reactions of the CyP^tBu_2 and PCy_3 complexes by this analysis because the y-intercepts of their plots of $1/k_{obs}$ vs 1/[ArCl] were close to zero. However, the values of K_4k_5 calculated from Figures 13 and 14 were similar to each other in both cases. This equivalence, and the clear dissociative mechanism for reaction of **2,** suggest that complexes **3** and **4** also react with aryl chlorides by a dissociative mechanism.

Most generally, our data show unambiguously that the irreversible step for addition of chloroarenes involves a monophosphine species and that the number of phosphine ligands in the Pd(0) species involved in the irreversible step of the oxidative addition of chloroarenes is identical for each of the Pd(0) complexes in this study. Moreover, these data show that the number of phosphines in the Pd(0) species in the irreversible step of the oxidative additions of chloroarenes is different than that in the Pd(0) species that reacts in the irreversible step of the oxidative additions of iodoarenes.

2.5. Mechanism of Oxidative Addition of Bromoarenes.

Like the rate data on the oxidative addition of PhCl and PhI, the rate data on the oxidative addition of PhBr to each of the $L_2Pd(0)$ complexes **2–4** were closely related to each other. The oxidative additions of bromoarenes to all three complexes depended positively on the concentration of bromoarene, and each reaction occurred with little (L=PCy_3) or no (L=1-AdP^tBu_2, CyP^tBu_2) dependence on the concentration of ligand.

This lack of dependence of k_{obs} on the concentration of ligand is similar to that for oxidative addition of PhI and is distinct from the strong dependence of k_{obs} on the concentration of ligand for oxidative addition of PhCl. As shown below, a detailed assessment of the dependence of the rate constant on the concentration of bromoarene implies that two pathways for the oxidative addition of bromoarenes occur concurrently. One pathway clearly occurs by irreversible dissociation of ligand, as was deduced for reaction of the chloroarene, and the second pathway could occur by irreversible associative displacement of ligand by the bromoarene, as was deduced for the reactions of iodobenzene.

The dependence of k_{obs} on [L] was nearly zeroth-order for the addition of PhBr to all three complexes. Thus, the irreversible step of these oxidative addition processes involves a bisphosphine Pd(0) species. Again, the coordination number of the species involved in the irreversible step of the oxidative addition of bromoarenes was identical for all of the Pd(0) species in this study.

Although this conclusion is the most concrete and the major conclusion we wish to draw from our studies on the oxidative addition of bromoarenes is the coordination number of the species reacting in the rate-limiting step of the major pathway, we can draw some additional conclusions about the mechanism of the oxidative addition of bromoarenes. The presence of a y-intercept implies that the reactions likely occur by two competing mechanisms involving bisphosphine species. For reactions of complexes **2** and **3**, plots of k_{obs} vs [PhBr] were linear, but they also contained a non-zero y-intercept. The non-zero y-intercepts in these plots suggest two pathways involving bisphosphine

complexes in the rate-determining step compete, one that is dependent on the concentration of bromoarene and one that is independent of the concentration of bromoarene. Of the mechanisms considered, only the mechanism involving initial, irreversible dissociation of ligand (Scheme 25) is independent of the concentration of ligand and haloarene ($k_{obs} = k_4$). Thus, we conclude that the value of the y-intercept roughly corresponds to the rate constant for reaction by this path.[52]

Two other paths predict rate constants that would be independent of the concentration of ligand and positively dependent on the concentration of haloarene: direct C–X bond cleavage to form a four-coordinate intermediate (Scheme 23) and irreversible associative displacement of ligand, followed by carbon–halogen bond cleavage (Scheme 24). We consider the pathway involving direct C–X bond cleavage to form a four-coordinate intermediate the least likely. Besides forming a crowded intermediate, microscopic reversibility implies that the elimination of ArBr from LPd(Ar)(Br) would occur through a four-coordinate intermediate. Previous studies on reductive elimination of ArBr from (P^tBu_3)Pd(*o*-tol)Br implied that the elimination involves a three-coordinate intermediate (Scheme 26).[53] Although reductive elimination of ArBr from aryl palladium(II) halide complexes of AdP^tBu_2 and CyP^tBu_2 have not been reported, the steric properties of these phosphines make the formation of a bisphosphine intermediate $L_2Pd(Ar)(X)$ and a change in mechanism from that of the reactions of P^tBu_3 complex **1** unlikely.

Therefore, we conclude, based on the presence of the y-intercepts, the addition of PhBr to complexes **2** and **3** most likely occurs by two competitive paths involving rate-

determining reactions of bisphosphine complexes to give rise to mono-phosphine intermediates. One pathway could occur by irreversible dissociation of ligand. The second by irreversible associative displacement of ligand prior to the carbon-halogen bond cleavage step (Scheme 28).

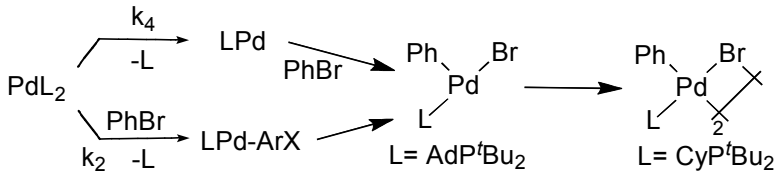

$$rate = k_{obs}[PdL_2];\ k_{obs} = k_4 + k_2[PhBr]$$

Scheme 28. Two concurrent mechanisms for the oxidative addition of PhBr to **2** and **3**.

In contrast, the oxidative addition of PhBr to PCy_3-ligated **4** appears to occur by a single mechanism involving associative displacement of the ligand or oxidative addition to the two-coordinate species. The rate of the oxidative addition of PhBr to PCy_3-ligated **4** was measured at a temperature in which the major Pd(0) species was the L_2Pd complex. The data in Figure 16 showed that this oxidative addition occurred with a positive dependence on the concentration of bromobenzene and only a weak dependence on the concentration of added ligand. The small slope and large y-intercept of the plot of $1/k_{obs}$ vs [L] is consistent with the rate equations corresponding to nearly irreversible associative substitution of PCy_3 by PhBr (Scheme 24) or nearly irreversible oxidative addition to the two-coordinate species to generate a four-coordinate product (Scheme 23). The small slope implies that the product of the equilibrium and rate constants in the second term of the equation (K_2k_3) are large, relative to the rate constant (k_2) in the first

term. Because both processes would be favorable with the smaller PCy_3 ligand, we cannot distinguish between these two mechanisms. However, we can conclude in general that a major pathway for reactions of bromoarenes with the $L_2Pd(0)$ complexes **2-4** occurs by irreversible reaction of the bromoarene with the bisphosphine complex. This irreversible reaction could occur by associative displacement of ligand followed by oxidative addition or by direct oxidative addition.

2.6 Conclusions

The observed kinetic data are summarized in Table 1, and this table shows that the dependence of the rate constants depends on the identity of the halide more than the steric bulk of the ligand. The reactions of iodobenzene were all zeroth order in added ligand, the reactions of bromobenzene were all zeroth, or nearly zeroth order, in added ligand, and the reactions of chlorobenzene were all inverse first order in added ligand. Moreover, all reactions depended positively on the concentration of haloarene. Thus, all the reactions of the iodoarenes occur by rate-determining reaction with a bisphosphine complex, while all of the reactions of the chloroarene occur by rate-determining reaction with a monophosphine complex. The reactions of the bromoarenes occur by rate-determining reaction of a bisphosphine complex. Our data imply that the reactions of chloroarenes occur by reversible formation of a monophosphine intermediate, while the reactions of iodobenzene occur by an irreversible reaction of the starting bisphosphine species. The oxidative additions of bromoarenes appear to occur by a combination of irreversible reaction of the bromoarene with the two-coordinate Pd(0) species and

dissociation of phosphine prior to reaction with the bromoarene. In particular, the reactions of bromoarenes with Pd(1-Ad$P^tBu_2)_2$ (**2**) appeared to occur by a combination of both associative and dissociative substitution of the ligand by haloarene, and this result reveals the fine balance between these two mechanisms for generation of the monophosphine intermediates.

We propose that the iodoarenes react with the bisphosphine species in an irreversible process because they are softer and more reactive than the other haloarenes, while addition of chloroarenes requires generation of the more reactive monophosphine species because they are poorer ligands and require a more reactive intermediate to cleave the less reactive C–Cl bond. These conclusions are supported by the low barriers for oxidative addition of chloroarenes to monophosphine palladium(0) species and high barriers for oxidative addition of chloroarenes to bisphosphine palladium(0) species calculated recently by DFT methods.[34,36]

Table 1. Summary of the experimental observations and suggested mechanisms for the oxidative addition of ArX to complexes **2**–**4**.

		$Pd(1\text{-}AdP^tBu_2)_2$	$Pd(CyP^tBu_2)_2$	$Pd(PCy_3)_n$ n = 2,3	General Conclusion
ArI	Order in ArI	1	1	1	The ArI reacts with the PdL2 species
	Order in L	Zeroth	Zeroth	-1 for n = 3, 0 for n = 2	
	Conclusion	Irreversible associative displacement of L by ArI		Reaction of ArI with L_2Pd	
ArCl	Order ArCl	1	1	1	The C–X bond cleavage step occurs after reversible dissociation or displacement of one phosphine from PdL2 to form PdL or LPd–ArX
	Order in L	-1	-1	-1	
	Conclusion	Reversible exchange of L with PhCl prior to C–X bond cleavage.			
ArBr	Order ArBr	1	1	1	The C–X bond cleavage step appears to occur by two pathways of similar energy. One major pathway clearly occurs by reaction of ArBr with the $L_2Pd(0)$ species. This step could occur by irreversible displacement of one L to form LPd–ArX or by irreversible direct C-X bond cleavage. The second, less defined pathway is zeroth order in ArBr, and appears to occur by irreversible dissociation of L to form LPd.
	y-intercept of k_{obs} vs [ArBr]	non-zero	non-zero	zero	
	Order in L	Zeroth	Zeroth	Nearly zeroth	
	Conclusion	One path by reaction of the ArBr with L_2Pd, most likely by associative displacement of L to form LPd–ArX. A second competing pathway appears to occur that is zeroth order in ArBr, most likely by initial dissociation of L, followed by rapid reaction with ArBr.		Reaction of the ArBr with the bisphosphine complex L_2Pd as the major pathway (by nearly irreversible associative displacement of L by PhBr prior to C–X bond cleavage or nearly irreversible direct oxidative addition)	

2.7 Experimental

General Methods. All manipulations were conducted in an inert atmosphere dry box or using standard Schlenk techniques unless otherwise specified. ^{1}H spectra were recorded on a 400 or 500 MHz spectrometer; ^{13}C spectra were recorded at 125 MHz with solvent resonances as reference; $^{31}P\{^{1}H\}$ NMR spectra were recorded at 160 or 200 MHz with external H_3PO_4 as a reference. CH_2Cl_2, THF, diethyl ether, toluene, and pentane were dried with a solvent purification system containing a 1 m column with activated alumina. All reagents were obtained from commercial sources and used without further purification. The solvents and haloarenes were added to the kinetic experiment samples with a micropipette. For volumes lower than 10 μL, a microsyringe was used.

Synthesis of $[(P^tBu_3)Pd(Ph)(Cl)]_2$ (9). In a Schlenk flask was placed 100 mg (0.26 mmol) of $(Py)_2Pd(Ph)(Cl)$ (**20**) and 107.3 mg (0.52 mmol) of P^tBu_3. The solids were suspended in 10 mL of toluene. The reaction mixture was stirred at room temperature for 30 min. The solvent was evaporated under vacuum to leave a yellow and white residue. The flask was brought into the glove box, and the solid was treated with toluene. The yellow product dissolved in the toluene, and the white starting material remained. The yellow solution was then filtered, and the solvent was evaporated under vacuum. The resulting solid was washed with pentane and dried under vacuum to yield 47.5 mg (42% yield) of yellow product. ^{1}H NMR (C_6D_6, 400 MHz) δ 7.48 (ddd, J = 8.0, 3.0, 1.0 Hz, 2H), 6.86 (t, J = 7.5 Hz, 2H), 6.78 (tt, J = 6.7, 1.5 Hz, 1H), 1.30 (d, J = 12.0 Hz, 27H) ; ^{13}C NMR (C_6D_6, 125 MHz) δ 143.22, 138.31 (d, J = 2.3 Hz), 127.18 (d, J = 1.8 Hz),

123.72, 41.27 (d, J = 7.9 Hz), 33.51 (d, J = 3.9 Hz); $^{31}P\{^{1}H\}$ NMR (C_6D_6) δ 72.8. Anal. calcd. for $C_{18}H_{32}ClPPd$: C, 51.32; H, 7.66. Found: C, 51.60; H, 7.80.

Synthesis of [(P^tBu_3)Pd(2-CF_3-C_6H_4)(Cl)]$_2$ (10). Into a Schlenk flask was placed 200 mg (0.39 mmol) of Pd(P^tBu_3)$_2$. The solid was dissolved in 15 mL of 2-CF_3-C_6H_4Cl, and the resulting solution was heated under nitrogen at 80 °C for 1 h. The solvent was evaporated under vacuum at 50 °C, and the resulting orange residue was redissolved in toluene. The resulting solution was filtered, concentrated, layered with pentane. Cooling at −35 °C generated 114 mg of orange product (0.23 mmol, 59% yield). Recrystallization of the product in toluene layered with pentane yielded crystals suitable for X-ray diffraction. ^{1}H NMR (C_6D_6, 400 MHz) δ 1.26 (d, J = 12.4 Hz, 27H), 6.67 (br, 1H), 6.74 (br, 1H), 7.35 (br, 1H), 7.84 (br, 1H); ^{13}C NMR (CD_2Cl_2, 125 MHz) 139.95, 138.49, 136.09 (q, J = 28.7 Hz), 128.21, 127.48, 124.86 (q, J = 273 Hz), 123.69, 41.36 (d, J = 8.9 Hz), 32.89 (d, J = 2.7 Hz); $^{31}P\{^{1}H\}$ NMR (C_6D_6) δ 70.8; $^{19}F\{^{1}H\}$ NMR (C_6D_6, 375 MHz) δ −55.0. Anal. calcd. for $C_{19}H_{31}Cl_1F_3PPd$: C, 46.64; H, 6.39. Found: C, 46.90; H, 6.56.

Determination of Molecular Weight in Solution[54] of [(P^tBu_3)Pd(2-CF_3-C_6H_4)(Cl)]$_2$ (10). Into a 1.0 mL volumetric flask was placed 29.3 mg (0.0599 mol) of [(P^tBu_3)Pd(2-CF_3-C_6H_4)(Cl)]$_2$ (10), and the flask was filled with THF to the mark. The reference solution was prepared in a similar manner with 8.4 mg (0.045 mmol) of ferrocene. A Signer apparatus was loaded with 0.8 mL of the solution of the complex in one arm and 0.8 mL of the solution of ferrocene in the other arm. The

solutions were frozen in liquid N_2, and the apparatus was evacuated to about 20 mtorr. The apparatus was then allowed to stand at room temperature. The volume in each arm was measured periodically until the volumes were constant. From the final concentrations, the molecular weight was calculated to be 530 g/mol. The molecular weight of the monomeric complex would be 489.29 g/mol, and the molecular weight of the dimeric complex would be 978.58 g/mol. The molecular weight calculated by the same method in C_6H_6 solvent is 505 g/mol.

Independent synthesis of [(1-AdP^{t}Bu$_2$)Pd(Ph)(Cl)]$_2$ (11). The complex was obtained following a procedure previously reported by reaction of tetraoctylammoniun chloride with (1-AdP^{t}Bu$_2$)Pd(Ph)(CF_3SO_3).[37] In a small vial, 30 mg (0.049 mmol) of (1-AdP^{t}Bu$_2$)Pd(Ph)(CF_3SO_3) was dissolved in 1 mL of toluene. In a separate vial, N(octyl)$_4$Cl (26mg, 0.052 mmol) was dissolved in 1 mL of toluene. The chloride solution was added dropwise to the stirring vial containing the Pd solution. The reaction was stirred for 2 min. At this time, the reaction was filtered through a plug of Celite and concentrated to approximately 1 mL. The resulting bright yellow solution was layered with pentane and cooled to −35 °C. After 16 h, bright yellow crystals and colorless crystals formed in the vial. The crystals were washed repeatedly with ether until only the yellow crystals remained. These crystals were dried under vacuum to yield 21 mg of product (86% yield). Crystals suitable for X-ray diffraction were obtained by recrystallization from toluene solution layered with pentane at −35 °C. ^{1}H NMR (C_6D_6, 400 MHz) δ 7.54 – 7.57 (m, 2H), 6.89 (t, J = 7.2 Hz, 2H), 6.80 (t, J = 7.2 Hz, 1H), 2.38

(br s, 6H), 1.81 (br, 3H), 1.50 – 1.63 (br m, 6H), 1.23 (d, J = 12.0 Hz, 18H); ^{13}C NMR (C_6D_6, 100 MHz) δ 141.8, 138.2 (d, J = 3.0 Hz), 127.3 (br), 123.8, 47.8 (d, J = 6.0 Hz), 42.0, 41.5 (d, J = 7.8 Hz), 36.9, 33.6 (d, J = 2.2 Hz), 29.9 (d, J = 8.1 Hz); ^{31}P{^{1}H} NMR (C_6D_6) δ 69.2. Anal. calcd. for $C_{24}H_{38}ClPPd$: C, 57.72; H, 7.67. Found: C, 57.73; H, 7.92.

Independent synthesis of [(1-AdP^{t}Bu$_2$)Pd(2-CF$_3$-C$_6$H$_4$)(Cl)]$_2$ (12). In a small vial, 150 mg (0.225 mmol) Pd(1-AdP^{t}Bu$_2$)$_2$ (**2**) was suspended in 6.74 mL (50.6 mmol) *o*-chlorobenzotrifluoride. The mixture was heated in an oil bath at 100 ^{o}C with stirring for 20 min. The resulting orange solution was concentrated to dryness under vacuum. The residue was next triturated with 3 mL acetonitrile for 1.5 hrs. The resulting yellow precipitate was collected and washed with 4x1 mL pentane. The process was repeated a second time, and the resulting solid was dried under vacuum to give 50 mg (39%, 0.089 mmol) **12**. Crystals suitable for X-ray diffraction were obtained by slow evaporation of a THF solution at room temperature. ^{1}H NMR (C_6D_6, 500 MHz) δ 1.28 (br, 18H), 1.50 (br, 3H), 1.58 (br, 3H), 1.80 (br, 3H), 2.42 (br, 6H), 6.64 (br, 1H), 6.75 (br, 1H), 7.31 (br, 1H), 7.92 (br, 1H); ^{13}C NMR (C_6D_6, 125 MHz) 139.94, 139.01, 136.57 (q, J = 27.3 Hz), 128.53, 127.63, 125.48 (q, J = 274 Hz), 123.61, 47.69 (d, J = 5.8 Hz), 41.53 (d, J = 6.9 Hz), 41.30, 36.58, 33.25 (br), 29.50; ^{31}P{^{1}H} NMR (C_6D_6, 200 MHz) δ 70.6; ^{19}F{^{1}H} NMR (C_6D_6, 470 MHz) δ −54.9. Anal. calcd. for $C_{25}H_{37}ClF_3PPd$: C, 52.92; H, 6.57. Found: C, 53.10; H, 6.84.

Independent synthesis of $[(CyP^tBu_2)_2Pd(3,5\text{-}(CF_3)_2C_6H_3)(I)]_2$ (13). Inside the glove box, 100 mg (0.18 mmol) of $Pd(CyP^tBu_2)_2$ (**3**) was weighed into a small vial, and 300 μL of 3,5-$(CF_3)_2C_6H_3I$ and 3 mL of toluene were added. The reaction mixture was stirred at room temperature for 2 h, after which time the solvent and excess iodoarene was evaporated under vacuum. The yellow product was redissolved in toluene, and the solution was filtered, concentrated, layered with pentane and cooled at −35 °C. After a second recrystallization under the same conditions, 60.7 mg (51%, 0.090 mmol) of yellow solid was obtained. ^{1}H NMR (C_6D_6, 400 MHz) δ 8.08 (s, 2H), 6.86 (s, 1H), 1.68 (br, 3H), 1.09 (br, 4H), 0.85 (br, 18H), 0.52 (br, 2H), 0.40 (br, 2H); ^{13}C NMR (CD_2Cl_2, 125 MHz) δ 155.64, 138.53, 128.90 (q, J = 31.9 Hz), 124.48 (q, J = 272.7 Hz), 116.79 (m), 41.06, 39.74 (d, J = 11.1 Hz), 32.49, 31.73, 28.28 (d, J = 9.7 Hz), 26.74; ^{19}F{^{1}H} NMR (C_6D_6, 375 MHz) δ −65.0; ^{31}P{^{1}H} NMR (C_6D_6) δ 63.3 (br). Anal. calcd for $C_{22}H_{32}F_6IPPd$: C, 39.16; H, 4.78. Found: C, 39.28; H, 4.72.

Independent synthesis of $[(CyP^tBu_2)Pd(Ph)(I)]_2$ (14). Inside the glove box, 100 mg (0.18 mmol) of $Pd(CyP^tBu_2)_2$ (**3**) was weighed into a small vial and mixed with 1.5 mL of PhI. The reaction was stirred at 60 °C for 40 min, after which time the excess PhI was evaporated under vacuum. The yellow product was dissolved in toluene, and the resulting solution was filtered, concentrated, and layered with pentane. Cooling at −35 °C and recrystallization of the resulting yellow solid by layering a toluene solution with pentane yielded 42.2 mg (44%, 0.078 mmol) of yellow powder. ^{1}H NMR (C_6D_6, 500 MHz) δ 7.46 (d, J = 7.3 Hz, 2H), 6.88 (t, J = 7.3, 2H), 6.74 (t, J = 6.7 Hz, 1H), 2.27 (br, 2H), 2.09 (br,

1H), 1.61 (br, 4H), 1.48 (d, J = 10.4 Hz, 18H), 1.15 (br m, 2H), 0.87 (br, 2H); ^{13}C NMR (CD_2Cl_2, 125 MHz) δ 152.39, 138.48, 127.25, 122.64, 40.04 (br), 39.09 (d, J = 10.3 Hz), 32.33, 31.67, 28.06 (d, J = 9.8 Hz), 26.70; ^{31}P{^{1}H} NMR (CD_2Cl_2) δ 59.8. Anal. calcd for $C_{20}H_{34}IPPd$: C,44.58, H, 6.36. Found: C, 44.86; H, 6.26.

Independent synthesis of [(CyP^{t}Bu$_2$)Pd(Ph)(Br)]$_2$ (15). Inside the glove box, 100 mg (0.18 mmol) of Pd(CyP^{t}Bu$_2$)$_2$ (**3**) was weighed into a small vial, and mixed with 3.0 mL of PhBr. The reaction mixture was stirred at 70 °C for 1 h, after which time the excess bromobenzene was evaporated under vacuum. The yellow product was redissolved in toluene, and the solution was filtered, concentrated, layered with pentane and cooled at −35 °C. After a second recrystallization, 61.1 mg (70%, 0.12 mmol) of yellow solid was obtained. Crystals suitable for X-ray diffraction were obtained upon further recrystallization of the product under the same conditions. ^{1}H NMR (C_6D_6, 500 MHz) δ 7.64 (d, J = 6.5 Hz, 2H), 6.94 (t, J = 7.3 Hz, 2H), 6.82 (t, J = 7.0 Hz, 1H), 2.16 (br, 3H), 1.5 – 1.2 (br, 5H), 1.37 (d, J = 11.5 Hz, 18H), 0.91 (br m, 1H), 0.77 (br, 2H); ^{13}C NMR (C_6D_6, 125 MHz) δ 150.51, 137.84, 127.37, 123.47, 39.65 (d, J = 10.6 Hz), 39.00 (d, J = 11.6 Hz), 32.39, 31.93, 28.32 (d, J = 8.5 Hz), 27.04; ^{31}P{^{1}H} NMR (C_6D_6) δ 62.58. Anal. calcd. For $C_{20}H_{34}BrPPd$: C, 48.85; H, 6.97. Found: C, 50.08; H, 6.9.

Determination of Molecular Weight in Solution[54] of [(CyP^{t}Bu$_2$)Pd(Ph)(Br)]$_2$ (15). Into a 1.0 mL volumetric flask was placed 11 mg (0.011 mmol) of [(CyP^{t}Bu$_2$)Pd(Ph)(Br)]$_2$ (**15**), and the flask was filled with THF to the mark. The

reference solution was prepared in a similar manner with 3.3 mg (0.018 mmol) of ferrocene. A Signer apparatus was loaded with 1.0 mL of the solution of the complex in one arm and 1.0 mL of the solution of ferrocene in the other arm. The solutions were frozen in liquid N_2, and the apparatus was evacuated to about 50 mTorr. The apparatus was then allowed to stand at room temperature. The volume in each arm was measured periodically until the volumes were constant. From the final concentrations, the molecular weight was calculated to be 523 g/mol. The molecular weight of the monomeric complex would be 491.78 g/mol, and the molecular weight of the dimeric complex would be 983.56 g/mol.

Independent synthesis of [(CyP^{t}Bu$_2$)Pd(Ph)(Cl)]$_2$ (16). Inside the glove box, 100 mg (0.18 mmol) of Pd(CyP^{t}Bu$_2$)$_2$ (**3**) was weighed into a small vial, and mixed with 3.0 mL of PhCl. The reaction mixture was stirred at 70 °C for 2 h, after which time the excess chlorobenzene was evaporated under vacuum. The yellow product was redissolved in toluene, and the solution was filtered, concentrated, layered with pentane and cooled at −35 °C. After a second recrystallization under the same conditions, 50.5 mg (64%, 0.11 mmol) of yellow solid was obtained. ^{1}H NMR (C_6D_6, 500 MHz) δ 7.62 (br, 2H), 6.94 (br, 2H), 6.84 (br m, 1H), 2.14 (br, 2H), 2.07 (br, 1H), 1.2–1.7 (br, 5H), 1.39 (d, J = 10.9 Hz, 18H), 0.89 (br m, 1H), 0.71 (br, 2H). ^{13}C NMR (C_6D_6, 125 MHz) δ 148.69, 137.04, 126.76, 123.14, 39.00 (d, J = 13.5), 38.40 (d, J = 13.0), 31.80, 31.42, 27.92 (d, J = 9.9), 26.63; ^{31}P{^{1}H} NMR (C_6D_6) δ 64.06. Anal calcd For $C_{20}H_{34}ClPPd$: C, 53.70; H, 7.66. Found: C, 53.58; H, 7.52

Synthesis of *trans*-$(Py)_2Pd(Ph)(Cl)$ (20). In a Schlenk flask, was placed 800 mg of $Pd_2(dba)_3$ (0.87 mmol) and 80 mg of P^tBu_3 (0.40 mmol). To these solids was added a mixture of 0.7 mL of pyridine (8.6 mmol) and 5 mL of PhCl. The reaction was stirred under N_2 at 45 °C for 1.5 h. $(Py)_2Pd(Ph)(Cl)$ precipitated from the reaction mixture as a white solid. This solid was rinsed with ether and redissolved in CH_2Cl_2. The solution was filtered through plug of Celite and layered with pentane at −35 °C. The resulting white crystalline solid was isolated by filtration and dried under vacuum to obtain 361 mg (55 % yield) of product. ^{1}H NMR (CD_2Cl_2, 400 MHz) δ 8.81 (dt, *J* = 5.2, 1.5 Hz, 4H), 7.73 (tt, *J* = 7.6, 1.6 Hz, 2H), 7.25 (ddd, *J* = 7.5, 5.3, 1.6 Hz, 4H), 7.19 (dd, *J* = 7.4, 0.9 Hz, 2H) 6.86 (m, 3H) ; ^{13}C NMR (CD_2Cl_2, 125 MHz) δ 153.42, 153.21, 138.07, 134.31, 127.46, 125.00, 123.91. Anal. calcd. for $C_{16}H_{15}ClN_2Pd$: C, 50.95; H, 4.01. Found: C, 50.72; H, 3.83.

General procedure for kinetic experiments. The amounts and reagents used to prepare each sample are described below. The solvents and haloarenes were added to the samples with a micropipette. The sample solutions were transferred to a screw top NMR tube and capped with a Teflon septum. A sealed capillary tube with a THF or DMF solution of H_3PO_4 (0.35 M) was placed inside the NMR tube to be used as an external standard. Before inserting the sample into the NMR probe, the temperature was adjusted. The temperature was measured with a type K thermocouple; the thermocouple probe was inserted into an NMR sample tube, which was lowered inside the spectrometer probe.

Once the temperature was stable, the tube with the sample was inserted into the NMR probe and ^{31}P NMR spectra were acquired at fixed time intervals throughout the length of experiment with the aid of an automated data collection program.

Representative procedure for the oxidative addition of PhBr to Pd(P^tBu_3)$_2$ (1). The palladium complex Pd(P^tBu_3)$_2$ (**1**) was weighed in a small vial (10.2 mg, 0.02 mmol). Into this vial was placed 40 μL of a 2.5 M (0.1 mmol) solution of P^tBu_3. Toluene (354 μL), PhBr (100 μL, 0.95 mmol) and phosphazene base were added (6 μL, 0.02 mmol) to the sample. The solution was transferred to a screw capped NMR tube, and the sample tube was placed into a preheated NMR spectrometer probe at 90°C. The disappearance of the Pd complex peak was monitored by ^{31}P NMR spectroscopy with the aid of an automated acquisition program.

Representative procedure for the oxidative addition of ArX (X= I, Br, Cl) to Pd(1-AdP^tBu_2)$_2$ (2). Into a small vial was placed the palladium complex Pd(1-AdP^tBu_2)$_2$ (6.7 mg, 0.010 mmol) and ligand 1-AdP^tBu_2 (28.0 mg, 0.10 mmol). The complex was suspended in 100 μL of toluene. The suspension was transferred to an NMR sample tube with a total of three portions of 100 μL of toluene and 100 μL ArX to ensure that all of the solid was transferred to the tube. Total sample volume equal 400 μL. Into the sample tube was added 2 μL (0.006 mmol) of phosphazene base. The sample was placed into the preheated probe at 80 – 100 °C. At this high temperature, the complex Pd(1-AdP^tBu_2)$_2$

solubilized and the sample became homogeneous. The decay of the Pd complex was monitored by ^{31}P NMR spectroscopy with the aid of an automated acquisition program.

Representative procedure for the oxidative addition of PhX (X=I, Br, Cl) to Pd(CyP^{t}Bu$_2$)$_2$ (3). Into a small vial, weighed the palladium complex Pd(CyP^{t}Bu$_2$)$_2$ (**3**) (10.2 mg, 0.018 mmol) and the ligand CyP^{t}Bu$_2$ (22.8 mg, 0.10 mmol). The necessary amounts of toluene and PhX were added to the vial to adjust to the desired haloarene concentration and make the final volume 500 μL. The solution was transferred to a screw capped NMR tube, and the sample was placed into a preheated NMR spectrometer probe at 50 – 80°C. The decay of the Pd complex was measured by ^{31}P NMR spectroscopy with the aid of an automated acquisition program.

Representative procedure for the oxidative addition of PhI to Pd(PCy$_3$)$_2$ (4). Into a small vial was weighed 141 mg of PCy$_3$ (0.503 mmol). This material was dissolved in 500 μL of toluene to prepare a 1.00 M stock solution. Into a separate vial was weighed 6.3 mg (0.0094 mmol) of the palladium complex Pd(PCy$_3$)$_2$ (**4**). To this vial, 30 μL of the phosphine stock solution (0.030 mmol) and 270 μL of toluene were added. The solution was transferred to a screw capped NMR tube and cooled to −78 °C. Then, a solution of 20 μL of PhI and 180 μL of toluene was added by syringe. The sample was introduced into the NMR spectrometer probe that was pre-cooled to −80 °C, and the decay of the Pd complex was measured by ^{31}P NMR spectroscopy with the aid of an automated acquisition program.

Representative procedure for the oxidative addition of PhCl to $Pd(PCy_3)_2$ (4). Into a small vial was weighed 14.1 mg of PCy_3 (0.0503 mmol). This material was dissolved in 500 μL of toluene to prepare a 0.100 M stock solution. Into a separate vial, 6.3 mg (0.0094 mmol) of the palladium complex $Pd(PCy_3)_2$ (**4**) were weighed. To this vial 50 μL of the phosphine stock solution (0.0050 mmol), 40 μL of PhCl and 410 μL of toluene were added to make the final volume 500 μL. The solution was transferred to a screw capped NMR tube, and the sample was placed into a preheated NMR spectrometer probe at 70°C. The decay of the Pd complex was measured by ^{31}P NMR spectroscopy with the aid of an automated acquisition program.

Representative procedure for the oxidative addition of PhBr to $Pd(PCy_3)_2$ (4). The phosphine PCy_3 (25.0 mg, 0.089 mmol) and the palladium complex $Pd(PCy_3)_2$ (**4**) (6.3 mg, 0.0094 mmol) were weighed into a small vial. To this vial was added 400 μL of toluene, and the resulting solution was transferred to a screw-capped NMR tube. The sample was cooled in ice bath, and 100 μL of PhBr were added to the tube with a syringe. The sample was introduced into the NMR spectrometer probe pre-cooled at 10 °C. The decay of the Pd complex was measured by ^{31}P NMR spectroscopy with the aid of an automated acquisition program.

Derivation of the rate expressions. Scheme 24.

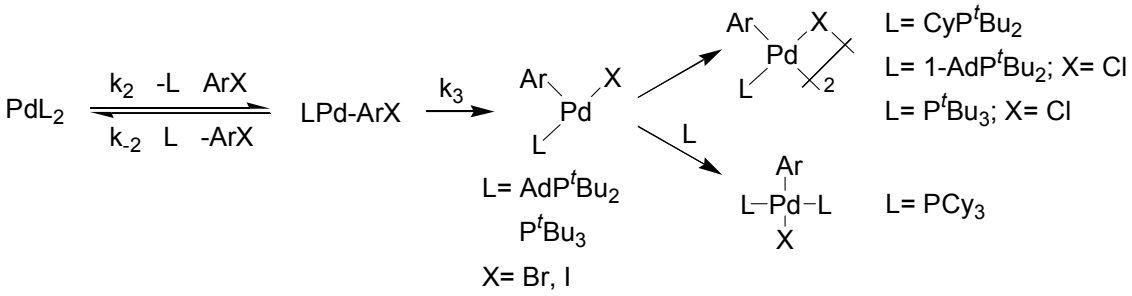

$$rate = [\mathrm{PdL_2}]k_{obs}$$

$$1/k_{obs} = \frac{1}{k_2[\mathrm{ArX}]} + \frac{[\mathrm{L}]}{K_2k_3[\mathrm{ArX}]} \qquad \text{If } k_3 >> k_{-2}[\mathrm{L}]$$

$$k_{obs} = \frac{k_2k_3[\mathrm{ArX}]}{k_3 + k_{-2}[\mathrm{L}} \qquad 1/k_{obs} = \left(\frac{1}{k_2} + \frac{[\mathrm{L}]}{K_2k_3}\right)\frac{1}{[\mathrm{ArX}]} \qquad k_{obs} = k_2[\mathrm{ArX}]$$

Under the steady state approximation,

$$\frac{\mathrm{d}[\mathrm{LPd(ArX)}]}{\mathrm{d}t} = 0 = k_2[\mathrm{PdL_2}][\mathrm{ArX}] - k_{-2}[\mathrm{LPd(ArX)}][\mathrm{L}] - k_3[\mathrm{LPd(ArX)}]$$

Solving for [LPd(ArX)],

$$[\mathrm{LPd(ArX)}] = \frac{k_2[\mathrm{ArX}][\mathrm{PdL_2}]}{k_3 + k_{-2}[\mathrm{L}]}$$

$$rate = k_3[\mathrm{LPd(ArX)}] = \frac{k_2k_3[\mathrm{ArX}][\mathrm{PdL_2}]}{k_3 + k_{-2}[\mathrm{L}]}$$

$rate = k_{obs}[\mathrm{PdL_2}]$; therefore,

$$k_{obs} = \frac{k_2k_3[\mathrm{ArX}]}{k_3 + k_{-2}[\mathrm{L}]}$$

If $k_3 >> k_{-2}[L]$; the term $k_{-2}[L]$ in k_{obs} denominator can be ignored and the expression for k_{obs} gets reduced to $k_{obs} = k_2[ArX]$.

Derivation of the rate expressions. Scheme 25.

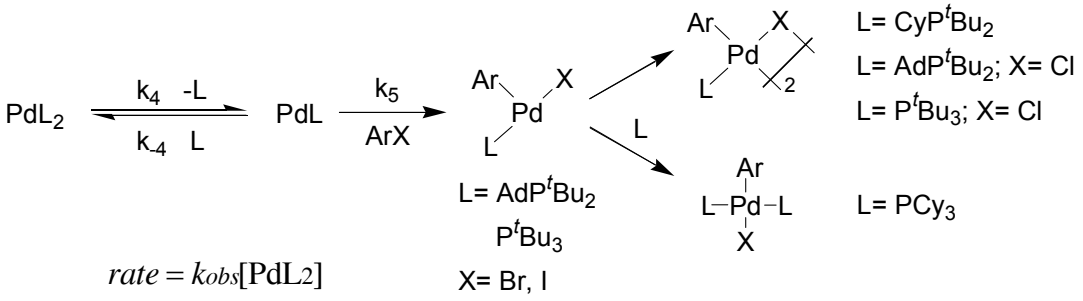

$rate = k_{obs}[PdL_2]$

$$k_{obs} = \frac{k_4 k_5[ArX]}{k_5[ArX] + k_{-4}[L]} \qquad 1/k_{obs} = \frac{1}{k_4} + \frac{[L]}{K_4 k_5[ArX]}$$

If $k_5[ArX] >> k_{-4}[L]$ $k_{obs} = k_4$

Under the steady state approximation,

$$\frac{d[PdL]}{dt} = 0 = k_4[PdL_2] - k_{-4}[PdL][L] - k_5[PdL][ArX]$$

Solving for [PdL],

$$[PdL] = \frac{k_2[PdL_2]}{k_{-4}[L] + k_5[ArX]}$$

$$rate = k_5[PdL][ArX] = \frac{k_4 k_5[PdL_2][ArX]}{k_{-4}[L] + k_5[ArX]}$$

$rate = k_{obs}[PdL_2]$; therefore,

$$k_{obs} = \frac{k_4 k_5[ArX]}{k_{-4}[L] + k_5[ArX]}$$

If k_5[ArX] >> k_{-4}[L]

The term k_{-4}[L] in k_{obs} denominator can be ignored and the expression for k_{obs} gets reduced to $k_{obs} = k_4$.

Derivation of the rate expressions. Scheme 27.

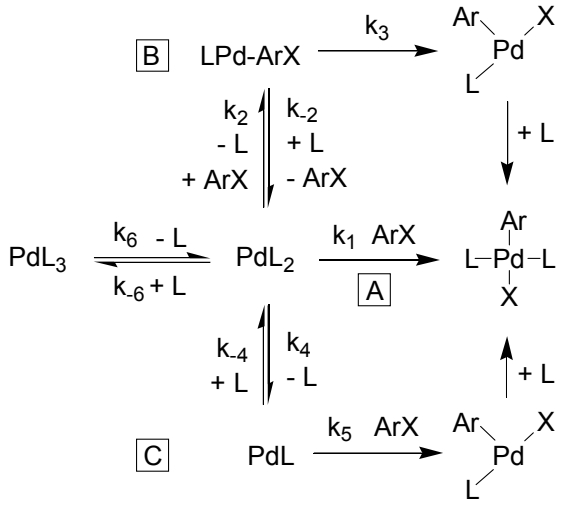

$$rate = [PdL_3]k_{obs}$$

A. Direct reaction to L_2Pd

$$k_{obs} = \frac{k_6 k_1[ArX]}{k_1[ArX] + k_{-6}[L]}$$

$$1/k_{obs} = \frac{1}{k_6} + \frac{[L]}{K_6 k_1[ArX]}$$

B. Associative displacement of the ligand in L_2Pd

$$k_{obs} = \frac{k_6 k_2 k_3[ArX]}{k_2 k_3[ArX] + k_3 k_{-6}[L] + k_{-6} k_{-2}[L]^2}$$

$$1/k_{obs} = \frac{1}{k_6} + \frac{[L]}{K_6 k_2[ArX]} + \frac{[L]^2}{K_6 K_2 k_3[ArX]}$$

C. Dissociation of ligand from

L_2Pd

$$k_{obs} = \frac{k_6 k_4 k_5[\mathrm{ArX}]}{k_4 k_5[\mathrm{ArX}] + k_5 k_{-6}[\mathrm{ArX}][\mathrm{L}] + k_{-6} k_{-4}[\mathrm{L}}$$

$$1/k_{obs} = \frac{1}{k_6} + \frac{[\mathrm{L}]}{K_6 k_4} + \frac{[\mathrm{L}]^2}{K_6 K_4 k_5[\mathrm{ArX}]}$$

Path A

Under the steady state approximation,

$$\frac{\mathrm{d}[\mathrm{PdL}_2]}{\mathrm{d}t} = 0 = k_6[\mathrm{PdL}_3] - k_{-6}[\mathrm{PdL}_2][\mathrm{L}] - k_1[\mathrm{PdL}_2][\mathrm{ArX}]$$

Solving for $[PdL_2]$,

$$[\mathrm{PdL}_2] = \frac{k_6[\mathrm{PdL}_3]}{k_{-6}[\mathrm{L}] + k_1[\mathrm{ArX}]}$$

$$rate = k_1[\mathrm{PdL}_2][\mathrm{ArX}] = \frac{k_6 k_1[\mathrm{PdL}_3][\mathrm{ArX}]}{k_{-6}[\mathrm{L}] + k_1[\mathrm{ArX}]}$$

$rate = k_{obs}[PdL_3]$; therefore,

$$k_{obs} = \frac{k_6 k_1[\mathrm{ArX}]}{k_{-6}[\mathrm{L}] + k_1[\mathrm{ArX}]}$$

Path B

Under the steady state approximation,

$$\frac{\mathrm{d}[\mathrm{LPd(ArX)}]}{\mathrm{d}t} = 0 = k_2[\mathrm{PdL}_2][\mathrm{ArX}] - k_{-2}[\mathrm{LPd(ArX)}][\mathrm{L}] - k_3[\mathrm{LPd(ArX)}]$$

(1)

$$\frac{\mathrm{d}[\mathrm{PdL_2}]}{\mathrm{d}t} = 0 = k_6[\mathrm{PdL_3}] + k_{-2}[\mathrm{LPd(ArX)}][\mathrm{L}] - k_{-6}[\mathrm{PdL_2}][\mathrm{L}] - k_2[\mathrm{PdL_2}][\mathrm{ArX}] \quad (2)$$

Solving for [LPd(ArX)],

$$[\mathrm{LPd(ArX)}] = \frac{k_2[\mathrm{PdL_2}][\mathrm{ArX}]}{k_{-2}[\mathrm{L}] + k_3} \quad (3)$$

Adding equations (1) and (2),

$$0 = k_6[\mathrm{PdL_3}] - k_{-6}[\mathrm{PdL_2}][\mathrm{L}] - k_3[\mathrm{LPd(ArX)}]$$

Solving for [PdL_2],

$$[\mathrm{PdL_2}] = \frac{k_6[\mathrm{PdL_3}] - k_3[\mathrm{LPd(ArX)}]}{k_{-6}[\mathrm{L}]}$$

Substituting [PdL_2] into (3),

$$[\mathrm{LPd(ArX)}] = \frac{k_6k_2[\mathrm{PdL_3}][\mathrm{ArX}] - k_2k_3[\mathrm{LPd(ArX)}][\mathrm{ArX}]}{k_{-6}k_{-2}[\mathrm{L}]^2 + k_{-6}k_3[\mathrm{L}]}$$

Solving for [LPd(ArX)],

$$[\mathrm{LPd(ArX)}] = \frac{k_6k_2[\mathrm{PdL_3}][\mathrm{ArX}]}{k_{-6}k_{-2}[\mathrm{L}]^2 + k_{-6}k_3[\mathrm{L}] + k_2k_3[\mathrm{ArX}]}$$

$$rate = k_6[\mathrm{LPd(ArX)}] = \frac{k_6k_2k_3[\mathrm{PdL_3}][\mathrm{ArX}]}{k_{-6}k_{-2}[\mathrm{L}]^2 + k_{-6}k_3[\mathrm{L}] + k_2k_3[\mathrm{ArX}]} = k_{obs}[\mathrm{PdL_3}]$$

Therefore,

$$k_{obs} = \frac{k_6k_2k_3[\mathrm{ArX}]}{k_{-6}k_{-2}[\mathrm{L}]^2 + k_{-6}k_3[\mathrm{L}] + k_2k_3[\mathrm{ArX}]}$$

Path C

Under the steady state approximation,

$$\frac{\mathrm{d}[\mathrm{PdL}]}{\mathrm{d}t} = 0 = k_4[\mathrm{PdL}_2] - k_{-4}[\mathrm{PdL}][\mathrm{L}] - k_5[\mathrm{PdL}][\mathrm{ArX}] \quad (4)$$

$$\frac{\mathrm{d}[\mathrm{PdL}_2]}{\mathrm{d}t} = 0 = k_6[\mathrm{PdL}_3] + k_{-4}[\mathrm{PdL}][\mathrm{L}] - k_{-6}[\mathrm{PdL}_2][\mathrm{L}] - k_4[\mathrm{PdL}_2]$$

(5)

Solving for [PdL],

$$[\mathrm{PdL}] = \frac{k_4[\mathrm{PdL}_2]}{k_{-4}[\mathrm{L}] + \mathrm{k}_5[\mathrm{ArX}]}$$

(6)

Adding equations (4) and (5),

$$0 = k_6[\mathrm{PdL}_3] - k_{-6}[\mathrm{PdL}_2][\mathrm{L}] - k_5[\mathrm{PdL}][\mathrm{ArX}]$$

Solving for [PdL_2],

$$[\mathrm{PdL}_2] = \frac{k_6[\mathrm{PdL}_3] - k_5[\mathrm{ArX}][\mathrm{PdL}]}{k_{-6}[\mathrm{L}]}$$

Substituting [PdL_2] into (3),

$$[\mathrm{PdL}] = \frac{k_6k_4[\mathrm{PdL}_3] - k_4k_5[\mathrm{ArX}][\mathrm{PdL}]}{k_{-6}k_{-4}[\mathrm{L}]^2 + k_{-6}k_5[\mathrm{ArX}][\mathrm{L}]}$$

Solving for [PdL],

$$[\mathrm{PdL}] = \frac{k_6k_4[\mathrm{PdL}_3]}{k_{-6}k_{-4}[\mathrm{L}]^2 + k_{-6}k_5[\mathrm{ArX}][\mathrm{L}] + k_4k_5[\mathrm{ArX}]}$$

$$rate = k_5[\mathrm{PdL}][\mathrm{ArX}] = \frac{k_6k_4k_5[\mathrm{PdL}_3][\mathrm{ArX}]}{k_{-6}k_{-4}[\mathrm{L}]^2 + k_{-6}k_5[\mathrm{ArX}][\mathrm{L}] + k_4k_5[\mathrm{ArX}]} = k_{obs}[\mathrm{PdL}_3]$$

Therefore,

$$k_{obs} = \frac{k_6 k_4 k_5 [\mathrm{ArX}]}{k_{-6} k_{-4} [\mathrm{L}]^2 + k_{-6} k_5 [\mathrm{ArX}][\mathrm{L}] + k_4 k_5 [\mathrm{ArX}]}$$

X ray crystallographic data for $[(P^tBu_3)Pd(2\text{-}CF_3C_6H_4)(Cl)]_2$ (10)

Data Collection

A pale yellow plate crystal of $C_{38}H_{62}Cl_2F_6P_2Pd_2$ having approximate dimensions of 0.20 x 0.20 x 0.08 mm^3 was mounted with epoxy cement on the tip of a fine glass fiber. All measurements were made on a Nonius KappaCCD diffractometer with graphite monochromated Mo-Kα radiation.

Cell constants and an orientation matrix for data collection corresponded to a primitive monoclinic cell with dimensions:

a = 8.2900(17) Å α = 90 °

b = 24.948(5) Å β = 106.86(3) °

c = 10.626(2) Å γ = 90 °

V = 2103.2(7) $Å^3$

For Z = 2 and F.W. = 978.52, the calculated density is 1.545 g/cm^3. Based on a statistical analysis of intensity distribution, and the successful solution and refinement of the structure, the space group was determined to be $P2_1$ (#4).

The data were collected at a temperature of 173(2) K to a maximum 2θ value of 56.52 °. Four omega scans consisting of 108, 85, 101, and 42 data frames, respectively, were collected with a frame width of 0.7 ° and a detector-to-crystal distance, Dx, of 35.0 mm. Each frame was exposed twice (for the purpose of de-zingering) for a total of 84 s. The data frames were processed and scaled using the DENZO software package.[55]

Data Reduction

A total of 8016 reflections were collected of which 8016 were unique and observed (R_{int} = 0.000, Friedel pairs not merged). The linear absorption coefficient, μ, for Mo-Kα radiation is 11.11 cm^{-1}, and no absorption correction was applied. The data were corrected for Lorentz and polarization effects.

Structure Solution and Refinement

The structure was solved by direct methods and expanded using Fourier techniques.[56] The non-hydrogen atoms were refined anisotropically, and hydrogen atoms were treated as idealized contributions. The final cycle of full-matrix least-squares refinement[3] on F was based on 8016 observed reflections ($I > 2.00\sigma(I)$) and 559 variable parameters and converged with unweighted and weighted agreement factors of:

$$R = \Sigma \, ||Fo| - |Fc|| \, / \, \Sigma \, |Fo| = 0.0427$$

$$R_W = \{\Sigma[w \, (F_o^2 - F_c^2)^2] \, / \, \Sigma[w(F_o^2)^2]\}^{1/2} = 0.1089$$

The maximum and minimum peaks on the final difference Fourier map corresponded to 1.301 and –0.838 $e^-/Å^3$ respectively.

Structural Description

The compound crystallized in the chiral monoclinic space group $P2_1$ with one molecule in the asymmetric unit and two molecules in the unit cell. Pd(1) and Pd(2) are

separated by 3.61 Å and bridged by two μ_2-chloride ligands. The chloride ligands bond nearly symmetrically with the Pd-Cl bond distances ranging from 2.3913(16) to 2.4817(17) Å. The mean deviations of the palladium coordination planes are 0.04 Å for Pd(1) and 0.11 Å for Pd(2) and these planes intersect at an angle of 145.6 ° as illustrated in Figure 1.

The molecule possesses a pseudo-center of inversion but the molecular symmetry is disrupted by severe disorder. Although the environment about Pd(1) is well-ordered, the phosphine and aryl groups bonded to Pd(2) are disordered over several positions. Two of the *tert*-butyl groups, C(20-23) and C(24-27), were refined with alternate positions at occupancy factor ratios of 50:50. All components were refined with anisotropic displacement parameters. As illustrated in Figure 2 the alternate location of the aryl group is offset from the primary component by 180 °. The occupancy factor for this group was refined to 70:30 and the minor component was refined with isotropic displacement parameters.

The molecule was refined as a racemic twin and thus the absolute configuration could not be unambiguously determined. There are no significant intermolecular contacts.

Table 2. Crystal data and structure refinement for $[(P^tBu_3)Pd(2\text{-}CF_3C_6H_4)(Cl)]_2$ (**10**)

Empirical formula	$C_{38}\ H_{62}\ Cl_2\ F_6\ P_2\ Pd_2$	
Formula weight	978.52	
Temperature	173(2) K	
Wavelength	0.71073 Å	
Crystal system	Monoclinic	
Space group	P2(1)	
Unit cell dimensions	a = 8.2900(17) Å	□= 90°.
	b = 24.948(5) Å	□= 106.86(3)°.
	c = 10.626(2) Å	□ = 90°.
Volume	2103.2(7) Å^3	
Z	2	
Density (calculated)	1.545 g/cm^3	
Absorption coefficient	11.11 cm^{-1}	
F(000)	1000	
;	0.20 x 0.20 x 0.08 mm^3	
Theta range for data collection	2.57 to 28.26°.	
Index ranges	-11<=h<=11, -33<=k<=23, -14<=l<=14	
Reflections collected	8016	
Independent reflections	8016 [R(int) = 0.0000]	
Completeness to theta = 28.26°	99.2 %	
Absorption correction	None	
Max. and min. transmission	0.9164 and 0.8084	
Refinement method	Full-matrix least-squares on F^2	
Data / restraints / parameters	8016 / 1 / 559	
Goodness-of-fit on F^2	1.015	
Final R indices [I>2sigma(I)]	R1 = 0.0427, wR2 = 0.1089	
R indices (all data)	R1 = 0.0514, wR2 = 0.1146	
Absolute structure parameter	0.17(3)	
Largest diff. peak and hole	1.301 and -0.838 e.Å^{-3}	

Table 3. Atomic coordinates (x 10^4) and equivalent isotropic displacement parameters ($Å^2$x 10^3) for [(P^tBu_3)Pd(2-$CF_3C_6H_4$)(Cl)]$_2$ (**10**). U(eq) is defined as one third of the trace of the orthogonalized U^{ij} tensor.

	x	y	z	U(eq)
Pd(1)	8676(1)	3424(1)	7418(1)	34(1)
Pd(2)	6889(1)	2167(1)	8043(1)	34(1)
P(1)	8705(2)	3967(1)	5601(1)	32(1)
P(2)	5695(2)	1789(1)	9609(2)	37(1)
Cl(2)	8147(2)	2513(1)	6442(2)	49(1)
Cl(1)	8672(2)	2899(1)	9300(2)	50(1)
F(1)	5627(5)	4686(2)	8326(6)	81(1)
F(2)	5733(6)	4126(3)	9872(5)	82(2)
F(3)	5743(4)	3851(2)	7980(4)	59(1)
C(1)	10203(6)	3610(3)	4771(6)	41(1)
C(2)	10712(8)	3965(3)	3724(7)	51(2)
C(3)	9451(8)	3102(3)	4075(7)	51(2)
C(4)	11777(7)	3460(3)	5894(6)	49(2)
C(5)	6488(6)	3968(3)	4385(6)	41(1)
C(6)	6386(8)	4090(3)	2955(7)	53(2)
C(7)	5686(6)	3418(3)	4459(7)	52(2)
C(8)	5367(7)	4375(3)	4827(7)	51(2)
C(9)	9430(8)	4709(3)	5852(7)	45(1)
C(10)	8931(9)	5035(3)	4580(8)	57(2)
C(11)	8651(9)	4993(3)	6826(7)	50(2)
C(12)	11352(8)	4741(3)	6505(7)	57(2)
C(13)	9295(7)	4007(2)	8740(6)	36(1)
C(14)	11062(7)	4090(3)	9296(7)	44(1)
C(15)	11692(9)	4441(3)	10334(7)	55(2)

Table 3 (cont.)

C(16)	10605(10)	4714(3)	10880(7)	59(2)
C(17)	8897(9)	4615(3)	10382(6)	49(2)
C(18)	8244(8)	4271(3)	9333(6)	41(1)
C(19)	6369(8)	4231(3)	8863(7)	47(2)
C(20)	7540(9)	1576(3)	11071(7)	57(2)
C(21)	7440(40)	1450(20)	12370(40)	121(16)
C(22)	8110(30)	981(7)	10686(18)	73(5)
C(23)	9037(18)	1910(8)	11252(16)	65(4)
C(21')	6970(30)	1345(14)	12220(30)	75(8)
C(22')	8912(17)	1363(9)	10602(15)	67(4)
C(23')	8340(20)	2135(8)	11863(16)	72(4)
C(24)	4450(9)	2347(3)	10164(8)	56(2)
C(25)	3591(17)	2689(6)	9007(15)	53(3)
C(26)	3380(20)	2199(10)	11030(20)	50(5)
C(27)	5826(17)	2748(6)	11098(15)	47(3)
C(25')	2600(20)	2346(7)	9010(20)	72(5)
C(26')	4070(30)	2256(11)	11460(30)	72(7)
C(27')	5110(30)	2848(7)	10000(30)	88(6)
C(28)	4208(12)	1177(4)	9166(8)	69(2)
C(29)	3541(14)	984(4)	10269(10)	86(3)
C(30)	2740(20)	1286(8)	8033(15)	205(12)
C(31)	5120(30)	718(5)	8700(20)	184(11)
C(36)	4782(10)	1150(3)	4649(7)	53(2)
C(32)	5427(10)	1775(3)	6507(8)	35(2)
C(33)	3878(15)	2008(6)	5882(15)	60(3)
C(34)	2857(18)	1821(6)	4720(13)	67(3)
C(35)	3334(16)	1378(5)	4093(11)	69(3)
C(37)	5872(12)	1349(4)	5871(9)	43(2)

Table 3 (cont.)

C(38)	7578(15)	1063(5)	6379(12)	55(3)
F(4)	8431(8)	1159(3)	7603(6)	70(2)
F(5)	7409(12)	537(3)	6287(10)	86(2)
F(6)	8597(10)	1179(3)	5626(8)	83(2)
C(32')	6210(20)	1559(8)	6737(19)	29(3)
C(33')	7210(30)	1112(8)	6840(20)	33(4)
C(34')	6990(40)	742(15)	5790(30)	58(7)
C(35')	5720(30)	766(10)	4750(30)	52(5)
C(37')	4880(20)	1578(8)	5583(18)	30(3)
C(38')	3640(40)	2029(11)	5220(30)	44(6)
F(4')	2071(19)	1826(8)	4940(20)	80(6)
F(5')	3742(17)	2385(7)	6145(14)	61(4)
F(6')	3670(20)	2297(6)	4169(14)	63(4)

Table 4. Bond lengths [Å] and angles [°] for $[(P^tBu_3)Pd(2\text{-}CF_3C_6H_4)(Cl)]_2$ (**10**).

Pd(1)-C(13)	1.984(6)
Pd(1)-P(1)	2.3645(15)
Pd(1)-Cl(1)	2.3913(16)
Pd(1)-Cl(2)	2.4814(17)
Pd(2)-C(32)	1.985(8)
Pd(2)-C(32')	2.02(2)
Pd(2)-P(2)	2.3650(15)
Pd(2)-Cl(2)	2.3994(15)
Pd(2)-Cl(1)	2.4817(17)
P(1)-C(5)	1.916(6)
P(1)-C(1)	1.937(5)
P(1)-C(9)	1.940(7)
P(2)-C(20)	1.913(7)
P(2)-C(24)	1.923(7)
P(2)-C(28)	1.933(7)
F(1)-C(19)	1.338(8)
F(2)-C(19)	1.350(8)
F(3)-C(19)	1.328(8)
C(1)-C(3)	1.508(10)
C(1)-C(4)	1.537(8)
C(1)-C(2)	1.573(8)
C(5)-C(6)	1.527(9)
C(5)-C(7)	1.536(10)
C(5)-C(8)	1.539(9)
C(9)-C(10)	1.529(10)
C(9)-C(11)	1.542(9)
C(9)-C(12)	1.545(9)
C(13)-C(18)	1.382(8)

Table 4 (cont.)

C(13)-C(14)	1.427(8)
C(14)-C(15)	1.385(10)
C(15)-C(16)	1.384(12)
C(16)-C(17)	1.382(10)
C(17)-C(18)	1.387(9)
C(18)-C(19)	1.492(9)
C(20)-C(21)	1.44(4)
C(20)-C(22')	1.467(18)
C(20)-C(23)	1.461(19)
C(20)-C(21')	1.54(3)
C(20)-C(22)	1.645(18)
C(20)-C(23')	1.66(2)
C(24)-C(27')	1.40(2)
C(24)-C(25)	1.496(16)
C(24)-C(26)	1.50(2)
C(24)-C(26')	1.52(3)
C(24)-C(27)	1.622(15)
C(24)-C(25')	1.67(2)
C(28)-C(30)	1.466(17)
C(28)-C(29)	1.512(11)
C(28)-C(31)	1.531(16)
C(36)-C(35')	1.22(3)
C(36)-C(35)	1.305(15)
C(36)-C(37')	1.44(2)
C(36)-C(37)	1.437(12)
C(32)-C(33)	1.391(15)
C(32)-C(37)	1.368(13)
C(33)-C(34)	1.361(19)

Table 4 (cont.)

C(34)-C(35)	1.41(2)
C(37)-C(38)	1.535(16)
C(38)-F(4)	1.310(14)
C(38)-F(5)	1.322(14)
C(38)-F(6)	1.352(14)
C(32')-C(37')	1.39(3)
C(32')-C(33')	1.38(3)
C(33')-C(34')	1.42(4)
C(34')-C(35')	1.29(4)
C(37')-C(38')	1.50(3)
C(38')-F(4')	1.35(3)
C(38')-F(6')	1.31(3)
C(38')-F(5')	1.31(3)

C(13)-Pd(1)-P(1)	95.52(17)
C(13)-Pd(1)-Cl(1)	82.62(17)
P(1)-Pd(1)-Cl(1)	178.14(6)
C(13)-Pd(1)-Cl(2)	160.88(18)
P(1)-Pd(1)-Cl(2)	103.04(5)
Cl(1)-Pd(1)-Cl(2)	78.81(6)
C(32)-Pd(2)-C(32')	23.7(5)
C(32)-Pd(2)-P(2)	95.8(2)
C(32')-Pd(2)-P(2)	95.4(5)
C(32)-Pd(2)-Cl(2)	83.2(2)
C(32')-Pd(2)-Cl(2)	82.9(5)
P(2)-Pd(2)-Cl(2)	177.57(6)
C(32)-Pd(2)-Cl(1)	158.6(2)
C(32')-Pd(2)-Cl(1)	157.7(5)

Table 4 (cont.)

P(2)-Pd(2)-Cl(1)	102.69(5)
Cl(2)-Pd(2)-Cl(1)	78.65(6)
C(5)-P(1)-C(1)	108.1(3)
C(5)-P(1)-C(9)	106.9(3)
C(1)-P(1)-C(9)	106.7(3)
C(5)-P(1)-Pd(1)	108.46(19)
C(1)-P(1)-Pd(1)	105.53(19)
C(9)-P(1)-Pd(1)	120.7(2)
C(20)-P(2)-C(24)	109.0(4)
C(20)-P(2)-C(28)	106.3(4)
C(24)-P(2)-C(28)	106.6(4)
C(20)-P(2)-Pd(2)	106.5(2)
C(24)-P(2)-Pd(2)	107.4(2)
C(28)-P(2)-Pd(2)	120.7(2)
Pd(2)-Cl(2)-Pd(1)	95.38(5)
Pd(1)-Cl(1)-Pd(2)	95.59(6)
C(3)-C(1)-C(4)	108.2(5)
C(3)-C(1)-C(2)	106.6(5)
C(4)-C(1)-C(2)	110.2(5)
C(3)-C(1)-P(1)	112.4(4)
C(4)-C(1)-P(1)	105.7(4)
C(2)-C(1)-P(1)	113.7(4)
C(6)-C(5)-C(7)	109.2(6)
C(6)-C(5)-C(8)	108.0(5)
C(7)-C(5)-C(8)	105.3(5)
C(6)-C(5)-P(1)	115.9(4)
C(7)-C(5)-P(1)	108.0(4)
C(8)-C(5)-P(1)	109.9(4)

Table 4 (cont.)

C(10)-C(9)-C(11)	106.8(6)
C(10)-C(9)-C(12)	110.4(5)
C(11)-C(9)-C(12)	104.7(6)
C(10)-C(9)-P(1)	113.1(5)
C(11)-C(9)-P(1)	111.0(4)
C(12)-C(9)-P(1)	110.5(5)
C(18)-C(13)-C(14)	116.7(6)
C(18)-C(13)-Pd(1)	127.2(4)
C(14)-C(13)-Pd(1)	115.1(4)
C(15)-C(14)-C(13)	121.8(6)
C(14)-C(15)-C(16)	120.2(6)
C(15)-C(16)-C(17)	118.1(7)
C(16)-C(17)-C(18)	122.4(7)
C(13)-C(18)-C(17)	120.8(6)
C(13)-C(18)-C(19)	123.3(6)
C(17)-C(18)-C(19)	115.9(6)
F(3)-C(19)-F(1)	105.5(6)
F(3)-C(19)-F(2)	105.1(5)
F(1)-C(19)-F(2)	105.4(5)
F(3)-C(19)-C(18)	116.1(5)
F(1)-C(19)-C(18)	113.0(5)
F(2)-C(19)-C(18)	110.9(6)
C(21)-C(20)-C(22')	121(2)
C(21)-C(20)-C(23)	106.5(12)
C(22')-C(20)-C(23)	62.5(11)
C(21)-C(20)-C(21')	17.1(15)
C(22')-C(20)-C(21')	125.3(16)
C(23)-C(20)-C(21')	123.6(12)

Table 4 (cont.)

C(21)-C(20)-C(22)	98(2)
C(22')-C(20)-C(22)	44.0(10)
C(23)-C(20)-C(22)	104.6(11)
C(21')-C(20)-C(22)	92.1(17)
C(21)-C(20)-C(23')	80.0(19)
C(22')-C(20)-C(23')	103.9(12)
C(23)-C(20)-C(23')	41.9(9)
C(21')-C(20)-C(23')	94.7(15)
C(22)-C(20)-C(23')	141.2(12)
C(21)-C(20)-P(2)	125.6(15)
C(22')-C(20)-P(2)	109.9(7)
C(23)-C(20)-P(2)	113.4(7)
C(21')-C(20)-P(2)	113.0(9)
C(22)-C(20)-P(2)	105.6(8)
C(23')-C(20)-P(2)	106.5(7)
C(27')-C(24)-C(25)	59.8(13)
C(27')-C(24)-C(26)	128.3(14)
C(25)-C(24)-C(26)	114.9(11)
C(27')-C(24)-C(26')	116.0(15)
C(25)-C(24)-C(26')	130.9(13)
C(26)-C(24)-C(26')	24.2(9)
C(27')-C(24)-C(27)	45.0(12)
C(25)-C(24)-C(27)	103.5(9)
C(26)-C(24)-C(27)	102.2(10)
C(26')-C(24)-C(27)	80.3(11)
C(27')-C(24)-C(25')	102.6(13)
C(25)-C(24)-C(25')	43.7(9)
C(26)-C(24)-C(25')	82.6(10)

Table 4 (cont.)

C(26')-C(24)-C(25')	106.2(13)
C(27)-C(24)-C(25')	141.8(10)
C(27')-C(24)-P(2)	110.2(9)
C(25)-C(24)-P(2)	109.3(6)
C(26)-C(24)-P(2)	118.4(11)
C(26')-C(24)-P(2)	116.3(11)
C(27)-C(24)-P(2)	106.8(6)
C(25')-C(24)-P(2)	103.6(7)
C(30)-C(28)-C(29)	107.1(10)
C(30)-C(28)-C(31)	103.9(13)
C(29)-C(28)-C(31)	109.7(10)
C(30)-C(28)-P(2)	111.8(8)
C(29)-C(28)-P(2)	114.4(5)
C(31)-C(28)-P(2)	109.4(7)
C(35')-C(36)-C(35)	149.5(15)
C(35')-C(36)-C(37')	127.8(16)
C(35)-C(36)-C(37')	81.5(10)
C(35')-C(36)-C(37)	88.5(14)
C(35)-C(36)-C(37)	120.9(9)
C(37')-C(36)-C(37)	39.5(8)
C(33)-C(32)-C(37)	115.7(10)
C(33)-C(32)-Pd(2)	116.5(9)
C(37)-C(32)-Pd(2)	127.0(7)
C(32)-C(33)-C(34)	122.3(14)
C(33)-C(34)-C(35)	120.9(13)
C(36)-C(35)-C(34)	118.4(10)
C(32)-C(37)-C(36)	121.7(8)
C(32)-C(37)-C(38)	122.7(9)

Table 4 (cont.)

C(36)-C(37)-C(38)	115.6(8)
F(4)-C(38)-F(5)	105.6(10)
F(4)-C(38)-F(6)	107.4(10)
F(5)-C(38)-F(6)	103.9(10)
F(4)-C(38)-C(37)	116.2(10)
F(5)-C(38)-C(37)	111.6(10)
F(6)-C(38)-C(37)	111.3(9)
C(37')-C(32')-C(33')	113.7(19)
C(37')-C(32')-Pd(2)	124.9(16)
C(33')-C(32')-Pd(2)	120.8(15)
C(34')-C(33')-C(32')	122(2)
C(33')-C(34')-C(35')	122(3)
C(36)-C(35')-C(34')	117(3)
C(32')-C(37')-C(36)	117.0(16)
C(32')-C(37')-C(38')	124(2)
C(36)-C(37')-C(38')	118.6(19)
F(4')-C(38')-F(6')	105(3)
F(4')-C(38')-F(5')	106(2)
F(6')-C(38')-F(5')	106(2)
F(4')-C(38')-C(37')	109(2)
F(6')-C(38')-C(37')	115.0(19)
F(5')-C(38')-C(37')	115(3)

Table 5. Anisotropic displacement parameters ($Å^2 x\ 10^3$) for $[(P^tBu_3)Pd(2\text{-}CF_3C_6H_4)(Cl)]_2$ (**10**).The anisotropic displacement factor exponent takes the form: $-2\pi^2[h^2 a^{*2} U^{11} + ... + 2 h k a^* b^* U^{12}]$

	U^{11}	U^{22}	U^{33}	U^{23}	U^{13}	U^{12}
Pd(1)	32(1)	34(1)	35(1)	1(1)	10(1)	-8(1)
Pd(2)	36(1)	33(1)	32(1)	3(1)	9(1)	-4(1)
P(1)	25(1)	37(1)	33(1)	1(1)	8(1)	-5(1)
P(2)	41(1)	35(1)	34(1)	1(1)	11(1)	-5(1)
Cl(2)	68(1)	40(1)	46(1)	-4(1)	29(1)	-16(1)
Cl(1)	64(1)	46(1)	37(1)	1(1)	12(1)	-21(1)
F(1)	56(2)	64(3)	113(4)	11(3)	9(2)	13(2)
F(2)	61(3)	136(5)	58(3)	-6(3)	33(2)	-8(3)
F(3)	37(2)	75(3)	66(3)	-14(2)	18(2)	-5(2)
C(1)	25(2)	53(4)	48(3)	3(3)	15(2)	0(2)
C(2)	39(3)	64(4)	54(4)	12(3)	23(3)	-2(3)
C(3)	52(3)	54(4)	57(4)	2(3)	30(3)	6(3)
C(4)	31(2)	59(4)	57(4)	13(4)	14(2)	7(3)
C(5)	24(2)	61(4)	37(3)	2(3)	6(2)	-1(2)
C(6)	39(3)	71(5)	42(4)	8(3)	1(3)	3(3)
C(7)	28(2)	70(4)	51(4)	-1(4)	3(2)	-16(3)
C(8)	29(3)	64(4)	58(4)	10(3)	12(3)	11(3)
C(9)	45(3)	39(3)	49(4)	11(3)	13(3)	-10(3)
C(10)	59(4)	50(4)	63(5)	15(4)	17(3)	-8(3)
C(11)	57(3)	32(3)	62(4)	3(3)	20(3)	2(3)
C(12)	56(4)	50(4)	59(4)	-12(4)	5(3)	-26(3)
C(13)	38(3)	36(3)	31(3)	-2(2)	8(2)	-4(2)
C(14)	34(3)	44(3)	46(4)	2(3)	-1(2)	-6(2)
C(15)	52(4)	52(4)	48(4)	9(3)	-5(3)	-10(3)

Table 5 (cont.)

C(16) 75(5)	48(4)	43(4)	-2(3)	0(3)	-14(4)
C(17) 70(4)	40(3)	35(3)	1(3)	15(3)	-7(3)
C(18) 47(3)	39(3)	36(3)	2(3)	10(3)	-4(2)
C(19) 52(3)	41(4)	50(4)	1(3)	20(3)	3(3)
C(20) 59(4)	64(5)	45(4)	20(4)	9(3)	15(3)
C(21) 66(19)	230(40)	54(14)	9(17)	-1(13)	-80(20)
C(22) 98(13)	64(11)	61(10)	29(9)	28(9)	46(10)
C(23) 48(8)	91(12)	48(9)	6(9)	1(6)	13(7)
C(21') 37(11)	140(20)	30(10)	48(13)	-13(8)	-27(12)
C(22') 42(7)	95(13)	49(9)	26(9)	-9(6)	-1(8)
C(23') 89(11)	72(11)	45(8)	8(9)	3(8)	-5(10)
C(24) 62(4)	53(4)	59(4)	3(3)	30(4)	9(3)
C(25) 46(7)	53(8)	59(9)	-5(7)	14(6)	15(6)
C(26) 40(8)	67(12)	46(10)	-21(9)	19(7)	5(8)
C(27) 55(7)	41(7)	47(8)	-20(6)	16(6)	-7(6)
C(25') 56(8)	65(10)	99(14)	19(9)	28(9)	27(8)
C(26') 105(19)	53(11)	73(18)	-9(12)	50(14)	-5(14)
C(27') 95(14)	52(11)	130(20)	16(12)	52(15)	8(9)
C(28) 98(6)	64(5)	56(5)	-23(4)	38(4)	-47(4)
C(29) 118(8)	74(6)	80(6)	-15(5)	49(6)	-57(6)
C(30) 155(13)	260(20)	132(11)	70(13)	-69(10)	-177(16)
C(31) 250(20)	74(8)	320(30)	-98(12)	220(20)	-83(11)
C(36) 68(4)	57(4)	37(4)	-7(3)	22(3)	-17(3)
C(32) 34(4)	35(4)	32(4)	1(4)	3(3)	-4(3)
C(33) 62(7)	71(9)	43(7)	11(6)	10(5)	14(6)
C(34) 43(7)	82(9)	63(8)	1(7)	-6(6)	0(7)
C(35) 74(7)	74(8)	42(6)	-1(6)	-9(5)	-30(6)
C(37) 55(5)	37(5)	42(5)	3(4)	21(4)	-7(4)

Table 5 (cont.)

C(38)	57(6)	63(8)	50(7)	3(6)	22(6)	-2(5)
F(4)	65(4)	89(5)	57(4)	-2(3)	20(3)	33(3)
F(5)	110(6)	47(4)	101(7)	0(4)	30(5)	17(4)
F(6)	90(5)	94(5)	86(5)	31(4)	58(4)	35(4)
F(4')	27(7)	97(13)	105(15)	20(10)	1(8)	17(8)
F(5')	65(8)	66(10)	43(8)	-1(7)	-2(6)	44(7)
F(6')	91(10)	62(9)	44(7)	0(6)	29(7)	3(7)

Table 6. Hydrogen coordinates (x 10^4) and isotropic displacement parameters (Å^{2}x 10^3) for [(P^tBu_3)Pd(2-$CF_3C_6H_4$)(Cl)]$_2$ (**10**).

	x	y	z	U(eq)
H(2A)	11467	3761	3343	76
H(2B)	11290	4289	4150	76
H(2C)	9697	4067	3026	76
H(3A)	10241	2940	3656	77
H(3B)	8392	3185	3404	77
H(3C)	9231	2850	4713	77
H(4A)	12597	3282	5531	73
H(4B)	11456	3216	6505	73
H(4C)	12280	3785	6363	73
H(6A)	5205	4084	2419	79
H(6B)	7022	3819	2630	79
H(6C)	6866	4445	2900	79
H(7A)	4543	3411	3852	77
H(7B)	5638	3355	5358	77
H(7C)	6367	3137	4216	77
H(8A)	4234	4371	4204	76
H(8B)	5853	4734	4856	76
H(8C)	5299	4277	5704	76
H(10A)	9310	5407	4770	86
H(10B)	7702	5029	4205	86
H(10C)	9460	4880	3950	86
H(11A)	9024	5367	6929	74
H(11B)	9015	4812	7680	74
H(11C)	7419	4980	6487	74

Table 6 (cont.)

H(12A)	11697	5118	6630	86
H(12B)	11940	4566	5939	86
H(12C)	11639	4560	7360	86
H(14A)	11827	3901	8945	53
H(15A)	12873	4494	10672	65
H(16A)	11021	4962	11577	71
H(17A)	8143	4790	10773	58
H(21A)	8557	1353	12936	181
H(21B)	6664	1147	12316	181
H(21C)	7016	1762	12736	181
H(22A)	9061	850	11404	110
H(22B)	8457	1009	9880	110
H(22C)	7164	732	10544	110
H(23A)	9934	1782	12013	97
H(23B)	8762	2282	11401	97
H(23C)	9421	1891	10463	97
H(21D)	7964	1243	12938	112
H(21E)	6265	1028	11917	112
H(21F)	6323	1616	12531	112
H(22D)	9852	1255	11356	100
H(22E)	9294	1641	10101	100
H(22F)	8507	1052	10036	100
H(23D)	9295	2045	12625	108
H(23E)	7472	2319	12160	108
H(23F)	8725	2370	11269	108
H(25A)	2958	2973	9288	80
H(25B)	2816	2468	8335	80
H(25C)	4437	2849	8641	80

Table 6 (cont.)

H(26A)	2827	2520	11232	74
H(26B)	4098	2043	11850	74
H(26C)	2532	1937	10579	74
H(27A)	5242	3040	11401	71
H(27B)	6547	2896	10598	71
H(27C)	6521	2549	11858	71
H(25D)	1870	2623	9207	108
H(25E)	2062	1995	8983	108
H(25F)	2771	2421	8150	108
H(26D)	3435	2563	11649	108
H(26E)	5124	2218	12169	108
H(26F)	3392	1930	11405	108
H(27D)	4464	3129	10283	131
H(27E)	5034	2901	9070	131
H(27F)	6292	2867	10530	131
H(29A)	2794	677	9966	130
H(29B)	2911	1274	10534	130
H(29C)	4486	877	11020	130
H(30A)	2021	968	7837	307
H(30B)	3126	1376	7268	307
H(30C)	2105	1588	8236	307
H(31A)	4360	408	8467	276
H(31B)	6125	618	9404	276
H(31C)	5444	833	7926	276
H(33A)	3519	2309	6279	72
H(34A)	1808	1992	4328	81
H(35A)	2619	1247	3282	82
H(33B)	8070	1049	7640	39

Table 6 (cont.)

H(34B)	7812	468	5856	69
H(35B)	5520	496	4093	62

X ray crystallographic data for $[(1\text{-AdP}^t\text{Bu}_2)\text{Pd(Ph)(Cl)}]_2$ (11)

Data Collection

A pale yellow plate crystal of $C_{48}H_{76}Cl_2P_2Pd_2$ having approximate dimensions of 0.20 x 0.20 x 0.08 mm^3 was mounted with epoxy cement on the tip of a fine glass fiber. All measurements were made on a Nonius KappaCCD diffractometer with graphite monochromated Mo-Kα radiation.

Cell constants and an orientation matrix for data collection corresponded to a primitive monoclinic cell with dimensions:

a = 15.251(3) Å α = 90 °

b = 14.575(3) Å β = 90.64(3) °

c = 20.401(4) Å γ = 90 °

V = 4534.3(16) $Å^3$

For Z = 4 and F.W. = 998.73, the calculated density is 1.463 g/cm^3. Based on a statistical analysis of intensity distribution, and the successful solution and refinement of the structure, the space group was determined to be $P2_1/n$ (#14).

The data were collected at a temperature of 173(2) K to a maximum 2θ value of 56.58 °. Four omega scans consisting of 47, 47, 43, and 21 data frames, respectively, were collected with a frame width of 1.6 ° and a detector-to-crystal distance, Dx, of 35.0 mm. Each frame was exposed twice (for the purpose of de-zingering) for a total of 80 s. The data frames were processed and scaled using the DENZO software package.[55]

Data Reduction

A total of 17957 reflections were collected of which 11194 were unique and observed (R_{int} = 0.0282). The linear absorption coefficient, μ, for Mo-Kα radiation is 10.14 cm^{-1}, and no absorption correction was applied. The data were corrected for Lorentz and polarization effects.

Structure Solution and Refinement

The structure was solved by direct methods and expanded using Fourier techniques.[56] The non-hydrogen atoms were refined anisotropically, and hydrogen atoms were treated as idealized contributions. The final cycle of full-matrix least-squares refinement[5] on F was based on 11194 observed reflections ($I > 2.00\sigma(I)$) and 487 variable parameters and converged with unweighted and weighted agreement factors of:

$$R = \Sigma \, ||Fo| - |Fc|| \, / \, \Sigma \, |Fo| = 0.0386$$

$$R_W = \{\Sigma[w \, (F_o^2 - F_c^2)^2] \, / \, \Sigma[w(F_o^2)^2]\}^{1/2} = 0.0954$$

The maximum and minimum peaks on the final difference Fourier map corresponded to 0.409 and –0.772 $e^-/Å^3$ respectively.

Structural Description

The compound crystallized in the monoclinic space group $P2_1/n$ with one molecule in the asymmetric unit and four molecules in the unit cell. Pd(1) and Pd(2) are separated by 3.78 Å and bridged by two μ_2-chloride ligands that are separated by 3.12 Å. The chloride ligands possess dissimilar Pd-Cl bond distances with shorter Pd-Cl(1) bonds than Pd-

Cl(2) on the order of 0.1 Å. This is probably caused by the steric congestion of the neighboring phosphine ligands. The mean deviations of the palladium coordination planes are 0.06 Å for Pd(1) and 0.15 Å for Pd(2) and these planes intersect at an angle of 166.3 ° as illustrated in Figure 3. The molecule possesses a pseudo-mirror plane that bisects the Cl-Cl vector. The asymmetry is caused by slight differences in the palladium planes and the offsetting orientations of the their respective phenyl rings (88.1 vs. 99.5 °).

There are no significant intermolecular contacts.

Table 7. Crystal data and structure refinement for $[(1\text{-AdP}^t\text{Bu}_2)\text{Pd(Ph)(Cl)}]_2$ (**11**).

Empirical formula	$C_{48}\ H_{76}\ Cl_2\ P_2\ Pd_2$	
Formula weight	998.73	
Temperature	173(2) K	
Wavelength	0.71073 Å	
Crystal system	Monoclinic	
Space group	P2(1)/n	
Unit cell dimensions	a = 15.251(3) Å	□= 90°.
	b = 14.575(3) Å	□= 90.64(3)°.
	c = 20.401(4) Å	□ = 90°.
Volume	4534.3(16) $Å^3$	
Z	4	
Density (calculated)	1.463 g/cm^3	
Absorption coefficient	10.14 cm^{-1}	
F(000)	2080	
Crystal size	0.20 x 0.08 x 0.08 mm^3	
Theta range for data collection	1.68 to 28.29°.	
Index ranges	-20<=h<=20, -19<=k<=19, -27<=l<=27	
Reflections collected	17957	
Independent reflections	11194 [R(int) = 0.0282]	
Completeness to theta = 28.29°	99.3 %	
Absorption correction	None	
Max. and min. transmission	0.9233 and 0.8229	
Refinement method	Full-matrix least-squares on F^2	
Data / restraints / parameters	11194 / 0 / 487	
Goodness-of-fit on F^2	1.006	
Final R indices [I>2sigma(I)]	R1 = 0.0386, wR2 = 0.0954	
R indices (all data)	R1 = 0.0600, wR2 = 0.1042	
Largest diff. peak and hole	0.409 and -0.772 $e.Å^{-3}$	

Table 8. Atomic coordinates (x 10^4) and equivalent isotropic displacement parameters ($Å^2$x 10^3) for [(1-AdP^tBu_2)Pd(Ph)(Cl)]$_2$ (**11**). U(eq) is defined as one third of the trace of the orthogonalized U^{ij} tensor.

	x	y	z	U(eq)
Pd(1)	59(1)	10049(1)	3337(1)	21(1)
Pd(2)	-1397(1)	7955(1)	3300(1)	19(1)
Cl(1)	-1300(1)	9467(1)	3775(1)	24(1)
Cl(2)	-129(1)	8615(1)	2686(1)	36(1)
P(1)	1428(1)	10607(1)	3012(1)	21(1)
P(2)	-1415(1)	6393(1)	3001(1)	19(1)
C(1)	1490(2)	10497(2)	2068(1)	23(1)
C(2)	598(2)	10827(2)	1785(2)	30(1)
C(3)	2240(2)	11029(2)	1731(2)	29(1)
C(4)	1602(2)	9485(2)	1861(1)	25(1)
C(5)	563(2)	10735(2)	1038(2)	35(1)
C(6)	1307(2)	11287(3)	732(2)	40(1)
C(7)	2190(2)	10919(3)	982(2)	37(1)
C(8)	2278(2)	9916(2)	795(2)	40(1)
C(9)	1543(2)	9372(2)	1109(2)	34(1)
C(10)	660(2)	9730(3)	859(2)	40(1)
C(11)	2280(2)	9811(2)	3423(2)	28(1)
C(12)	2402(2)	10094(2)	4147(2)	40(1)
C(13)	1912(2)	8828(2)	3431(2)	33(1)
C(14)	3186(2)	9792(2)	3101(2)	34(1)
C(15)	1777(2)	11855(2)	3207(2)	28(1)
C(16)	1595(2)	12156(2)	3913(2)	35(1)
C(17)	2768(2)	12008(2)	3102(2)	36(1)

Table 8 (cont.)

C(18)	1241(2)	12534(2)	2776(2)	35(1)
C(19)	-161(2)	11112(2)	3917(1)	24(1)
C(20)	36(2)	11071(2)	4585(2)	29(1)
C(21)	-234(2)	11757(2)	5003(2)	35(1)
C(22)	-711(2)	12492(2)	4763(2)	43(1)
C(23)	-908(2)	12544(2)	4102(2)	39(1)
C(24)	-643(2)	11853(2)	3676(2)	29(1)
C(25)	-1244(2)	6347(2)	2065(1)	21(1)
C(26)	-1831(2)	7127(2)	1778(1)	24(1)
C(27)	-281(2)	6572(2)	1893(1)	25(1)
C(28)	-1471(2)	5433(2)	1718(1)	26(1)
C(29)	-1718(2)	7194(2)	1030(2)	29(1)
C(30)	-762(2)	7420(2)	887(2)	32(1)
C(31)	-173(2)	6647(2)	1144(2)	28(1)
C(32)	-420(2)	5748(2)	814(2)	33(1)
C(33)	-1366(2)	5522(2)	971(2)	29(1)
C(34)	-1969(2)	6279(2)	709(2)	33(1)
C(35)	-2421(2)	5625(2)	3184(2)	25(1)
C(36)	-2217(2)	4599(2)	3104(2)	37(1)
C(37)	-2777(2)	5746(2)	3886(2)	34(1)
C(38)	-3187(2)	5869(2)	2728(2)	29(1)
C(39)	-426(2)	5846(2)	3448(2)	28(1)
C(40)	332(2)	6543(2)	3457(2)	36(1)
C(41)	-660(2)	5680(3)	4168(2)	40(1)
C(42)	-86(2)	4943(2)	3156(2)	39(1)
C(43)	-2540(2)	7877(2)	3748(2)	25(1)
C(44)	-2579(2)	7828(2)	4431(2)	36(1)
C(45)	-3385(3)	7864(3)	4739(2)	50(1)

Table 8 (cont.)

C(46)	-4145(3)	7975(2)	4381(2)	51(1)
C(47)	-4113(2)	8059(2)	3701(2)	43(1)
C(48)	-3303(2)	8014(2)	3385(2)	29(1)

Table 9. Bond lengths [Å] and angles [°] for [(1-AdP^{t}Bu$_2$)Pd(Ph)(Cl)]$_2$ (**11**).

Pd(1)-C(19)	1.980(3)	C(11)-C(12)	1.542(5)
Pd(1)-P(1)	2.3436(9)	C(15)-C(16)	1.534(4)
Pd(1)-Cl(1)	2.4193(9)	C(15)-C(17)	1.545(4)
Pd(1)-Cl(2)	2.4922(9)	C(15)-C(18)	1.550(4)
Pd(2)-C(43)	1.979(3)	C(19)-C(24)	1.392(4)
Pd(2)-P(2)	2.3571(9)	C(19)-C(20)	1.393(4)
Pd(2)-Cl(1)	2.4110(8)	C(20)-C(21)	1.380(4)
Pd(2)-Cl(2)	2.5086(10)	C(21)-C(22)	1.382(5)
P(1)-C(11)	1.926(3)	C(22)-C(23)	1.380(5)
P(1)-C(1)	1.936(3)	C(23)-C(24)	1.393(4)
P(1)-C(15)	1.937(3)	C(25)-C(28)	1.545(4)
P(2)-C(39)	1.926(3)	C(25)-C(27)	1.549(4)
P(2)-C(25)	1.930(3)	C(25)-C(26)	1.557(4)
P(2)-C(35)	1.940(3)	C(26)-C(29)	1.541(4)
C(1)-C(4)	1.544(4)	C(27)-C(31)	1.541(4)
C(1)-C(3)	1.548(4)	C(28)-C(33)	1.540(4)
C(1)-C(2)	1.548(4)	C(29)-C(30)	1.527(4)
C(2)-C(5)	1.530(4)	C(29)-C(34)	1.532(4)
C(3)-C(7)	1.537(4)	C(30)-C(31)	1.530(5)
C(4)-C(9)	1.545(4)	C(31)-C(32)	1.519(4)
C(5)-C(10)	1.518(5)	C(32)-C(33)	1.518(4)
C(5)-C(6)	1.529(5)	C(33)-C(34)	1.529(4)
C(6)-C(7)	1.532(5)	C(35)-C(38)	1.528(4)
C(7)-C(8)	1.517(5)	C(35)-C(36)	1.536(4)
C(8)-C(9)	1.519(5)	C(35)-C(37)	1.546(4)
C(9)-C(10)	1.526(5)	C(39)-C(42)	1.537(4)
C(11)-C(13)	1.539(4)	C(39)-C(41)	1.534(4)
C(11)-C(14)	1.538(4)	C(39)-C(40)	1.539(4)

Table 9 (cont.)

C(43)-C(48)	1.387(4)	C(25)-P(2)-C(35)	106.67(13)
C(43)-C(44)	1.396(4)	C(39)-P(2)-Pd(2)	105.67(10)
C(44)-C(45)	1.387(5)	C(25)-P(2)-Pd(2)	106.79(9)
C(45)-C(46)	1.373(6)	C(35)-P(2)-Pd(2)	120.91(10)
C(46)-C(47)	1.393(6)	C(4)-C(1)-C(3)	105.8(2)
C(47)-C(48)	1.403(4)	C(4)-C(1)-C(2)	107.1(2)
		C(3)-C(1)-C(2)	109.3(2)
C(19)-Pd(1)-P(1)	93.18(9)	C(4)-C(1)-P(1)	110.93(19)
C(19)-Pd(1)-Cl(1)	84.39(8)	C(3)-C(1)-P(1)	116.4(2)
P(1)-Pd(1)-Cl(1)	174.68(3)	C(2)-C(1)-P(1)	107.0(2)
C(19)-Pd(1)-Cl(2)	162.88(8)	C(5)-C(2)-C(1)	111.4(3)
P(1)-Pd(1)-Cl(2)	103.74(3)	C(7)-C(3)-C(1)	111.1(3)
Cl(1)-Pd(1)-Cl(2)	78.96(3)	C(1)-C(4)-C(9)	111.6(2)
C(43)-Pd(2)-P(2)	93.28(8)	C(10)-C(5)-C(6)	109.5(3)
C(43)-Pd(2)-Cl(1)	85.28(8)	C(10)-C(5)-C(2)	108.8(3)
P(2)-Pd(2)-Cl(1)	170.91(3)	C(6)-C(5)-C(2)	110.0(3)
C(43)-Pd(2)-Cl(2)	160.06(9)	C(5)-C(6)-C(7)	109.5(3)
P(2)-Pd(2)-Cl(2)	104.30(3)	C(8)-C(7)-C(6)	109.5(3)
Cl(1)-Pd(2)-Cl(2)	78.80(3)	C(8)-C(7)-C(3)	110.3(3)
Pd(2)-Cl(1)-Pd(1)	102.81(3)	C(6)-C(7)-C(3)	109.1(3)
Pd(1)-Cl(2)-Pd(2)	98.04(3)	C(7)-C(8)-C(9)	109.2(3)
C(11)-P(1)-C(1)	110.11(14)	C(8)-C(9)-C(10)	109.5(3)
C(11)-P(1)-C(15)	107.05(14)	C(8)-C(9)-C(4)	109.1(3)
C(1)-P(1)-C(15)	105.41(13)	C(10)-C(9)-C(4)	109.7(3)
C(11)-P(1)-Pd(1)	105.47(10)	C(5)-C(10)-C(9)	109.7(3)
C(1)-P(1)-Pd(1)	107.86(9)	C(13)-C(11)-C(14)	108.5(3)
C(15)-P(1)-Pd(1)	120.75(10)	C(13)-C(11)-C(12)	106.2(3)
C(39)-P(2)-C(25)	109.91(13)	C(14)-C(11)-C(12)	108.3(3)
C(39)-P(2)-C(35)	106.66(14)	C(13)-C(11)-P(1)	108.7(2)
		C(14)-C(11)-P(1)	115.4(2)

Table 9 (cont.)

C(12)-C(11)-P(1)	109.3(2)	C(32)-C(31)-C(30)	110.0(3)
C(16)-C(15)-C(17)	106.1(3)	C(32)-C(31)-C(27)	110.4(3)
C(16)-C(15)-C(18)	104.5(3)	C(30)-C(31)-C(27)	108.8(2)
C(17)-C(15)-C(18)	109.9(3)	C(31)-C(32)-C(33)	109.0(3)
C(16)-C(15)-P(1)	114.2(2)	C(32)-C(33)-C(34)	109.8(3)
C(17)-C(15)-P(1)	112.0(2)	C(32)-C(33)-C(28)	109.6(3)
C(18)-C(15)-P(1)	109.9(2)	C(34)-C(33)-C(28)	109.7(2)
C(24)-C(19)-C(20)	119.0(3)	C(33)-C(34)-C(29)	109.5(2)
C(24)-C(19)-Pd(1)	119.2(2)	C(38)-C(35)-C(36)	108.4(2)
C(20)-C(19)-Pd(1)	121.0(2)	C(38)-C(35)-C(37)	105.3(2)
C(21)-C(20)-C(19)	120.8(3)	C(36)-C(35)-C(37)	106.5(2)
C(20)-C(21)-C(22)	120.1(3)	C(38)-C(35)-P(2)	110.4(2)
C(23)-C(22)-C(21)	119.8(3)	C(36)-C(35)-P(2)	112.3(2)
C(22)-C(23)-C(24)	120.6(3)	C(37)-C(35)-P(2)	113.5(2)
C(19)-C(24)-C(23)	119.8(3)	C(42)-C(39)-C(41)	108.6(3)
C(28)-C(25)-C(27)	106.6(2)	C(42)-C(39)-C(40)	108.3(3)
C(28)-C(25)-C(26)	109.4(2)	C(41)-C(39)-C(40)	106.0(3)
C(27)-C(25)-C(26)	107.6(2)	C(42)-C(39)-P(2)	115.9(2)
C(28)-C(25)-P(2)	116.8(2)	C(41)-C(39)-P(2)	109.2(2)
C(27)-C(25)-P(2)	110.87(19)	C(40)-C(39)-P(2)	108.4(2)
C(26)-C(25)-P(2)	105.25(19)	C(48)-C(43)-C(44)	119.7(3)
C(29)-C(26)-C(25)	110.4(2)	C(48)-C(43)-Pd(2)	118.9(2)
C(31)-C(27)-C(25)	110.7(2)	C(44)-C(43)-Pd(2)	120.7(2)
C(33)-C(28)-C(25)	110.8(2)	C(45)-C(44)-C(43)	119.8(4)
C(30)-C(29)-C(34)	109.9(3)	C(46)-C(45)-C(44)	120.7(4)
C(30)-C(29)-C(26)	108.7(2)	C(45)-C(46)-C(47)	120.0(3)
C(34)-C(29)-C(26)	109.7(2)	C(46)-C(47)-C(48)	119.7(4)
C(29)-C(30)-C(31)	109.6(3)	C(43)-C(48)-C(47)	120.0(3)

Table 10. Anisotropic displacement parameters ($Å^2 x\ 10^3$) $[(1\text{-}AdP^tBu_2)Pd(Ph)(Cl)]_2$ (**11**). The anisotropic displacement factor exponent takes the form: $-2\pi^2[\ h^2\ a^{*2}U^{11} + ... + 2\ h\ k\ a^*\ b^*\ U^{12}\ ]$

	U^{11}	U^{22}	U^{33}	U^{23}	U^{13}	U^{12}
Pd(1)	21(1)	18(1)	23(1)	-2(1)	1(1)	-3(1)
Pd(2)	19(1)	19(1)	20(1)	-2(1)	2(1)	-3(1)
Cl(1)	23(1)	20(1)	30(1)	-4(1)	4(1)	-2(1)
Cl(2)	35(1)	31(1)	41(1)	-15(1)	18(1)	-15(1)
P(1)	20(1)	20(1)	23(1)	1(1)	-1(1)	-2(1)
P(2)	19(1)	18(1)	20(1)	-1(1)	1(1)	0(1)
C(1)	23(1)	23(2)	22(2)	2(1)	-1(1)	-2(1)
C(2)	27(2)	30(2)	32(2)	5(1)	-3(1)	0(1)
C(3)	26(2)	33(2)	30(2)	6(1)	3(1)	-3(1)
C(4)	24(2)	28(2)	25(2)	2(1)	2(1)	1(1)
C(5)	30(2)	44(2)	30(2)	5(2)	-8(1)	2(2)
C(6)	45(2)	48(2)	28(2)	13(2)	0(2)	2(2)
C(7)	35(2)	47(2)	29(2)	11(2)	4(1)	-8(2)
C(8)	42(2)	55(2)	22(2)	2(2)	6(1)	5(2)
C(9)	38(2)	37(2)	26(2)	-4(1)	-2(1)	2(2)
C(10)	48(2)	47(2)	24(2)	-1(2)	-7(2)	-5(2)
C(11)	25(2)	30(2)	30(2)	5(1)	-4(1)	4(1)
C(12)	47(2)	45(2)	27(2)	1(2)	-8(2)	9(2)
C(13)	35(2)	28(2)	35(2)	9(1)	1(1)	4(1)
C(14)	25(2)	36(2)	41(2)	0(2)	-5(1)	7(1)
C(15)	27(2)	24(2)	33(2)	-2(1)	2(1)	-7(1)
C(16)	33(2)	31(2)	42(2)	-9(2)	-2(1)	-10(1)
C(17)	32(2)	35(2)	40(2)	-1(2)	1(1)	-16(1)

Table 10 (cont.)

C(18)	40(2)	19(2)	47(2)	1(1)	2(2)	-3(1)
C(19)	24(2)	20(1)	27(2)	-2(1)	2(1)	-5(1)
C(20)	36(2)	26(2)	25(2)	4(1)	2(1)	-1(1)
C(21)	43(2)	35(2)	27(2)	-7(1)	1(1)	-6(2)
C(22)	46(2)	35(2)	49(2)	-16(2)	9(2)	-1(2)
C(23)	33(2)	23(2)	59(2)	-6(2)	-5(2)	5(1)
C(24)	25(2)	25(2)	37(2)	-1(1)	-2(1)	-2(1)
C(25)	22(1)	21(1)	21(2)	-2(1)	1(1)	0(1)
C(26)	25(2)	22(2)	25(2)	-3(1)	2(1)	2(1)
C(27)	26(2)	26(2)	22(2)	-3(1)	3(1)	0(1)
C(28)	29(2)	19(2)	29(2)	-2(1)	1(1)	-1(1)
C(29)	34(2)	27(2)	26(2)	3(1)	-4(1)	3(1)
C(30)	43(2)	31(2)	23(2)	1(1)	8(1)	-5(2)
C(31)	28(2)	32(2)	25(2)	1(1)	9(1)	-2(1)
C(32)	41(2)	32(2)	25(2)	-6(1)	6(1)	4(2)
C(33)	36(2)	26(2)	24(2)	-8(1)	0(1)	-3(1)
C(34)	39(2)	35(2)	23(2)	-6(1)	-4(1)	0(2)
C(35)	26(2)	23(2)	27(2)	0(1)	6(1)	-7(1)
C(36)	45(2)	22(2)	44(2)	1(2)	7(2)	-3(2)
C(37)	38(2)	30(2)	35(2)	6(1)	11(1)	-7(1)
C(38)	19(1)	33(2)	35(2)	-10(1)	3(1)	-7(1)
C(39)	27(2)	32(2)	25(2)	2(1)	-4(1)	6(1)
C(40)	23(2)	53(2)	31(2)	-5(2)	-7(1)	5(2)
C(41)	40(2)	51(2)	28(2)	6(2)	-3(2)	8(2)
C(42)	37(2)	40(2)	41(2)	6(2)	2(2)	15(2)
C(43)	24(2)	20(2)	30(2)	-3(1)	9(1)	-5(1)
C(44)	41(2)	38(2)	28(2)	-5(1)	11(1)	-11(2)
C(45)	62(3)	44(2)	44(2)	-16(2)	31(2)	-20(2)

Table 10 (cont.)

C(46)	42(2)	36(2)	77(3)	-16(2)	39(2)	-11(2)
C(47)	28(2)	25(2)	77(3)	-5(2)	9(2)	-4(1)
C(48)	25(2)	19(2)	42(2)	1(1)	5(1)	0(1)

Table 11. Hydrogen coordinates (x 10^4) and isotropic displacement parameters (Å^{2}x 10^3) for [(1-AdP^{t}Bu$_2$)Pd(Ph)(Cl)]$_2$ (**11**).

	x	y	z	U(eq)
H(2A)	121	10459	1978	36
H(2B)	505	11477	1908	36
H(3A)	2199	11688	1845	35
H(3B)	2812	10797	1894	35
H(4A)	1141	9110	2068	31
H(4B)	2178	9258	2019	31
H(5A)	-13	10969	870	42
H(6A)	1248	11943	851	48
H(6B)	1275	11236	249	48
H(7A)	2675	11277	778	45
H(8A)	2853	9677	948	47
H(8B)	2245	9850	312	47
H(9A)	1603	8709	992	41
H(10A)	622	9658	376	48
H(10B)	180	9371	1056	48
H(12A)	2835	9691	4357	59
H(12B)	1841	10041	4373	59
H(12C)	2608	10731	4169	59
H(13A)	2337	8418	3644	49
H(13B)	1804	8622	2980	49
H(13C)	1361	8818	3673	49
H(14A)	3575	9379	3347	50
H(14B)	3435	10412	3102	50
H(14C)	3126	9574	2649	50

Table 11 (cont.)

H(16A)	1787	12792	3975	53
H(16B)	1916	11757	4219	53
H(16C)	965	12112	3997	53
H(17A)	2919	12645	3209	54
H(17B)	2911	11884	2643	54
H(17C)	3104	11593	3387	54
H(18A)	1418	13164	2881	53
H(18B)	615	12458	2864	53
H(18C)	1352	12410	2313	53
H(20A)	359	10566	4754	35
H(21A)	-92	11723	5457	42
H(22A)	-902	12961	5052	52
H(23A)	-1227	13055	3936	46
H(24A)	-791	11887	3223	35
H(26A)	-2453	7002	1879	29
H(26B)	-1667	7719	1984	29
H(27A)	-108	7158	2102	29
H(27B)	109	6083	2066	29
H(28A)	-1079	4943	1886	31
H(28B)	-2082	5259	1818	31
H(29A)	-2104	7692	852	35
H(30A)	-598	8005	1102	39
H(30B)	-682	7492	409	39
H(31A)	452	6795	1045	34
H(32A)	-31	5250	975	39
H(32B)	-349	5802	334	39
H(33A)	-1529	4927	758	34
H(34A)	-2586	6129	809	39

Table 11 (cont.)

H(34B)	-1912	6327	228	39
H(36A)	-2741	4238	3205	55
H(36B)	-1739	4426	3404	55
H(36C)	-2041	4478	2651	55
H(37A)	-3282	5341	3947	51
H(37B)	-2957	6385	3949	51
H(37C)	-2316	5589	4205	51
H(38A)	-3691	5479	2829	43
H(38B)	-3015	5770	2272	43
H(38C)	-3346	6514	2790	43
H(40A)	843	6273	3680	53
H(40B)	150	7097	3692	53
H(40C)	485	6704	3006	53
H(41A)	-157	5406	4398	60
H(41B)	-1163	5264	4190	60
H(41C)	-809	6266	4375	60
H(42A)	421	4729	3412	59
H(42B)	88	5045	2701	59
H(42C)	-551	4479	3168	59
H(44A)	-2055	7770	4684	43
H(45A)	-3410	7812	5202	60
H(46A)	-4694	7993	4597	62
H(47A)	-4638	8146	3453	52
H(48A)	-3276	8077	2922	35

X ray crystallographic data for $[(CyP^tBu_2)Pd(Ph)(Br)]_2$ (15)

Data Collection

A pale yellow block crystal of $C_{40}H_{68}Br_2P_2Pd_2$ having approximate dimensions of 0.25 x 0.2 x 0.2 mm was mounted on a glass fiber. All measurements were made on a Nonius KappaCCD diffractometer with graphite monochromated Mo-Kα radiation.

Cell constants and an orientation matrix for data collection corresponded to a primitive monoclinic cell with dimensions:

a = 14.549(3) Å $\alpha = 90^o$

b = 14.689(3) Å $\beta = 97.19(3)^o$

c = 20.017(4) Å $\gamma = 90^o$

V = 4244.3(15) $Å^3$

For Z = 4 and F.W. = 983.5, the calculated density is 1.539 g/cm^3. Based on a statistical analysis of intensity distribution, and the successful solution and refinement of the structure, the space group was determined to be: $P2_1/c$ (#14)

The data were collected at a temperature of 296(2)K to a maximum 2θ value of 55.94^o. Three omega scans consisting of 68, 68, and 49 data frames, respectively, were collected with a frame width of 1.5° and a detector-to-crystal distance, Dx, of 35 mm. Each frame was exposed twice (for the purpose of de-zingering) for 20s. The data frames were processed and scaled using the DENZO software package.[55]

Data Reduction

A total of 18273 reflections were collected of which 10077 were unique and observed (R_{int} = 0.0610). The linear absorption coefficient, μ, for Mo-Kα radiation is 28.31 cm^{-1} and no absorption correction was applied. The data were corrected for Lorentz and polarization effects.

Structure Solution and Refinement

The structure was solved by direct methods and expanded using Fourier techniques.[56] The non-hydrogen atoms were refined anisotropically and hydrogen atoms were refined isotropically. The final cycle of full-matrix least-squares refinement[5] on F was based on 10077 observed reflections ($I > 2.00\sigma(I)$) and 415 variable parameters and converged with unweighted and weighted agreement factors of:

$$R = \Sigma \, ||Fo| - |Fc|| \, / \, \Sigma \, |Fo| = 0.0419$$

$$R_W = [\Sigma \, w \, (|Fo| - |Fc|)^2 \, / \, \Sigma \, w \, Fo^2]^{1/2} = 0.0827$$

The maximum and minimum peaks on the final difference Fourier map corresponded to 0.459 and -0.561 $e^-/Å^3$, respectively.

Structural Description

The compound crystallized in the monoclinic space group $P2_1/c$ with one molecule in the asymmetric unit and four in the unit cell. The geometry about the palladium atoms is square planar with acute Br-Pd-Br angles measured at 82.787(18) and 82.526(18)˚. The planes defined by Pd(1), C(1), P(1), Br(1), Br(2) and Pd(2), C(21), P(2), Br(1), Br(2)

have mean deviations of 0.0578 and 0.0820Å respectively and are offset by 20.7˚ (see Figure 4).

Most interesting is the presence of a pseudo-mirror plane with the phosphine ligands in a "*cis*-like" arrangement. The Pd-Br bond lengths are asymmetric with Br(1) possessing lengths ~0.1Å longer than Br(2) which is certainly a direct effect of the pseudo-mirror plane and the steric bulk imparted by the phosphine ligands. A search of the Cambridge Crystallographic Database (v. 5.23, April 2002) yielded only three examples $[(PR_x)(R)Pd(\mu\text{-}X)]_2$ with a similar "cis-like" arrangement. Two of the examples involve bulky P-C-chelating ligands while the third is a fragment of a more complicated tetramer.

Table 12. Crystal data and structure refinement for $[(CyP^tBu_2)Pd(Ph)(Br)]_2$ (**15**).

Empirical formula	$C_{40}H_{68}Br_2P_2Pd_2$	
Formula weight	983.50	
Temperature	296(2) K	
Wavelength	0.71073 Å	
Crystal system	Monoclinic	
Space group	P2(1)/c	
Unit cell dimensions	a = 14.549(3) Å	□= 90°.
	b = 14.689(3) Å	□= 97.19(3)°.
	c = 20.017(4) Å	□ = 90°.
Volume	4244.3(15) $Å^3$	
Z	4	
Density (calculated)	1.539 g/cm^3	
Absorption coefficient	28.31 mm^{-1}	
F(000)	2000	
Crystal size	0.25 x 0.20 x 0.20 mm^3	
Theta range for data collection	2.31 to 27.97°.	
Index ranges	-19<=h<=19, -17<=k<=19, -26<=l<=26	
Reflections collected	18273	
Independent reflections	10077 [R(int) = 0.0610]	
Completeness to theta = 27.97°	98.4 %	
Absorption correction	None	
Max. and min. transmission	0.6013 and 0.5379	
Refinement method	Full-matrix least-squares on F^2	
Data / restraints / parameters	10077 / 0 / 415	
Goodness-of-fit on F^2	0.914	
Final R indices [I>2sigma(I)]	R1 = 0.0419, wR2 = 0.0677	
R indices (all data)	R1 = 0.1119, wR2 = 0.0827	
Largest diff. peak and hole	0.459 and -0.561 $e.Å^{-3}$	

Table 13. Atomic coordinates (x 10^4) and equivalent isotropic displacement parameters ($Å^2$x 10^3) for $[(CyP^tBu_2)Pd(Ph)(Br)]_2$ (**15**). U(eq) is defined as one third of the trace of the orthogonalized U^{ij} tensor.

	x	y	z	U(eq)
Pd(1)	2851(1)	9501(1)	2515(1)	35(1)
Pd(2)	1891(1)	11689(1)	3139(1)	34(1)
Br(1)	1875(1)	9968(1)	3459(1)	51(1)
Br(2)	2439(1)	11073(1)	2090(1)	54(1)
P(2)	1531(1)	12370(1)	4124(1)	33(1)
P(1)	3358(1)	8061(1)	2884(1)	33(1)
C(1)	3437(3)	9404(2)	1667(2)	37(1)
C(2)	2867(3)	9271(3)	1068(2)	48(1)
C(3)	3223(4)	9265(3)	463(2)	60(1)
C(4)	4151(4)	9407(3)	435(2)	67(2)
C(5)	4716(4)	9566(3)	1025(2)	62(1)
C(6)	4370(3)	9572(3)	1636(2)	47(1)
C(7)	3860(3)	7407(3)	2215(2)	41(1)
C(8)	3136(3)	7140(3)	1620(2)	49(1)
C(9)	3603(4)	6879(3)	1008(2)	71(2)
C(10)	4290(4)	6114(3)	1170(2)	75(2)
C(11)	4995(4)	6351(3)	1769(2)	67(1)
C(12)	4522(3)	6602(3)	2378(2)	50(1)
C(13)	2397(3)	7344(3)	3175(2)	42(1)
C(14)	1517(3)	7529(3)	2685(2)	61(1)
C(15)	2605(3)	6320(3)	3173(2)	58(1)
C(16)	2176(3)	7601(3)	3883(2)	59(1)
C(17)	4330(3)	8199(3)	3599(2)	46(1)

Table 13 (cont.)

C(18)	4082(3)	8955(3)	4079(2)	58(1)
C(19)	5188(3)	8539(3)	3297(2)	59(1)
C(20)	4577(3)	7328(3)	4011(2)	63(1)
C(21)	1893(3)	12876(2)	2651(2)	34(1)
C(22)	1130(3)	13101(3)	2199(2)	44(1)
C(23)	1118(4)	13862(3)	1799(2)	57(1)
C(24)	1887(4)	14413(3)	1826(2)	62(1)
C(25)	2663(4)	14187(3)	2247(2)	56(1)
C(26)	2670(3)	13424(3)	2654(2)	44(1)
C(27)	1110(3)	13568(2)	3986(2)	36(1)
C(28)	173(3)	13633(3)	3544(2)	46(1)
C(29)	7(3)	14595(3)	3280(2)	60(1)
C(30)	25(4)	15273(3)	3858(2)	62(1)
C(31)	914(3)	15189(3)	4334(2)	52(1)
C(32)	1110(3)	14232(3)	4586(2)	45(1)
C(33)	617(3)	11712(3)	4523(2)	41(1)
C(34)	1040(3)	10871(3)	4906(2)	54(1)
C(35)	-116(3)	11386(3)	3958(2)	57(1)
C(36)	136(3)	12286(3)	5030(2)	61(1)
C(37)	2644(3)	12436(3)	4727(2)	43(1)
C(38)	3239(3)	13193(3)	4469(2)	57(1)
C(39)	2531(3)	12637(3)	5471(2)	55(1)
C(40)	3185(3)	11547(3)	4687(2)	59(1)

Table 14. Bond lengths [Å] and angles [°] for [(CyP^{t}Bu$_2$)Pd(Ph)(Br)]$_2$ (**15**).

Pd(1)-C(1)	1.998(4)	C(13)-C(16)	1.539(5)
Pd(1)-P(1)	2.3306(11)	C(17)-C(19)	1.537(6)
Pd(1)-Br(2)	2.5067(6)	C(17)-C(18)	1.540(5)
Pd(1)-Br(1)	2.5939(8)	C(17)-C(20)	1.540(5)
Pd(2)-C(21)	1.999(4)	C(21)-C(22)	1.381(5)
Pd(2)-P(2)	2.3286(11)	C(21)-C(26)	1.387(5)
Pd(2)-Br(2)	2.5052(7)	C(22)-C(23)	1.374(5)
Pd(2)-Br(1)	2.6082(7)	C(23)-C(24)	1.377(6)
P(2)-C(27)	1.872(4)	C(24)-C(25)	1.362(6)
P(2)-C(37)	1.897(4)	C(25)-C(26)	1.387(5)
P(2)-C(33)	1.900(4)	C(27)-C(28)	1.533(5)
P(1)-C(7)	1.870(4)	C(27)-C(32)	1.548(5)
P(1)-C(17)	1.893(4)	C(28)-C(29)	1.517(5)
P(1)-C(13)	1.899(4)	C(29)-C(30)	1.525(5)
C(1)-C(2)	1.385(5)	C(30)-C(31)	1.511(6)
C(1)-C(6)	1.389(6)	C(31)-C(32)	1.509(5)
C(2)-C(3)	1.376(5)	C(33)-C(35)	1.532(5)
C(3)-C(4)	1.374(7)	C(33)-C(34)	1.541(5)
C(4)-C(5)	1.371(6)	C(33)-C(36)	1.552(5)
C(5)-C(6)	1.380(5)	C(37)-C(40)	1.532(5)
C(7)-C(12)	1.535(5)	C(37)-C(38)	1.537(5)
C(7)-C(8)	1.539(5)	C(37)-C(39)	1.548(5)
C(8)-C(9)	1.523(5)		
C(9)-C(10)	1.511(6)	C(1)-Pd(1)-P(1)	92.96(11)
C(10)-C(11)	1.518(7)	C(1)-Pd(1)-Br(2)	83.53(10)
C(11)-C(12)	1.520(6)	P(1)-Pd(1)-Br(2)	175.15(3)
C(13)-C(15)	1.534(5)	C(1)-Pd(1)-Br(1)	165.65(11)
C(13)-C(14)	1.537(6)	P(1)-Pd(1)-Br(1)	100.94(3)

Table 14 (cont.)

Br(2)-Pd(1)-Br(1)	82.787(18)	C(12)-C(7)-C(8)	108.7(3)
C(21)-Pd(2)-P(2)	93.01(10)	C(12)-C(7)-P(1)	122.3(3)
C(21)-Pd(2)-Br(2)	83.45(10)	C(8)-C(7)-P(1)	113.2(3)
P(2)-Pd(2)-Br(2)	173.39(3)	C(9)-C(8)-C(7)	110.8(4)
C(21)-Pd(2)-Br(1)	165.06(10)	C(10)-C(9)-C(8)	111.4(4)
P(2)-Pd(2)-Br(1)	101.44(3)	C(9)-C(10)-C(11)	111.2(4)
Br(2)-Pd(2)-Br(1)	82.526(18)	C(10)-C(11)-C(12)	111.1(4)
Pd(1)-Br(1)-Pd(2)	93.111(18)	C(11)-C(12)-C(7)	110.5(3)
Pd(2)-Br(2)-Pd(1)	97.807(19)	C(15)-C(13)-C(14)	108.7(3)
C(27)-P(2)-C(37)	106.48(18)	C(15)-C(13)-C(16)	107.9(3)
C(27)-P(2)-C(33)	107.85(18)	C(14)-C(13)-C(16)	106.9(4)
C(37)-P(2)-C(33)	110.14(18)	C(15)-C(13)-P(1)	112.9(3)
C(27)-P(2)-Pd(2)	112.55(11)	C(14)-C(13)-P(1)	107.1(3)
C(37)-P(2)-Pd(2)	107.25(13)	C(16)-C(13)-P(1)	113.2(3)
C(33)-P(2)-Pd(2)	112.42(12)	C(19)-C(17)-C(18)	106.0(3)
C(7)-P(1)-C(17)	106.01(19)	C(19)-C(17)-C(20)	109.5(4)
C(7)-P(1)-C(13)	107.70(18)	C(18)-C(17)-C(20)	108.9(3)
C(17)-P(1)-C(13)	109.64(18)	C(19)-C(17)-P(1)	107.6(3)
C(7)-P(1)-Pd(1)	112.10(13)	C(18)-C(17)-P(1)	109.8(3)
C(17)-P(1)-Pd(1)	108.59(13)	C(20)-C(17)-P(1)	114.6(3)
C(13)-P(1)-Pd(1)	112.58(13)	C(22)-C(21)-C(26)	116.9(4)
C(2)-C(1)-C(6)	118.0(4)	C(22)-C(21)-Pd(2)	118.6(3)
C(2)-C(1)-Pd(1)	118.2(3)	C(26)-C(21)-Pd(2)	123.6(3)
C(6)-C(1)-Pd(1)	123.3(3)	C(23)-C(22)-C(21)	121.8(4)
C(3)-C(2)-C(1)	120.9(4)	C(22)-C(23)-C(24)	120.2(5)
C(4)-C(3)-C(2)	120.9(4)	C(25)-C(24)-C(23)	119.2(4)
C(5)-C(4)-C(3)	118.6(4)	C(24)-C(25)-C(26)	120.4(5)
C(4)-C(5)-C(6)	121.2(5)	C(25)-C(26)-C(21)	121.3(4)
C(5)-C(6)-C(1)	120.4(4)	C(28)-C(27)-C(32)	108.8(3)
		C(28)-C(27)-P(2)	113.3(3)

Table 14 (cont.)

C(32)-C(27)-P(2)	120.6(3)
C(29)-C(28)-C(27)	110.5(4)
C(28)-C(29)-C(30)	111.0(3)
C(31)-C(30)-C(29)	110.9(4)
C(32)-C(31)-C(30)	113.4(4)
C(31)-C(32)-C(27)	110.2(3)
C(35)-C(33)-C(34)	108.3(3)
C(35)-C(33)-C(36)	108.9(4)
C(34)-C(33)-C(36)	107.2(3)
C(35)-C(33)-P(2)	107.9(3)
C(34)-C(33)-P(2)	111.1(3)
C(36)-C(33)-P(2)	113.3(3)
C(40)-C(37)-C(38)	106.5(3)
C(40)-C(37)-C(39)	109.2(3)
C(38)-C(37)-C(39)	108.5(3)
C(40)-C(37)-P(2)	109.1(3)
C(38)-C(37)-P(2)	107.2(3)
C(39)-C(37)-P(2)	116.0(3)

Table 15. Anisotropic displacement parameters ($Å^2 x\ 10^3$) for $[(CyP^tBu_2)Pd(Ph)(Br)]_2$ (**15**). The anisotropic displacement factor exponent takes the form: $-2\pi^2[\ h^2\ a^{*2}U^{11} + ...\ + 2\ h\ k\ a^*\ b^*\ U^{12}\ ]$

	U^{11}	U^{22}	U^{33}	U^{23}	U^{13}	U^{12}
Pd(1)	47(1)	30(1)	29(1)	0(1)	8(1)	2(1)
Pd(2)	42(1)	30(1)	30(1)	-1(1)	8(1)	0(1)
Br(1)	79(1)	35(1)	43(1)	2(1)	25(1)	5(1)
Br(2)	93(1)	34(1)	38(1)	4(1)	25(1)	15(1)
P(2)	36(1)	36(1)	29(1)	-3(1)	7(1)	-3(1)
P(1)	37(1)	31(1)	31(1)	3(1)	5(1)	-1(1)
C(1)	55(3)	25(2)	33(2)	0(2)	13(2)	8(2)
C(2)	62(3)	43(3)	39(3)	0(2)	7(2)	8(2)
C(3)	97(4)	50(3)	34(3)	1(2)	10(3)	15(3)
C(4)	112(5)	52(3)	44(3)	6(2)	38(3)	7(3)
C(5)	71(4)	56(3)	66(3)	9(3)	30(3)	-2(3)
C(6)	64(3)	39(3)	41(2)	3(2)	20(2)	-2(2)
C(7)	48(3)	37(3)	41(2)	4(2)	9(2)	2(2)
C(8)	68(3)	34(3)	46(3)	1(2)	11(2)	5(2)
C(9)	108(5)	57(3)	49(3)	0(2)	12(3)	18(3)
C(10)	114(5)	53(3)	68(3)	-1(3)	42(3)	25(3)
C(11)	79(4)	50(3)	78(4)	2(3)	28(3)	17(3)
C(12)	56(3)	36(3)	58(3)	4(2)	12(2)	11(2)
C(13)	48(3)	32(2)	49(3)	2(2)	14(2)	-5(2)
C(14)	42(3)	65(3)	76(3)	-3(3)	4(3)	-11(3)
C(15)	68(4)	35(3)	73(3)	2(2)	22(3)	-12(3)
C(16)	75(4)	43(3)	64(3)	2(2)	30(3)	-6(3)
C(17)	47(3)	45(3)	45(2)	4(2)	-3(2)	-7(2)
C(18)	70(4)	62(3)	39(2)	-1(2)	-5(2)	-12(3)

Table 15 (cont.)

C(19)46(3)	64(3)	65(3)	6(2)	-3(2)	-12(3)
C(20)69(4)	62(3)	55(3)	18(2)	-12(2)	0(3)
C(21)45(3)	29(2)	30(2)	-4(2)	11(2)	6(2)
C(22)53(3)	45(3)	34(2)	0(2)	9(2)	1(2)
C(23)68(4)	63(3)	40(3)	7(2)	8(2)	22(3)
C(24)97(5)	37(3)	55(3)	11(2)	24(3)	21(3)
C(25)74(4)	36(3)	63(3)	-3(2)	28(3)	-5(3)
C(26)48(3)	41(3)	46(3)	-1(2)	14(2)	3(2)
C(27)39(3)	37(2)	35(2)	-6(2)	16(2)	-3(2)
C(28)47(3)	48(3)	43(2)	-12(2)	2(2)	7(2)
C(29)72(4)	57(3)	49(3)	-1(2)	3(2)	14(3)
C(30)92(4)	41(3)	53(3)	1(2)	13(3)	13(3)
C(31)68(3)	43(3)	50(3)	-15(2)	24(3)	2(2)
C(32)55(3)	44(3)	39(2)	-10(2)	16(2)	-1(2)
C(33)46(3)	41(3)	39(2)	-3(2)	17(2)	-9(2)
C(34)66(3)	48(3)	50(3)	7(2)	16(2)	-7(3)
C(35)48(3)	58(3)	66(3)	-3(2)	7(2)	-18(3)
C(36)66(4)	62(3)	62(3)	-2(2)	36(3)	-7(3)
C(37)37(3)	55(3)	37(2)	-6(2)	0(2)	-1(2)
C(38)40(3)	75(4)	53(3)	-9(2)	-1(2)	-10(3)
C(39)62(3)	67(3)	33(2)	-7(2)	-6(2)	-3(3)
C(40)46(3)	67(3)	60(3)	-4(2)	-4(2)	7(3)

Table 16. Hydrogen coordinates (x 10^4) and isotropic displacement parameters ($Å^2$x 10^3) for $[(CyP^tBu_2)Pd(Ph)(Br)]_2$ (**15**).

	x	y	z	U(eq)
H(2A)	2234	9186	1074	57
H(3A)	2830	9162	66	72
H(4A)	4390	9396	26	80
H(5A)	5344	9672	1012	75
H(6A)	4765	9688	2029	56
H(7A)	4245	7858	2019	50
H(8A)	2772	6631	1749	59
H(8B)	2719	7648	1506	59
H(9A)	3136	6691	646	85
H(9B)	3922	7405	856	85
H(10A)	4607	5994	781	90
H(10B)	3961	5565	1269	90
H(11A)	5371	6858	1652	81
H(11B)	5401	5834	1878	81
H(12A)	4987	6763	2751	60
H(12B)	4179	6082	2514	60
H(14A)	1014	7176	2816	92
H(14B)	1622	7361	2237	92
H(14C)	1365	8164	2695	92
H(15A)	2100	5992	3325	87
H(15B)	3163	6198	3468	87
H(15C)	2682	6131	2724	87
H(16A)	1689	7217	4004	89
H(16B)	1982	8225	3885	89

Table 16 (cont.)

H(16C)	2720	7521	4202	89
H(18A)	4577	9024	4441	87
H(18B)	3522	8795	4259	87
H(18C)	3992	9518	3836	87
H(19A)	5694	8613	3649	89
H(19B)	5051	9114	3078	89
H(19C)	5354	8104	2975	89
H(20A)	5075	7453	4360	95
H(20B)	4763	6862	3720	95
H(20C)	4045	7125	4209	95
H(22A)	611	12727	2164	52
H(23A)	587	14006	1508	69
H(24A)	1877	14934	1561	74
H(25A)	3190	14547	2260	68
H(26A)	3207	13276	2936	53
H(27A)	1548	13841	3709	43
H(28A)	162	13214	3168	56
H(28B)	-318	13461	3805	56
H(29A)	-589	14625	3003	72
H(29B)	482	14755	3001	72
H(30A)	-30	15887	3679	74
H(30B)	-499	15162	4103	74
H(31A)	1425	15395	4105	63
H(31B)	879	15587	4716	63
H(32A)	642	14047	4863	54
H(32B)	1708	14213	4861	54
H(34A)	565	10551	5103	80
H(34B)	1515	11062	5254	80

Table 16 (cont.)

H(34C)	1304	10476	4599	80
H(35A)	-587	11051	4148	86
H(35B)	170	11000	3656	86
H(35C)	-390	11902	3716	86
H(36A)	-316	11919	5215	92
H(36B)	-164	12801	4802	92
H(36C)	590	12493	5387	92
H(38A)	3809	13247	4765	85
H(38B)	2909	13759	4458	85
H(38C)	3372	13043	4024	85
H(39A)	3131	12660	5733	83
H(39B)	2169	12164	5642	83
H(39C)	2224	13211	5501	83
H(40A)	3749	11576	4991	88
H(40B)	3328	11462	4236	88
H(40C)	2816	11046	4809	88

2.8 References

(1) Crabtree, R. H. *The Organometallic Chemistry of the Transition Metals*; 4th ed.; John Wiley & Sons, Inc.: Hoboken, NJ, 2005.
(2) Hartwig, J. F. In *Handbook of Organopalladium Chemistry for Organic Synthesis*; Negishi, E.-I., Ed.; John Wiley & Sons, Inc.: Hoboken, N.J., 2002; Vol. 1, p 1051.
(3) Hartwig, J. F. In *Modern Arene Chemistry*; Astruc, D., Ed.; Wiley-VCH: Weinheim, Germany, 2002, p 107.
(4) Yang, B. H.; Buchwald, S. L. *J. Organomet. Chem.* **1999**, *576*, 125.
(5) Beletskaya, I. P.; Cheprakov, A. V. *Chem. Rev.* **2000**, *100*, 3009.
(6) Shibasaki, M.; Vogl, E. M.; Ohshima, T. *Adv. Synth. Catal.* **2004**, *346*, 1533.
(7) Suzuki, A. In *Modern Arene Chemistry*; Astruc, D., Ed.; Wiley-VCH: Weinheim, Germany, 2002, p 53.
(8) Zapf, A. In *Transition Metals for Organic Synthesis*; 2nd ed.; Beller, M., Bolm, C., Eds.; Wiley-VCH: Weinheim, Germany, 2004; Vol. 1, p 211.
(9) Bellina, F.; Carpita, A.; Rossi, R. *Synthesis* **2004**, 2419.
(10) Herrmann, W. A. In *Applied Homogeneous Catalysis with Organometallic Compounds*; 2nd ed.; Cornils, B., Herrmann, W. A., Eds.; Wiley-VCH: Weinheim, Germany, 2002; Vol. 1, p 591.
(11) Espinet, P.; Echavarren, A. M. *Angew. Chem., Int. Ed.* **2004**, *43*, 4704.
(12) Stille, J. K. *Angew. Chem., Int. Ed. Engl.* **1986**, *25*, 508.
(13) Hartwig, J. F.; Kawatsura, M.; Hauck, S. I.; Shaughnessy, K. H.; Alcazar-Roman, L. M. *J. Org. Chem.* **1999**, *64*, 5575.
(14) Stambuli, J. P.; Kuwano, R.; Hartwig, J. F. *Angew. Chem., Int. Ed. Engl.* **2002**, *41*, 4746.
(15) Littke, A. F.; Fu, G. C. *Angew. Chem., Int. Ed.* **2002**, *41*, 4176.
(16) Surry, D. S.; Buchwald, S. L. *Angew. Chem., Int. Ed.* **2008**, *47*, 6338.
(17) Brunel, J. M. *Mini-Reviews in Organic Chemistry* **2004**, *1*, 249.
(18) Amatore, C.; Pfluger, F. *Organometallics* **1990**, *9*, 2276.
(19) Fauvarque, J.-F.; Pflüger, F. *J. Organomet. Chem.* **1981**, *208*, 419.
(20) Hartwig, J. F.; Paul, F. *J. Am. Chem. Soc.* **1995**, *117*, 5373.
(21) Barrios-Landeros, F.; Hartwig, J. F. *J. Am. Chem. Soc.* **2005**, *127*, 6944.
(22) Stambuli, J. P.; Buhl, M.; Hartwig, J. F. *J. Am. Chem. Soc.* **2002**, *124*, 9346.
(23) Stambuli, J. P.; Incarvito, C. D.; Buehl, M.; Hartwig, J. F. *J. Am. Chem. Soc.* **2004**, *126*, 1184.
(24) Amatore, C.; Broeker, G.; Jutand, A.; Khalil, F. *J. Am. Chem. Soc.* **1997**, *119*, 5176.
(25) Amatore, C.; Carre, E.; Jutand, A.; Mbarki, M. A. *Organometallics* **1995**, *14*, 1818.
(26) Amatore, C.; Jutand, A. *J. Organomet. Chem.* **1999**, *576*, 254.
(27) Galardon, E.; Ramdeehul, S.; Brown, J. M.; Cowley, A.; Hii, K. K.; Jutand, A. *Angew. Chem., Int. Ed.* **2002**, *41*, 1760.
(28) Portnoy, M.; Milstein, D. *Organometallics* **1993**, *12*, 1665.

(29) Lewis, A. K. d. K.; Caddick, S.; Cloke, G. N.; Billingham, N. C.; Hitchcock, P. B.; Leonard, J. *J. Am. Chem. Soc.* **2003**, *125*, 10066.
(30) Alcazar-Roman, L. M.; Hartwig, J. F.; Rheingold, A. L.; Liable-Sands, L. M.; Guzei, I. A. *J. Am. Chem. Soc.* **2000**, *122*, 4618.
(31) Alcazar-Roman, L. M.; Hartwig, J. F. *Organometallics* **2002**, *21*, 491.
(32) Shekhar, S.; Ryberg, P.; Hartwig, J. F. *Org. Lett.* **2006**, *8*, 851.
(33) For computational studies of these effects, see the following three references.
(34) Lam, K. C.; Marder, T. B.; Lin, Z. *Organometallics* **2007**, *26*, 758.
(35) Ahlquist, M.; Fristrup, P.; Tanner, D.; Norrby, P.-O. *Organometallics* **2006**, *25*, 2066.
(36) Ahlquist, M.; Norrby, P.-O. *Organometallics* **2007**, *26*, 550.
(37) Stambuli, J. P. Ph.D. Dissertation, Yale University, 2003.
(38) White, L. M.; Morris, R. T. *Anal. Chem.* **1952**, *24*, 1063.
(39) Ozawa, F.; Kawasaki, N.; Okamoto, H.; Yamamoto, T.; Yamamoto, A. *Organometallics* **1987**, *6*, 1640.
(40) Huser, M.; Youinou, M. T.; Osborn, J. A. *Angew. Chem.* **1989**, *101*, 1427.
(41) Macgregor, S. A.; Roe, D. C.; Marshall, W. J.; Bloch, K. M.; Bakhmutov, V. I.; Grushin, V. V. *J. Am. Chem. Soc.* **2005**, *127*, 15304.
(42) Barrios-Landeros, F.; Carrow, B. P.; Hartwig, J. F. *J. Am. Chem. Soc.* **2008**, *130*, 5842.
(43) Mann, B. E.; Musco, A. *J. Chem. Soc., Dalton Trans.: Inorg. Chem.* **1975**, 1673.
(44) Musco, A.; Kuran, W.; Silvani, A.; Anker, M. W. *J. Chem. Soc., Chem. Commun.* **1973**, 938.
(45) Mitchell, E. A.; Baird, M. C. *Organometallics* **2007**, *26*, 5230.
(46) As we treated the data here, the linear curve fit at low [PCy3] corresponds to the hypothetical case of reaction of $[Pd(PCy_3)_3]$ under these conditions. We did not fit the data to the full system that would include situations in which a significant concentration of both the $[Pd(PCy_3)_3]$ and $[Pd(PCy_3)_2]$ complexes are present.
(47) Some reactions contained almost neat haloarene. However, the rates of these reactions are not strongly affected by solvent polarity (ref 18 and qualitative measurements with compound **2**), and the dielectric constant of chlorobenzene is between that of benzene and THF. Thus, a high concentration of ArCl should not give rise to a large medium effect.
(48) Yoshida, T.; Otsuka, S. *Inorg. Synth.* **1990**, *28*, 113.
(49) Otsuka, S.; Yoshida, T.; Matsumoto, M.; Nakatsu, K. *J. Am. Chem. Soc.* **1976**, *98*, 5850.
(50) The derivation of the rate expression is included in the Supporting Information.
(51) Roy, A. H.; Hartwig, J. F. *Organometallics* **2004**, *23*, 1533.
(52) Unimolecular decomposition of the Pd(0) complex can be excluded as a significant contributor to the value of the y-intercept because $Pd(1\text{-}AdP^tBu_2)_2$ (**2**) was stable in toluene at 100 °C. Our values for the y-intercepts of the plots of k_{obs} vs. [PhBr] in Figures 14 and 15 are similar. If these correspond to the rate constants for oxidative addition by an irreversible dissociation of ligand, one might expect the value of the y-intercept to be larger for reaction of the complex

containing the more sterically bulky 1-AdP^tBu_2 compared to that containing CyP^tBu_2. However, comparison of these y-intercept values is complicated because they represent only an approximate value for the rate of ligand dissociation. A quantitative value for the rate constant for ligand dissociation k_4 cannot be obtained from simple extrapolation of the plot of k_{obs} vs [ArBr] over the linear range investigated because the plots become non-linear as [ArBr] approaches zero.

(53) Roy, A. H.; Hartwig, J. F. *J. Am. Chem. Soc.* **2003**, *125*, 13944.

(54) Zoellner, R. W. *J. Chem. Ed.* **1990**, *67*, 714.

(55) Otwinowski, Z.; Minor, W. In *Macromolecular Crystallography, part A*; C.W. Carter, J., Sweet, R. M., Eds.; Academic Press: 1997; Vol. 276.

(56) Sheldrick, G. M. *Acta Crystallographica Section A* **1990**, *46*, 467-473.

(57) Least Squares function minimized: $\Sigma w(F_o^2-F_c^2)^2$

Chapter 3. Autocatalytic Oxidative Addition of PhBr to $Pd(P^tBu_3)_2$ via $Pd(P^tBu_3)_2(H)(Br)$

3.1 Introduction

The oxidative addition of aryl halides or sulfonates to Pd(0) complexes is the first step in classic and recently developed cross coupling reactions. Among the most active catalysts for many coupling reactions are complexes of P^tBu_3.[1-3] Recently, we reported the isolation of unusual 3-coordinated products from oxidative addition of bromoarenes to Pd(0) complexes of P^tBu_3.[4-5] We have now studied the mechanism of the oxidative addition of bromoarenes to $Pd(P^tBu_3)_2$, and this mechanism is equally unusual. The reaction in the absence of a strong base is autocatalytic, and a side product, $Pd(P^tBu_3)_2(H)(Br)$, is capable of acting as the catalyst. In contrast to the typically higher reactivity of haloarenes with Pd(0) species than with Pd(II), the reaction of bromobenzene with $Pd(P^tBu_3)_2(H)(Br)$ occurs faster than with $Pd(P^tBu_3)_2$ to form $Pd(P^tBu_3)(Ph)(Br)$. Studies that support these conclusions are reported here.

3.2 Results and Discussion

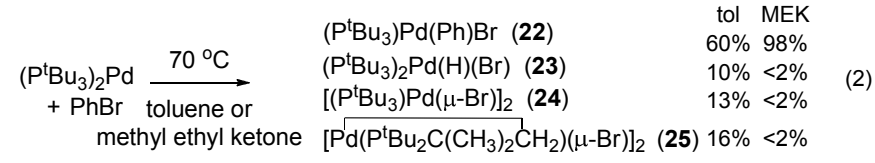

(2)

The oxidative addition of PhBr to $Pd(P^tBu_3)_2$ (**21**) produces the 3-coordinate $(P^tBu_3)Pd(Ph)(Br)$ (**22**).[4-5] The yields of **22** and side products in polar and non-polar

solvents are shown in eq 2. The reaction in polar solvents, such as methyl ethyl ketone, formed **22** in high yield. Reactions in toluene were slower, and this slower rate allowed decomposition of the product (*vide infra*) to occur in parallel with the oxidative addition. Thus, a typical product distribution in toluene was **22** (60%), $(P^tBu_3)_2Pd(H)(Br)$[6] (**23**) (10%), $[(P^tBu_3)Pd(\mu\text{-}Br)]_2$[7] (**24**) (13%), and $[Pd(P^tBu_2C(CH_3)_2CH_2)(\mu\text{-}Br)]_2$[8] (**25**) (16%). Protonated phosphine $[HP^tBu_3]^+$ (**26**) (12%) was also detected by ^{31}P NMR spectroscopy; the anion in this salt lacks an NMR active nucleus and is likely to be bromide. Each of the side products[6-8] was identified by independent synthesis and comparison of ^{31}P NMR chemical shifts to those of the reaction mixture.

The rate of reaction of the Pd(0) complex **21** with bromobenzene was measured by ^{31}P NMR spectroscopy with [**21**] = 0.040 M and [PhBr] = 1.9 M in toluene, THF, and 2-butanone solvent at 70 °C. The reaction of **21** in toluene in the absence of any additive (open squares, Figure 18) was clearly not exponential and was characteristic of an autocatalytic reaction. To determine the origin of this kinetic behavior, the rate of the reaction of PhBr with **21** was conducted with 5 mol % of $(P^tBu_3)Pd(Ph)(Br)$ (**22**) and **2**5 mol % of the individual, independently synthesized side-products. Each of these species accelerated the oxidative addition process, but to different extents. The degree of acceleration by the different additives followed the trend $(P^tBu_3)Pd(Ph)(Br) \approx (HP^tBu_3)Br < [(P^tBu_3)Pd(\mu\text{-}Br)]_2 < (P^tBu_3)_2Pd(H)(Br)$. Added cyclometallated **25** did not affect the reaction of **21** with PhBr. Reactions in toluene in the presence of 5 mol % added $(P^tBu_3)_2Pd(H)(Br)$ occurred in less than half of the roughly 3.5 h required in the absence of additive.

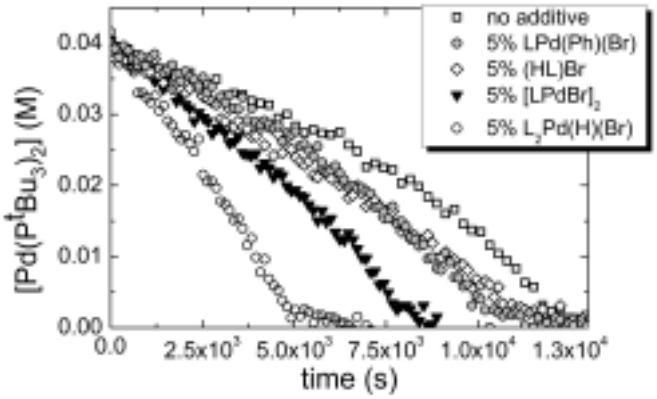

Figure 18. Decay of $Pd(P^tBu_3)_2$ (**21**) during the oxidative addition of PhBr in toluene at 70 °C in the presence of additives (L= P^tBu_3).

Because several of the compounds that affected the oxidative addition product contained HBr, we sought to determine if the accelerating effect of these additives resulted from H^+, Br^-, or a combination of the two. The oxidative additions of PhBr to **21** in the presence of 5 mol % $NEt_3 \cdot HBr$ occurred faster than in the absence of this additive and with an exponential decay possessing a half-life of about 30 min (Figure 19). The reaction in the presence of 50 mol % of NBu_4Br (0.020 M) occurred with an exponential decay possessing a half-life of about 30 min. Oxidative additions of PhBr to **21** in the presence of the strong, neutral phosphazene base *tert*-butylimino-trispyrrolidino phosphorane (BTPP)[9-10,11] also occurred with an exponential decay, in this case with a much longer half-life of 6.5 h. Reactions conducted with weaker bases, such as NEt_3, did not quench the autocatalysis.[12] These data show that both Br^- and H^+ contribute to the autocatalysis, and that a strong base is needed to quench the autocatalysis.

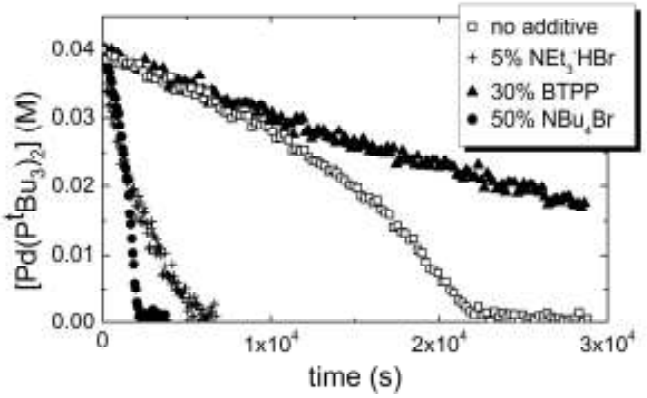

Figure 19. Decay of Pd(P^{t}Bu$_3$) (**21**), during the oxidative addition of PhBr in THF at 70 °C in the presence of 5 mol % NEt_3·HBr, 30 mol % phosphazene base *tert*-butylimino-trispyrrolidino phosphorane (BTPP), or 50 mol% NBu_4Br.

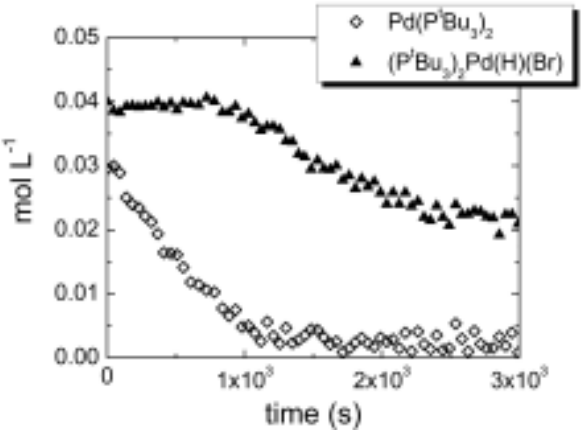

Figure 20. Decay of a 1:1 mixture of Pd(P^{t}Bu$_3$)$_2$ (**21**) (0.039 M) and (P^{t}Bu$_3$)$_2$Pd(H)(Br) (**23**) (0.041 M) during oxidative addition of PhBr (0.95 M) in toluene at 70 ^{o}C.

Because HBr adds to Pd(P^{t}Bu$_3$)$_2$ to form hydridopalladium bromide **23**, and because complex **23** had the largest accelerating effect on the oxidative addition, we focused on how this complex could affect the reactions of PhBr with Pd(P^{t}Bu$_3$)$_2$. Profiles of the reaction of PhBr with a 1:1 mixture of Pd(0) complex **21** and the hydrido bromide **23** at 70 °C in toluene (Fig 20) show that the concentration of **23** decreased only after Pd(0) complex **21** had been consumed. Because the oxidative addition to **21** was faster in the

presence of **23**, but the concentration of **23** did not change during the consumption of **21**, complex **23** plays the unexpected role of a catalyst for this addition of PhBr to **21**.

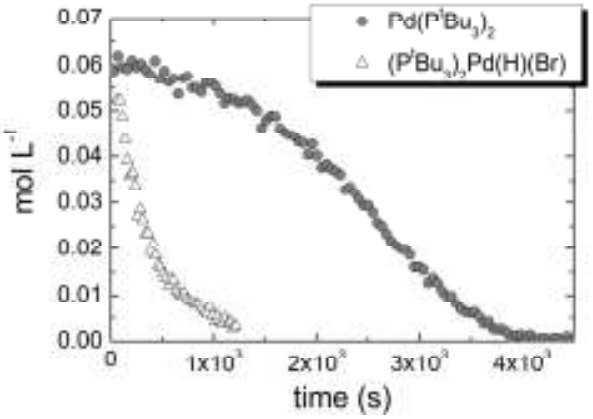

Figure 21. Relative decay of Pd(P^{t}Bu$_3$)$_2$ (**21)** and (P^{t}Bu$_3$)$_2$Pd(H)(Br) **23** during the oxidative addition of PhBr in 2-butanone at 70 °C.

To probe the origin of the accelerating affect of hydrido bromide complex **23** on the reaction of PhBr with Pd(0) complex **21**, we studied the reaction of **23** with PhBr and compared the rates of these reactions to those of **21** with PhBr. The reaction of PhBr with hydrido bromide complex **23** at 70 °C in toluene occurred faster than that with Pd(0) complex **21**. The yield of **22** was modest (32% at 77% conversion), just as it was for reaction of **21** with PhBr in toluene (vide supra) because the decomposition products **25** and (HP^{t}Bu$_3$)$_2$[PdBr$_4$] (**27**)[13] increased at higher conversion of **23**.[14]

The high yields of the reaction of **23** with bromoarenes at 70 °C in 2-butanone allowed a clearer illustration of the difference between the rates of reactions of the Pd(II) complex **23** and the Pd(0) complex **21**.[15] Figure 21 shows the decay of **21** from reaction with PhBr and the decay of hydrido bromide **23**. The reaction of PhBr with **23** to form **22** occurred to 90% conversion after about 900 s with a decay profile that was similar to that in

toluene. In contrast, the reaction with **21** under the same conditions for the same time occurred to less than 10% conversion. We propose that $L_2Pd(H)(Br)$ reacts with bromobenzene by reversible reductive elimination to generate the ionic species $[^tBu_3PH][Pd(^tBu_3P)(Br)]$ containing a Pd(0) anion that would be expected to add bromoarenes rapidly.[16-18,19]

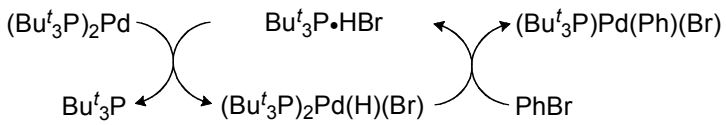

Scheme 28. Mechanism of autocatalysis

These observations lead to the basic steps of a catalytic cycle for oxidative addition of ArBr to Pd(0) complex **21** shown in Scheme 28. By this mechanism, reaction of the bromoarene with hydrido bromide complex **23** via the proposed unsaturated, anionic intermediate forms arylpalladium bromide complex **22** and $^tBu_3P$•HBr (**26**). The liberated equivalent of HBr then transfers to Pd(0) complex **21** to regenerate hydrido bromide **23** and liberate P^tBu_3.

This mechanism requires the generation of **26** or hydrido bromide complex **23** from the combination of Pd(0) complex **21** and PhBr to initiate the autocatalysis. To determine the origin of these species, we studied the relative stabilities of the initial products from reaction of PhBr with complex **21** at different temperatures. These studies showed that thermal decomposition of arylpalladium bromide **22** at 50 ^oC in toluene forms μ-Br complex **24**[20] and that complex **24** degrades at 80 ^oC in toluene to form hydridopalladium bromide **23** (5%), cyclometallated **25** (42%), and the phosphonium salt (53%). Thus, the

decomposition of the simple oxidative addition product **22** to μ-Br complex **24** and then $^{t}Bu_3P$•HBr appears to initiate the autocatalysis.

3.3 Conclusions

In conclusion, we have shown that the oxidative addition to $Pd(P^{t}Bu_3)_2$ occurs, at least under certain conditions, by an unusual and complex autocatalytic mechanism, and these studies led to the counterintuitive observation that bromobenzene reacts faster with the palladium(II) complex $L_2Pd(H)(Br)$ than with the related palladium(0) species L_2Pd. The formation of $L_2Pd(H)(Br)$ from a cascade beginning with the oxidative addition product, along with the faster reaction of the bromoarene with $L_2Pd(H)(Br)$ than with L_2Pd, can account for this autocatalysis. The fact that these processes occur in the absence of base or in the presence of bases of modest strength could make the autocatalytic pathway relevant to the mechanisms of Stille cross-couplings,[21-22] certain Suzuki couplings,[23-24] and Heck reactions.[25] In fact, complex **23** is the resting state of the Heck reaction catalyzed by Pd(0) complexes of $P^{t}Bu_3$ under some conditions.[26]

3.4 Experimental

General Methods. All manipulations were conducted in an inert atmosphere dry box or using standard Schlenk techniques unless otherwise specified. ^{1}H spectra were recorded on a 400 or 500 MHz spectrometer; ^{13}C spectra were recorded at 125 MHz with solvent resonances as reference; $^{31}P\{^{1}H\}$ NMR spectra were recorded at 160 or 200 MHz with external H_3PO_4 as a reference. Toluene, dichloromethane, THF, diethyl ether, and

pentane were dried with a solvent purification system by percolation through neutral alumina under positive pressure of argon. 2-butanone was purchased from Aldrich (ACS grade) and dried over anhydrous calcium sulphate. The complexes $Pd(P^tBu_3)_2$[27] (**21**), $(P^tBu_3)Pd(Ph)(Br)$[28-29] (**22**), and $(P^tBu_3)_2Pd(H)(Br)$[30-31] (**23**) were prepared by published procedures. The complex $[(P^tBu_3)Pd(\mu\text{-}Br)]_2$[7] (**24**) was obtained from Johnson Matthey. All other reagents were obtained from commercial sources and used without further purification.

Independent synthesis of $P^tBu_3 \cdot HBr$ (26). P^tBu_3 (100 mg, 0.49 mmol) and pyridinium bromide (72 mg, 0.45 mmol) were weighed into a small vial. Acetonitrile (2 mL) was added, and the mixture was stirred until the solution was homogeneous, at which time 5 mL of ether were added. Upon addition of the ether, a white solid precipitated immediately. The product was separated by filtration, rinsed with ether, and dried under vacuum to give 117 mg of the phosphonium salt (92 % yield). ^{1}H NMR (CD_2Cl_2, 500 MHz) δ 8.57 (d, J = 472 Hz, 1H), 1.63 (d, J = 14.9 Hz, 27H); ^{13}C NMR (CD_2Cl_2, 125 MHz) δ 37.28 (d, J = 28.0 Hz), 30.44; ^{31}P{^{1}H} NMR (CD_2Cl_2, 165 MHz) δ 40.97. Anal. calcd. for $C_{12}H_{28}BrP$: C, 50.89; H, 9.96. Found: C, 50.84; H, 10.16.

Independent synthesis of $[Pd(P(t\text{-}Bu)_3)_2(C(CH_3)_2CH_2)(\mu\text{-}Br)]_2$ (25).[30-32] Inside the glove box, the palladium(I) dimer $[Pd(P^tBu_3)(\mu\text{-}Br)]_2$ (**24**) (200 mg, 0.26 mmol) was weighed into a small vial and dissolved in 2.0 mL of dry toluene. The solution was stirred at 80 °C for 2 h. The vial was then opened to air, and the reaction mixture was filtered

through a plug of Celite to separate the dark solid from the orange solution. The solvent was evaporated under vacuum to yield an orange residue. The residue was dissolved in CH_2Cl_2, and the resulting solution flushed through a plug of silica. The methylene chloride solution was concentrated to about 0.5 ml, layered with pentane, and placed in the freezer at -35 °C overnight. Yellow crystalline product formed, which was collected by filtration and dried under vacuum to afford 81 mg of dimeric complex (40% yield). ^{1}H NMR (CD_2Cl_2, 500 MHz) δ 1.56 (d, J = 14.0 Hz, 18H), 1.48 (d, J = 14.5 Hz, 6H), 1.15 (b, 2H); ^{13}C NMR (C_6D_6, 125 MHz) δ 50.12 (d, J = 18.7 Hz), 38.83 (d, J = 9.4 Hz), 32.45 (d, J = 2.8 Hz), 31.52, 14.18 (d, J = 27.2 Hz); ^{31}P{^{1}H} NMR (CD_2Cl_2, 165 MHz) δ -8.44. Anal. Calcd. for $C_{12}H_{26}BrPPd$: C, 37.18; H, 6.76. Found: C, 37.35; H, 6.55.

Independent synthesis of $(HP^tBu_3)_2[PdBr_4]$ (27). Into a small vial was weighed P^tBu_3·HBr (**26**) (42 mg, 0.15 mmol) and $PdBr_2$ (18 mg, 0.068 mmol). The solids were mixed with 2 mL of THF and 100 μL of MeCN. The reaction mixture was stirred at room temperature, and the orange product precipitated from solution. The reaction should be stirred until the dark starting palladium salt can no longer be observed (approximately 1 h). After this time, the orange solid was isolated by filtration, rinsed with pentane, and dried under vacuum to afford 49 mg of product (87 % yield). ^{1}H NMR (CD_2Cl_2, 500 MHz) δ 8.19 (d, J = 467.0 Hz, 1H), 1.77 (d, J = 15.0 Hz, 27H) ; ^{13}C NMR (CD_2Cl_2, 125 MHz) δ 37.97 (d, J = 28.0 Hz), 30.90; ^{31}P{^{1}H} NMR (CD_2Cl_2, 165 MHz) δ 44.52. Anal. calcd. for $C_{24}H_{56}Br_4P_2Pd$: C, 34.62; H, 6.78. Found: C, 34.34; H, 6.71.

General procedure for kinetic experiments. The amounts and reagents used to prepare each sample are described below. The solvents and bromoarenes were added to the samples with a micropipette or microliter syringe. The sample solutions were transferred to a screw top NMR tube and sealed with a cap containing a Teflon-lined septum. A sealed capillary tube with a THF or DMF solution of H_3PO_4 (0.35 M) was placed inside the NMR tube to be used as an external standard for calculation of yields and conversions. Before inserting the sample into the NMR probe, the temperature was adjusted. The temperature was measured with a type K thermocouple; the thermocouple probe was inserted into an NMR sample tube, which was lowered inside the spectrometer probe. Once the temperature was stable, the tube with the sample was inserted into the NMR probe, and ^{31}P NMR spectra were acquired at fixed time intervals throughout the length of experiment with the aid of an automated data collection program.

Representative procedure for the reaction of PhBr with 21. Complex $Pd(P^tBu_3)_2$ (**21**) was weighed into a small vial (10 mg, 0.020 mmol) and dissolved in a mixture of 400 μL of THF (or toluene) and 100 μL PhBr (0.95 mmol). The sample was handled following the general procedure for the kinetic experiments described above. The reaction was performed at 70 °C.

Representative procedure for the reaction of 21 with PhBr in the presence of additives. Into a small vial, 8 mg (0.01 mmol) of $[Pd(P^tBu_3)(\mu\text{-}Br)]_2$ (**24**) were weighed. This material was dissolved in 1.0 mL of toluene to prepare a 0.010 M stock solution. Into a separate vial, was weighed 10 mg (0.020 mmol) of $Pd(P^tBu_3)_2$ (**21**). To this vial

was added 100 μL of the stock solution of $[Pd(P^tBu_3)(\mu\text{-}Br)]_2$ (0.001 mmol), 300 μL of toluene and 100 μL PhBr (0.95 mmol). The sample was handled following the general procedure for the kinetic experiments described above. The reaction was heated at 70 °C.

Representative procedure for the reaction of 21 with PhBr in the presence of tetraalkylammonium salt. $Pd(P^tBu_3)_2$ (**21**) (10 mg, 0.020 mmol) and $N(butyl)_4Br$ (3 mg, 0.01 mmol) were weighed into a small vial and dissolved in 400 μL of THF and 100 μL PhBr (0.95 mmol). The sample was handled following the general procedure for the kinetic experiments described above and the reaction was heated at 70 °C.

Representative procedure for the reaction of 21 with PhBr in the presence of trialkylammonium salts. $NEt_3 \cdot HBr$ (4 mg, 0.02 mmol) was weighed into a small vial and dissolved in 2.0 mL of THF to prepare a 0.010 M stock solution. Into a separate vial was weighed 10 mg (0.02 mmol) of $Pd(P^tBu_3)_2$ (**21**). To this vial was added 100 μL of the stock solution of $NEt_3 \cdot HBr$ (0.001 mmol), 300 μL of THF, and 100 μL PhBr (0.95 mmol). The sample was handled following the general procedure for the kinetic experiments described above. The reaction was heated at 70 °C.

Reaction of PhBr with a 1:1 mixture of 21 and 23. Into a small vial, was weighed 10 mg of **21** (0.020 mmol) and 12 mg of **23** (0.020 mmol). The complexes were dissolved in 400 μL of toluene and 100 μL PhBr. The sample was handled following the general

procedure for the kinetic experiments described above, and the reaction was heated at 70 °C. A plot of the concentrations of **21** and **23** vs time is shown in Figure 19.

Thermolysis of arylpalladium halide complex 22: Complex **22** (20 mg, 0.043 mmol) was dissolved in 700 μL C_6D_6 and heated in a sealed NMR tube at 50 ^oC. Degradation of the starting complex was monitored by ^1H and ^{31}P NMR spectroscopy. After 3 hours the μ-Br dimer **24** was the only new species observed by ^{31}P NMR, present in a 1:2.5 ratio with unreacted **22**.

Representative procedure for the reaction of PhBr with 23. $(P^tBu_3)_2Pd(H)(Br)$ (**23**) (12 mg, 0.020 mmol) was weighed into a small vial and dissolved in 400 μL of degassed 2-butanone and 100 μL PhBr (0.95 mmol). The sample was handled following the general procedure for the kinetic experiments described above. The reaction was heated at 70 °C.

3.5 References

(1) Hartwig, J. F.; Kawatsura, M.; Hauck, S. I.; Shaughnessy, K. H.; Alcazar-Roman, L. M. *J. Org. Chem.* **1999**, *64*, 5575-5580.
(2) Littke, A. F.; Fu, G. C. *Angew. Chem. Int. Ed.* **2002**, *41*, 4176-4211.
(3) Dubbaka, S. R. *Synlett* **2005**, 709-710.
(4) Stambuli, J. P.; Bühl, M.; Hartwig, J. F. *J. Am. Chem. Soc.* **2002**, *124*, 9346-9347.
(5) Stambuli, J. P.; Incarvito, C. D.; Bühl, M.; Hartwig, J. F. *J. Am. Chem. Soc.* **2004**, *126*, 1184-1194.
(6) Dura-Vila, V.; Mingos, D. M. P.; Vilar, R.; White, A. J. P.; Williams, D. J. *J. Organomet. Chem.* **2000**, *600*, 198-205.
(7) Vilar, R.; Mingos, D. M. P.; Cardin, C. J. *J. Chem. Soc., Dalton Trans.: Inorg. Chem.* **1996**, 4313-4314.
(8) Clark, H. C.; Goel, A. B.; Goel, S. *Inorg. Chem.* **1979**, *18*, 2803-2808.
(9) Kisanga, P. B.; Verkade, J. G.; Schwesinger, R. *J. Org. Chem.* **2000**, *65*, 5431-5432.
(10) Schwesinger, R.; Hasenfratz, C.; Schlemper, H.; Walz, L.; Peters, E. M.; Peters, K.; von Schnering, H. G. *Angew. Chem. Int. Ed. Engl.* **1993**, *32*, 1361-1363.
(11) Control experiments have shown that the phosphazene base does not displace P^tBu_3 from the Pd(0) reactant or Pd(II) products.
(12) The pk_a (28.24, $CH2_3CN$) of BTPP is significantly higher than $NEt2_3$ (18.28, $CH2_3CN$) and P^tBu2_3 (11.24, $CH2_3NO2_2$). see (a) Kaljurand, I; Kütt, I.; Sooväli, L.; Rodima, T.; Mäemets, V.; Leito, I.; Koppel, I. *J. Org. Chem.* **2005**, 20*70*, 1019-1028. (b) Allman, T.; Goel, R. G. *Can. J. Chem.* **1982**, **20***60*, 2716-2722.
(13) See experimental section for characterication of isolated **7**.
(14) The products (normalized relative to **23**) observed by ^{31}P NMR at 91% conversion of **23** are: **22** (0.13), **25** (0.24), **24** (0.01), P^tBu_3 (0.37) and HP^tBu_3 (0.19).
(15) The reaction of **23** with PhBr in MEK occured in 92% yield with 0.5 equiv of added P^tBu_3. The same reaction without added ligand gave 63% of **22** and 23% of **25** at 92% conversion of **23**.
(16) Alcazar-Roman, L. M.; Hartwig, J. F. *J. Am. Chem. Soc.* **2001**, *123*, 12905-12906.
(17) Shekhar, S.; Hartwig, J. F. *Organometallics* **2007**, *26*, 340-351.
(18) Amatore, C.; Carré, E.; Jutand, A.; M'Barki, M. A.; Meyer, G. *Organometallics* **1995**, *14*, 5605-5614.
(19) Goodson, F. E.; Wallow, T. I.; Novak, B. M. *J. Am. Chem. Soc.* **1997**, *119*, 12441-12453.
(20) The organic products biphenyl (19%), bromobenzene (14%), and benzene (16%) were identified by ^1H NMR spectroscopy at 49% conversion of **22**.
(21) Espinet, P.; Echavarren, A. M. *Angew. Chem. Int. Ed.* **2004**, *43*, 4704-4734.
(22) Littke, A. F.; Schwarz, L.; Fu, G. C. *J. Am. Chem. Soc.* **2002**, *124*, 6343-6348.
(23) Zapf, A. *Transition Metals for Organic Synthesis (2nd Edition)* **2004**, *1*, 211-229.
(24) Bellina, F.; Carpita, A.; Rossi, R. *Synthesis* **2004**, 2419-2440.
(25) Beletskaya, I. P.; Cheprakov, A. V. *Chem.Rev.* **2000**, *100*, 3009-3066.
(26) Hills, I. D.; Fu, G. C. *J. Am. Chem. Soc.* **2004**, *126*, 13178-13179.
(27) Dai, C.; Fu, G. C. *J. Am. Chem. Soc.* **2001**, *123*, 2719-2724.
(28) Stambuli, J. P.; Incarvito, C. D.; Buehl, M.; Hartwig, J. F. *J. Am. Chem. Soc.* **2004**, *126*, 1184-1194.
(29) Stambuli, J. P.; Buhl, M.; Hartwig, J. F. *J. Am. Chem. Soc.* **2002**, *124*, 9346-9347.
(30) Clark, H. C.; Goel, A. B.; Goel, S. *Inorg. Chem.* **1979**, *18*, 2803-2808.
(31) Clark, H. C.; Goel, A. B.; Goel, S. *J. Organomet. Chem.* **1979**, *166*, C29-C32.

(32) Geissler, H.; Gross, P.; Guckes, B.; (Hoechst A.-G., Germany). DE, 1998, p 6 pp.

Chapter 4. Preparation and Evaluation of Ligandless, Anionic Arylpalladium Complexes as Intermediates in Mizoroki-Heck Reactions

---

4.1 Introduction to the Mizoroki-Heck Reaction

The prevalence of vinylarenes as structural motifs in bioactive molecules, synthetic intermediates, and materials precursors has inspired the development of many synthetic methods for their construction. Palladium-catalyzed cross-coupling has emerged as a premier strategy for the synthesis of vinylarenes. The cross-coupling of an organic electrophile, typically a haloarene or pseudo-halide, with an alkenyl organometallic reagent forms the corresponding vinylarene with high regio- and stereoselectivity (Scheme 29). Common organometallic reagents for this transformation include alkenyl-boron, silicon, zinc, tin, and magnesium compounds.

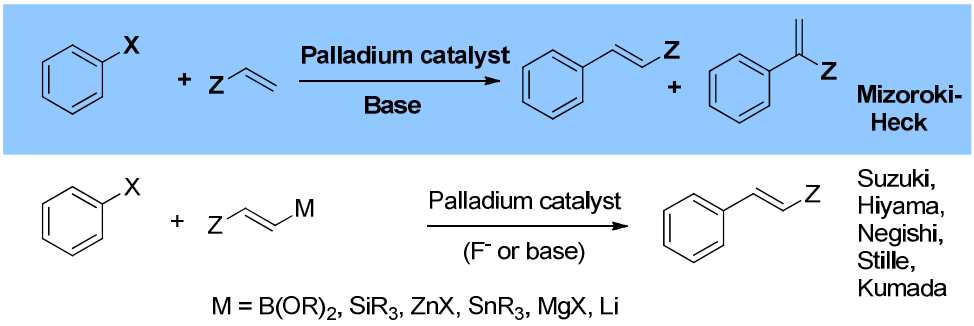

Scheme 29. Palladium-Catalyzed Coupling Reactions

A more direct and atom-efficient method for the construction of vinylarenes is the Mizoroki-Heck reaction, which is the palladium-mediated coupling of an organic electrophile with an olefin in the presence of base (Scheme 29).[1-7] Whereas cross-coupling reactions require the preparation or commercial availability of an alkenyl-metal

reagent, the Mizoroki-Heck reaction necessitates the availability of only the parent olefin.[8] Unlike the high regioselectivity observed for cross-coupling reactions, Mizoroki-Heck reactions can form both internal and terminal olefin products. Thus, the development of catalysts that are able to control the regioselectivity of the Mizoroki-Heck reaction has been an area of intense research.

Since the seminal reports by Heck and Mizoroki,[9-10,11-13] a great number of mechanistic and methodological studies have propelled this coupling reaction to one of the most commonly employed palladium-catalyzed reactions in laboratory and industrial settings. Advances in catalyst design have extended the scope of haloarene electrophiles from the more reactive iodoarenes and bromoarenes to less reactive chloroarenes, as well as pseudo-halides such as arenesulfonates. The intramolecular coupling of alkyl electrophiles has been reported recently as well.[14] The development of catalysts ligated by chiral bisphosphine ligands have also led to both intra- and intermolecular, enantioselective versions of this transformation.[15-16]

The attractive features of the Heck reaction can be highlighted by the ever increasing number of complex molecule syntheses[17] and pharmaceutical targets[18] in which one or more C-C bonds are constructed by this method. A few elegant examples include: the carbon framework of Merck's singular®, which is an LTD_4 antagonist for the treatment of asthma, is completed by the Heck reaction of an iodoarene and allylic alcohol (Scheme 30). Upon olefin migration of the substituted allylic alcohol product and tautomerization of the enol, the resulting ketone product is elaborated to singulair®, as well as a number of derivatives.[19] It is worthy of note that singulair® accounted for greater than $3 billion

in retail sales in 2009.[20] A second example of the Heck reaction in industrial-scale synthesis is Aventis' preparation of naproxen, an anti-inflammatory agent, by the coupling of ethylene and a naphthyl bromide derivative (Scheme 31).[18] Hydroxycarbonylation and resolution of the resulting vinylarene product affords naproxen in a step-economic route. [21]

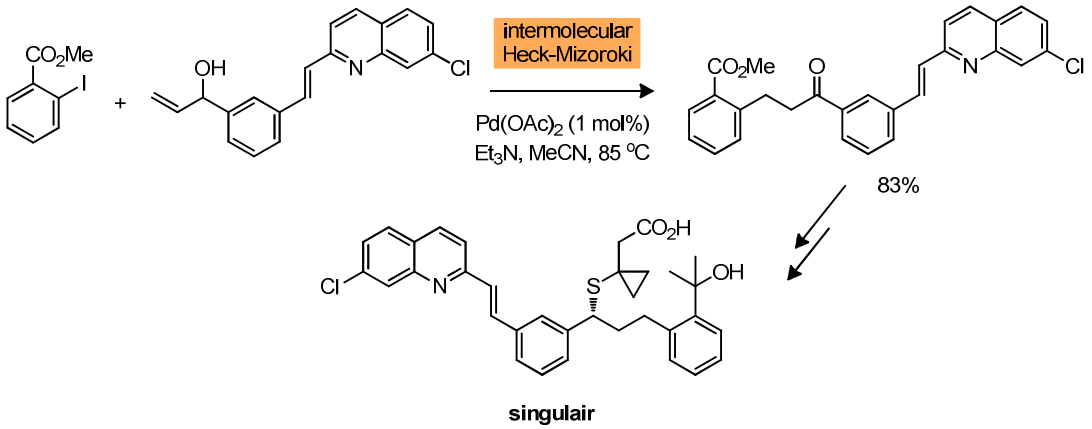

Scheme 30. Mizoroki-Heck Reaction in the Synthesis of Singulair®

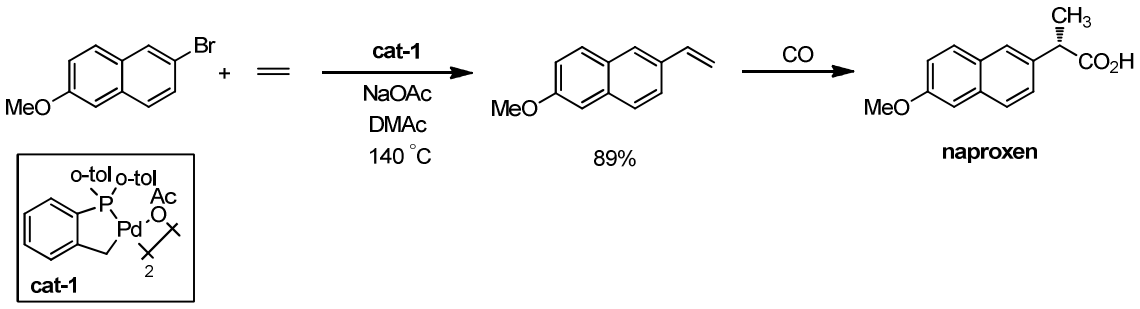

Scheme 31. Mizoroki-Heck Reaction in the Synthesis of Naproxen

In the context of complex molecule synthesis, Tietze has reported a synthesis of estrone where construction of the steroid skeleton is accomplished first by an intermolecular Heck reaction of an alkenyl bromide and a cyclohexene derivative followed by an intramolecular Heck reaction to close the B ring and complete the ABCD

steroid core (Scheme 32). Danishefsky also utilized a Heck reaction in the synthesis of the taxol skeleton (Scheme 33).[22] The intramolecular reaction of an enol triflate with a terminal olefin completes the core ABC ring system. These four syntheses that utilize the Heck reaction not only point out the impressive range of electrophiles and olefins that undergo coupling, but also emphasize that this reaction has become a preferred strategic disconnect of vinylic C-C bonds. Additionally, the impact of this synthetic method was recently recognized when Richard Heck was one of three scientists awarded the 2010 Nobel Prize in Chemistry for the discovery and development of palladium-catalyzed coupling reactions.

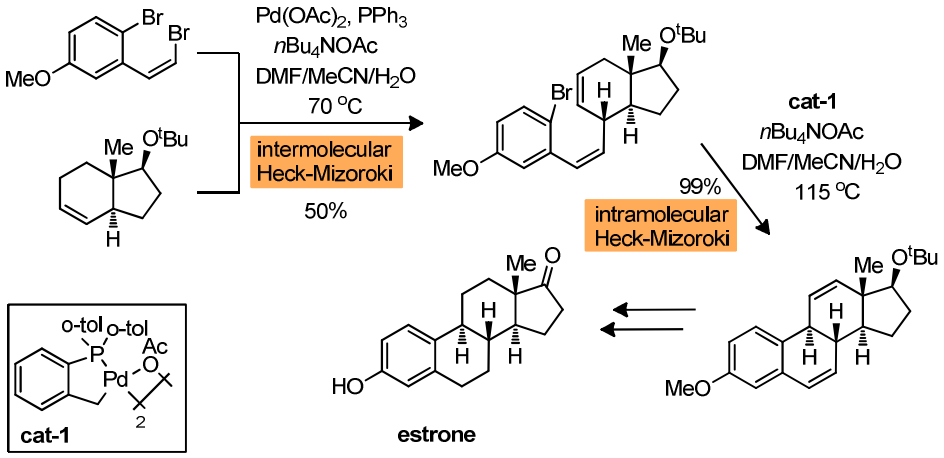

Scheme 32. Mizoroki-Heck Reactions in the Synthesis of Estrone

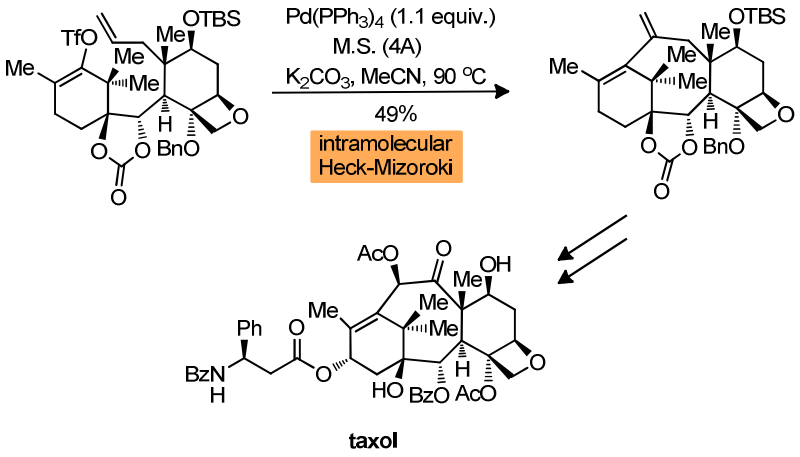

Scheme 33. Mizoroki-Heck Reaction in the Synthesis of Taxol

4.2 Mechanism of the Mizoroki-Heck Reaction

Although the Heck reaction is often associated with cross-coupling reactions, the catalytic cycle is distinct following the first step that is common to the two classes of coupling reactions. Cross-coupling reactions are established to occur by oxidative addition, transmetallation of an appropriate organometallic nucleophile, and C-C bond-forming reductive elimination (Scheme 34). However, C-C bond formation occurs instead in the Heck reaction by migratory insertion of an olefin into the Pd-C bond resulting from oxidative addition.

The general mechanism of the Mizoroki-Heck begins with oxidative addition of an organic electrophile to a palladium(0) complex, followed by migratory insertion of an olefin across the Pd-C bond, β-hydrogen elimination to generate the olefin product, and finally the Pd(0) complex is regenerated by base-assisted reductive elimination of HX

(Scheme 34).[23-24] Oxidative addition is common among the Heck reaction and other cross-coupling reactions and has been discussed in the first three Chapters. Reductive elimination is also common to the Heck reaction and other cross-coupling reactions. However, the ligands involved in the reductive elimination process are carbon-based or H and X (X = I, Br, Cl, OSO_2Ar, etc.) for cross-coupling and Heck reactions, respectively.

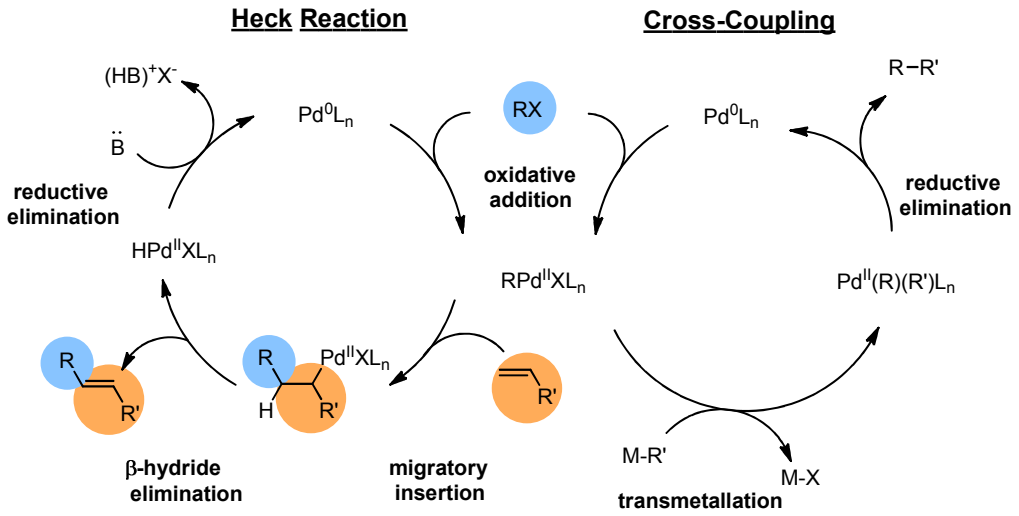

Scheme 34. Mechanisms of the Heck and Cross-Coupling Reactions

Carbon-carbon bond-forming reductive elimination has been studied extensively,[25] but the mechanism of H-X reductive elimination in the Heck reaction has not been studied to the same extent as that of C-C reductive elimination. In fact, studies of reductive elimination of H-X from isolated palladium hydride complexes are rare. One recent report by Fu details the reversible base-assisted reductive elimination from a palladium hydride complex $L_2Pd(H)(Cl)$ (L = PCy_3 or P^tBu_3) in the presence of Cs_2CO_3 or trialkylamine.[26] This study concluded that the stronger base Cy_2MeN led to full conversion of $(^tBu_3P)_2Pd(H)(Cl)$ to $(^tBu_3P)_2Pd^0$, whereas the weaker base afforded no reductive elimination product. Furthermore, $(Cy_3P)_2Pd(H)(Cl)$ did not react with amine

base to afford a detectable amount of $(Cy_3P)_2Pd^0$. Analysis of X-ray crystal structures of $(^tBu_3P)_2Pd(H)(Cl)$ and $(Cy_3P)_2Pd(H)(Cl)$, as well as an observed inverse dependence of the rate on the concentration of free phosphine for the reaction of $(^tBu_3P)_2Pd(H)(Cl)$ with amine base, led the authors to conclude that reductive elimination occurs through a three-coordinate monophosphine intermediate. The increased steric bulk of P^tBu_3 versus PCy_3 presumably accounts for the increased extent of reductive elimination by lowering the barrier to dissociation of the ligand from $L_2Pd(H)(Cl)$. However, other details about the reductive elimination step in the Heck reaction remain unclear, such as whether olefin remains bound prior to cleavage of the Pd-H bond. Mechanistic details such as these are important since the persistence of the palladium hydride complex with bound olefin can lead to migration of the double bond in the initial Heck product and the formation of thermodynamic mixtures of olefin isomers.

Migratory insertion in the Heck reaction is the step of the catalytic cycle responsible for the formation of the C-C bond in the organic product. Arylation can occur at the α or β position of a terminal olefin, thus migratory insertion also controls the regioselectivity of the Heck reaction and ultimately the yield of the desired product. Migratory insertion of an olefin into the metal-carbon occurs by *syn* addition across the π system.[27-29] Similarly, the mechanism of β-hydrogen elimination has been studied and is proposed to occur first by generation of an open coordination site on the metal followed by *syn* elimination.[30-31] However, identification of the structure of palladium complexes that undergo migratory insertion and β-hydrogen elimination in catalyst systems commonly used for Heck reactions is a more challenging endeavor. Knowledge of these

intermediates is desirable both to understand the factors that affect the regioselectivity of olefin insertion,[7] and to facilitate the evolution of catalyst design towards both higher activity and selectivity.

Proposed mechanisms for coordination-insertion in the Heck reaction generally fall into two categories: neutral pathway and ionic pathway. These two mechanisms are distinct by the dissociation of a dative or ionic ligand from palladium prior to olefin coordination, respectively. When the anionic ligand X in the oxidative addition product $L_2Pd(Ar)(X)$ is weakly coordinating (e.g. $^-OSO_2CF_3$) or abstracted by an anion scavenger (e.g. Ag^+ or Tl^+), then the ionic pathway often dominates. This is especially true if the dative ligands do not readily dissociate to facilitate the neutral pathway, such as for chelating bisphosphine ligands.[7,32-33] Monophosphine and halide ligands bound to palladium are proposed to promote coordination-insertion through the neutral pathway. When the ionic pathway is operative, the regioselectivity of migratory insertion is influenced more by the electronic properties of the olefin than by steric properties. Conversely, catalysts that operate through the neutral pathway are argued to be more influenced by steric properties of the olefin. However, the extent to which the ligands on palladium can override the influence of the substrate with regard to the regioselectivity of olefin insertion is unclear in many cases, especially for recently developed bulky monophosphine ligands.[7]

Although the number of catalysts and reaction conditions developed for the Heck reaction likely numbers in the hundreds, the majority of small and large-scale syntheses involving the Heck reaction utilize one of four general catalyst systems. The original

conditions reported by Heck using only simple palladium salts such as $Pd(OAc)_2$ and no added dative ligand (and Jeffery's variation on these conditions)[34-35] remain one of the most utilized methods for couplings of iodoarenes and some bromoarenes.[9-10,11-13] Additionally, palladium complexes ligated by PPh_3,[36] and the bulkier P(*o*-tol)$_3$,[37-38] constitute the most often used phosphine-ligated catalysts for the Heck reaction of iodo-, bromo-, and some activated chloroarenes with terminal and di-substituted olefins. Finally, the recent development of palladium catalysts ligated by bulky, electron-rich trialkylphosphines (e.g. P^{t}Bu$_3$) by Hartwig and Fu has expanded the scope of the organic electrophile to deactivated bromo- and chloroarenes.[39-43] The later method is arguably the state-of-the-art for Heck reactions of haloarenes with mono- and di-substituted olefins; often reactions conducted with these catalysts occur at room temperature.

Heck reactions conducted with palladium catalysts lacking added dative ligand, often described as "Jeffery conditions" when ionic additives are used,[34-35] are run on both small and industrial scale despite the development of modern phosphine and carbene ligands. Studies to reveal the mechanism of reactions under these "ligandless" conditions are more challenging than those of systems known to react through discrete complexes containing supporting ligands.[44]

Studies of "ligandless" systems have identified the presence of colloidal palladium in such reactions[45-48] and molecular species generated from these nanoparticles have been proposed as the active catalyst in solution,[48] but conclusions about the structures of such species have been largely speculative. Reetz used transmission electron microscopy (TEM) to directly observe palladium nanoparticles formed during catalytic reactions

conducted with $Pd(OAc)_2$.[45] A debate ensued as to whether a homogeneous, molecular complex accounts for catalysis, with the nanoparticles simply acting as a reservoir for such a species, or heterogeneous catalysis occurs directly on the surface of the palladium nanoparticles.

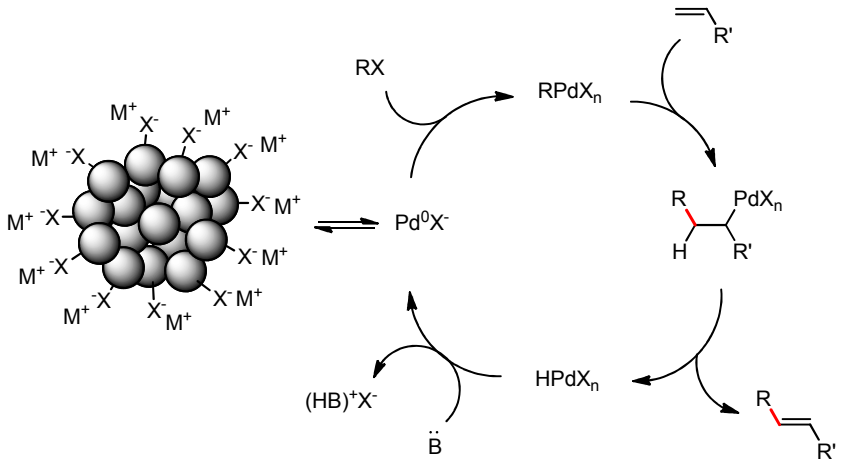

Scheme 35. Mechanism of "Ligandless" Mizoroki-Heck Reactions

The anionic species $[(Ar)PdX_2]^-$ and $[PdX_3]^-$ lacking dative ligands have been detected in solution by mass spectrometry and small angle X-ray techniques,[46,48] and complexes of the formula $[(Ar)PdX_2]_2^{2-}$ containing perhalogenated aryl groups have been isolated.[49-50] These spectroscopic studies indirectly suggest a molecular catalyst is operative. Furthermore, de Vries reported that decreased catalyst loading resulted in higher turnover frequency for ligandless Heck reactions.[51] This counterintuitive inverse dependence of the rate on the concentration of catalyst is proposed to arise from the higher concentration of a molecular species (argued to be the active catalyst) that is in equilibrium with higher-order aggregates when the concentration of palladium is decreased. On the basis of these observations, Reetz and de Vries propose that

nanoparticles serve as a reservoir for molecular species that catalyzes Heck reactions run under "ligandless" conditions (Scheme 35).[47] However, ligandless arylpalladium halide complexes lacking the stability imparted by a perhaloaryl group have never been isolated, and the reactions of discrete, "ligandless" anionic arylpalladium halide complexes have not been described.[52] Thus, the efficacy of such anionic palladium complexes to serve as molecular catalysts have not been evaluated empirically.

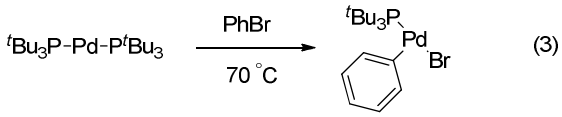

(3)

The more recently developed catalysts for Heck reactions involving palladium complexes ligated by P(*t*-Bu)$_3$ are arguably the most active to date. However, investigations of the mechanism of olefin insertion into complexes of P(*t*-Bu)$_3$ are rare. Stambuli and Hartwig found that the product of oxidative addition of haloarenes to palladium complexes of P(*t*-Bu)$_3$ formed unusual three-coordinate, T-shaped products (Eq 3).[53-54] The mechanism of oxidative addition of haloarenes to palladium complexes has been reported.[55-57] The reaction of the T-shaped (L)Pd(Ph)(Br) (L = 1-adamantyl-di-*tert*-butylphosphine) with styrene was also reported and occurred with an inverse order in free phosphine. [53] The authors concluded that the inverse order in added ligand signifies coordinated phosphine is absent during the rate-determining step of migratory insertion to form stilbene, but did not specify what the rate-determining step was in this system. With the exception of this report, the intermediates involved in migratory insertion for Heck reactions conducted with these highly active palladium complexes containing bulky trialkylphosphine ligands have not been identified.

4.3 Results and Discussion

4.3.1 Preparation and Characterization of Ligandless, Anionic Arylpalladium Halide Complexes

Here, the synthesis, isolation, structural characterization, and reactivity of anionic arylpalladium halide complexes $[(Ar)PdBr_2]_2^{2-}$ lacking a dative ligand is reported. Mechanistic data imply that these complexes are intermediates in Heck reactions catalyzed by ligandless palladium. However, we also provide data that imply that that such "ligandless" species are also intermediates in reactions catalyzed by complexes of some of the most commonly used phosphines, including those catalyzed by the combination of palladium and a bulky trialkylphosphine.

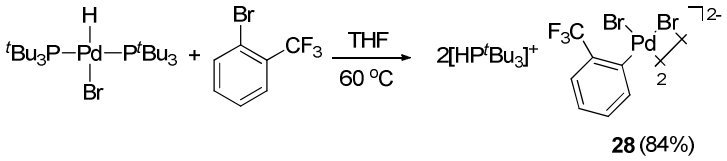

28 (84%) (4)

We first observed the formation of anionic arylpalladium complexes lacking dative ligands from the combination of 2-bromobenzotrifluoride and the Pd(II) complex $(^tBu_3P)_2Pd(H)(Br)$ (Eq 4).[55,58] This reaction formed the anionic 2-trifluoromethyl-phenyl complex **28** lacking any neutral, L-type, ligands in high yield. The ^1H NMR spectrum of **28** contained a doublet at 5.49 ppm for the proton of the phosphonium salt, in addition to the resonances for the palladium-bound aryl group and the *tert*-butyl groups on phosphorus. The $^{31}P\{^1H\}$ NMR spectrum consisted of a signal with a chemical shift similar to that of $[HP^tBu_3]Br$.

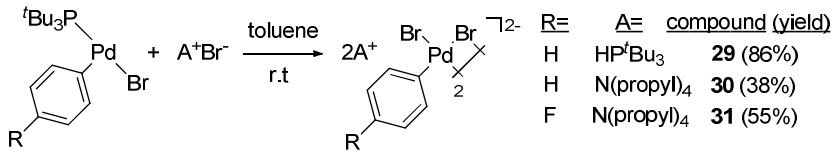

Scheme 36. Synthesis of Ligandless, Anionic Arylpalladium Halide Complexes

A more general synthesis of dimeric, dianionic arylpalladium halide complexes is shown in Scheme 36. Phenyl and 4-fluorophenyl complexes **29-31** were prepared from the reaction of trialkylphosphonium and tetraalkylammonium halides with (^{t}Bu$_3$P)Pd(Ar)(Br).[53-54] The products were obtained directly from a nonpolar reaction solvent in 38-86% yield. Complexes **28**-**31** are air-stable, crystalline solids. Single-crystal X-ray diffraction indicates that they are dimeric complexes containing two μ-halide ligands in the solid state. Conductivity measurements indicate that the complexes remain dimeric in solution. The conductivity of a 1 mM solution of **30** in nitrobenzene was 49 ohm^{-1} cm^2 mol^{-1}. This value falls in the range of conductivities of 2:1 electrolytes, and a 2:1 electrolyte is consistent with a dianionic, dimeric structure.[59]

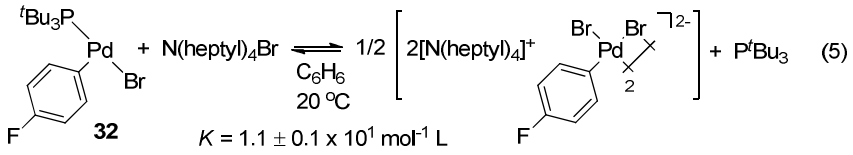

The combination of halide and neutral, phosphine-ligated arylpalladium halide complexes equilibrates with the combination of the anionic complexes and free phosphine. Exchange of halide for phosphine occurred immediately upon mixing the neutral complex **32** with NR_4Br (Eq 5). The equilibrium constant determined by ^{19}F and ^{31}P NMR spectroscopy at 20 °C was 1.1 ± 0.1 x 10^1 mol^{-1} L.[60]

4.3.2 Reactions of Isolated Ligandless, Anionic Arylpalladium Halide Complexes with Olefins

Anionic complexes **29** and **30** react with alkenes and vinylarenes under mild conditions (Scheme 37). Complex **29** reacted with styrene in a mixture of acetonitrile and toluene with added $MeCy_2N$ to form *trans*-stilbene in high yield within 10 min at 25 °C. Reactions occurred in the absence of base; however higher yields of the vinylarenes (ca 10%) were obtained in the presence of added amine, presumably because the consumption of the H-Pd-X product prevents unproductive consumption of the starting complex. Reactions of the anionic complexes with olefins typically result in fast precipitation of a black solid (presumably Pd^0) during the reaction. In the case of the reaction of **29** with styrene (Scheme 37), the soluble palladium products were quantified by ^{31}P NMR spectroscopy. The only species observed in solution was $Pd(P^tBu_3)_2$ (25%). The remaining palladium product is likely the precipitated species.

To assess whether the phosphonium cation generates a phosphine ligand and the reaction occurs through this phosphine complex, we studied the reactions of alkenes and vinylarenes with complex **30** containing an ammonium, rather than a phosphonium, ion. Acrylates and styrene reacted with **30** to give the cinnamate and stilbene products in high yield. Even 3,3-dimethyl-1-butene reacted to form a vinylarene product at room temperature. 1,2-Disubstituted alkenes react more slowly than less substituted alkenes in the Heck arylation, but the anionic complex **30** reacted with *trans*-methyl cinnamate to afford the tri-substituted olefin product in good yield at only 50 ^oC.

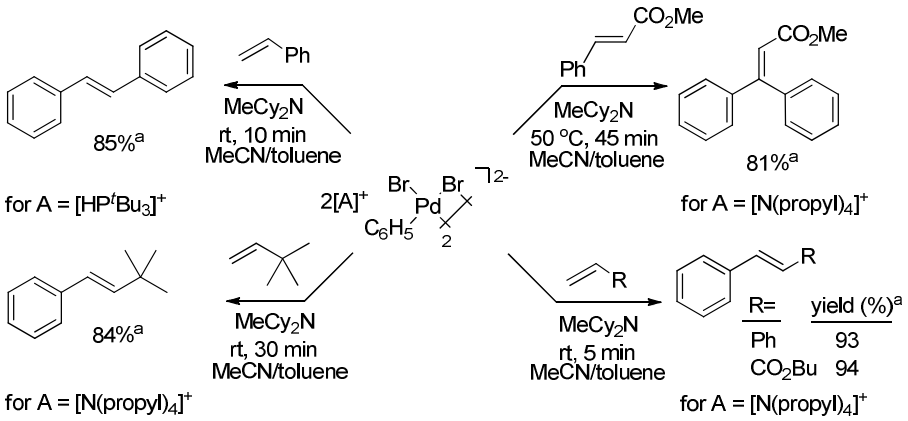

[a]Based on GC analysis with *n*-$C_{14}H_{30}$ as internal standard.

Scheme 37. Reactions of **29** and **30** with Olefins

These results show that the anionic complex $[(Ar)PdX_2]_2^{2-}$ is competent to be an intermediate in Heck reactions catalyzed by ligandless palladium systems that typically occur over several hours at elevated temperature.[61-63] Moreover, these results show that the anionic arylpalladium complexes are more reactive than neutral analogs ligated by PPh_3.[64-65-67] The faster reactions of alkenes with these anionic complexes than with related neutral complexes runs counter to the typically faster insertions of alkenes into the M-C bonds of more electrophilic complexes.

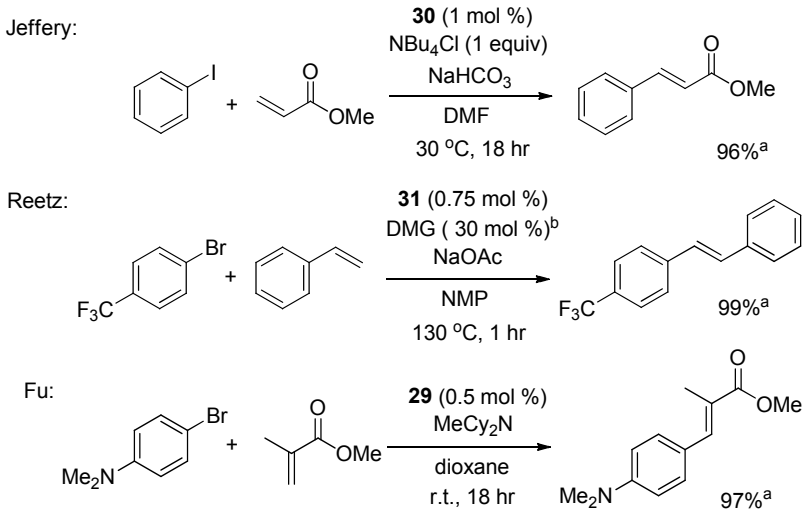

[a]Isolated yield. [b]DMG = *N,N*-dimethylglycine.

Scheme 38. Catalytic Mizoroki-Heck Reactions

To assess the competence of **29-31** to be intermediates in the Heck reaction, we conducted reactions of aryl halides with olefins catalyzed by **29-31** under three common sets of reaction conditions (Scheme 38). The reaction of iodobenzene with methyl acrylate catalyzed by the parent phenyl complex **30** at 30 °C gave *trans*-methyl cinnamate in 96% yield. Similarly, the reaction of 4-bromo-benzotrifluoride with styrene catalyzed by *p*-fluorophenyl complex **31** at 130 °C gave the substituted stilbene in high yield. Finally, the reaction of the deactivated aryl bromide 1-bromo-4-*N,N*-dimethyl-aniline with methyl methacrylate occurred in the presence of **29** to give the substituted cinnamate product in high yield at room temperature. Presumably the phosphonium cation in **29** releases free P(*t*-Bu)$_3$ in the presence of amine base[68] and forms a highly active P(*t*-Bu)$_3$-ligated Pd(0) species for oxidative addition.[69] These data on the reactions of the anionic species imply that the isolated complexes are competent to be

intermediates in the Heck reactions of iodo- and bromoarenes with terminal and di-substituted olefins.

Further studies implied that these ligandless complexes are also intermediates in Heck reactions conducted under some of the mildest conditions developed recently.[39-43] Because "ligandless" complexes **29-31** were prepared from arylpalladium complexes ligated by P(*t*-Bu)$_3$, ligandless, anionic complexes would be formed reversibly in a catalytic system involving P(*t*-Bu)$_3$-ligated palladium complexes. If the anionic complexes were more reactive than the neutral species, then the products would actually result from reaction of the alkene with the species lacking any dative ligand. Thus, we conducted experiments to compare the rates of reactions of the anionic arylpalladium complexes to those of neutral P(*t*-Bu)$_3$-ligated analogs. These experiments revealed the unexpected result that the anionic complexes react *faster* than the neutral analogs ligated by P(*t*-Bu)$_3$.

Comparisons of the rates of reactions of styrene with ligandless and P(*t*-Bu)$_3$-ligated arylpalladium halide complexes **31** and **32** are shown in Figure 22. Reaction of anionic **31** with styrene and MeCy$_2$N in a mixture of acetonitrile and toluene (4:1) at 20 °C occurred with a k_{obs} value of 2.9 x 10^{-3} s^{-1}. This value was much faster than that of the analogous reaction of the neutral, three-coordinate **32** with the same quantity of styrene in the presence of MeCy$_2$N[70] (0.05 M) and P^{t}Bu$_3$ (0.17 M).

The rate of decay of the neutral, three-coordinate species in the presence of added halide (Figure 21) was measured to test the potential that the anionic species are intermediates in reactions of phosphine-ligated complexes. Reaction of (^{t}Bu$_3$P)Pd(C$_6$H$_4$-

p-F)(Br) (**32**) with styrene in the presence of N(heptyl)$_4$Br (0.68 M) occurred in good yield (92% yield as determined by ^{19}F NMR spectroscopy) and to 90% conversion after 7 h (k_{obs} = 8.9 x 10^{-5} s^{-1}), while the same reaction conducted in absence of added bromide proceeded to only 13% conversion over the same time.[71]

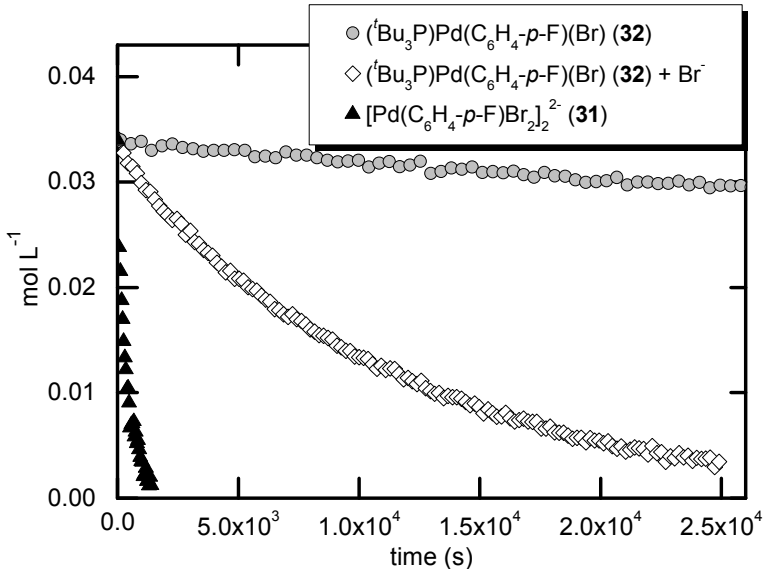

Figure 22. Decay of **32** (0.034 M) in the presence of styrene (0.17 M), P^{t}Bu$_3$ (0.17 M), N(heptyl)$_4$Br (0-0.68 M) and MeCy$_2$N (0.05 M)[70] in acetonitrile and toluene (4:1) at 20 °C, and decay of **31** (0.017 M) in the presence of styrene (0.17 M) and MeCy$_2$N (0.05 M) in acetonitrile and toluene (4:1) at 20 °C as monitored by ^{19}F NMR spectroscopy.

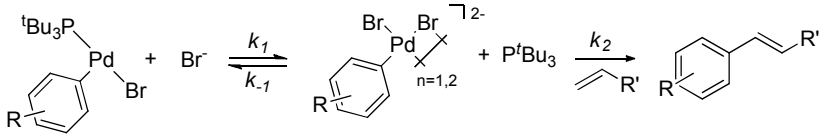

$$\text{rate} = k_{obs}\,[(^t\text{Bu}_3\text{P})\text{Pd(Ar)(Br)}]$$

$$k_{obs} = \frac{k_1 k_2\ [\text{Br}^-]\ [\text{olefin}]}{k_{-1}\ \ [\text{P}^t\text{Bu}_3]}$$

Scheme 39. Mechanism for Migratory Insertion

We also conducted detailed kinetic studies to further evaluate the intermediacy of ligandless, anionic palladium complexes during migratory insertion with catalysts ligated

by bulky alkyl phosphines. A mechanism for reaction of (^{t}Bu$_3$P)Pd(Ar)(Br) with olefin involving the intermediacy of [(Ar)Pd(Br)$_2$]$^-$ is shown in Scheme 39. Initial reversible displacement of phosphine in (^{t}Bu$_3$P)Pd(Ar)(Br) by halide generates an anionic intermediate, which then coordinates olefin. Migratory insertion and β-hydrogen elimination generates the organic product. According to this mechanism the rate of the stoichiometric reaction should occur with a first-order dependence on the concentration of halide and olefin, and with an inverse first-order dependence on the concentration of phosphine. Kinetic reactions of isolated (^{t}Bu$_3$P)Pd(Ar)(Br) with styrene were conducted to probe the validity of the mechanism outlined in Scheme 39.

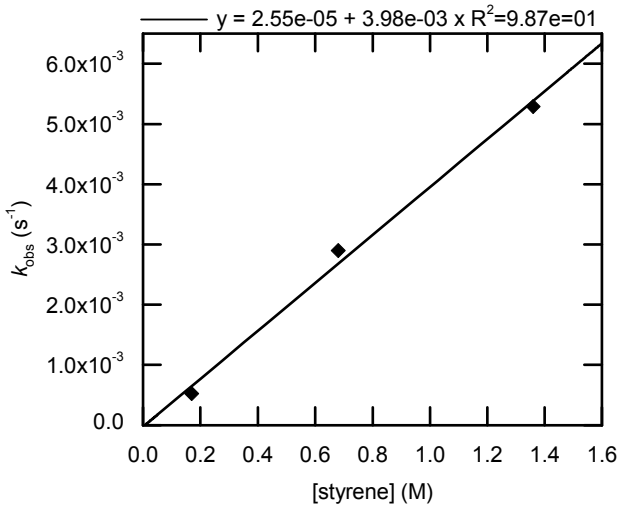

Figure 23. Dependence of observed rate constant on the concentration of styrene (0.17-1.3 M) for the reaction of (^{t}Bu$_3$P)Pd(C$_6$H$_4$-*p*-F)(Br) (**32**) (0.034 M) with styrene in the presence of P(*t*-Bu$_3$) (0.17 M) and N(heptyl)$_4$Br (0.17 M) in benzene at 20 °C.

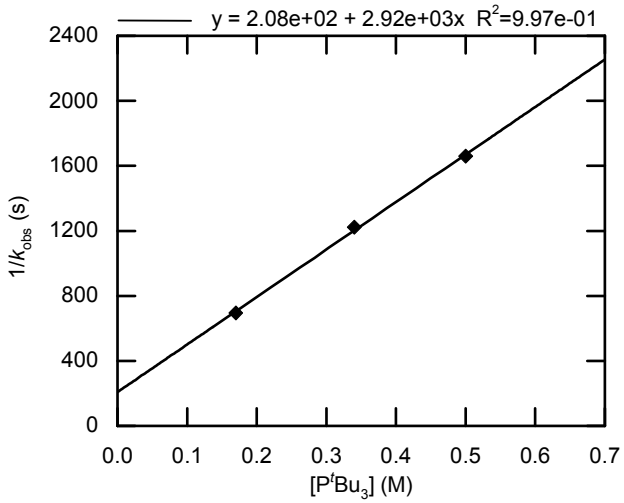

Figure 24. Dependence of observed rate constant on the concentration of P(*t*-Bu$_3$) (0.17-0.54 M) for the reaction of (^{t}Bu$_3$P)Pd(C$_6$H$_4$-*p*-F)(Br) (**32**) (0.034 M) with styrene (0.68 M) in the presence of N(heptyl)$_4$Br (0.10 M) in benzene at 20 °C.

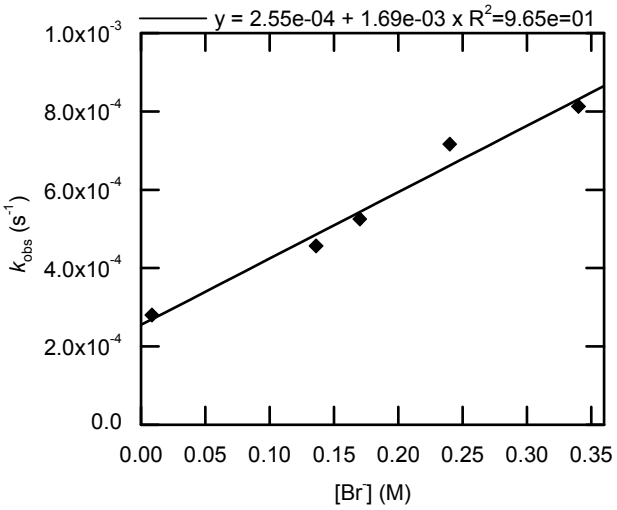

Figure 25. Dependence of observed rate constant on the concentration of N(heptyl)$_4$Br (0.0085-0.34 M) for the reaction of (^{t}Bu$_3$P)Pd(C$_6$H$_4$-*p*-F)(Br) (**32**) (0.034 M) with styrene (0.68 M) in the presence of P(*t*-Bu$_3$) (0.17 M) in benzene at 20 °C.

The rate constants for the reactions of (^{t}Bu$_3$P)Pd(C$_6$H$_4$-*p*-F)(Br) (**32**) with styrene to form 4-fluoro-*trans*-stilbene in the presence of P(*t*-Bu)$_3$ and N(heptyl)$_4$Br were measured in benzene at 20 °C by ^{19}F NMR spectroscopy. The plot of k_{obs} versus [styrene] indicates

that the reaction is first order in olefin (Fig 23). The plot of $1/k_{obs}$ versus [P^{t}Bu$_3$] indicates that the reaction is inverse first order in phosphine (Fig 24). Finally, the plot of k_{obs} versus [N(heptyl)$_4$Br] indicates that the reaction is first order in bromide (Fig 25). These data are consistent with the mechanism of Scheme 39, which involves the reversible formation of the ligandless, anionic arylpalladium halide complex followed by rate-limiting migratory insertion into the ligandless species.

4.3.3 Competition Studies to Probe for Ligandless Palladium Intermediates in Reactions Conducted with Phosphine-Ligated Catalysts

To test the potential that the ligandless and P(*t*-Bu)$_3$-ligated complexes react with olefins through a common intermediate, we evaluated the ratios of products formed from the isolated anionic complexes and from reactions conducted with common catalysts for the Heck reaction. Because prior studies[72-74] have indicated that the distribution of isomers formed from the Heck reaction varies with the steric and electronic properties of the electrophile, olefin, and catalyst, we considered that this selectivity could be used to probe for an intermediate that is common to reactions initiated with different catalyst precursors.

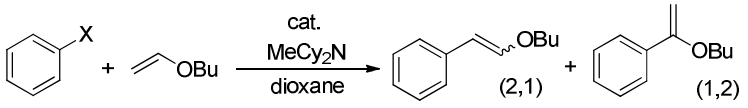

	X=	cat.=	temp (time)	(2,1):(1,2)
(a)	Br	Pd_2dba_3/P^tBu_3	8 hr (rt)	77:23
(b)	Br	Pd_2dba_3/P^tBu_3	20 min (100 °C)	72:28
(c)	Br	$Pd(PPh_3)_4$	36 hr (120 °C)	12:88
(d)	I	$Pd(OAc)_2/PPh_3$	3 hr (100 °C)	33:67
(e)	OTf	$Pd(OAc)_2$/dppp	5 hr (80 °C)	<1:99

Scheme 40. Catalytic Mizoroki-Heck Reactions with *n*-Butyl Vinyl Ether

In particular, Heck reactions of vinyl ethers form different ratios of isomeric products with different catalysts, and we measured the isomeric ratios of products of the reactions catalyzed by palladium complexes of triphenylphosphine, 1,3-bis-(diphenyl-phosphino)propane (dppp), and P(*t*-Bu)$_3$ under the same conditions. The distribution of products from the reaction of bromobenzene or iodobenzene with butyl vinyl ether catalyzed by Pd(PPh$_3$)$_4$ or the combination of Pd(OAc)$_2$ and PPh$_3$, as well as that from the reaction of phenyl triflate and butyl vinyl ether catalyzed by Pd(OAc)$_2$ and dppp (Scheme 40) were much different from that obtained from reaction of Pd$_2$dba$_3$ and P(*t*-Bu)$_3$. Thus, we concluded this selectivity would be a valid probe for a common intermediate.

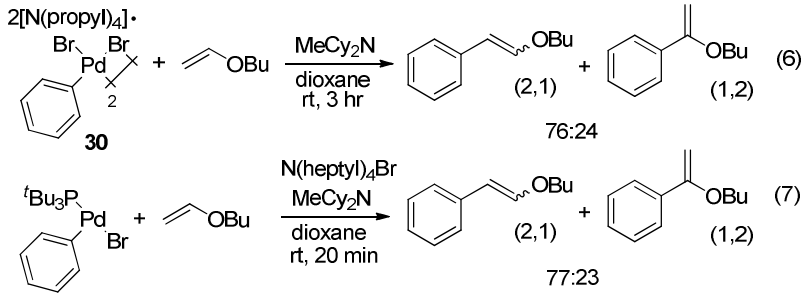

The reaction of butyl vinyl ether with the isolated anionic **30** and with the combination of (^{t}Bu$_3$P)Pd(Ph)(Br) and a tetraalkylammonium bromide salt are shown in eq 6 and 7. These two stoichiometric reactions occurred with similar regioselectivity. Moreover, this regioselectivity was indistinguishable from that of the catalytic reaction conducted with Pd$_2$dba$_3$ and P(*t*-Bu)$_3$. The similarity of these regioselectivities is consistent with the presence of a common intermediate that reacts with the olefin. The selectivity from the stoichiometric reaction of the vinyl ether with complex **30** indicates

that this common intermediate is the "ligandless," anionic arylpalladium halide complex we isolated.

4.3.4 DFT Calculations of CO Stretching Frequencies of Neutral and Anionic Palladium Complexes

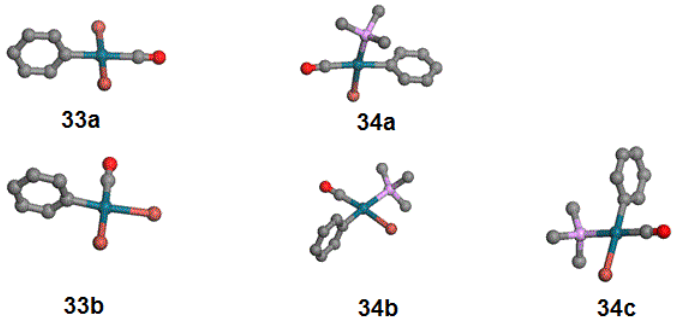

Figure 26. B3LYP optimized geometries of $[(Ph)Pd(CO)(Br)_2]^-$ and $(Me_3P)Pd(CO)(Ph)(Br)$. Color code: **Pd**, turquoise; **C**, gray; **P**, purple; **Br**, bronze; **O**, red).

Table 17. Calculated carbonyl stretching frequencies and selected bond distances for $[(Ph)Pd(CO)(Br)_2]^-$ and $(Ph)Pd(CO)(Br)(PMe_3)$ shown in Figure 25.

	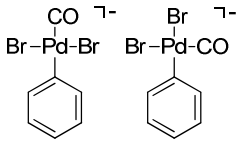		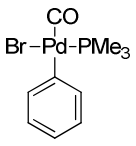	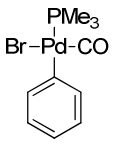	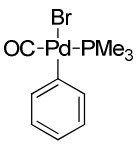
	33a	**33b**	**34a**	**34b**	**34c**
ν_{CO} (cm^{-1}):	2145	2129	2175	2153	2190
Pd-C (Å):	1.900	2.032	2.032	1.909	1.971
C-O (Å):	1.140	1.144	1.137	1.141	1.135

The activity of the ligandless arylpalladium complexes towards migratory insertion of olefins is surprising because this class of reactions tends to be faster for more electrophilic metal complexes.[75-76] However, it is not trivial to ascertain if, or to what extent, the anionic $[Pd(Ar)(Br)_2]_2^{2-}$ is more electron-rich compared to the neutral complex $(^tBu_3P)Pd(Ar)(Br)$ ligated by a trialkylphosphine that is a strong σ-donor. In order to gain

quantitative data about the electronic properties of these two complexes, DFT calculations were carried out with carbonyl complexes of the an anionic $[Pd(Ar)(Br)_2]^-$ and neutral $(R_3P)Pd(Ar)(Br)$. Optimized geometries for isomers of $[Pd(CO)(Ph)(Br)_2]^-$ and $(Me_3P)Pd(CO)(Ar)(Br)$ are shown in Figure 26. The stretching frequencies of these complexes were used as a gauge of the relative electron density at the metal center (Table 17). If the carbonyl ligands are oriented *cis* to the aryl ligand, as would be the orientation of an olefin prior to migratory insertion, the stretching frequencies indicate the anionic $[Pd(CO)(Ph)(Br)_2]^-$ is indeed more electron-rich than the neutral $(Me_3P)Pd(CO)(Ar)(Br)$. As such, the fast rates of migratory insertion of alkenes into the Pd-C bond of $[Pd(Ar)(Br)_2]^-$ complexes are attributed to steric factors that dominate the counteracting electronic effects typically observed for olefin insertions.

4.3.5 Mechanism of Olefin Insertion into Ligandless, Anionic Arylpalladium Halide Complexes

The kinetic analysis of the reactions of the neutral complex ($^tBu_3P)Pd(C_6H_4$-*p*-F)(Br) (**32**) with styrene (Section 4.3.2) provide detailed information of the mechanism of migratory insertion of olefins through the intermediacy of the anionic $[(Ar)Pd(Br)_2]_2^{2-}$ formed reversibly from the neutral complex. However, a firm understanding of the mechanism of migratory insertion into the anionic $[(Ar)Pd(Br)_2]_2^{2-}$ is also desired in order to learn how to control the regioselectivity in Heck reactions that involve such intermediates. Thus, we monitored the reaction of anionic **31** with styrene at low temperature in order to detect the presence of transient intermediates, and we also

conducted kinetic experiments to distinguish between possible mechanisms of migratory insertion.

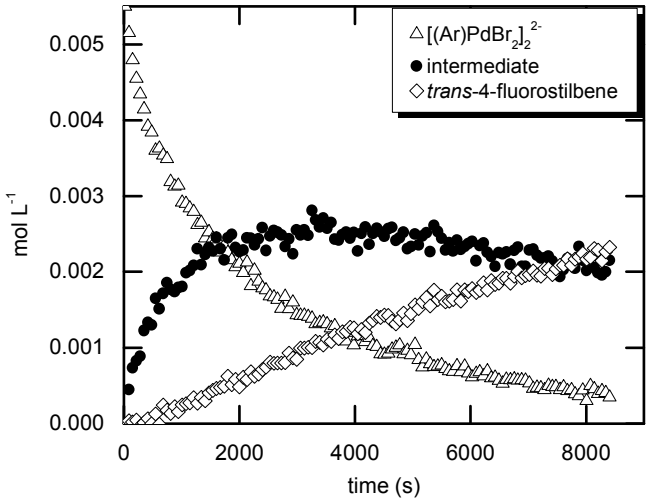

Figure 27. Decay of $2(NPr_4)\cdot[Pd(C_6H_4\text{-}p\text{-}F)(Br_2)]_2$ (**31**) (0.011 M) in the presence of styrene (0.11 M) in CH_2Cl_2 at -40 °C as monitored by ^{19}F NMR spectroscopy. The appearance of an intermediate (δ -118.8 ppm) and 4-fluoro-*trans*-stilbene, formed concurrently with the decay of **31**, were also monitored by ^{19}F NMR spectroscopy.

The reaction of anionic **31** with styrene was monitored by ^{19}F NMR spectroscopy at low temperature (Fig 27). The decay of **31** (0.011 M) in the presence of styrene (0.11 M) in CH_2Cl_2 at -40 °C occurred with an observed rate constant of 5.02×10^{-4} s^{-1}. During the course of the reaction of **31** with styrene, an unknown intermediate (δ -118.8 ppm) accumulated. The accumulation of the intermediate peaked at approximately one half-life, after which the concentration began to decrease. Additionally, 4-fluoro-*trans*-stilbene was observed by ^{19}F NMR spectroscopy during the reaction. The formation of the organic product occurred by an apparent zeroth-order process, suggesting that the final step of the reaction is an intramolecular process (i.e. β-hydrogen elimination or olefin dissociation).

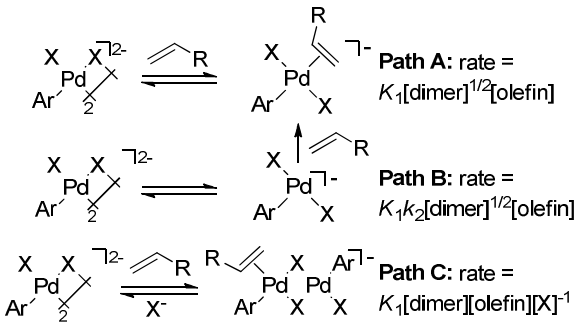

Scheme 41. Mechanisms for Migratory Insertion

The mechanism of migratory insertion during the reaction of the anionic $[(Ar)Pd(Br)_2]_2^{2-}$ with olefins has not been previously studied. Because the dimeric anionic complex $[(Ar)Pd(Br)_2]_2^{2-}$ is coordinatively saturated, it is unlikely to react directly with olefins through five-coordinate intermediates. We propose three mechanisms that could account for migratory insertion starting from the dimeric $[(Ar)Pd(Br)_2]_2^{2-}$ (Scheme 41). Associative or dissociative displacement of the bridging halide ligands by olefin account for two of the potential reaction pathways. The third mechanism involves displacement of a non-bridging halide ligand by olefin. Determination of the order in dimer, halide, and olefin for the reaction of $[(Ar)Pd(Br)_2]_2^{2-}$ with alkenes should distinguish between these potential mechanisms and could also provide insight as to the structure of the intermediate observed during the reaction of **4** with styrene at -40 °C (vide supra).

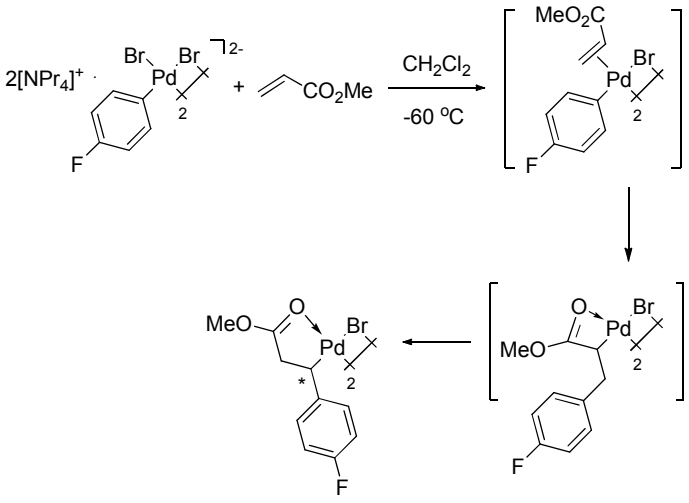

Scheme 42. Migratory Insertion of Methyl Acrylate

The reaction of anionic **31** with methyl acrylate was chosen as the system for kinetic analysis. Brookhart and Mecking have previously characterized by ^{1}H NMR spectroscopy the products of migratory insertion of methyl acrylate into a cationic methylpalladium complex ligated by a bulky α-diimine.[77] If stable intermediates also form during reaction of **31** with acrylates at low temperature, identification of the structures by correlation to published data for complexes containing α-diimine ligands may be possible. A potential pathway for the reaction of **31** with methyl acrylate outlined in Scheme 42 is similar to the mechanism proposed by Brookhart and Mecking whereby initial coordination and 2,1-insertion of methyl acrylate affords a four-membered chelate as the immediate product, which undergoes fast rearrangement to the more stable five-membered chelate. The coordination of the carbonyl oxygen to the vacant coordination site imparts stability to the resulting palladium alkyl complex. The formation of monomeric intermediates is also possible, and kinetic analysis of the reaction of **31** with

acrylates will facilitate identification of the structure and nuclearity of the palladium complex formed during migratory insertion.

Unfortunately, characterization by ^{1}H NMR spectroscopy of the intermediate palladium complex formed at -40 °C from the reaction of **31** with methyl acrylate was complicated by the observation of complex resonances that were difficult to assign. If the dimeric complex remains intact, the chelate that forms upon migratory insertion of methyl acrylate would generate several diastereomers from the combinations of the two stereogenic centers of the two alkyl ligands per molecule in addition to the *anti* and *syn* conformations of the palladium dimer. Such a scenario could explain the complexity of the ^{1}H NMR spectrum obtained for reaction of **31** with methyl acrylate, but conclusions are tenuous. Thus, we turned to kinetic studies to obtain information about the mechanism and structure of the complexes involved in the reactions of ligandless, anionic complexes with olefins.

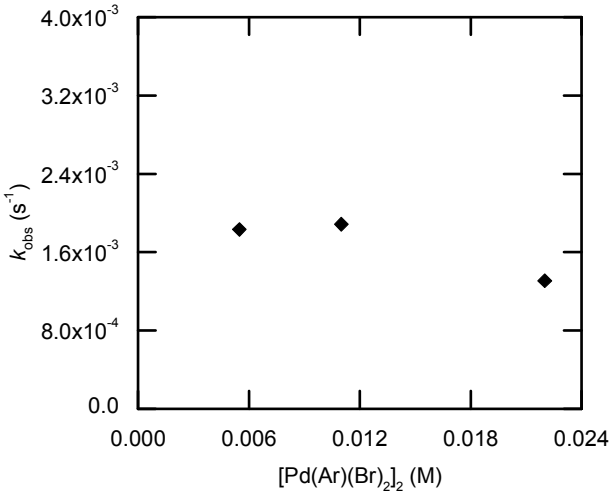

Figure 28. Dependence of observed rate constant on the concentration of $2(NPr_4)\cdot[Pd(C_6H_4\text{-}p\text{-}F)(Br_2)]_2$ (**31**) (0.0055-0.022 M) during the reaction with methyl acrylate (0.22 M) in the presence of $N(heptyl)_4Br$ (0.034 M) in CH_2Cl_2 at -40 °C.

The decay of **31** in the presence of styrene was previously shown (Fig 27) to occur by a first-order exponential decay, even though the starting complex is dimeric. Similarly, the decay of anionic **31** in the presence of methyl acrylate occurs by first-order decay, as measured by ^{19}F NMR spectroscopy. The dependence of the observed rate constant on the concentration of **31** (0.0055-0.022 M) with methyl acrylate (0.22 M) in the presence of N(heptyl)$_4$Br (0.034 M) was measured in CH_2Cl_2 at -40 °C (Fig 28). The observed rate constant does not vary significantly ($1.7 \pm 0.3 \times 10^{-3}$ s^{-1}) when the concentration of **31** is varied by a factor of four, indicating that the decay is indeed a first order process. These data rule out Path A and Path B mechanisms for migratory insertion illustrated in Scheme 41, the rates of which would occur with a half-order dependence on the concentration of **31**.

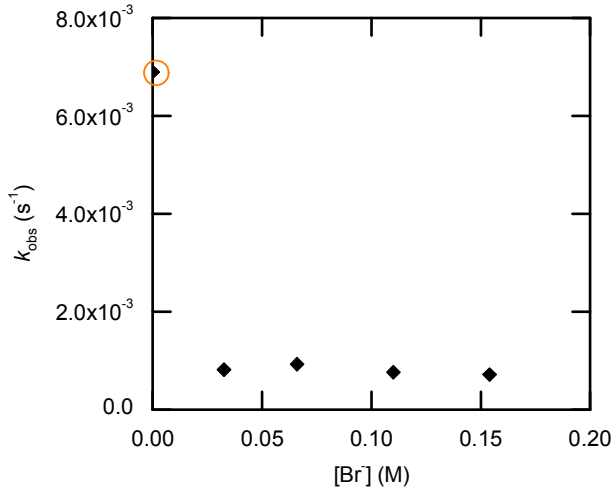

Figure 29. Dependence of observed rate constant on the concentration of N(heptyl)$_4$Br (0-0.15 M) for the reaction of 2(NPr$_4$)·[Pd(C$_6$H$_4$-*p*-F)(Br$_2$)]$_2$ (**31**) (0.011 M) with methyl acrylate (0.11 M) in CH_2Cl_2 at -40 °C.

The dependence of the observed rate constant on the concentration of added bromide was complex. The reaction of **31** with methyl acrylate conducted in the absence of added bromide occurs faster than reactions conducted in the presence of added bromide. The dependence of the observed rate constant for the reaction of **31** (0.011 M) with methyl acrylate (0.11 M) in the presence of $N(heptyl)_4Br$ (0.033-0.15 M) was measured by ^{19}F NMR spectroscopy in CH_2Cl_2 at -40 °C (Fig 29). The rate constant ($8.1 \pm 0.9 \times 10^{-4}$ s^{-1}) did not vary significantly when the concentration of bromide was varied by a factor of ca 5. These data suggest that the presence of free bromide ions cause a change in mechanism for migratory insertion or that bromide scavenges a species from solution that accelerates the rate of insertion. In the absence of bromide, reversible dissociation of a non-bridging halide may occur. However, the zeroth-order dependence of the observed rate constant on the concentration of added bromide indicates that reversible dissociation of a non-bridging bromide is not possible in the presence of added bromide. Thus, Path C in Scheme 41 is also not operative. However, several variants of the Path C mechanism could account for the observed orders in reagents. Irreversible substitution of a non-bridging bromide for olefin, or substitution of a single bridging bromide in the dimeric **31** for olefin would be consistent with the observed first-order dependence on the concentration of **31** and zeroth-order dependence on the concentration of bromide ions.

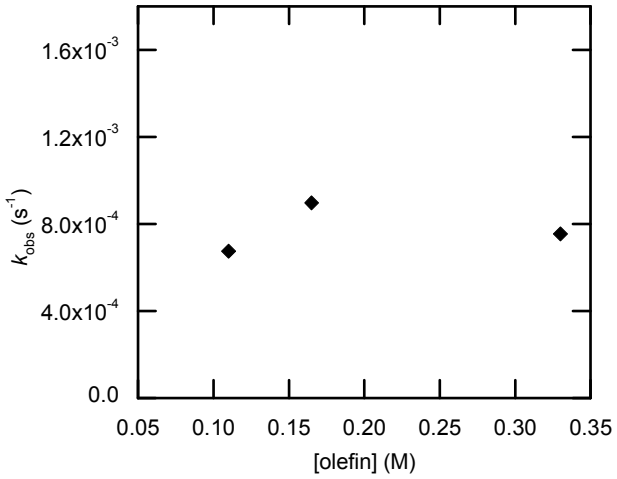

Figure 30. Dependence of observed rate constant on the concentration of methyl acrylate (0.11-0.33 M) for the reaction of $2(NPr_4)\cdot[Pd(C_6H_4\text{-}p\text{-}F)(Br_2)]_2$ (**31**) (0.011 M) with methyl acrylate in the presence of $N(heptyl)_4Br$ (0.034 M) in CH_2Cl_2 at -40 °C.

The dependence of the observed rate constant on the concentration of methyl acrylate was also measured by ^{19}F NMR spectroscopy (Fig 30). The reaction of **31** (0.011 M) with methyl acrylate (0.11-0.33 M) in the presence of $N(heptyl)_4Br$ (0.034 M) in CH_2Cl_2 occurred with an average observed rate constant of $7.8 \pm 1.1 \times 10^{-4}$ s^{-1}. The observed rate constant varied by only ca 14% when the concentration of olefin was varied by a factor of three, which is consistent with a zeroth-order dependence of the rate on the concentration of olefin. These kinetic data are consistent with three mechanisms for migratory insertion that are described in Scheme 43: irreversible dissociative substitution of a non-bridging halide (Path D), irreversible dissociative substitution of a bridging halide (Path E), and reversible dissociative substitution of a bridging halide (Path F). All three mechanisms involve dissociative substitution as the initial step, which is counterintuitive because associative substitution mechanisms for square planar, 16-electron transition metal complexes are typically observed.

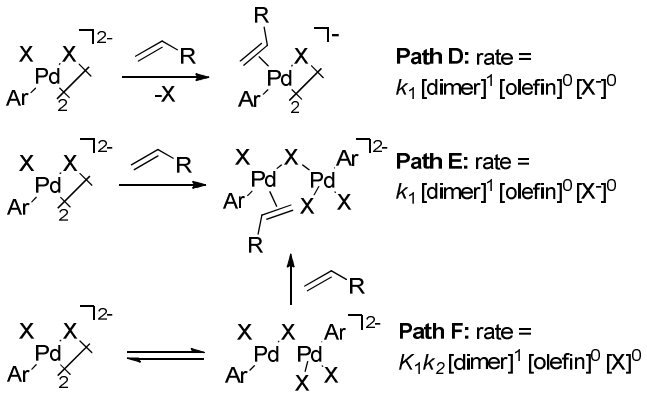

Scheme 43. Mechanisms for Migratory Insertion

The current data do not distinguish which of the three potential mechanisms outlined in Scheme 43 is operative, but the data does suggest that migratory insertions involving dimeric ligandless, anionic palladium complexes occur by a dissociative or solvent-assisted mechanism that does not depend on the concentration of olefin or bromide ions. Additionally, the first order dependence of the observed rate constant on the concentration of dimeric **31** indicates the palladium intermediate observed by ^{19}F NMR spectroscopy (Fig 28) for the reaction of **31** with styrene could exist as a dinuclear species.

The first-order dependence of the rate on the concentration of olefin for the reaction of the neutral complex **32** with olefin in the presence of halide contrasts the zeroth-order dependence of the rate on olefin for the reaction of anionic **31** with olefin, even though the former is proposed to undergo migratory insertion of olefins through the intermediacy of the later. However, the rate-limiting step of the two sets of reactions is not revealed by these studies and could be different. Such a circumstance could account for the discrepancy in the order of olefin. The reaction of neutral (L)Pd(Ar)(X) could also

proceed by generation of monomeric anionic $[Pd(Ar)(X)_2]^-$ which is trapped by olefin prior to dimerization. Additional experiments are needed to test these hypotheses.

4.3.6 Probing the Intermediacy of Ligandless, Anionic Arylpalladium Halide Complexes in Other Catalytic Processes

Facile and reversible generation of ligandless, anionic palladium complexes by exchange of halide for bulky phosphine ligands in T-shaped LPd(Ar)(X) complexes begs the question: what other phosphine ligands and metal geometries are susceptible to exchange of phosphine for halide? The answer to this question will begin to explore the range of palladium complexes, and by corollary the cross-coupling reactions, which may proceed by reaction of the reactive ligandless, anionic palladium species with an olefin or organometallic reagent. To begin, we initially monitored reactions of isolated T-shaped complexes containing phosphines other than P(*t*-Bu)$_3$ with olefins in the presence and absence of added halide.

Reactions of the T-shaped (1-AdP^tBu_2)Pd(Ph)(Br) (**35**) with styrene occurred with a marked acceleration in the presence of added bromide (Ad = adamantyl). The reacton of **35** (0.032 M) with styrene (0.33 M) in the presence of 1-AdP^tBu_2 (0.031 M) and N(heptyl)$_4$Br (0.093 M) in THF produced *trans*-stilbene in 85% yield after 65 min at room temperature, as monitored by GC analysis versus *n*-tetradecane as internal standard (Fig 31). The same reaction conducted in the absence of added bromide produced only 34% yield of *trans*-stilbene over the same period of time. These data are analogous to reactions of T-shaped ($^tBu_3P$)Pd(Ar)(Br) with olefins in the presence of added bromide,

which have been shown to proceed by initial formation of the ligandless, anionic palladium complex $[(Ar)Pd(Br)_2]_2^{2-}$ by displacement of the bulky phosphine ligand on palladium by halide.

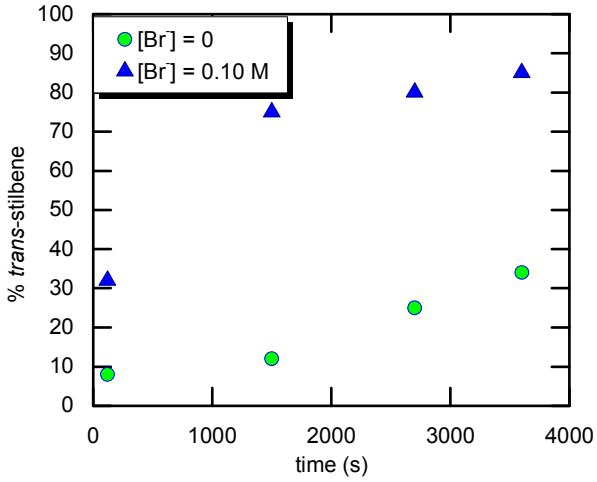

Figure 31. Appearance of *trans*-stilbene during the reaction of (1-AdP^tBu_2)Pd(Ph)(Br) (**35**) (0.032 M) with styrene (0.33 M) in the presence of N(heptyl)$_4$Br (0-0.093 M) and 1-AdP^tBu_2 (0.031 M) in THF at room temperature as monitored by GC versus *n*-tetradecane as internal standard. (Ad = adamantyl)

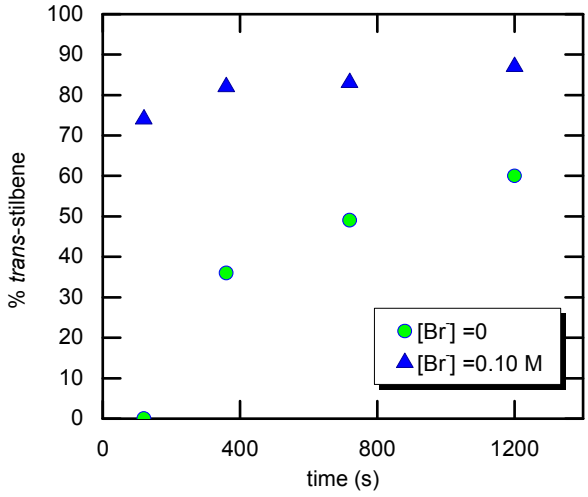

Figure 32. Appearance of *trans*-stilbene during the reaction of (QPhos)Pd(Ph)(Br) (**36**) (0.032 M) with styrene (0.33 M) in the presence of N(heptyl)$_4$Br (0-0.097 M) in THF at room temperature as monitored by GC versus *n*-tetradecane as internal standard. (QPhos = 1,2,3,4,5-Pentaphenyl-1′-(di-*tert*-butylphosphino)ferrocene)

Similar to reactions of the T-shaped complexes LPd(Ar)(X) ligated by P(*t*-Bu)$_3$ and (1-Ad)P^{t}Bu$_2$, the reaction of (QPhos)Pd(Ph)(Br) (QPhos = 1,2,3,4,5-Pentaphenyl-1′-(di-*tert*-butylphosphino)ferrocene) with styrene also exhibited a marked acceleration in the presence of added bromide ions. The reaction of (QPhos)Pd(Ph)(Br) (**36**) (0.032 M) with styrene (0.33 M) in the presence of N(heptyl)$_4$Br (0.097 M) in THF at room temperature produced *trans*-stilbene in 87% yield in 20 min, as monitored by GC analysis versus *n*-tetradecane as internal standard (Fig 32). The same reaction conducted in the absence of bromide produced *trans*-stilbene in only 60% yield over the same period of time. At earlier reaction time (2 min), the difference in yield of the organic product in the presence and absence of added bromide is even more pronounced: 74% and 0%, respectively.

Palladium complexes ligated by P(*o*-tol)$_3$ constitute one of the most widely used classes of catalysts for the Heck reaction.[24] The oxidative addition of aryl halides to palladium(0) complexes in the presence of P(*o*-tol)$_3$ generate three-coordinate, dimeric products of the form [LPd(Ar)(μ-X]$_2$. Similar to the T-shaped monomeric complexes LPd(Ar)(X) (L = P(*t*-Bu)$_3$, (1-Ad)P^{t}Bu$_2$, or QPhos), arylpalladium halide complexes ligated by P(*o*-tol)$_3$ are also three-coordinate, but the lower steric bulk of the phosphine ligand leads to a stable dimeric configuration.[78] Because catalysts containing P(*o*-tol)$_3$ are common catalysts for the Heck reaction, we also studied reactions of [Pd{P(*o*-tol)$_3$}(Ar)(μ-X]$_2$ complexes with olefins in the presence and absence of halide salts to probe the potential intermediacy of ligandless, anionic palladium complexes.

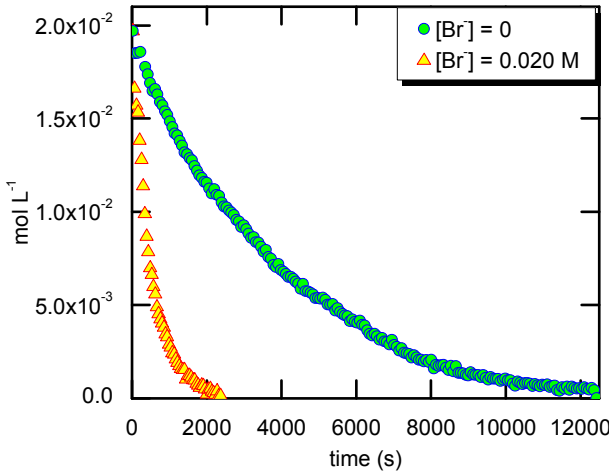

Figure 33. Decay of [Pd{P(*o*-tol)$_3$}(C$_6$H$_4$-*p*-F)(μ-Br)]$_2$ (**37**) (0.020 M) in the presence of butyl acrylate (0.20 M), N(heptyl)$_4$Br (0-0.20 M), P(*o*-tol)$_3$ (0.20 M), and MeCy$_2$N (0.040 M) in THF at 45 °C as monitored by ^{19}F NMR spectroscopy.

The reaction of [Pd{P(*o*-tol)$_3$}(C$_6$H$_4$-*p*-F)(μ-Br)]$_2$ (**37**) with butyl acrylate was monitored by ^{19}F NMR spectroscopy and occurred by a first order exponential decay (Fig 33). The decay of **37** (0.020 M) and butyl acrylate (0.20 M) in the presence of P(*o*-tol)$_3$ (0.20 M), MeCy$_2$N (0.040 M), and N(heptyl)$_4$Br (0-0.20 M) was monitored in THF at 45 °C and occurred with an observed rate constant of 2.06 x 10^{-3} s^{-1}. The same reaction conducted in the absence of added halide occurred with an observed rate constant of 2.38 x 10^{-4} s^{-1}. The slower reaction of the dimeric **37** with acrylate in the absence of added halide suggests that an anionic species may be generated prior to migratory insertion. Note that the starting complex in its dimeric form is ligated by two halides, an aryl ligand, and P(*o*-tol)$_3$. Thus, in addition to the potential formation of the ligandless, anionic arylpalladium complex by substitution of phosphine for halide, a second structure must be considered (Scheme 44). Substitution of a bridging halide in [Pd{P(*o*-

tol)$_3$}(Ar)(μ-X)]$_2$ by X$^-$ could also generate monomeric [Pd{P(*o*-tol)$_3$}(Ar)(X)$_2$]$^-$, which like the starting complex contains two halide ligands, an aryl ligand, and P(*o*-tol)$_3$.

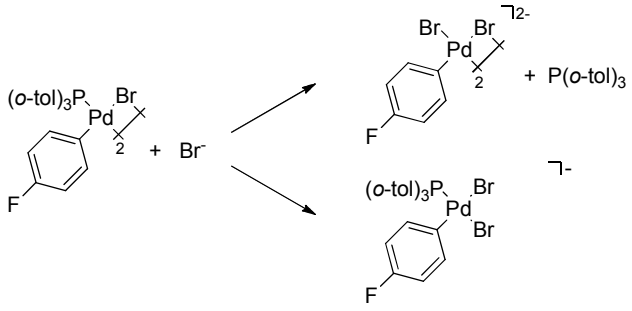

Scheme 44. Reaction of [Pd{P(*o*-tol)$_3$}(C$_6$H$_4$-*p*-F)(μ-Br)]$_2$ with Bromide

The combination of [Pd{P(*o*-tol)$_3$}(C$_6$H$_4$-*p*-F)(μ-Br)]$_2$ (**37**) and NPr$_4$Br in a 1:1 ratio in CH_2Cl_2 was monitored by ^{19}F NMR spectroscopy. The signal of the starting material (δ -122.7 ppm) dissipates upon mixing, and a new signal (δ -125.9 ppm) is observed. The chemical shift of the product is very similar to that of 2(NPr$_4$)·[Pd(C$_6$H$_4$-*p*-F)(Br$_2$)]$_2$ (**31**) (δ -126.0, -126.1 ppm for the major/minor diastereomer). However, the new signal is unlikely to correspond to the ligandless, anionic [(Ar)Pd(Br)$_2$]$_2^{2-}$ for several reasons. First, the ligandless, anionic complex is always observed as a pair of syn/anti diastereomers by ^{19}F NMR spectroscopy, yet a single resonance is observed as the product from reaction of [Pd{P(*o*-tol)$_3$}(C$_6$H$_4$-*p*-F)(μ-Br)]$_2$ (**37**) and NPr$_4$Br. Second, the interchange of neutral (^{t}Bu$_3$P)Pd(Ar)(Br) and [(Ar)Pd(Br)$_2$]$_2^{2-}$ is an equilibrium reaction with a small equilibrium constant. Thus, it seems unlikely that the interchange of [Pd{P(*o*-tol)$_3$}(C$_6$H$_4$-*p*-F)(μ-Br)]$_2$ and [(Ar)Pd(Br)$_2$]$_2^{2-}$ would occur with a very large equilibrium constant favoring the ligandless species. Third, the notion that the ligandless, anionic complex forms as the sole product from the combination of **37** and NPr$_4$Br

contradicts the slower reaction of **37** with styrene compared to the reaction of (^{t}Bu$_3$P)Pd(C$_6$H$_4$-*p*-F)(Br) (**32**) with styrene in the presence of similar concentrations of olefin, free phosphine, and bromide salt. Recall that the combination of (^{t}Bu$_3$P)Pd(C$_6$H$_4$-*p*-F)(Br) (**32**) and bromide forms a modest concentration of the ligandless, anionic species (vide supra). We propose that the identity of the product (δ -125.9 ppm) is instead a phosphine-ligated anionic monomer [Pr$_4$N]$^+$[Pd{P(*o*-tol)$_3$}(C$_6$H$_4$-*p*-F)(Br)$_2$]$^-$ (Scheme 44).

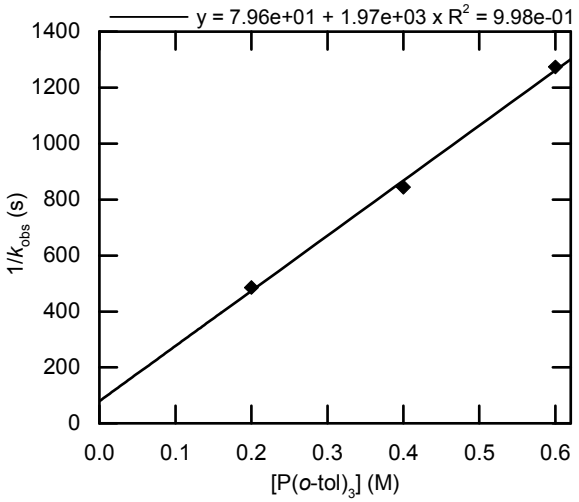

Figure 34. Dependence of the observed rate constant on the concentration of P(*o*-tol)$_3$ (0.20-0.60 M) for the reaction of [Pd{P(*o*-tol)$_3$}(C$_6$H$_4$-*p*-F)(μ-Br)]$_2$ (**37**) (0.020 M) with butyl acrylate (0.20 M), N(heptyl)$_4$Br (0.20 M), and MeCy$_2$N (0.040 M) in THF at 45 °C.

To probe whether the reaction of [Pd{P(*o*-tol)$_3$}(C$_6$H$_4$-*p*-F)(μ-Br)]$_2$ (**37**) with olefins proceeds by an anionic species lacking coordinated phosphine, the dependence of the rate constant on the concentration of P(*o*-tol)$_3$ for reactions of **37** with butyl acrylate was determined. The decay of **37** (0.020 M) with butyl acrylate (0.20 M) in the presence of N(heptyl)Br (0.020 M), MeCy$_2$N (0.040 M), and P(*o*-tol)$_3$ (0.20-0.60 M) was monitored

in THF at 45 °C by ^{19}F NMR spectroscopy. The plot of $1/k_{obs}$ versus [P(*o*-tol)$_3$] (Fig 34) indicates that the reaction is inverse first-order in ligand, which is consistent with a mechanism for migratory insertion that involves a palladium complex lacking coordinated phosphine. Although these data do not specifically identify the structure of the ligandless species, dissociation of phosphine from [Pd{P(*o*-tol)$_3$}(Ar)(X)$_2$]$^-$, which forms from the reaction of halide with [Pd{P(*o*-tol)$_3$}(Ar)(μ-X)]$_2$, could generate monomeric or dimeric ligandless [(Ar)Pd(Br)$_2$]$_n^{n-}$ (n = 1,2) by dissociation of phosphine prior to migratory insertion. Although additional kinetic data are needed to probe this hypothesis, these initial mechanistic studies suggest that migratory insertion in Heck reactions conducted with catalysts ligated by P(*o*-tol)$_3$, including Hermann's catalyst,[79] may proceed through the same ligandless, anionic palladium intermediate as was determined for reactions with complexes of bulkier monophosphines and for "ligandless" Heck reactions.

4.4 Conclusions

The studies described above reveal some basic principles about the reactivity of alkenes with transition-metal complexes and the design of catalysts for reactions occurring by alkene insertion. First, these studies show that alkene insertion can be fast, even for complexes lacking a positive charge or electron-poor dative ligands. The faster reactions of the anionic complex versus that of the neutral species contrasts the typical trend of faster insertions of alkenes into the metal-carbon bonds of complexes that are more electrophilic,[75] including cationic organopalladium complexes.[76] The anionic

complexes are more electron-rich, as probed by computed CO stretching frequencies, and therefore, we suggest that the anionic complexes in this work are more reactive than neutral, phosphine-ligated analogs because they are less hindered.

Second, these studies show that the fast rates of the catalyst containing the strongly donating P(*t*-Bu)$_3$ ligand relies on the ability of this ligand to fully dissociate to generate a less hindered "ligandless" species. At the same time, these studies show that efforts to use ancillary ligands to control *selectivity* should focus on dative ligands more tightly bound than P(*t*-Bu)$_3$ or on anionic additives. Lastly, kinetic studies indicate that complexes ligated by P(*o*-tol)$_3$, a common ligand for Heck reactions, may also react with olefins through anionic species. Future studies will test this hypothesis and explore the role of these species in other palladium-catalyzed processes.

4.5 Experimental

General Methods. All manipulations were conducted in an inert atmosphere dry box or using standard Schlenk techniques unless otherwise specified. ^{1}H spectra were recorded on a 400 or 500 MHz spectrometer; ^{13}C spectra were recorded at 100 or 125 MHz with solvent resonances as reference; ^{31}P{^{1}H} NMR spectra were recorded at 160 or 200 MHz with external H_3PO_4 as a reference; ^{19}F{^{1}H} NMR spectra were recorded at 375 or 470 MHz with external $CFCl_3$ as a reference. Toluene, benzene, and pentane were dried with a solvent purification system by percolation through neutral alumina under positive pressure of argon. Acetonitrile was distilled from CaH_2. The complexes Pd(P^{t}Bu$_3$)$_2$,[80] (^{t}Bu$_3$P)Pd(Ph)(Br),[53-54] (^{t}Bu$_3$P)$_2$Pd(H)(Br),[81-82] HP^{t}Bu$_3$Br[55], (1-

$AdP^tBu_2)Pd(Ph)(Br)$,[53] (QPhos)Pd(Ph)(Br),[54] and $[Pd\{P(o\text{-tol})_3\}(C_6H_4\text{-}p\text{-}F)(\mu\text{-}Br)]_2$[78] were prepared by published procedures. All other reagents were obtained from commercial sources and used without further purification. Conductivity measurements were made with a VWR Traceable™ conductivity meter.

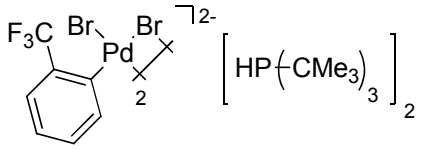

28

$[(2\text{-}CF_3C_6H_4)PdBr_2]_2[HP^tBu_3]_2$ (28). $(^tBu_3P)_2Pd(H)(Br)$ was weighed into a small vial (30 mg, 0.051 mmol) and dissolved in a mixture of THF (1.0 mL) and 2-bromobenzotrifluoride (0.30 mL, 0.18 mmol). The reaction mixture was heated without stirring at 60 ^oC for 60 min during which time the orange product crystallized from solution. After this time, the orange solid was isolated by filtration, rinsed once with toluene, twice with pentane, and dried under vacuum to afford 26 mg of product (84% yield). Recrystallization of the solid from an acetonitrile solution layered with toluene afforded orange crystals suitable for X-ray diffraction. A mixture of anti/syn diastereomers were observed by ^1H and ^{19}F NMR spectroscopy in a 12:1 ratio upon dissolution of the recrystallized material in CD_3CN. ^1H NMR (CD_3CN, 500 MHz) major diastereomer: δ 7.48 (d, J = 8.0 Hz, 1H), 7.15 (d, J = 8.0 Hz, 1H), 6.89 (t, J = 7.5 Hz, 1H), 6.736 (t, J = 7.5 Hz, 1H), 5.49 (d, J = 444 Hz, 1H), 1.59 (d, J = 15.5 Hz, 27H); minor diastereomer: δ ~7.5 (overlaps major δ 7.48), 7.31 (d, J = 7.5 Hz), 7.07 (t, J = 6.5 Hz), 6.97 (t, J = 7.4 Hz) ^{13}C NMR (CD_3CN, 125 MHz) δ 140.35, 139.72, 135.37 (q, J =

28.5 Hz), 127.78, 125.75, 125.47 (q, J = 273 Hz), 122.06, 37.79 (d, J = 27.6 Hz), 30.09; $^{19}F\{^{1}H\}$ NMR (CD_3CN, 470 MHz) δ major diastereomer: -55.95; minor diastereomer: -57.48; $^{31}P\{^{1}H\}$ NMR (CD_3CN, 200 MHz) δ 56.51; Anal. Calc'd for $C_{38}H_{64}Br_4F_6P_2Pd_2$: C, 37.13; H, 5.25. Found: C, 37.14; H, 5.16.

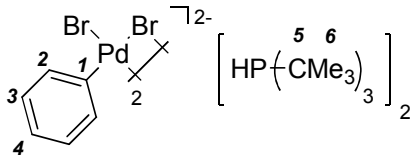

29

$[(C_6H_5)PdBr_2]_2[HP^tBu_3]_2$ (29). (^{t}Bu$_3$P)Pd(Ph)(Br) (30 mg, 0.064 mmol) and HP^{t}Bu$_3$Br (9.5 mg, 0.034 mmol) were weighed into a small vial, and toluene (2.0 mL) was added. The heterogeneous solution was stirred vigorously for 1.5 h, after which time a fine orange solid precipitated and was collected by vacuum filtration. The solid was rinsed with toluene and then pentane and was dried under vacuum. Recrystallization from a concentrated acetonitrile solution layered with toluene afforded 15 mg of orange crystalline product suitable for X-ray diffraction (86% yield). A mixture of anti/syn diastereomers were observed by ^{13}C NMR spectroscopy for C1, C3, and C4 upon dissolution of the recrystallized material in CD_2Cl_2; all other chemical shifts for the two isomers were indistinguishable. ^{1}H NMR (CD_3CN, 500 MHz) δ 7.04 (d, J = 7.5 Hz, 2H), 6.70 (br, 2H), 6.59 (br, 1H), 5.72 (d, J = 446 Hz, 1H), 1.60 (d, J = 15.5 Hz, 27H); ^{13}C NMR (CD_2Cl_2, 0 ^{o}C, 100 MHz) major diastereomer: δ 140.96 (C1), 137.35 (C2), 125.89 (C3), 122.12 (C4), 37.68 (d, J = 28.2 Hz, C5), 30.61 (C6); minor diastereomer: 141.66

(C1), 126.10 (C3), 122.32 (C4); $^{31}P\{^{1}H\}$ NMR (CD_3CN, 200 MHz) δ 54.39; Anal. Calc'd for $C_{36}H_{66}Br_4P_2Pd_2$: C, 39.55; H, 6.08. Found: C, 39.29 ; H, 6.10.

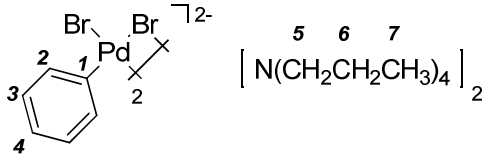

30

$[(C_6H_5)PdBr_2]_2[N(C_3H_7)_4]_2$ (30). ($^{t}Bu_3P$)Pd(Ph)(Br) (60 mg, 0.13 mmol) and $N(C_3H_7)_4Br$ (34 mg, 0.13 mmol) were weighed into a small vial, and toluene (4.0 mL) was added. The heterogeneous solution was stirred vigorously for 1.5 h, after which time the resulting fine yellow solid was collected by vacuum filtration. The solid was rinsed with toluene and then pentane, and was dried under vacuum. Recrystallization from a CH_2Cl_2 (0.5 mL) solution layered with toluene (1 mL) afforded 26 mg of orange crystalline product (38% yield). A mixture of anti/syn diastereomers were observed by ^{13}C NMR spectroscopy for C1, C3, and C4 upon dissolution of the recrystallized material in CD_2Cl_2; all other chemical shifts for the two isomers were indistinguishable. ^{1}H NMR (CD_3CN, 500 MHz) δ 7.12 (d, *J* = 7.5 Hz, 2H), 6.70 (t, J = 7.5 Hz, 2H), 6.58 (t, *J* = 7.5 Hz, 1H), 3.05 (m, 8H), 1.62 (m, 8H), 0.91 (t, *J* = 7.5 Hz, 12H); ^{13}C NMR (CD_2Cl_2, 0 ^{o}C, 100 MHz) major diastereomer: δ 142.10 (C1), 137.61 (C2), 125.78 (C3), 121.95 (C4), 60.77 (C5), 16.12 (C6), 11.14 (C7); minor diastereomer: δ 141.24 (C1), 125.88 (C3), 122.04 (C4); Anal. Calc'd for $C_{36}H_{66}Br_4N_2Pd_2$: C, 40.81; H, 6.28.; N, 2.64 Found: C, 40.47 ; H, 6.34; N, 2.67.

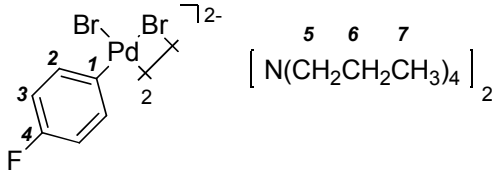

31

[(4-FC$_6$H$_4$)PdBr$_2$]$_2$[N(C$_3$H$_7$)$_4$]$_2$ (31). (^{t}Bu$_3$P)Pd(C$_6$H$_4$-*p*-F)(Br) (**32**) (42 mg, 0.087 mmol) was dissolved in toluene (1.5 mL) and added to a stirring suspension of N(C$_3$H$_7$)$_4$Br (23 mg, 0.087 mmol) in toluene (1.5 mL). The heterogeneous solution was stirred vigorously for 1.5 h, after which time the resulting fine yellow solid was collected by vacuum filtration. The solid was rinsed with toluene and then pentane, and was dried under vacuum. Recrystallization from a CH_2Cl_2 (0.5 mL) solution layered with toluene (1 mL) afforded 23 mg of orange crystalline product (55% yield). A mixture of anti/syn diastereomers (~60:40) were observed by ^{13}C (for C1, C3, C4) and ^{19}F NMR spectroscopy upon dissolution of the recrystallized material in CD_2Cl_2; all other chemical shifts for the two isomers were indistinguishable. ^{1}H NMR (CD_3CN, 500 MHz) δ 7.01 (m, 2H), 6.55 (t, *J* = 9.0 Hz, 2H) 3.04 (m, 8H), 1.64 (m, 8H), 0.93 (t, 8.0 Hz, 12H); ^{13}C NMR (CD_2Cl_2, -10 ^{o}C, 100 MHz) major diastereomer: δ 160.29 (d, *J* = 237 Hz, C4), 137.38 (C2), 133.79 (C1), 112.01 (d, *J* = 18.3 Hz, C3), 60.59 (C5), 15.93 (C6), 10.96 (C7); minor diastereomer: δ 160.38 (d, *J* = 237 Hz, C4), 133.019 (C1), 112.37 (d, *J* = 18.3 Hz, C3); ^{19}F{^{1}H} NMR (CD_2Cl_2, 470 MHz) minor diastereomer: δ -125.98; major diastereomer: δ -126.11; Anal. Calc'd for C$_{36}$H$_{64}$Br$_4$F$_2$N$_2$Pd$_2$: C, 39.47; H, 5.89.; N, 2.56 Found: C, 39.18 ; H, 5.65; N, 2.60.

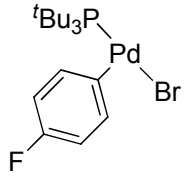

32

(^{t}Bu$_3$P)Pd(C$_6$H$_4$-*p*-F)(Br) (32). The preparation of **32** was adapted from a known procedure.[53-54] Pd(P^{t}Bu$_3$)$_2$ was weighed into a small vial (300 mg, 0.587 mmol) and suspended in 1-bromo-4-fluorobenzene (2.9 mL, 26 mmol). The reaction mixture was heated with vigorous stirring at 70 ^{o}C for 75 min. After this time, the solution was added to 40 mL of stirring pentane. After two hours, the resulting orange solid was collected, washed with pentane (4x2 mL), and dried under vacuum to afford 140 mg of product (49 % yield). ^{1}H NMR (C$_6$D$_6$, 500 MHz) δ 7.25 (m, 2H), 6.65 (t, *J* = 9.0 Hz, 2H), 1.09 (d, *J* = 12.0 Hz, 27H); ^{13}C NMR (C$_6$D$_6$, 125 MHz) δ 161.27 (d, *J* = 240 Hz), 137.33, 130.24, 113.96 (d, *J* = 22.1 Hz), 40.53 (d, *J* = 8.3 Hz), 32.37; ^{19}F{^{1}H} NMR (C$_6$D$_6$, 470 MHz) δ -122.27; ^{31}P{^{1}H} NMR (C$_6$D$_6$, 200 MHz) δ 66.95; Anal. Calc'd for C$_{18}$H$_{31}$BrFPPd: C, 44.69; H, 6.46. Found: C, 44.46; H, 6.50.

Representative Procedure for Determination of the Equilibrium Constant K_{eq} for formation of [Pd(4-FC$_6$H4)Br$_2$]$_2$[N(C$_7$H$_{15}$)$_4$]$_2$ from 32. (^{t}Bu$_3$P)Pd(*p*-FC$_6$H$_4$)(Br) (**32**) (8.2 mg, 0.017 mmol) and tetraheptylammonium bromide (8.3 mg, 0.017 mmol) were weighed into a small vial. A solution of tri-*tert*-butylphosphine (50 μL, 0.34 M) in benzene was added by microliter syringe, followed by benzene (450 μL). The resulting solution was transferred to an NMR tube and sealed with a septum. The relative ratios of

32, $[Pd(4\text{-}FC_6H4)Br_2]_2[N(C_7H_{15})_4]_2$, and P^tBu_3 were subsequently determined by ^{19}F and ^{31}P NMR spectroscopy at 20 ^oC.

Representative procedure for reactions of 29 or 30 and olefin (Scheme 37). $[Pd(C_6H_5)Br_2]_2[N(C_3H_7)_4]_2$ (**30**) (6.0 mg, 5.5 μmol) was weighed into a small vial. To the solid were added *n*-tetradecane (5.0 μL, internal standard) and acetonitrile (400 μL). After dissolution, a solution of butyl acrylate (9 μL, 0.07 mmol) and *N,N*-dicyclohexylmethylamine (4 μL, 0.02 mmol) in toluene (100 μL) was added, and the mixture was stirred at room temperature. After 5 min, an aliquot (50 μL) was diluted in ethyl acetate and passed through a silica plug. The yield of olefin product was subsequently determined from the gas chromatography trace.

Reaction of iodobenzene with methyl acrylate catalyzed by $[Pd(C_6H_5)Br_2]_2$ $[N(C_3H_7)_4]_2$ (30) (Scheme 38).[34] Iodobenzene (102 mg, 0.500 mmol), methyl acrylate (86 mg, 1.0 mmol), tetrabutylammonium chloride (139 mg, 0.500 mmol), and sodium bicarbonate (105 mg, 1.25 mmol) were weighed into a small vial. A solution of $[Pd(C_6H_5)Br_2]_2$ $[N(C_3H_7)_4]_2$ (**30**) (5.3 mg, 5.0 μmol) in anhydrous DMF (1.0 mL) was then added by syringe. The mixture was stirred at 30 ^oC. After 18 h, the mixture was diluted in dichloromethane and washed with water then brine. The organic layer was dried over anhydrous $MgSO_4$ and evaporated. The crude material was purified by flash chromatography (5% ethyl acetate in hexane) to afford 78 mg (96 % yield) of spectroscopically pure *trans*-methyl cinnamate as a white solid.

Reaction of 4-bromobenzotrifluoride with styrene catalyzed by [(4-FC_6H_4)$PdBr_2$]$_2$[$N(C_3H_7)_4$]$_2$ (31) (Scheme 38).[63] 4-Bromobenzotrifluoride (113 mg, 0.502 mmol), styrene (73 mg, 0.70 mmol), sodium acetate (82 mg, 1.0 mmol), and *N,N*-dimethylglycine (15 mg, 0.15 mmol) were weighed into a small vial. A solution of [(4-FC_6H_4)$PdBr_2$]$_2$[$N(C_3H_7)_4$]$_2$ (**31**) (4.0 mg, 3.7 μmol) in anhydrous *N*-methylpyrrolidinone (500 μL) was then added by syringe. The mixture was stirred at 130 ^oC. After 1 h, the mixture was diluted in dichloromethane and washed with water then brine. The organic layer was dried over anhydrous $MgSO_4$ and evaporated. The crude material was purified by flash chromatography (100% hexane) to afford 123 mg (99 % yield) of spectroscopically pure *trans*-(4-trifluoromethyl)-stilbene as a white solid.

Reaction of 4-bromo-*N,N*-dimethylaniline with methyl methacrylate catalyzed by [(C_6H_5)$PdBr_2$]$_2$[HP^tBu_3]$_2$ (29) (Scheme 38).[39] 4-Bromo-*N,N*-dimethylaniline (100 mg, 0.500 mmol), methyl methacrylate (100 mg, 1.00 mmol), and *N,N*-dicyclohexylmethylamine (107 mg, 0.548 mmol) were weighed into a small vial. A suspension of [(C_6H_5)$PdBr_2$]$_2$[HP^tBu_3]$_2$ (**29**) (2.7 mg, 2.5 μmol) in dioxane (450 μL) was then added by syringe. The resulting mixture was stirred at room temperature. After 18 h, isolation of the product according to the reported procedure afforded 107 mg (97% yield) of spectroscopically pure (*E*)-3-(4-dimethylaminophenyl)-2-methyl acrylic acid methyl ester as a pale yellow solid.

Representative procedure for kinetic experiments (Figure 22). ($^tBu_3P$)Pd(C_6H_4-*p*-F)(Br) (**32**) (8.2 mg, 0.017 mmol) and tri-*tert*-butylphosphine (17 mg, 0.085 mmol) were

weighed into a small vial. Next, *N,N*-dicyclohexylmethylamine (5.0 μL, 0.024 mmol) and 1,4-difluorobenzene (3.0 μL, 0.029 mmol, internal standard) were added by microliter syringe. The reagents were then dissolved in acetonitrile (400 μL) and toluene (100 μL). The sample solution was transferred to an NMR tube and sealed with a septum. Before inserting the sample into the NMR probe, the temperature was adjusted to 20 ^{o}C using ethylene glycol as a temperature standard. Styrene (10 μL, 0.085 mmol) was added via syringe just prior to insertion of the sample into the NMR probe. ^{19}F NMR spectra were acquired at fixed time intervals throughout the length of experiment with the aid of an automated data collection program.

Representative procedure for kinetic experiments (Figures 23-25). (^{t}Bu$_3$P)Pd(C$_6$H$_4$-*p*-F)(Br) (**32**) (8.2 mg, 0.017 mmol), tri-*tert*-butylphosphine (52 mg, 0.26 mmol), and N(heptyl)$_4$Br (24 mg, 0.12 mmol) were weighed into a small vial. Next, benzene (0.42 mL) and 1,4-difluorobenzene (3.0 μL, 0.029 mmol, internal standard) were added by microliter syringe. The sample solution was transferred to an NMR tube and sealed with a septum. Before inserting the sample into the NMR probe, the temperature was adjusted to 20 ^{o}C using ethylene glycol as a temperature standard. Styrene (39 μL, 0.34 mmol) was added via microliter syringe just prior to insertion of the sample into the NMR probe. ^{19}F NMR spectra were acquired at fixed time intervals throughout the length of experiment with the aid of an automated data collection program.

Reaction of bromobenzene with butyl vinyl ether catalyzed by tri-*tert*-butylphosphine and Pd$_2$dba$_3$·CHCl$_3$ (Scheme 40, entry A).[39] Bromobenzene (79 mg,

0.50 mmol), butyl vinyl ether (55 mg, 0.55 mmol), and *N,N*-dicyclohexylmethylamine (107 mg, 0.548 mmol) were weighed into a small vial. A solution of tri-*tert*-butylphosphine in 1,4-dioxane (0.05 M, 0.005 mmol, 100 μL) was then added, followed by a solution of $Pd_2dba_3 \cdot CHCl_3$ in 1,4-dioxane (0.006 M, 0.003 mmol, 400 μL). The resulting mixture was stirred at room temperature. After 8 h, an aliquot (20 μL) was diluted in ethyl acetate and passed through a silica plug. The ratio of olefin products (uncorrected) was then determined by gas chromatography.

Reaction of bromobenzene with butyl vinyl ether catalyzed by tetrakis(triphenylphosphine)palladium (Scheme 40, entry C). Bromobenzene (79 mg, 0.50 mmol), butyl vinyl ether (55 mg, 0.55 mmol), *N,N*-dicyclohexylmethylamine (107 mg, 0.548 mmol), and tetrakis(triphenylphosphine)-palladium (17 mg, 0.015 mmol) were weighed into a small vial. Dioxane (500 μL) was added and the resulting mixture was stirred at 120 ^{o}C. After 36 h, an aliquot (20 μL) was diluted in ethyl acetate and passed through a silica plug. The ratio of olefin products (uncorrected) was then determined by gas chromatography.

Reaction of iodobenzene with butyl vinyl ether catalyzed by palladium acetate and triphenylphosphine (Scheme 40, entry D). Iodobenzene (102 mg, 0.50 mmol), butyl vinyl ether (55 mg, 0.55 mmol), and *N,N*-dicyclohexylmethylamine (107 mg, 0.548 mmol) were weighed into a small vial followed by addition of dioxane (0.5 mL). The resulting solution was added to a vial containing palladium acetate (2 mg, 0.01 mmol) and triphenylphosphine (5 mg, 0.02 mmol). The mixture was stirred at 100 ^{o}C. After 3 h,

an aliquot (30 μL) was diluted in ethyl acetate and passed through a silica plug. The ratio of olefin products (uncorrected) was then determined by gas chromatography.

Reaction of phenyl trifluoromethanesulfonate with butyl vinyl ether catalyzed by palladium acetate and 1,3-bis(diphenylphosphino)propane (Scheme 40, entry E).[72] Phenyl trifluoromethanesulfonate (113 mg, 0.50 mmol), butyl vinyl ether (55 mg, 0.55 mmol), and *N,N*-dicyclohexylmethylamine (107 mg, 0.548 mmol) were weighed into a small vial followed by addition of dioxane (0.5 mL). The resulting solution was added to a vial containing palladium acetate (2.8 mg, 0.012 mmol) and 1,3-bis(diphenylphosphino)propane (5.8 mg, 0.015 mmol). The mixture was stirred at 80 ^{o}C. After 5 h, an aliquot (30 μL) was diluted in ethyl acetate and passed through a silica plug. The ratio of olefin products (uncorrected) was then determined by gas chromatography.

Reaction of $[Pd(C_6H_5)Br_2]_2$ $[N(C_3H_7)_4]_2$ (30) and butyl vinyl ether (Eq 6). $[Pd(C_6H_5)Br_2]_2$ $[N(C_3H_7)_4]_2$ (**30**) (6.5 mg, 6.1 μmol) was weighed into a small vial. Dioxane (600 μL), butyl vinyl ether (63 μL, 0.49 mmol), and *N,N*-dicyclohexylmethylamine (5.0 μL, 0.024 mmol) were added by syringe, and the resulting heterogeneous suspension was stirred vigorously. After 3 h, an aliquot (100 μL) was diluted in ethyl acetate and passed through a silica plug. The ratio of olefin products (uncorrected) was then determined by gas chromatography.

Reaction of ($^{t}Bu_3P$)$Pd(C_6H_5)(Br)$ and butyl vinyl ether (Eq 7). ($^{t}Bu_3P$)$Pd(C_6H_5)(Br)$ (7.0 mg, 0.015 mmol) and tetraheptylammonium bromide (7.5 mg, 0.015 mmol) were weighed into a small vial. The solids were dissolved in dioxane (550

μL). *N,N*-Dicyclohexylmethylamine (5.0 μL, 0.024 mmol) and butyl vinyl ether (57 μL, 0.44 mmol) were added by microliter syringe. After 20 min, an aliquot (100 μL) was diluted in ethyl acetate and passed through a silica plug. The ratio of olefin products (uncorrected) was then determined by gas chromatography.

Computational details (Figure 26 and Table 18). DFT calculations were carried out using the B3LYP hybrid functional[83-85] and carried out via the Gaussian 03 package[86] with no symmetry restrictions placed on any structure. The optimized structures were visualized with the Molden program (Figure 25). Palladium was modeled with the LANL2DZ basis set[87] and all other atoms were modeled with the split valence 6-31G(d,p) basis set.[88-89] The resulting CO stretching frequencies for the anionic palladium complexes **33a-b** and the neutral, phosphine-ligated complexes **34a-c** are shown in Table 18.

Reaction of 31 with styrene at low temperatures (Figure 27). $[(C_6H_4$-*p*-$F)PdBr_2]_2[N(C_3H_7)_4]_2$ (**31**) (6.0 mg, 5.5 μmol) was weighed into a vial. 1,4-difluorobenzene (2 μL, internal standard) and CH_2Cl_2 (0.4 mL) were added to the vial. The resulting sample solution was transferred to a NMR tube, the tube was sealed with a septum, and the tube was placed in a -78 °C cold bath. In a separate vial styrene (6.3 μL, 55 μmol) was diluted in CH_2Cl_2 (0.1 mL), and the resulting solution was added to the chilled NMR tube by syringe. Before inserting the sample into the NMR probe, the temperature was adjusted to -40 ^oC using methanol as a temperature standard. ^{19}F NMR

spectra were acquired at fixed time intervals throughout the length of experiment with the aid of an automated data collection program.

Representative procedure for kinetic experiments (Figure 28-30). [(C_6H_4-*p*-F)$PdBr_2$]$_2$[$N(C_3H_7)_4$]$_2$ (**31**) (6.0 mg, 5.5 μmol) and N(heptyl)$_4$Br (8 mg, 0.02 mmol) were weighed into a vial. 1,4-difluorobenzene (3 μL, internal standard) and CH_2Cl_2 (0.5 mL) were added to the vial. The resulting sample solution was transferred to a NMR tube, the tube was sealed with a septum, and the tube was placed in a -78 °C cold bath. Before inserting the sample into the NMR probe, the temperature was adjusted to -40 ^oC using methanol as a temperature standard. Styrene (10 μL, 0.11 mmol) was added by syringe just prior to inserting the sample into the NMR probe. ^{19}F NMR spectra were acquired at fixed time intervals throughout the length of experiment with the aid of an automated data collection program.

Representative procedure for the reaction of 35 with styrene (Figure 31). (1-AdP^tBu_2)Pd(Ph)(Br) (**35**) (9.0 mg, 0.017 mmol), N(heptyl)$_4$Br (24 mg, 0.049 mmol), and 1-AdP^tBu_2 (4.5 mg, 0.017 mmol) were weighed into a small vial containing a magnetic stirring bar. *n*-tetradecane (5.0 μL, 0.019 mmol, internal standard) and THF (0.5 mL) were added to the vial, which was sealed with a septum cap. The vial was taken out of the glove box, and styrene (20 μL, 0.17 mmol) was added to the stirring solution at room temperature. Aliquots were extracted by syringe at regular time intervals, diluted in toluene, and passed through a plug of silica. The yield of *trans*-stilbene was determined by analysis of the gas chromatography trace versus the internal standard.

Representative procedure for the reaction of 36 with styrene (Figure 32). (QPhos)Pd(Ph)(Br) (**36**) (17 mg, 0.017 mmol) and $N(heptyl)_4Br$ (25 mg, 0.051 mmol), were weighed into a small vial containing a magnetic stirring bar. *n*-tetradecane (5.0 μL, 0.019 mmol, internal standard) and THF (0.5 mL) were added to the vial, which was sealed with a septum cap. The vial was taken out of the glove box, and styrene (20 μL, 0.17 mmol) was added to the stirring solution at room temperature. Aliquots were extracted by syringe at regular time intervals, diluted in toluene, and passed through a plug of silica. The yield of *trans*-stilbene was determined by analysis of the gas chromatography trace versus the internal standard.

Representative procedure for kinetic experiments (Figure 33). [Pd{P(*o*-tol)$_3$}(C_6H_4-*p*-F)(μ-Br)]$_2$ (**37**) (12 mg, 0.010 mmol), P(*o*-tol)$_3$ (31 mg, 0.10 mmol), $N(heptyl)_4Br$ (49 mg, 0.10 mmol) were weighed into a small vial. 1,4-diflurobenzene (3 μL, internal standard), $MeCy_2N$ (4.0 mL, 0.020 mmol), and THF (0.5 mL) were added to the vial. The resulting sample solution was transferred to a NMR tube, the tube was sealed with a septum. Before inserting the sample into the NMR probe, the temperature was adjusted to 45 ^oC using ethylene glycol as a temperature standard. Butyl acrylate (15 μL, 0.10 mmol) was added by syringe just prior to inserting the sample into the NMR probe. ^{19}F NMR spectra were acquired at fixed time intervals throughout the length of experiment with the aid of an automated data collection program.

Representative procedure for kinetic experiments (Figure 34). [Pd{P(*o*-tol)$_3$}(C_6H_4-*p*-F)(μ-Br)]$_2$ (**37**) (12 mg, 0.010 mmol), P(*o*-tol)$_3$ (61 mg, 0.20 mmol), N(heptyl)$_4$Br (49 mg, 0.10 mmol) were weighed into a small vial. 1,4-diflurobenzene (3 μL, internal standard), $MeCy_2N$ (4.0 μL, 0.020 mmol), and THF (0.5 mL) were added to the vial. The resulting sample solution was transferred to a NMR tube, the tube was sealed with a septum. Before inserting the sample into the NMR probe, the temperature was adjusted to 45 ^oC using ethylene glycol as a temperature standard. Butyl acrylate (15 μL, 0.10 mmol) was added by syringe just prior to inserting the sample into the NMR probe. ^{19}F NMR spectra were acquired at fixed time intervals throughout the length of experiment with the aid of an automated data collection program.

Table 18. Crystal data and structure refinement for $[(2\text{-}CF_3C_6H_4)PdBr_2]_2[HP^tBu_3]_2$ (**28**).

Empirical formula	$C_{38}H_{64}Br_4F_6P_2Pd_2$	
Formula weight	1229.27	
Temperature	297(2) K	
Wavelength	0.71073 Å	
Crystal system	Monoclinic	
Space group	P 21/n	
Unit cell dimensions	a = 10.6562(4) Å	a= 90°
	b = 9.0426(4) Å	b= 95.246(2)°
	c = 25.5092(11) Å	g = 90°
Volume	2447.76(18) $Å^3$	
Z	2	
Density (calculated)	1.668 Mg/m^3	
Absorption coefficient	4.112 mm^{-1}	
F(000)	1216	
Crystal color	orange	
Crystal size	0.31 x 0.07 x 0.05 mm^3	
Theta range for data collection	1.60 to 27.65°	
Index ranges	-13<=h<=13, -11<=k<=11, -30<=l<=33	
Reflections collected	34711	
Independent reflections	5623 [R(int) = 0.0503]	
Completeness to theta = 27.65°	98.7 %	
Absorption correction	Integration	
Max. and min. transmission	0.8252 and 0.4238	
Refinement method	Full-matrix least-squares on F^2	
Data / restraints / parameters	5623 / 172 / 273	
Goodness-of-fit on F^2	1.013	
Final R indices [I>2sigma(I)]	R1 = 0.0407, wR^2 = 0.0857	
R indices (all data)	R1 = 0.0920, wR^2 = 0.1040	
Largest diff. peak and hole	0.546 and -0.629 e.$Å^{-3}$	

Table 19. Atomic coordinates (x 10^4) and equivalent isotropic displacement parameters ($Å^2$ x 10^3) for $[(2\text{-}CF_3C_6H_4)PdBr_2]_2[HP^tBu_3]_2$ (**28**). U(eq) is defined as one third of the trace of the orthogonalized U^{ij} tensor.

	x	y	z	U(eq)
C(1)	-949(3)	4851(4)	1293(1)	59(1)
C(2)	-1681(4)	5897(4)	1523(2)	67(2)
C(3)	-2327(4)	5511(6)	1952(2)	87(2)
C(4)	-2241(4)	4080(6)	2151(1)	102(3)
C(5)	-1510(5)	3034(5)	1920(2)	107(3)
C(6)	-864(4)	3419(4)	1491(2)	82(2)
C(7)	-1786(7)	7424(10)	1356(3)	99(2)
F(1)	-1069(7)	8377(7)	1669(3)	116(2)
F(2)	-2964(6)	7945(8)	1392(4)	122(2)
F(3)	-1480(8)	7746(8)	868(2)	106(2)
Br(1)	-1538(1)	4373(1)	59(1)	65(1)
Br(2)	1802(1)	5922(1)	1401(1)	62(1)
Pd(1)	138(1)	5249(1)	717(1)	48(1)
P(1)	3284(1)	1942(2)	1122(1)	55(1)
C(8)	2411(6)	488(7)	725(3)	73(2)
C(9)	3299(8)	-788(8)	591(4)	115(3)
C(10)	1327(6)	-156(7)	1009(3)	91(2)
C(11)	1773(8)	1198(10)	223(3)	123(3)
C(12)	4731(5)	2636(7)	828(3)	70(2)
C(13)	4499(7)	2736(9)	228(3)	96(2)
C(14)	4998(7)	4207(8)	1023(3)	101(2)
C(15)	5874(6)	1629(9)	968(3)	103(3)
C(16)	3498(6)	1529(8)	1840(2)	80(2)

Table 19 (cont.)

C(17)	2227(7)	1698(10)	2066(2)	102(2)
C(18)	4061(8)	12(10)	1957(3)	118(3)
C(19)	4369(8)	2704(11)	2125(3)	125(3)
C(20)	-1942(11)	7362(12)	1306(4)	105(2)
F(4)	-2222(16)	8430(13)	1652(5)	119(3)
F(5)	-2953(11)	7460(14)	941(5)	113(3)
F(6)	-1008(12)	7975(16)	1049(6)	106(3)

Table 20. Bond lengths [Å] and angles [°] for $[(2\text{-}CF_3C_6H_4)PdBr_2]_2[HP^tBu_3]_2$ (**28**).

C(1)-C(2)	1.3900
C(1)-C(6)	1.3900
C(1)-Pd(1)	1.985(3)
C(2)-C(3)	1.3900
C(2)-C(7)	1.447(10)
C(2)-C(20)	1.453(11)
C(3)-C(4)	1.3900
C(3)-H(3)	0.9300
C(4)-C(5)	1.3900
C(4)-H(4)	0.9300
C(5)-C(6)	1.3900
C(5)-H(5)	0.9300
C(6)-H(6)	0.9300
C(7)-F(3)	1.348(7)
C(7)-F(2)	1.352(7)
C(7)-F(1)	1.360(7)
Br(1)-Pd(1)	2.4681(7)
Br(1)-Pd(1)#1	2.6064(7)
Br(2)-Pd(1)	2.4477(7)
Pd(1)-Br(1)#1	2.6064(7)
P(1)-C(8)	1.857(6)
P(1)-C(16)	1.864(6)
P(1)-C(12)	1.882(6)
P(1)-H(1)	1.18(5)
C(8)-C(11)	1.534(9)
C(8)-C(10)	1.535(9)

Table 20 (cont.)

C(8)-C(9)	1.549(9)
C(9)-H(9A)	0.9600
C(9)-H(9B)	0.9600
C(9)-H(9C)	0.9600
C(10)-H(10A)	0.9600
C(10)-H(10B)	0.9600
C(10)-H(10C)	0.9600
C(11)-H(11A)	0.9600
C(11)-H(11B)	0.9600
C(11)-H(11C)	0.9600
C(12)-C(14)	1.524(9)
C(12)-C(13)	1.531(8)
C(12)-C(15)	1.537(9)
C(13)-H(13A)	0.9600
C(13)-H(13B)	0.9600
C(13)-H(13C)	0.9600
C(14)-H(14A)	0.9600
C(14)-H(14B)	0.9600
C(14)-H(14C)	0.9600
C(15)-H(15A)	0.9600
C(15)-H(15B)	0.9600
C(15)-H(15C)	0.9600
C(16)-C(18)	1.516(10)
C(16)-C(17)	1.528(9)
C(16)-C(19)	1.548(10)
C(17)-H(17A)	0.9600
C(17)-H(17B)	0.9600
C(17)-H(17C)	0.9600

Table 20 (cont.)

C(18)-H(18A)	0.9600
C(18)-H(18B)	0.9600
C(18)-H(18C)	0.9600
C(19)-H(19A)	0.9600
C(19)-H(19B)	0.9600
C(19)-H(19C)	0.9600
C(20)-F(6)	1.359(8)
C(20)-F(4)	1.360(8)
C(20)-F(5)	1.360(8)

C(2)-C(1)-C(6)	120.0
C(2)-C(1)-Pd(1)	125.3(2)
C(6)-C(1)-Pd(1)	114.6(2)
C(1)-C(2)-C(3)	120.0
C(1)-C(2)-C(7)	123.8(4)
C(3)-C(2)-C(7)	116.1(4)
C(1)-C(2)-C(20)	123.7(5)
C(3)-C(2)-C(20)	116.0(5)
C(4)-C(3)-C(2)	120.0
C(4)-C(3)-H(3)	120.0
C(2)-C(3)-H(3)	120.0
C(3)-C(4)-C(5)	120.0
C(3)-C(4)-H(4)	120.0
C(5)-C(4)-H(4)	120.0
C(6)-C(5)-C(4)	120.0
C(6)-C(5)-H(5)	120.0
C(4)-C(5)-H(5)	120.0
C(5)-C(6)-C(1)	120.0

Table 20 (cont.)

C(5)-C(6)-H(6)	120.0
C(1)-C(6)-H(6)	120.0
F(3)-C(7)-F(2)	106.9(7)
F(3)-C(7)-F(1)	103.6(7)
F(2)-C(7)-F(1)	102.4(7)
F(3)-C(7)-C(2)	117.3(7)
F(2)-C(7)-C(2)	111.1(7)
F(1)-C(7)-C(2)	114.1(7)
Pd(1)-Br(1)-Pd(1)#1	92.58(2)
C(1)-Pd(1)-Br(2)	87.21(11)
C(1)-Pd(1)-Br(1)	90.55(11)
Br(2)-Pd(1)-Br(1)	175.43(3)
C(1)-Pd(1)-Br(1)#1	176.86(12)
Br(2)-Pd(1)-Br(1)#1	94.65(2)
Br(1)-Pd(1)-Br(1)#1	87.42(2)
C(8)-P(1)-C(16)	113.9(3)
C(8)-P(1)-C(12)	114.0(3)
C(16)-P(1)-C(12)	115.3(3)
C(8)-P(1)-H(1)	102(2)
C(16)-P(1)-H(1)	104(2)
C(12)-P(1)-H(1)	106(2)
C(11)-C(8)-C(10)	105.0(6)
C(11)-C(8)-C(9)	111.1(7)
C(10)-C(8)-C(9)	108.8(5)
C(11)-C(8)-P(1)	108.7(5)
C(10)-C(8)-P(1)	111.8(5)
C(9)-C(8)-P(1)	111.2(5)
C(8)-C(9)-H(9A)	109.5

Table 20 (cont.)

C(8)-C(9)-H(9B)	109.5
H(9A)-C(9)-H(9B)	109.5
C(8)-C(9)-H(9C)	109.5
H(9A)-C(9)-H(9C)	109.5
H(9B)-C(9)-H(9C)	109.5
C(8)-C(10)-H(10A)	109.5
C(8)-C(10)-H(10B)	109.5
H(10A)-C(10)-H(10B)	109.5
C(8)-C(10)-H(10C)	109.5
H(10A)-C(10)-H(10C)	109.5
H(10B)-C(10)-H(10C)	109.5
C(8)-C(11)-H(11A)	109.5
C(8)-C(11)-H(11B)	109.5
H(11A)-C(11)-H(11B)	109.5
C(8)-C(11)-H(11C)	109.5
H(11A)-C(11)-H(11C)	109.5
H(11B)-C(11)-H(11C)	109.5
C(14)-C(12)-C(13)	106.2(6)
C(14)-C(12)-C(15)	110.9(6)
C(13)-C(12)-C(15)	108.6(6)
C(14)-C(12)-P(1)	108.4(4)
C(13)-C(12)-P(1)	110.8(4)
C(15)-C(12)-P(1)	111.8(5)
C(12)-C(13)-H(13A)	109.5
C(12)-C(13)-H(13B)	109.5
H(13A)-C(13)-H(13B)	109.5
C(12)-C(13)-H(13C)	109.5
H(13A)-C(13)-H(13C)	109.5

Table 20 (cont.)

H(13B)-C(13)-H(13C)109.5
C(12)-C(14)-H(14A) 109.5
C(12)-C(14)-H(14B) 109.5
H(14A)-C(14)-H(14B)109.5
C(12)-C(14)-H(14C) 109.5
H(14A)-C(14)-H(14C)109.5
H(14B)-C(14)-H(14C)109.5
C(12)-C(15)-H(15A) 109.5
C(12)-C(15)-H(15B) 109.5
H(15A)-C(15)-H(15B)109.5
C(12)-C(15)-H(15C) 109.5
H(15A)-C(15)-H(15C)109.5
H(15B)-C(15)-H(15C)109.5
C(18)-C(16)-C(17) 111.4(6)
C(18)-C(16)-C(19) 108.6(6)
C(17)-C(16)-C(19) 105.6(6)
C(18)-C(16)-P(1) 112.7(5)
C(17)-C(16)-P(1) 108.5(4)
C(19)-C(16)-P(1) 109.8(5)
C(16)-C(17)-H(17A) 109.5
C(16)-C(17)-H(17B) 109.5
H(17A)-C(17)-H(17B)109.5
C(16)-C(17)-H(17C) 109.5
H(17A)-C(17)-H(17C)109.5
H(17B)-C(17)-H(17C)109.5
C(16)-C(18)-H(18A) 109.5
C(16)-C(18)-H(18B) 109.5
H(18A)-C(18)-H(18B)109.5

Table 20 (cont.)

C(16)-C(18)-H(18C)	109.5
H(18A)-C(18)-H(18C)	109.5
H(18B)-C(18)-H(18C)	109.5
C(16)-C(19)-H(19A)	109.5
C(16)-C(19)-H(19B)	109.5
H(19A)-C(19)-H(19B)	109.5
C(16)-C(19)-H(19C)	109.5
H(19A)-C(19)-H(19C)	109.5
H(19B)-C(19)-H(19C)	109.5
F(6)-C(20)-F(4)	103.7(10)
F(6)-C(20)-F(5)	102.3(9)
F(4)-C(20)-F(5)	100.9(9)
F(6)-C(20)-C(2)	115.6(9)
F(4)-C(20)-C(2)	116.5(9)
F(5)-C(20)-C(2)	115.6(9)

Symmetry transformations used to generate equivalent atoms:

#1 -x,-y+1,-z

Table 21. Anisotropic displacement parameters ($Å^2$ x 10^3) for $[(2\text{-}CF_3C_6H_4)PdBr_2]_2$ $[HP^tBu_3]_2$ (**28**). The anisotropic displacement factor exponent takes the form: $-2p^2[h^2a^{*2}U^{11} + ... + 2 h k a^* b^* U^{12}]$

	U^{11}	U^{22}	U^{33}	U^{23}	U^{13}	U^{12}
C(1)	61(3)	75(4)	41(3)	-1(3)	7(3)	-7(3)
C(2)	61(3)	93(5)	48(3)	-7(3)	4(3)	-4(3)
C(3)	85(5)	129(7)	52(4)	-9(4)	28(3)	-18(4)
C(4)	97(6)	148(8)	64(5)	14(5)	20(4)	-44(5)
C(5)	122(7)	119(7)	82(6)	40(5)	11(5)	-13(5)
C(6)	83(4)	94(5)	70(4)	27(4)	10(3)	-9(4)
C(7)	114(4)	95(4)	90(4)	-1(4)	23(4)	20(4)
F(1)	139(5)	97(4)	109(4)	-7(3)	2(4)	-1(4)
F(2)	105(4)	119(4)	144(5)	-7(4)	18(4)	33(4)
F(3)	140(5)	96(4)	82(4)	12(3)	17(4)	31(4)
Br(1)	61(1)	90(1)	46(1)	-10(1)	13(1)	-19(1)
Br(2)	73(1)	60(1)	51(1)	-1(1)	-3(1)	-5(1)
Pd(1)	56(1)	51(1)	38(1)	0(1)	9(1)	-4(1)
P(1)	59(1)	52(1)	52(1)	4(1)	2(1)	0(1)
C(8)	88(4)	57(4)	74(4)	-2(3)	3(4)	-15(3)
C(9)	126(7)	76(5)	150(8)	-42(5)	53(6)	-16(5)
C(10)	83(5)	64(4)	127(7)	1(4)	8(4)	-14(4)
C(11)	137(7)	133(7)	90(6)	9(5)	-38(5)	-52(6)
C(12)	63(4)	73(4)	74(4)	4(3)	12(3)	-6(3)
C(13)	107(6)	105(6)	78(5)	22(4)	27(4)	0(5)
C(14)	91(5)	79(5)	134(7)	-6(5)	27(5)	-28(4)
C(15)	66(4)	126(7)	120(7)	21(5)	15(4)	7(4)
C(16)	83(4)	105(5)	51(4)	15(4)	-2(3)	0(4)

Table 21 (cont.)

C(17)101(5)	146(8)	59(4)	19(4)	15(4)	5(5)
C(18)116(6)	139(8)	97(6)	51(5)	1(5)	31(6)
C(19)132(7)	178(9)	61(5)	-6(5)	-18(5)	-34(7)
C(20)120(5)	98(4)	99(5)	1(4)	17(4)	19(4)
F(4) 137(6)	111(5)	111(5)	-16(4)	15(5)	26(5)
F(5) 124(5)	106(5)	105(5)	16(5)	-2(5)	13(5)
F(6) 123(5)	91(5)	104(6)	10(5)	17(5)	10(5)

Table 22. Hydrogen coordinates (x 10^4) and isotropic displacement parameters (Å^2 x 10^3) for [(2-$CF_3C_6H_4$)$PdBr_2$]$_2$[HP^tBu_3]$_2$ (**28**).

	x	y	z	U(eq)
H(3)	-2816	6211	2107	105
H(4)	-2674	3822	2438	123
H(5)	-1453	2076	2053	129
H(6)	-374	2719	1337	98
H(1)	2570(50)	2930(60)	1092(19)	70(16)
H(9A)	3941	-409	387	172
H(9B)	2821	-1531	391	172
H(9C)	3684	-1214	911	172
H(10A)	849	-832	780	137
H(10B)	789	631	1106	137
H(10C)	1664	-670	1320	137
H(11A)	1284	466	23	184
H(11B)	2405	1586	16	184
H(11C)	1232	1985	317	184
H(13A)	5236	3125	87	143
H(13B)	3796	3376	135	143
H(13C)	4321	1768	85	143
H(14A)	5662	4626	840	151
H(14B)	5249	4190	1394	151
H(14C)	4250	4796	957	151
H(15A)	6046	1582	1343	155
H(15B)	6595	2022	816	155
H(15C)	5695	654	832	155

Table 22 (cont.)

H(17A)	2347	1667	2443	152
H(17B)	1679	906	1941	152
H(17C)	1855	2627	1955	152
H(18A)	3517	-730	1790	177
H(18B)	4147	-149	2331	177
H(18C)	4874	-47	1825	177
H(19A)	5197	2630	2007	188
H(19B)	4417	2538	2498	188
H(19C)	4035	3673	2047	188

Figure 35. ORTEP diagram of **28** at 50% thermal ellipsoids.

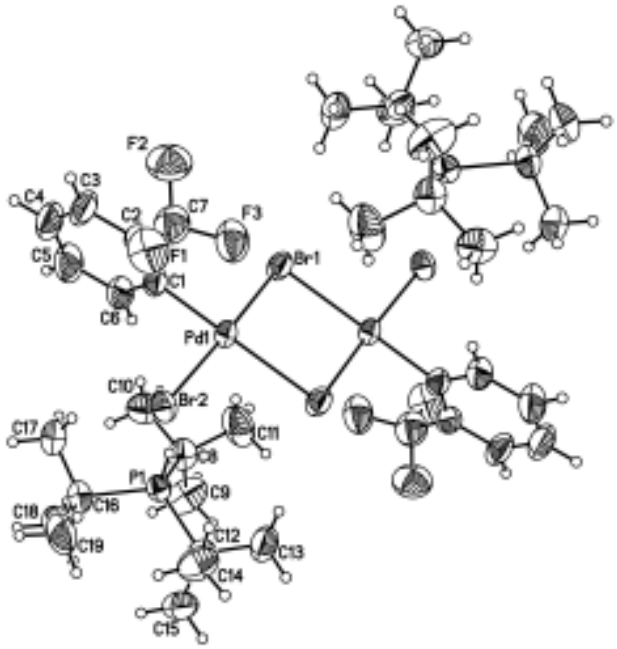

Table 23. Crystal data and structure refinement for $[(C_6H_5)PdBr_2]_2[HP^tBu_3]_2$ (**29**).

Empirical formula	$C_{36}H_{66}Br_4P_2Pd_2$	
Formula weight	1093.27	
Temperature	193(2) K	
Wavelength	0.71073 Å	
Crystal system	Monoclinic	
Space group	P 21	
Unit cell dimensions	a = 9.527(2) Å	a= 90°
	b = 19.163(4) Å	b= 110.754(3)°
	c = 12.549(3) Å	g = 90°
Volume	2142.4(8) $Å^3$	
Z	2	
Density (calculated)	1.695 Mg/m^3	
Absorption coefficient	4.667 mm^{-1}	
F(000)	1088	
Crystal color	dark orange	
Crystal size	0.12 x 0.10 x 0.07 mm^3	
Theta range for data collection	1.74 to 25.37°.	
Index ranges	-11<=h<=11, -23<=k<=23, -15<=l<=15	
Reflections collected	22094	
Independent reflections	7855 [R(int) = 0.0424]	
Completeness to theta = 25.37°	99.9 %	
Absorption correction	Integration	
Max. and min. transmission	0.7709 and 0.3889	
Refinement method	Full-matrix least-squares on F^2	
Data / restraints / parameters	7855 / 1 / 422	
Goodness-of-fit on F^2	0.984	
Final R indices [I>2sigma(I)]	R1 = 0.0330, wR^2 = 0.0613	
R indices (all data)	R1 = 0.0553, wR^2 = 0.0667	
Absolute structure parameter	0.437(7)	
Largest diff. peak and hole	0.882 and -0.495 $e.Å^{-3}$	

Table 24. Atomic coordinates (x 10^4) and equivalent isotropic displacement parameters ($Å^2$ x 10^3) for $[(C_6H_5)PdBr_2]_2[HP^tBu_3]_2$ (**29**). U(eq) is defined as one third of the trace of the orthogonalized U^{ij} tensor.

	x	y	z	U(eq)
C(1)	8565(6)	8196(3)	3334(5)	26(1)
C(2)	9791(7)	8416(4)	4143(6)	38(2)
C(3)	10424(7)	9057(4)	4035(5)	38(2)
C(4)	9725(7)	9476(4)	3095(6)	45(2)
C(5)	8419(7)	9241(4)	2276(6)	41(2)
C(6)	7822(7)	8597(4)	2399(5)	37(2)
C(7)	6668(6)	4662(3)	1790(5)	31(2)
C(8)	5402(6)	4414(4)	945(5)	37(2)
C(9)	4837(7)	3749(4)	1072(6)	43(2)
C(10)	5518(8)	3369(4)	2036(6)	44(2)
C(11)	6766(7)	3628(4)	2868(6)	45(2)
C(12)	7332(7)	4284(4)	2746(6)	38(2)
C(13)	3472(7)	4760(3)	4385(5)	43(2)
C(14)	4812(8)	4244(4)	4819(7)	60(2)
C(15)	3107(8)	4848(4)	3101(5)	51(2)
C(16)	2122(7)	4441(4)	4634(6)	50(2)
C(17)	5236(6)	5591(3)	6616(5)	34(1)
C(18)	5415(7)	6318(3)	7175(5)	46(2)
C(19)	6835(6)	5370(4)	6669(5)	48(2)
C(20)	4627(7)	5083(4)	7307(5)	47(2)
C(21)	2375(7)	6252(4)	4824(6)	46(2)
C(22)	2997(8)	6994(4)	4962(6)	58(2)
C(23)	1480(7)	6110(4)	5619(6)	61(2)

Table 24 (cont.)

C(24)	1288(7)	6166(4)	3582(6)	66(2)
C(25)	12618(6)	7805(3)	1420(5)	36(2)
C(26)	13386(7)	8367(4)	967(5)	46(2)
C(27)	13828(6)	7297(4)	2153(5)	48(2)
C(28)	11844(7)	8116(4)	2203(5)	50(2)
C(29)	9835(6)	7916(3)	-827(5)	37(2)
C(30)	8372(6)	7505(4)	-1442(5)	54(2)
C(31)	9435(7)	8545(4)	-220(6)	49(2)
C(32)	10496(7)	8190(4)	-1696(5)	49(2)
C(33)	11977(7)	6601(3)	-394(6)	41(2)
C(34)	12407(8)	5988(4)	472(6)	55(2)
C(35)	13319(7)	6826(4)	-687(6)	54(2)
C(36)	10753(8)	6302(4)	-1469(6)	60(2)
Br(1)	7803(1)	6977(1)	1483(1)	35(1)
Br(2)	6790(1)	5951(1)	3387(1)	41(1)
Br(3)	7664(1)	7420(1)	5303(1)	51(1)
Br(4)	8188(1)	5312(1)	124(1)	47(1)
P(1)	3979(2)	5628(1)	5091(1)	29(1)
P(2)	11182(2)	7321(1)	229(1)	30(1)
Pd(1)	7763(1)	7224(1)	3409(1)	29(1)
Pd(2)	7311(1)	5643(1)	1660(1)	29(1)

Table 25. Bond lengths [Å] and angles [°] for $[(C_6H_5)PdBr_2]_2[HP^tBu_3]_2$ (**29**).

C(1)-C(2)	1.316(8)
C(1)-C(6)	1.371(8)
C(1)-Pd(1)	2.029(6)
C(2)-C(3)	1.395(9)
C(2)-H(2)	0.9500
C(3)-C(4)	1.387(9)
C(3)-H(3)	0.9500
C(4)-C(5)	1.378(9)
C(4)-H(4)	0.9500
C(5)-C(6)	1.390(9)
C(5)-H(5)	0.9500
C(6)-H(6)	0.9500
C(7)-C(12)	1.351(9)
C(7)-C(8)	1.378(8)
C(7)-Pd(2)	2.001(6)
C(8)-C(9)	1.414(9)
C(8)-H(8)	0.9500
C(9)-C(10)	1.363(9)
C(9)-H(9)	0.9500
C(10)-C(11)	1.367(9)
C(10)-H(10)	0.9500
C(11)-C(12)	1.398(9)
C(11)-H(11)	0.9500
C(12)-H(12)	0.9500
C(13)-C(15)	1.532(8)
C(13)-C(16)	1.552(8)
C(13)-C(14)	1.553(9)

Table 25 (cont.)

C(13)-P(1)	1.864(6)
C(14)-H(14A)	0.9800
C(14)-H(14B)	0.9800
C(14)-H(14C)	0.9800
C(15)-H(15A)	0.9800
C(15)-H(15B)	0.9800
C(15)-H(15C)	0.9800
C(16)-H(16A)	0.9800
C(16)-H(16B)	0.9800
C(16)-H(16C)	0.9800
C(17)-C(18)	1.542(8)
C(17)-C(20)	1.548(8)
C(17)-C(19)	1.560(8)
C(17)-P(1)	1.865(5)
C(18)-H(18A)	0.9800
C(18)-H(18B)	0.9800
C(18)-H(18C)	0.9800
C(19)-H(19A)	0.9800
C(19)-H(19B)	0.9800
C(19)-H(19C)	0.9800
C(20)-H(20A)	0.9800
C(20)-H(20B)	0.9800
C(20)-H(20C)	0.9800
C(21)-C(22)	1.527(10)
C(21)-C(24)	1.544(9)
C(21)-C(23)	1.549(9)
C(21)-P(1)	1.875(6)
C(22)-H(22A)	0.9800

Table 25 (cont.)

C(22)-H(22B)	0.9800
C(22)-H(22C)	0.9800
C(23)-H(23A)	0.9800
C(23)-H(23B)	0.9800
C(23)-H(23C)	0.9800
C(24)-H(24A)	0.9800
C(24)-H(24B)	0.9800
C(24)-H(24C)	0.9800
C(25)-C(26)	1.519(8)
C(25)-C(27)	1.541(8)
C(25)-C(28)	1.542(8)
C(25)-P(2)	1.876(6)
C(26)-H(26A)	0.9800
C(26)-H(26B)	0.9800
C(26)-H(26C)	0.9800
C(27)-H(27A)	0.9800
C(27)-H(27B)	0.9800
C(27)-H(27C)	0.9800
C(28)-H(28A)	0.9800
C(28)-H(28B)	0.9800
C(28)-H(28C)	0.9800
C(29)-C(32)	1.533(8)
C(29)-C(31)	1.544(8)
C(29)-C(30)	1.548(8)
C(29)-P(2)	1.871(6)
C(30)-H(30A)	0.9800
C(30)-H(30B)	0.9800
C(30)-H(30C)	0.9800

Table 25 (cont.)

C(31)-H(31A)	0.9800
C(31)-H(31B)	0.9800
C(31)-H(31C)	0.9800
C(32)-H(32A)	0.9800
C(32)-H(32B)	0.9800
C(32)-H(32C)	0.9800
C(33)-C(35)	1.513(9)
C(33)-C(36)	1.547(9)
C(33)-C(34)	1.554(9)
C(33)-P(2)	1.872(6)
C(34)-H(34A)	0.9800
C(34)-H(34B)	0.9800
C(34)-H(34C)	0.9800
C(35)-H(35A)	0.9800
C(35)-H(35B)	0.9800
C(35)-H(35C)	0.9800
C(36)-H(36A)	0.9800
C(36)-H(36B)	0.9800
C(36)-H(36C)	0.9800
Br(1)-Pd(1)	2.4768(9)
Br(1)-Pd(2)	2.6223(10)
Br(2)-Pd(2)	2.4608(9)
Br(2)-Pd(1)	2.6060(10)
Br(3)-Pd(1)	2.4401(9)
Br(4)-Pd(2)	2.4398(9)
P(1)-H(1)	1.27(6)
P(2)-H(2A)	1.25(6)

Table 25 (cont.)

C(2)-C(1)-C(6)	121.9(6)
C(2)-C(1)-Pd(1)	120.3(5)
C(6)-C(1)-Pd(1)	117.8(5)
C(1)-C(2)-C(3)	120.2(6)
C(1)-C(2)-H(2)	119.9
C(3)-C(2)-H(2)	119.9
C(4)-C(3)-C(2)	119.9(6)
C(4)-C(3)-H(3)	120.1
C(2)-C(3)-H(3)	120.1
C(5)-C(4)-C(3)	118.7(7)
C(5)-C(4)-H(4)	120.7
C(3)-C(4)-H(4)	120.7
C(4)-C(5)-C(6)	120.3(7)
C(4)-C(5)-H(5)	119.9
C(6)-C(5)-H(5)	119.9
C(1)-C(6)-C(5)	119.0(6)
C(1)-C(6)-H(6)	120.5
C(5)-C(6)-H(6)	120.5
C(12)-C(7)-C(8)	120.3(6)
C(12)-C(7)-Pd(2)	121.0(5)
C(8)-C(7)-Pd(2)	118.1(5)
C(7)-C(8)-C(9)	119.3(6)
C(7)-C(8)-H(8)	120.4
C(9)-C(8)-H(8)	120.4
C(10)-C(9)-C(8)	120.0(6)
C(10)-C(9)-H(9)	120.0
C(8)-C(9)-H(9)	120.0
C(9)-C(10)-C(11)	119.7(7)

Table 25 (cont.)

C(9)-C(10)-H(10)	120.1
C(11)-C(10)-H(10)	120.1
C(10)-C(11)-C(12)	120.5(7)
C(10)-C(11)-H(11)	119.8
C(12)-C(11)-H(11)	119.8
C(7)-C(12)-C(11)	120.1(6)
C(7)-C(12)-H(12)	119.9
C(11)-C(12)-H(12)	119.9
C(15)-C(13)-C(16)	111.0(5)
C(15)-C(13)-C(14)	106.9(6)
C(16)-C(13)-C(14)	108.4(6)
C(15)-C(13)-P(1)	109.0(5)
C(16)-C(13)-P(1)	110.5(4)
C(14)-C(13)-P(1)	111.0(4)
C(13)-C(14)-H(14A)	109.5
C(13)-C(14)-H(14B)	109.5
H(14A)-C(14)-H(14B)	109.5
C(13)-C(14)-H(14C)	109.5
H(14A)-C(14)-H(14C)	109.5
H(14B)-C(14)-H(14C)	109.5
C(13)-C(15)-H(15A)	109.5
C(13)-C(15)-H(15B)	109.5
H(15A)-C(15)-H(15B)	109.5
C(13)-C(15)-H(15C)	109.5
H(15A)-C(15)-H(15C)	109.5
H(15B)-C(15)-H(15C)	109.5
C(13)-C(16)-H(16A)	109.5
C(13)-C(16)-H(16B)	109.5

Table 25 (cont.)

H(16A)-C(16)-H(16B)109.5
C(13)-C(16)-H(16C) 109.5
H(16A)-C(16)-H(16C)109.5
H(16B)-C(16)-H(16C)109.5
C(18)-C(17)-C(20) 108.5(5)
C(18)-C(17)-C(19) 106.1(5)
C(20)-C(17)-C(19) 111.1(5)
C(18)-C(17)-P(1) 111.1(4)
C(20)-C(17)-P(1) 111.5(4)
C(19)-C(17)-P(1) 108.4(4)
C(17)-C(18)-H(18A) 109.5
C(17)-C(18)-H(18B) 109.5
H(18A)-C(18)-H(18B)109.5
C(17)-C(18)-H(18C) 109.5
H(18A)-C(18)-H(18C)109.5
H(18B)-C(18)-H(18C)109.5
C(17)-C(19)-H(19A) 109.5
C(17)-C(19)-H(19B) 109.5
H(19A)-C(19)-H(19B)109.5
C(17)-C(19)-H(19C) 109.5
H(19A)-C(19)-H(19C)109.5
H(19B)-C(19)-H(19C)109.5
C(17)-C(20)-H(20A) 109.5
C(17)-C(20)-H(20B) 109.5
H(20A)-C(20)-H(20B)109.5
C(17)-C(20)-H(20C) 109.5
H(20A)-C(20)-H(20C)109.5
H(20B)-C(20)-H(20C)109.5

Table 25 (cont.)

C(22)-C(21)-C(24)	107.9(6)
C(22)-C(21)-C(23)	111.7(6)
C(24)-C(21)-C(23)	107.9(6)
C(22)-C(21)-P(1)	108.3(4)
C(24)-C(21)-P(1)	108.9(5)
C(23)-C(21)-P(1)	111.9(5)
C(21)-C(22)-H(22A)	109.5
C(21)-C(22)-H(22B)	109.5
H(22A)-C(22)-H(22B)	109.5
C(21)-C(22)-H(22C)	109.5
H(22A)-C(22)-H(22C)	109.5
H(22B)-C(22)-H(22C)	109.5
C(21)-C(23)-H(23A)	109.5
C(21)-C(23)-H(23B)	109.5
H(23A)-C(23)-H(23B)	109.5
C(21)-C(23)-H(23C)	109.5
H(23A)-C(23)-H(23C)	109.5
H(23B)-C(23)-H(23C)	109.5
C(21)-C(24)-H(24A)	109.5
C(21)-C(24)-H(24B)	109.5
H(24A)-C(24)-H(24B)	109.5
C(21)-C(24)-H(24C)	109.5
H(24A)-C(24)-H(24C)	109.5
H(24B)-C(24)-H(24C)	109.5
C(26)-C(25)-C(27)	108.3(5)
C(26)-C(25)-C(28)	111.6(5)
C(27)-C(25)-C(28)	106.8(5)
C(26)-C(25)-P(2)	111.4(4)

Table 25 (cont.)

C(27)-C(25)-P(2)	110.0(4)
C(28)-C(25)-P(2)	108.7(4)
C(25)-C(26)-H(26A)	109.5
C(25)-C(26)-H(26B)	109.5
H(26A)-C(26)-H(26B)	109.5
C(25)-C(26)-H(26C)	109.5
H(26A)-C(26)-H(26C)	109.5
H(26B)-C(26)-H(26C)	109.5
C(25)-C(27)-H(27A)	109.5
C(25)-C(27)-H(27B)	109.5
H(27A)-C(27)-H(27B)	109.5
C(25)-C(27)-H(27C)	109.5
H(27A)-C(27)-H(27C)	109.5
H(27B)-C(27)-H(27C)	109.5
C(25)-C(28)-H(28A)	109.5
C(25)-C(28)-H(28B)	109.5
H(28A)-C(28)-H(28B)	109.5
C(25)-C(28)-H(28C)	109.5
H(28A)-C(28)-H(28C)	109.5
H(28B)-C(28)-H(28C)	109.5
C(32)-C(29)-C(31)	108.6(5)
C(32)-C(29)-C(30)	110.1(5)
C(31)-C(29)-C(30)	107.9(5)
C(32)-C(29)-P(2)	111.2(4)
C(31)-C(29)-P(2)	110.7(4)
C(30)-C(29)-P(2)	108.2(4)
C(29)-C(30)-H(30A)	109.5
C(29)-C(30)-H(30B)	109.5

Table 25 (cont.)

H(30A)-C(30)-H(30B)109.5
C(29)-C(30)-H(30C) 109.5
H(30A)-C(30)-H(30C)109.5
H(30B)-C(30)-H(30C)109.5
C(29)-C(31)-H(31A) 109.5
C(29)-C(31)-H(31B) 109.5
H(31A)-C(31)-H(31B)109.5
C(29)-C(31)-H(31C) 109.5
H(31A)-C(31)-H(31C)109.5
H(31B)-C(31)-H(31C)109.5
C(29)-C(32)-H(32A) 109.5
C(29)-C(32)-H(32B) 109.5
H(32A)-C(32)-H(32B)109.5
C(29)-C(32)-H(32C) 109.5
H(32A)-C(32)-H(32C)109.5
H(32B)-C(32)-H(32C)109.5
C(35)-C(33)-C(36) 109.5(5)
C(35)-C(33)-C(34) 110.4(6)
C(36)-C(33)-C(34) 105.0(5)
C(35)-C(33)-P(2) 113.2(5)
C(36)-C(33)-P(2) 110.3(5)
C(34)-C(33)-P(2) 108.1(4)
C(33)-C(34)-H(34A) 109.5
C(33)-C(34)-H(34B) 109.5
H(34A)-C(34)-H(34B)109.5
C(33)-C(34)-H(34C) 109.5
H(34A)-C(34)-H(34C)109.5
H(34B)-C(34)-H(34C)109.5

Table 25 (cont.)

C(33)-C(35)-H(35A)	109.5
C(33)-C(35)-H(35B)	109.5
H(35A)-C(35)-H(35B)	109.5
C(33)-C(35)-H(35C)	109.5
H(35A)-C(35)-H(35C)	109.5
H(35B)-C(35)-H(35C)	109.5
C(33)-C(36)-H(36A)	109.5
C(33)-C(36)-H(36B)	109.5
H(36A)-C(36)-H(36B)	109.5
C(33)-C(36)-H(36C)	109.5
H(36A)-C(36)-H(36C)	109.5
H(36B)-C(36)-H(36C)	109.5
Pd(1)-Br(1)-Pd(2)	92.22(3)
Pd(2)-Br(2)-Pd(1)	92.98(3)
C(13)-P(1)-C(17)	114.7(3)
C(13)-P(1)-C(21)	115.2(3)
C(17)-P(1)-C(21)	113.2(3)
C(13)-P(1)-H(1)	109(2)
C(17)-P(1)-H(1)	106(2)
C(21)-P(1)-H(1)	96(2)
C(29)-P(2)-C(33)	115.5(3)
C(29)-P(2)-C(25)	112.7(3)
C(33)-P(2)-C(25)	114.1(3)
C(29)-P(2)-H(2A)	105(2)
C(33)-P(2)-H(2A)	105(3)
C(25)-P(2)-H(2A)	103(2)
C(1)-Pd(1)-Br(3)	92.82(16)
C(1)-Pd(1)-Br(1)	89.63(16)

Table 25 (cont.)

Br(3)-Pd(1)-Br(1)	177.52(3)
C(1)-Pd(1)-Br(2)	175.98(16)
Br(3)-Pd(1)-Br(2)	91.05(3)
Br(1)-Pd(1)-Br(2)	86.51(3)
C(7)-Pd(2)-Br(4)	91.19(16)
C(7)-Pd(2)-Br(2)	89.42(16)
Br(4)-Pd(2)-Br(2)	172.03(3)
C(7)-Pd(2)-Br(1)	172.46(16)
Br(4)-Pd(2)-Br(1)	93.75(3)
Br(2)-Pd(2)-Br(1)	86.48(3)

Symmetry transformations used to generate equivalent atoms:

Table 26. Anisotropic displacement parameters ($Å^2$ x 10^3) for $[(C_6H_5)PdBr_2]_2[HP^tBu_3]_2$ (**29**). The anisotropic displacement factor exponent takes the form: $-2p^2[h^2a^{*2}U^{11} + ... + 2 h k a^* b^* U^{12}]$

	U^{11}	U^{22}	U^{33}	U^{23}	U^{13}	U^{12}
C(1)	26(3)	29(4)	29(3)	4(3)	17(3)	13(3)
C(2)	39(4)	40(5)	42(4)	7(3)	23(3)	14(3)
C(3)	28(3)	49(5)	37(4)	-12(3)	15(3)	-1(3)
C(4)	50(4)	36(5)	61(5)	-8(4)	32(4)	0(3)
C(5)	34(4)	40(5)	51(4)	2(4)	16(3)	9(3)
C(6)	36(3)	38(4)	43(4)	-11(3)	23(3)	-5(3)
C(7)	35(3)	37(4)	29(4)	-6(3)	22(3)	-5(3)
C(8)	37(4)	40(5)	40(4)	-3(3)	20(3)	1(3)
C(9)	33(4)	41(5)	57(5)	-18(4)	19(3)	-16(3)
C(10)	55(5)	30(4)	60(5)	-4(4)	36(4)	-5(4)
C(11)	46(4)	37(5)	58(5)	10(4)	24(4)	2(4)
C(12)	38(4)	32(4)	49(4)	-4(3)	20(3)	-4(3)
C(13)	44(4)	37(4)	51(4)	-8(3)	23(3)	-8(3)
C(14)	65(5)	41(5)	73(5)	-12(4)	25(4)	14(4)
C(15)	59(4)	54(5)	47(4)	-18(4)	26(4)	-24(4)
C(16)	64(5)	45(5)	49(4)	-2(4)	28(4)	-17(4)
C(17)	31(3)	34(4)	35(3)	2(3)	9(2)	4(3)
C(18)	59(4)	49(4)	34(4)	-8(3)	23(3)	-8(4)
C(19)	37(4)	64(5)	38(4)	6(4)	5(3)	2(4)
C(20)	45(4)	49(5)	41(4)	10(3)	10(3)	1(3)
C(21)	44(4)	47(5)	50(4)	17(4)	22(3)	22(3)
C(22)	79(5)	42(5)	59(5)	14(4)	31(4)	23(4)

Table 26 (cont.)

C(23) 50(4)	78(7)	64(5)	14(5)	32(4)	23(4)
C(24) 52(5)	83(6)	56(5)	24(4)	10(4)	26(4)
C(25) 34(3)	38(4)	37(4)	-4(3)	15(3)	0(3)
C(26) 39(4)	51(5)	51(4)	-5(3)	21(3)	-8(3)
C(27) 34(3)	64(5)	39(4)	3(3)	5(3)	10(3)
C(28) 44(4)	67(5)	35(4)	-16(4)	10(3)	4(4)
C(29) 34(3)	44(4)	33(3)	4(3)	13(3)	-2(3)
C(30) 29(3)	87(6)	37(4)	8(4)	2(3)	-8(4)
C(31) 42(4)	49(5)	55(5)	6(4)	16(3)	3(3)
C(32) 39(4)	61(5)	47(4)	24(3)	15(3)	6(3)
C(33) 48(4)	35(4)	51(4)	-5(3)	31(4)	0(3)
C(34) 68(5)	31(4)	75(5)	3(4)	34(4)	0(4)
C(35) 54(4)	60(6)	59(5)	-14(4)	35(4)	1(4)
C(36) 78(5)	56(5)	51(4)	-19(4)	28(4)	-22(4)
Br(1) 42(1)	34(1)	33(1)	-3(1)	20(1)	-8(1)
Br(2) 57(1)	34(1)	45(1)	-7(1)	34(1)	-11(1)
Br(3) 79(1)	46(1)	39(1)	-7(1)	33(1)	-8(1)
Br(4) 66(1)	47(1)	38(1)	-6(1)	30(1)	-6(1)
P(1) 27(1)	31(1)	33(1)	2(1)	15(1)	-1(1)
P(2) 27(1)	36(1)	29(1)	2(1)	11(1)	-2(1)
Pd(1) 30(1)	30(1)	30(1)	-2(1)	14(1)	-1(1)
Pd(2) 31(1)	31(1)	28(1)	-3(1)	12(1)	-3(1)

Table 27. Hydrogen coordinates (x 10^4) and isotropic displacement parameters (Å^2 x 10^3) for $[(C_6H_5)PdBr_2]_2[HP^tBu_3]_2$ (**29**).

	x	y	z	U(eq)
H(2)	10247	8138	4802	46
H(3)	11332	9206	4605	45
H(4)	10138	9916	3017	54
H(5)	7925	9521	1626	50
H(6)	6911	8438	1844	44
H(8)	4915	4686	284	45
H(9)	3983	3567	485	51
H(10)	5127	2927	2130	53
H(11)	7252	3360	3534	54
H(12)	8185	4465	3336	46
H(14A)	4509	3789	4454	89
H(14B)	5116	4192	5647	89
H(14C)	5657	4425	4630	89
H(15A)	3027	4387	2745	76
H(15B)	3907	5115	2970	76
H(15C)	2152	5097	2767	76
H(16A)	1976	3956	4369	76
H(16B)	1214	4711	4234	76
H(16C)	2325	4455	5456	76
H(18A)	6105	6288	7967	68
H(18B)	4434	6485	7158	68
H(18C)	5818	6645	6755	68
H(19A)	7532	5391	7459	72

Table 27 (cont.)

H(19B)	7176	5687	6198	72
H(19C)	6800	4892	6381	72
H(20A)	5238	5120	8119	70
H(20B)	4673	4604	7048	70
H(20C)	3583	5202	7193	70
H(22A)	2173	7324	4624	87
H(22B)	3724	7035	4575	87
H(22C)	3492	7099	5773	87
H(23A)	643	6440	5445	91
H(23B)	2143	6169	6415	91
H(23C)	1089	5632	5502	91
H(24A)	518	6530	3405	99
H(24B)	809	5706	3489	99
H(24C)	1849	6207	3064	99
H(26A)	14152	8599	1606	68
H(26B)	12640	8710	532	68
H(26C)	13860	8153	470	68
H(27A)	14509	7543	2821	72
H(27B)	14400	7113	1702	72
H(27C)	13346	6910	2404	72
H(28A)	12607	8264	2923	75
H(28B)	11196	7762	2355	75
H(28C)	11235	8519	1828	75
H(30A)	7628	7816	-1966	81
H(30B)	7976	7319	-877	81
H(30C)	8586	7118	-1872	81
H(31A)	8637	8819	-773	74
H(31B)	10326	8839	115	74

Table 27 (cont.)

H(31C)	9090	8378	383	74
H(32A)	9801	8527	-2202	74
H(32B)	10649	7800	-2148	74
H(32C)	11459	8418	-1295	74
H(34A)	12656	5576	111	83
H(34B)	11558	5880	713	83
H(34C)	13277	6121	1138	83
H(35A)	13703	6426	-987	80
H(35B)	14106	7002	-1	80
H(35C)	13017	7195	-1264	80
H(36A)	11155	5897	-1744	90
H(36B)	10447	6660	-2064	90
H(36C)	9883	6158	-1279	90
H(1)	4680(60)	5980(30)	4580(40)	44
H(2A)	10410(60)	7020(30)	720(40)	45

Figure 36. ORTEP diagram of **29** at 50% thermal ellipsoids.

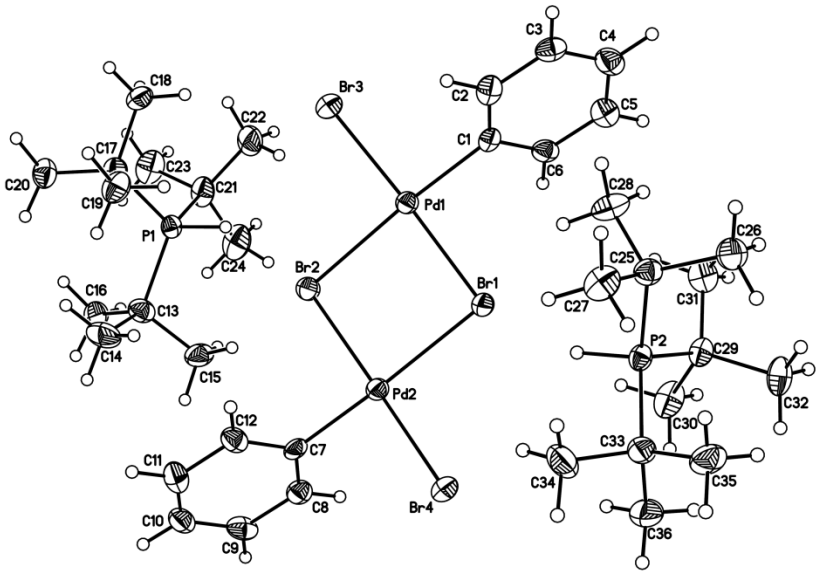

4.6 References

(1) Bräse, S.; Meijere, A. D. In *Metal-Catalyzed Cross-Coupling Reactions*; Wiley-VCH Verlag GmbH: 2008, p 217-315.
(2) Beletskaya, I. P.; Cheprakov, A. V. *Chem. Rev.* **2000**, *100*, 3009-3066.
(3) Heck, R. F. *Org. React. (N.Y.)* **1982**, *27*, 345.
(4) Jeffery, T. In *Advances in Metal-Organic Chemistry*; Liebeskind, L. S., Ed.; JAI: London, 1996; Vol. 5, p 153-260.
(5) Crisp, G. T. *Chem. Soc. Rev.* **1998**, *27*, 427.
(6) Daves, G. D.; Hallberg, A. *Chem. Rev.* **1989**, *89*, 1433-1445.
(7) Cabri, W.; Candiani, I. *Acc. Chem. Res.* **1995**, *28*, 2-7.
(8) The reaction of an alkenyl electrophile with an aryl organometallic reagent is an alternative strategy for the formation of vinylarenes by cross-coupling.
(9) Heck, R. F.; Nolley, J. P. *J. Org. Chem.* **1972**, *37*, 2320-2322.
(10) Mizoroki, T.; Mori, K.; Ozaki, A. *Bull. Chem. Soc. Jpn.* **1971**, *44*, 581.
(11) Reetz, M. T.; Breinbauer, R.; Wanninger, K. *Tetrahedron Lett.* **1996**, *37*, 4499-4502.
(12) Beller, M.; Fischer, H.; Kühlein, K.; Reisinger, C. P.; Herrmann, W. A. *J. Organomet. Chem.* **1996**, *520*, 257-259.
(13) Reetz, M. T.; Lohmer, G.; Schwickardi, R. *Angew. Chem., Int. Ed.* **1998**, *37*, 481-483.
(14) Firmansjah, L.; Fu, G. C. *J. Am. Chem. Soc.* **2007**, *129*, 11340-11341.
(15) Overman, L. E. *Pure Appl. Chem.* **1994**, *66*, 1423.
(16) Shibasaki, M.; Boden, C. D. J.; Kojima, A. *Tetrahedron* **1997**, *53*, 7371.
(17) Nicolaou, K. C.; Bulger, P. G.; Sarlah, D. *Angew. Chem. Int. Ed.* **2005**, *44*, 4442-4489.
(18) Prashad, M. *Top. Organomet. Chem.* **2004**, *6*, 181–203.
(19) Smith, G. B.; Dezeny, G. C.; Hughes, D. L.; King, A. O.; Verhoeven, T. R. *J. Org. Chem.* **1994**, *59*, 8151-8156
(20) http://www.drugs.com/top200.html
(21) Tietze, L. F.; Noebel, T.; Spescha, M. *J. Am. Chem. Soc.* **1998**, *120*, 8971.
(22) Danishefsky, S. J.; Masters, J. J.; Young, W. B.; Link, J. T.; Snyder, L. B.; Magee, T. V.; Jung, D. K.; Isaacs, R. C. A.; Bornmann, W. G.; Alaimo, C. A.; Coburn, C. A.; Di Grandi, M. J. *J. Am. Chem. Soc.* **1996**, *118*, 2843-2859.
(23) Hartwig, J. F. *Organotransition Metal Chemistry*; University Science Books: Sausalito, California, 2010.
(24) *The Mizoroki-Heck Reaction*; Oestreich, M., Ed.; John Wiley and Sons, Ltd: West Sussex, United Kingdom, 2009.
(25) Brown, J. M.; Cooley, N. A. *Chem. Rev.* **1988**, *88*, 1031-1046.
(26) Hills, I. D.; Fu, G. C. *J. Am. Chem. Soc.* **2004**, *126*, 13178-13179.
(27) Thorn, D. L.; Hoffmann, R. *J. Am. Chem. Soc.* **1978**, *100*, 2079-2090.
(28) Flood, T. C.; Bitler, S. P. *J. Am. Chem. Soc.* **1984**, *106*, 6076-6077.
(29) Cossee, P. *Journal of Catalysis* **1964**, *3*, 80-88.
(30) Stille, J. K.; Huang, F.; Regan, M. T. *J. Am. Chem. Soc.* **1974**, *96*, 1518-1522.
(31) Loiseleur, O.; Hayashi, M.; Schmees, N.; Pfaltz, A. *Synthesis* **1997**, *1997*, 1338,1345.
(32) Cabri, W.; Candiani, I.; DeBernardinis, S.; Francalanci, F.; Penco, S.; Santo, R. *J. Org. Chem.* **1991**, *56*, 5796-5800.

(33) Ozawa, F.; Kubo, A.; Hayashi, T. *J. Am. Chem. Soc.* **1991**, *113*, 1417.
(34) Jeffery, T. *J. Chem. Soc., Chem. Commun* **1984**, 1287-1289.
(35) Jeffery, T. *Tetrahedron Lett.* **1985**, *26*, 2667-2670.
(36) Dieck, H. A.; Heck, R. F. *J. Am. Chem. Soc.* **1974**, *96*, 1133.
(37) Patel, B. A.; Ziegler, C. B.; Cortese, N. A.; Plevyak, J. E.; Zebovitz, T. C.; Terpko, M.; Heck, R. F. *J. Org. Chem.* **1977**, *42*, 3903-3907.
(38) Spencer, A. *J. Organomet. Chem.* **1983**, *258*, 101-108.
(39) Littke, A. F.; Fu, G. C. *J. Am. Chem. Soc.* **2001**, *123*, 6989-7000.
(40) Shaughnessy, K. H.; Kim, P.; Hartwig, J. F. *J. Am. Chem. Soc.* **1999**, *121*, 2123-2132.
(41) Ehrentraut, A.; Zapf, A.; Beller, M. *Synlett* **2000**, *120*, 1589-1592.
(42) Littke, A. F.; Fu, G. C. *J. Org. Chem.* **1999**, *64*, 10-11.
(43) Stambuli, J. P.; Stauffer, S. R.; Shaughnessy, K. H.; Hartwig, J. F. *J. Am. Chem. Soc.* **2001**, *123*, 2677-2678.
(44) The term "ligandless" refers to palladium complexes lacking dative ligands such as phosphines, amines, or *N*-heterocyclic carbenes.
(45) Reetz, M. T.; Westermann, E. *Angew. Chem. Int. Ed.* **2000**, *39*, 165-168.
(46) Evans, J.; O'Neill, L.; Kambhampati, V. L.; Rayner, G.; Turin, S.; Genge, A.; Dent, A. J.; Neisius, T. *J. Chem. Soc., Dalton Trans.* **2002**, 2207-2212.
(47) de Vries, J. G. *J. Chem. Soc., Dalton Trans.* **2006**, 421–429.
(48) de Vries, A. H. M.; Parlevliet, F. J.; Schmieder-van de Vondervoort, L.; Mommers, J. H. M.; Henderickx, H. J. W.; Walet, M. A. M.; de Vries, J. G. *Adv. Synth. Catal.* **2002**, *344*, 996-1002.
(49) Albeniz, A. C.; Espinet, P.; Martin-Ruiz, B.; Milstein, D. *J. Am. Chem. Soc.* **2001**, *123*, 11504-11505.
(50) Usón, R.; Forniés, J.; Nalda, J. A.; Lozano, M. J.; Espinet, P.; Albéniz, A. C. *Inorg. Chim. Acta* **1989**, *156*, 251-256.
(51) de Vries, A. H. M.; Mulders, J. M. C. A.; Mommers, J. H. M.; Henderickx, H. J. W.; de Vries, J. G. *Org. Lett.* **2003**, *5*, 3285-3288.
(52) Amatore, C.; Carré, E.; Jutand, A.; M'Barki, M. *Organometallics* **1995**, *14*, 1818-1826.
(53) Stambuli, J. P.; Bühl, M.; Hartwig, J. F. *J. Am. Chem. Soc.* **2002**, *124*, 9346-9347.
(54) Stambuli, J. P.; Incarvito, C. D.; Bühl, M.; Hartwig, J. F. *J. Am. Chem. Soc.* **2004**, *126*, 1184-1194.
(55) Barrios-Landeros, F.; Carrow, B. P.; Hartwig, J. F. *J. Am. Chem. Soc.* **2008**, *130*, 5842-5843.
(56) Barrios-Landeros, F.; Carrow, B. P.; Hartwig, J. F. *J. Am. Chem. Soc.* **2009**, *131*, 8141-8154.
(57) Barrios-Landeros, F.; Hartwig, J. F. *J. Am. Chem. Soc.* **2005**, *127*, 6944-6945.
(58) Amatore, C.; Jutand, A. *Acc. Chem. Res.* **2000**, *33*, 314-321.
(59) Geary, W. J. *Coord. Chem. Rev.* **1971**, *7*, 81-122.
(60) The equilibrium constant was found to be sensitive to the polarity of the medium.
(61) Reetz, M. T.; de Vries, J. G. *Chem. Commun.* **2004**, 1559-1563.
(62) Guertler, C.; Buchwald, S. L. *Chem. Eur. J.* **1999**, *5*, 3107-3112.
(63) Reetz, M. T.; Westermann, E.; Lohmer, R.; Lohmer, G. *Tetrahedron Lett.* **1998**, *39*, 8449-8452.
(64) The reactions of PPh_3 complexes with styrene or acrylates require elevated temperature in the absence of additives and give modest to poor yields of the stilbene or cinnamate products.
(65) Amatore, C.; Carré, E.; Jutand, A.; M'Barki, M. A.; Meyer, G. *Organometallics* **1995**, *14*, 5605-5614.

(66) Dieck, H. A.; Heck, R. F. *J. Am. Chem. Soc.* **1974**, *96*, 1133-1136.
(67) Lee Kyoung, H.; Youngim, N.; Junseong, L.; Youngkyu, D.; Sukbok, C. *Angew. Chem. Int. Ed.* **2005**, *44*, 6166-6169.
(68) Netherton, M. R.; Fu, G. C. *Org. Lett.* **2001**, *3*, 4295-4298.
(69) Consistent with this assertion, the reaction of 1-bromo-4-*N,N*-dimethylaniline with methyl methacrylate catalyzed by the parent complex **30** containing an ammonium, rather than a phosphonium, cation did not form any cinnamate product, even at 100 °C.
(70) In the absence of added halide, rate acceleration by the palladium product $(^{t}Bu_3P)_2Pd(H)(Br)$ was observed and addition of $MeCy_2N$ was necessary to scavenge HBr. The resulting salt ($MeCy_2N \cdot HBr$) subsequently crystallized from solution during the course of the reaction.
(71) No intermediates were observed and the olefin product was formed with a rate constant that was similar to that of the decay of starting complex **32** (k_{obs} = 7.4 x 10^{-5} s^{-1}).
(72) Cabri, W.; Candiani, I.; Bedeschi, A.; Santi, R. *J. Org. Chem.* **1992**, *57*, 3558-3563.
(73) Cabri, W.; Candiani, I.; Bedeschi, A.; Penco, S.; Santi, R. *J. Org. Chem.* **1992**, *57*, 1481-1486.
(74) Andersson, C. M.; Hallberg, A.; Daves Jr., G. D. *J. Org. Chem.* **1987**, *52*, 3529-3536.
(75) Svejda, S. A.; Brookhart, M. *Organometallics* **1998**, *18*, 65-74.
(76) Szabo, M. J.; Jordan, R. F.; Michalak, A.; Piers, W. E.; Weiss, T.; Yang, S.-Y.; Ziegler, T. *Organometallics* **2004**, *23*, 5565-5572.
(77) Mecking, S.; Johnson, L. K.; Wang, L.; Brookhart, M. *J. Am. Chem. Soc.* **1998**, *120*, 888.
(78) Paul, F.; Patt, J.; Hartwig, J. F. *Organometallics* **1995**, *14*, 3030-3039.
(79) Louie, J.; Hartwig, J. F. *Angew. Chem. Int. Ed. Engl.* **1996**, *35*, 2359-2361.
(80) Dai, C.; Fu, G. C. *J. Am. Chem. Soc.* **2001**, *123*, 2719-2724.
(81) Clark, H. C.; Goel, A. B.; Goel, S. *Inorg. Chem.* **1979**, *18*, 2803-2808.
(82) Clark, H. C.; Goel, A. B.; Goel, S. *J. Organomet. Chem.* **1979**, *166*, C29-C32.
(83) Lee, C. T.; Yang, W. T.; Parr, R. G. *Phys. Rev. B: Condes. Matter Mater. Phys.* **1988**, *37*, 785-789.
(84) Becke, A. D. *J. Chem. Phys.* **1993**, *98*, 5648-5652.
(85) Stephens, P. J.; Devlin, F. J.; Chabalowski, C. F.; Frisch, M. J. *J. Phys. Chem. A* **1994**, *98*, 11623-11627.
(86) M. J. Frisch, G. W. T., H. B. Schlegel, G. E. Scuseria, M. A. Robb, J. R. Cheeseman, J. A. Montgomery, Jr., T. Vreven, K. N. Kudin, J. C. Burant, J. M. Millam, S. S. Iyengar, J. Tomasi, V. Barone, B. Mennucci, M. Cossi, G. Scalmani, N. Rega, G. A. Petersson, H. Nakatsuji, M. Hada, M. Ehara, K. Toyota, R. Fukuda, J. Hasegawa, M. Ishida, T. Nakajima, Y. Honda, O. Kitao, H. Nakai, M. Klene, X. Li, J. E. Knox, H. P. Hratchian, J. B. Cross, V. Bakken, C. Adamo, J. Jaramillo, R. Gomperts, R. E. Stratmann, O. Yazyev, A. J. Austin, R. Cammi, C. Pomelli, J. W. Ochterski, P. Y. Ayala, K. Morokuma, G. A. Voth, P. Salvador, J. J. Dannenberg, V. G. Zakrzewski, S. Dapprich, A. D. Daniels, M. C. Strain, O. Farkas, D. K. Malick, A. D. Rabuck, K. Raghavachari, J. B. Foresman, J. V. Ortiz, Q. Cui, A. G. Baboul, S. Clifford, J. Cioslowski, B. B. Stefanov, G. Liu, A. Liashenko, P. Piskorz, I. Komaromi, R. L. Martin, D. J. Fox, T. Keith, M. A. Al-Laham, C. Y. Peng, A. Nanayakkara, M. Challacombe, P. M. W. Gill, B. Johnson, W. Chen, M. W. Wong, C. Gonzalez, and J. A. Pople *Gaussian 03, Revision E.01*; Gaussian, Inc.: Wallingford CT, 2004.

(87) Hay, P. J.; Wadt, W. R. *J. Chem. Phys.* **1985**, *82*, 299-310.
(88) Ditchfiled, R.; Hehre, W.; Pople, J. A. *J. Chem. Phys.* **1971**, *54*, 724-728.
(89) Hariharan, P. C.; Pople, J. A. *Theor. Chim. Acta* **1973**, *28*, 213– 222.

Chapter 5. Distinguishing Between Pathways for Transmetallation in the Suzuki-Miyaura Reaction

---

5.1 Introduction

The Suzuki-Miyaura reaction is one of the most practiced classes of catalytic C-C bond formation. The frequent application of the Suzuki-Miyaura reaction on laboratory and industrial-scale[1] can be attributed to a number of attractive features of this transformation such as: mild reactions conditions that tolerate a wide range of functional groups, access to a large catalog of commercially-available coupling partners, ease of synthesis and stability of organoboron coupling partners, and flexibility in the identity of the leaving group of the electrophile and the ligands on the organoboron compound. Although other cross-coupling reactions continue to be developed in parallel, few can boast all of the advantages of the Suzuki-Miyaura reaction. The extent to which the Suzuki-Miyaura reaction has been embraced as a strategic synthetic disconnect can perhaps be exemplified by the total synthesis of the marine natural product gymnocin A by Sasaki et al.[2-4] The convergent synthesis hinges on the coupling of four complex polycyclic ether fragments through a sequential one-pot hydroboration - Suzuki-Miyaura coupling strategy (Scheme 45). Notably, the first and second coupling sequences utilize two different vinyl electrophiles, but a single catalyst is effective in both cases. The flexibility and mildness of the Suzuki-Miyaura reaction demonstrated in this elegant natural product synthesis that involves the union of complex synthetic intermediates highlights the power of this method.

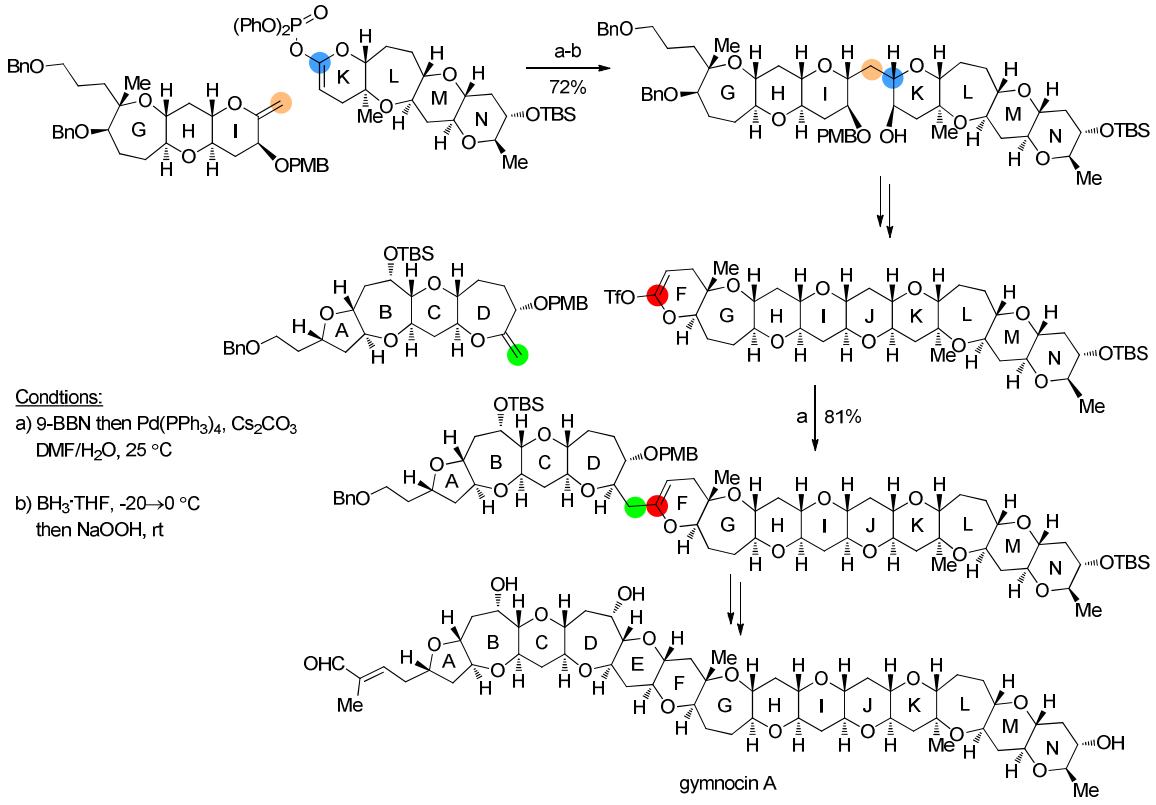

Scheme 45. Suzuki-Miyaura Reaction in the Synthesis of Gymnocin A

Like all cross-coupling reactions, the catalytic cycle of the Suzuki-Miyaura reaction begins by oxidative addition of an organic electrophile to a palladium(0) complex and is completed by bond-forming reductive elimination. These two fundamental steps of catalysis have been addressed in previous chapters. The mechanism of the intermediate step of the catalytic cycle, transmetallation, is unique to each class of cross-coupling reaction. Despite the widespread use of the Suzuki-Miyaura reaction in synthetic chemistry, significant efforts expended to understand the mechanism of transmetallation have yet to reveal many important details about this step. Future innovations in the Suzuki-Miyaura reaction would be facilitated by a more complete understanding of the mechanism of transmetallation. Comparison to mechanisms proposed for transmetallation

in other recently-developed transition metal-catalyzed reactions involving organoboron reagents such as rhodium-catalyzed 1,4-additions of arylboron reagents to conjugated carbonyl compounds and copper-catalyzed C-N and C-O cross-coupling reactions would also be possible with this knowledge.[5-7]

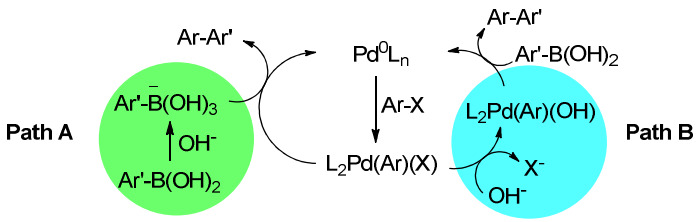

Scheme 46. Catalytic Cycle of the Suzuki-Miyaura Reaction

Two pathways are typically considered for transmetallation in the Suzuki-Miyaura reaction: conversion of an organoboron compound by base to form a nucleophilic boronate, followed by attack on a palladium halide complex (Scheme 46, Path A) or conversion of a palladium halide to a nucleophilic palladium hydroxo complex that subsequently reacts with a neutral organoboron compound (Scheme 46, Path B).[8] A number of studies have led to the conclusion that transmetallation occurs between the palladium halide and boronate,[9-15] but others have suggested that transmetallation occurs between the boronic acid and palladium hydroxo species.[16-20] Because transmetallation is often considered to be turnover-limiting and to dictate the choice of reaction conditions, a firm understanding of the mechanism of this step is important for the use of this common catalytic process.

5.2 Results and Discussion

5.2.1 Reactions of Isolated Arylpalladium Hydroxo and Halide Complexes with Arylboronic Acids and Aryltrihydroxyborates.

A systematic study involving the reactions of isolated arylpalladium hydroxo complexes and arylpalladium halide complexes containing the same ancillary ligands with arylboronic acids and aryltrihydroxyborates has been conducted. Quantitative information on the rates of reaction of boronic acids and trihydroxyborates with palladium hydroxide and halide complexes containing PPh_3 and PCy_3 as ligands and equilibrium constants for the interconversion of palladium hydroxide and halide complexes have been gained. These data provide strong evidence that, in the typical mixtures of water and organic solvent, transmetallation involving a palladium center that is ligated by two phosphine ligands occurs between the palladium hydroxo complex and a boronic acid, not between the palladium halide complex and a trihydroxyborate, as often proposed.

Our experimental design to assess the different proposed pathways focused on comparing the relative rates of the different stoichiometric reactions of isolated arylpalladium complexes and arylboron species. We studied the stoichiometric reaction of an isolated arylpalladium halide complex and trihydroxyborate in one case and an isolated arylpalladium hydroxo complex and boronic acid in the other. For this design, stable, arylpalladium hydroxo and halide complexes containing the same phosphine ligand were needed. The dimeric $[(Ph_3P)Pd(Ph)(\mu\text{-}OH)]_2$ (**37**) and $(Ph_3P)_2Pd(Ph)(X)$ (X = I, Br, and Cl) are isolable and were chosen for this study. Additionally, the monomeric

$(Cy_3P)_2Pd(Ph)(OH)$ (**41**) and $(Cy_3P)_2Pd(Ph)(X)$ (X = I, Br, and Cl)[21-25] are also isolable and were used in conjunction with complexes ligated by PPh_3. Catalysts containing either of these phosphine ligands are frequently used for Suzuki-Miyaura reactions. Alkali salts of aryltrihydroxyborates were found to be soluble in organic solvents in the presence of crown ether and were the boronates we used for this study.[26]

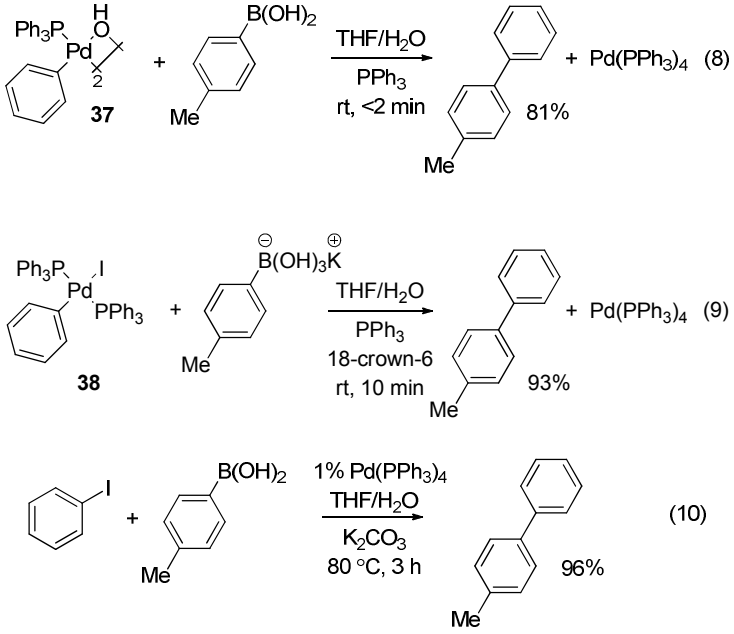

The reaction of hydroxo complex **37** with *p*-tolylboronic acid (Eq 8) at room temperature without base formed 4-methylbiphenyl within minutes in high yield (81%)[27] from transmetallation and reductive elimination.[28,29-30] Similarly, the reaction of $(Ph_3P)_2Pd(Ph)(I)$ (**38**) with potassium *p*-tolyltrihydroxyborate at room temperature formed 4-methylbiphenyl rapidly within minutes in high yield (Eq 9). The reaction of PhI with *p*-tolylboronic acid catalyzed by $Pd(PPh_3)_4$ occurred in 96% yield over 3 h at 80 °C (Eq 10).

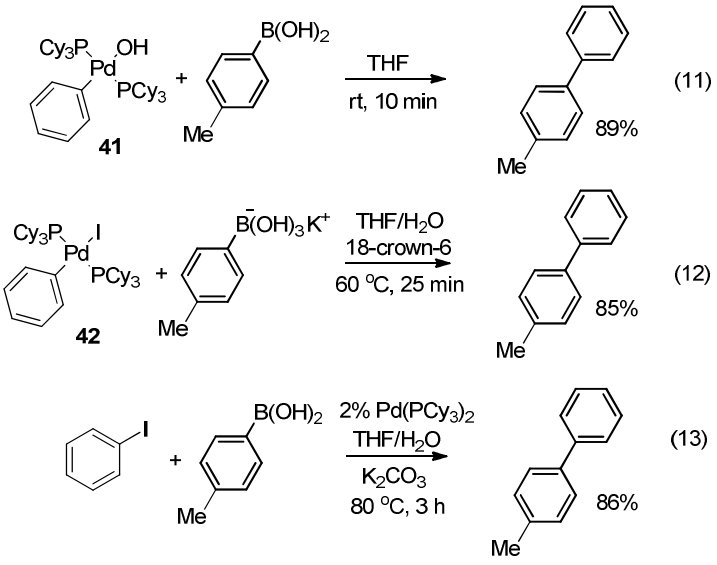

The reaction of hydroxo complex **41** with *p*-tolylboronic acid (Eq 11) at room temperature formed 4-methylbiphenyl from the combination of transmetallation and reductive elimination rapidly and in high yield (89%) in the absence of any additives. The reaction of $(Cy_3P)_2Pd(Ph)(I)$ (**42**) at 60 °C formed 4-methylbiphenyl rapidly in high yield (Eq 12). The reaction of PhI with $PhB(OH)_2$ catalyzed by $Pd(PCy_3)_2$ occurred in 86% yield over 3 h at 80 °C (Eq 13). Thus, both sets of stoichiometric reactions are much faster than the catalytic process and, therefore, could be the transmetallation step on the catalytic cycle for catalysts containing either PPh_3 or PCy_3 ligands.

The relative contribution of Path A and Path B to the transmetallation sequence in the catalytic reaction is dictated by the relative concentrations of the palladium halide and hydroxide, the relative concentrations of boronic acid and trihydroxyborate, and the relative rate constants for the two stoichiometric reactions of palladium halide and boronate and of palladium hydroxide and boronic acid (Scheme 47). The pathway with the largest product of the rate constant, concentration of palladium complex, and boron

reagent would be the one by which transmetallation occurs. Thus, we studied the interconversion of palladium hydroxo and halide complexes under aqueous conditions common to the catalytic Suzuki-Miyaura reaction, the equilibrium between boronic acid and trihydroxyborate, and the rate constants for the two stoichiometric reactions.

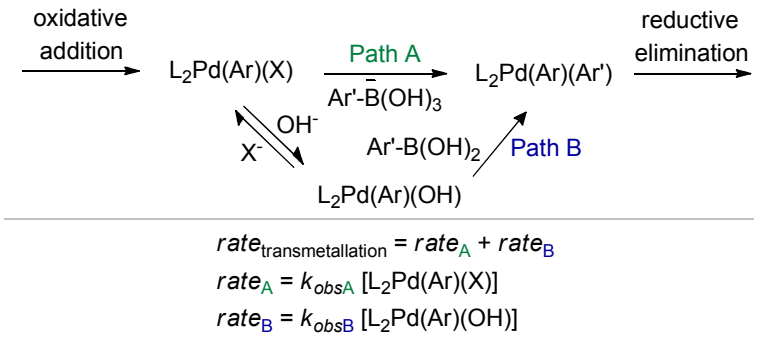

Scheme 47. Mechanisms of Transmetallation

5.2.2 Studies of Equilibriums Between Palladium Complexes and Equilibriums Between Organoboron Compounds.

The combination of 4-fluorophenylboronic acid (0.060 M) and the weak base potassium carbonate (0.03-0.15 M) typically used in Suzuki-Miyaura reactions (Eq 14) formed a mixture of boronic acid and trihydroxyborate, as determined by ^{11}B and ^{19}F NMR spectroscopy at room temperature in a 1:1 mixture of acetone and water.[31,32] The equilibrium between boronic acid and trihydroxyborate occurred on the NMR time scale, as evidenced by a single resonance at a chemical shift between that of the boronic acid and trihydroxyborate. From the observed chemical shift and the known chemical shifts of the boronic acid and trihydroxyborate, the ratio of boronic acid to trihydroxyborate could be determined. This ratio varied from 1:1 to 1:3 when the concentration of base was

increased from 0.03-0.15 M. Thus, the concentrations of boronic acid and trihydroxyborate are similar to each other in a medium containing weak base and water.

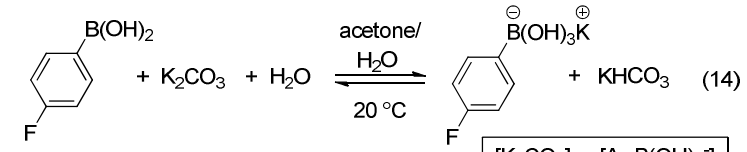

$[Ar\text{-}B(OH)_2]_o$ = 0.060 M

$[K_2CO_3]_o$	$[Ar\text{-}B(OH)_3^-]$
0.15 M	0.043 M
0.10 M	0.040 M
0.03 M	0.030 M

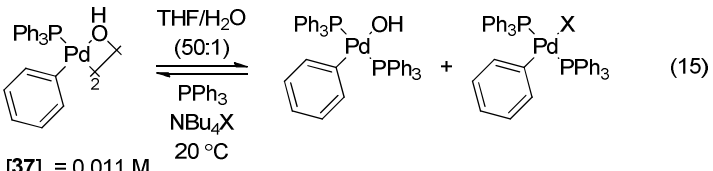

$[\mathbf{37}]_o$ = 0.011 M

X=	[**37**]	$[L_2Pd(Ph)(OH)]$	$[L_2Pd(Ph)(X)]$
I (**38**)	0.0049 M	0.0028 M	0.0032 M
Br (**39**)	0.0043 M	0.0038 M	0.0028 M
Cl (**40**)	0.0032 M	0.0045 M	0.0031 M

Our studies on the equilibriums between palladium hydroxo and halide complexes ligated by PPh_3 are summarized in Eq 15. The exchange of the halide in tetraalkylammonium halide salts (0.043 M) with the hydroxide in complex **37** (0.011 M) in aqueous THF (25:1) occurred upon mixing at room temperature, as determined by ^{31}P NMR spectroscopy (Eq 15). Equilibration was complete in the time required for acquisition of the ^{31}P NMR spectrum (<5 min). In addition to the formation of the corresponding aryl halide complex $(Ph_3P)_2Pd(Ph)(X)$ (X = I, Br, or Cl), monomeric $(Ph_3P)_2Pd(Ph)(OH)$ was detected.[22] The concentration of aryl halide complex was small (0.0028-0.0032 M), relative to the combined concentration of the dimeric and monomeric palladium hydroxo complexes (0.0077-0.0081 M) and appeared to be insensitive to the identity of the halide.

Direct comparison of the relative stabilities of hydroxo and halide complexes ligated by PPh_3 is complicated by the concurrent equilibrium between the monomeric and dimeric forms of the hydroxo complex. Thus, we also examined the equilibrium between the hydroxo and halide complexes for the related series of complexes ligated by PCy_3, which are both monomers.[21-25]

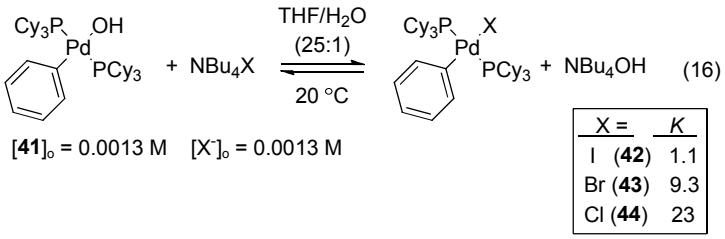

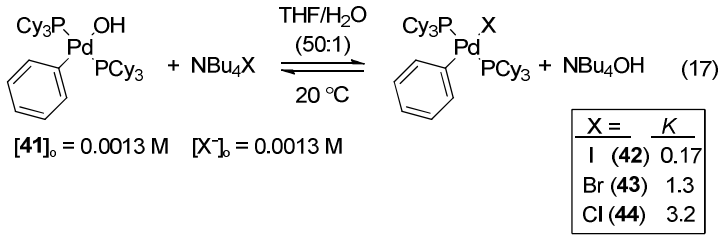

Equilibrium between PCy_3-ligated hydroxo and halide complexes are summarized in Eq 16 and Eq 17. In a 25:1 mixture of THF/H_2O the equilibrium constant for formation of $(Cy_3P)_2Pd(Ph)(I)$ (**42**) from the combination of $(Cy_3P)_2Pd(Ph)(OH)$ (**41**) (0.013 M) and tetrabutylammonium iodide (0.013 M) is approximately unity (K = 1.1) at 20 °C. Palladium bromide **43** and chloride **44** are more stable than iodide **42** (K = 9.3 and 23, respectively) (Eq 16), but the equilibrium constants are still small. In a similar medium containing less water (THF:water = 50:1), the equilibrium mixture of hydroxo **41** and each of the halide complexes (**42-44**) again contained substantial amounts of both halide and hydroxide complexes (Eq 17), but the concentration of hydroxide **41** increased in all

cases relative to the amount present in the 25:1 mixture of THF and H_2O. Presumably, the increased population of hydroxo complex at lower [H_2O] results from the decreased hydration of free hydroxide ions. From these data, we conclude that the concentration of palladium halide complex is higher than the concentration of palladium hydroxide complex in catalytic Suzuki-Miyaura reactions conducted with aqueous solvent mixtures, but that the populations of the palladium hydroxo and halide complexes in Eq 15-17 differ by less than an order of magnitude.

5.2.3 Comparison of the Rates of Reaction of Palladium Hydroxide with Boronic Acid and Palladium Halide Complexes with Trihydroxyborate

The observed rate constants for the reaction of hydroxide **37** with boronic acid and halide **39** with trihydroxyborate in a 50:1 mixture of THF/H_2O were measured by ^{31}P NMR spectroscopy. The reaction of **37** (0.015 M) with *p*-tolylboronic acid (0.15 M) in the presence of PPh_3 (0.15 M) was monitored (Fig 37) at -40 $^{\circ}C$ and occurred with an observed rate constant of 2.4 x 10^{-3} s^{-1}. An intermediate (δ 20.1 ppm) was detected as the initial product, which decays to biaryl and $Pd(PPh_3)_4$ upon warming. Spectrocopic characterization of the intermediate is complicated by the presence of excess reagents, but potential structures for the intermediate are proposed (vide infra) resulting from either the formation of a stable adduct of the hydroxide complex and boronic acid or β-elimination from the palladium boronate to form a stable *trans*-bis-aryl complex.[6]

In contrast to the fast reaction of palladium hydroxide **37** with *p*-tolylboronic acid at -40 °C, no reaction was observed between halide complex **39** and potassium *p*-

tolyltrihydroxyborate (0.15 M) in the presence of PPh_3 (0.03 M) and 18-crown-6 at -30 °C over the same period of time (Fig 37). In fact, less than 10% conversion of **39** occurred, even after 11 h. These data indicate that the rate constant for reaction of hydroxo complex **37** with boronic acid is much larger than that for reaction of halide complex **39** with trihydroxyborate.

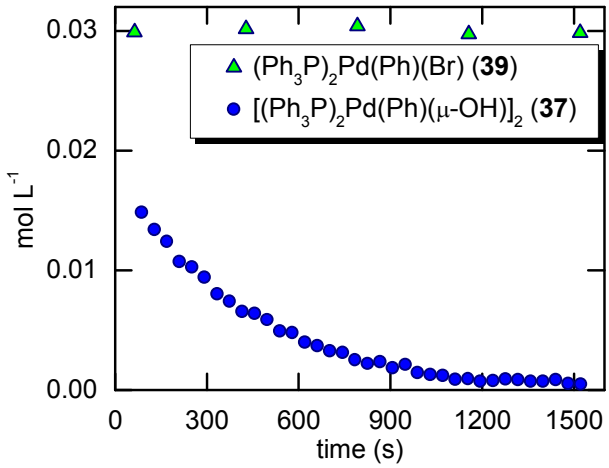

Figure 37. Decay of **37** (0.015 M) in the presence of *p*-tolylboronic acid (0.15 M) and PPh_3 (0.15 M) at -40 °C, and decay of **39** (0.030 M) in the presence of potassium *p*-tolyltrihydroxyborate (0.15 M), PPh_3 (0.03 M), and 18-crown-6 in THF/H_2O (50:1) at -30 °C as monitored by ^{31}P NMR spectroscopy.

The rate constant for reaction of halide complex **39** with *p*-tolyltrihydroxyborate at the -40 °C temperature of the reaction of hydroxo **37** with boronic acid was calculated from activation parameters for the reaction of **39** with trihydroxyborate (Fig 38). The estimated rate constant at -40 °C from these data is 1.7×10^{-7} s^{-1}. This rate constant is smaller than that for the reaction of hydroxo complex **37** with boronic acid at the same temperature by a factor of ca 1.4×10^4. Because the populations of hydroxo and halide complexes are similar and substantial amounts of boronic acid exist in media containing a

mixture of organic solvent and water, this large difference in rate constant implies that the reaction of hydroxo complex **37** with boronic acid is the pathway that accounts for transmetallation in the catalytic Suzuki-Miyaura reaction. In fact, this large difference implies that the reaction would occur through the hydroxo complex, even under conditions that would generate low concentrations of hydroxo complex **37** relative to halide complexes **38-40**.

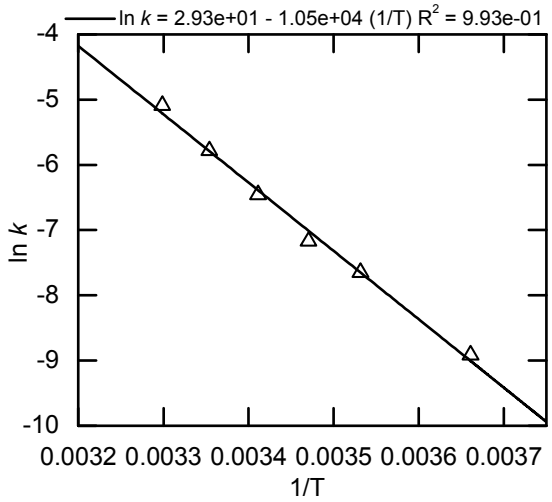

Figure 38. Arrhenius plot for the reaction of **39** (0.030 M) in the presence of potassium *p*-tolyltrihydroxyborate (0.15 M), PPh_3 (0.15 M), and 18-crown-6 in THF/H_2O (50:1) at 0-30 °C as monitored by ^{31}P NMR spectroscopy.

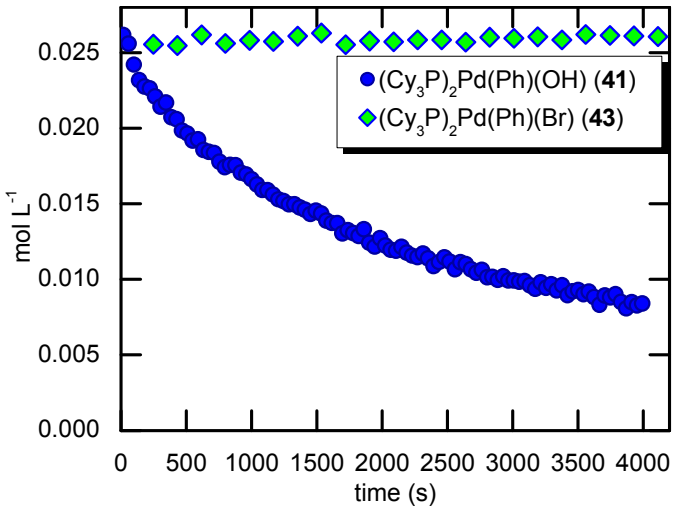

Figure 39. Decay of **41** (0.026 M) in the presence of *p*-tolylboronic acid (0.13 M) and PCy_3 (0.077 M), and decay of **43** (0.026 M) in the presence of potassium *p*-tolyltrihydroxyborate (0.13 M), PCy_3 (0.077 M), and 18-crown-6 in THF/H_2O (50:1) at -20 ^oC as monitored by ^{31}P NMR spectroscopy.

The kinetic behavior of the analogous series of palladium complexes ligated by PCy_3 was also examined. The reaction of $(Cy_3P)_2Pd(Ph)(OH)$ (**41**) (0.026 M) with *p*-tolylboronic acid (0.13 M) in the presence of PCy_3 (0.077 M) was monitored by ^{31}P NMR spectroscopy (Fig 39) at -20 ^oC and occurred with an observed rate constant of 6.4 x 10^{-4} s^{-1}.[33] In contrast, no conversion was observed during the reaction of halide complex **43** with potassium *p*-tolyltrihydroxyborate (0.13 M) in the presence of PCy_3 (0.077 M) and 18-crown-6 at -20 ^oC over the same period of time (Fig 39). In fact, less than 10% conversion of **43** occurred even after 2 days at room temperature. These data indicate that the reaction of hydroxo complex **41** with boronic acid is much faster than that of halide complex **43** with trihydroxyborate, analogous to the trends observed for complexes ligated by PPh_3.

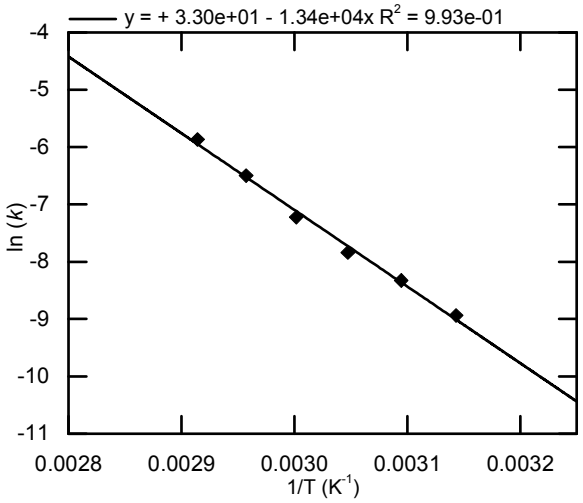

Figure 40. Arrhenius plot for the decay of **43** (0.026 M) in the presence of potassium *p*-tolyltrihydroxyborate (0.13 M), PCy_3 (0.13 M), and 18-crown-6 in THF/H_2O (50:1) from 45-70 °C as monitored by ^{31}P NMR spectroscopy.

The rate constant for reaction of halide complex **43** with *p*-tolyltrihydroxyborate was subsequently calculated by extrapolation of k_{obs} from an Arrhenius plot to -20 ^oC for the reaction of **43** with trihydroxyborate (Fig 40). The estimated rate constant at -20 ^oC from this plot (k_{obs} = 2.5 x 10^{-9} s^{-1}) is smaller by a factor of ca 2.5 x 10^5 than that for the reaction of hydroxo complex **41** with boronic acid at the same temperature. These data provide evidence that transmetallation also occurs in aqueous solvent mixtures by the reaction of palladium hydroxide with a neutral boronic acid for complexes ligated by PCy_3. In fact, the difference between the rate constants for the two stoichiometric reactions of complexes ligated by PCy_3 is larger by a factor of 17 than for complexes ligated by PPh_3.

5.2.4 Reactions of Palladium Hydroxide with Arylboronic Esters

The reaction of hydroxo complex **37** with arylboronic esters was also monitored by ^{31}P NMR spectroscopy. The reaction of **37** with catechol and neopentyl glycol esters of 4-fluorophenylboronic acid at -55 °C occurred with rates that were similar to that of the reaction of **37** with free boronic acid (Scheme 48). Formation of 4-fluorobiphenyl was observed by ^{19}F NMR spectroscopy upon warming to room temperature. The more sterically hindered 4-fluorophenylboronic acid pinacol ester also reacted with hydroxo complex **37** at -55 °C, albeit more slowly (>95% conversion after 1.5 h) than did the catechol and neopentyl glycol analogs. Thus, the reaction of **37** with all four neutral arylboron compounds occurs faster than the combination of halide complex **39** and trihydroxyborate. No reaction occurs between the latter combination over the same period of time, even at -30 °C. Assuming the borate analogs of the boronic esters do not react faster than the trihydroxyborates, these data suggest that transmetallation during Suzuki-Miyaura coupling of boronic esters also occurs by reaction of the neutral boron species with the palladium hydroxide (Path B).

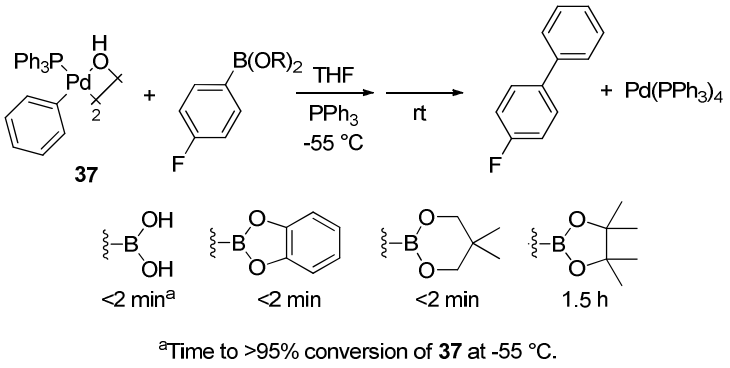

Scheme 48. Reaction of **37** with Arylboronic Esters

5.2.5 Competition Experiments of Electronically and Sterically-Distinct Arylboron Compounds

As an additional probe to assess whether the reaction of palladium hydroxide with boronic acid or palladium halide with trihydroxyborate is followed in the catalytic system, we compared the distribution of biaryl products from catalytic and stoichiometric reactions involving a set of arylboronic acids and their borate analogues. If one of the stoichiometric reactions forms a different ratio of products from the catalytic process, then it can then be ruled out as a step on the catalytic cycle. A similar strategy was recently followed to discriminate potential intermediates for olefin insertion in the Mizoroki-Heck reaction.[34]

The first series of competition experiments focused on the reaction of iodobenzene with two electronically-distinct boronic acids catalyzed by $Pd(PCy_3)_2$ (Scheme 49). The distribution of biaryl products in these reactions varied depending on the pH of the reaction medium. In the case of the weak base potassium carbonate, the two biaryl products were formed in roughly equimolar amounts (Scheme 49, entry 1). However, when potassium hydroxide was used as base the selectivity favored reaction with the electron-rich substrate (Scheme 49, entries 2-3).

We attribute the pH dependence on the observed selectivity to differences in the relative populations of the boronic acid and trihydroxyborates in solution for each substrate. Under weak base conditions the electron poor boronic acid would be expected to coordinate hydroxide preferentially because it is a stronger Lewis acid. Conversely, under strong base conditions all the boronic acid is converted to the trihydroxyborate.

Comparison of the selectivities across a range of solution pH is thus complicated by the inequivalent populations of the boronic acid and trihydroxyborate states for the two substrates.

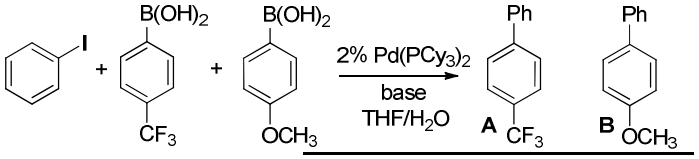

	Base	Temp.	Yield[a]	A:B
1.	K_2CO_3[b]	60 °C	98%	55:45
2.	KOH[c]	60 °C	99%	38:62
3.	KOH[d]	60 °C	100%	12:88

[a]Determined by GC versus *n*-tetradecane as internal standard. [b]2.5 equiv. [c]5 equiv. [d]10 equiv.

Scheme 49. Catalytic Suzuki-Miyaura Reactions of Electronically-Distinct Boronic Acids

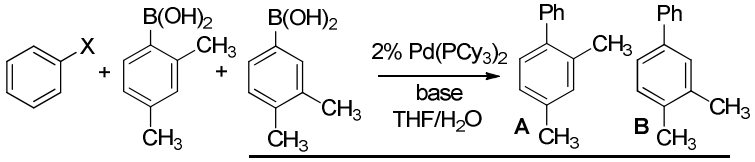

	X=	Base	Temp.	Yield[a]	A:B
1.	I	K_2CO_3[b]	60 °C	95%	94:6
2.	Br	K_2CO_3[b]	60 °C	93%	93:7
3.[d]	Cl	K_2CO_3[b]	80 °C	93%	90:10
4.	I	KOH[c]	rt	95%	95:5

[a]Determined by GC versus *n*-tetradecane as internal standard. [b]2.5 equiv. [c]11 equiv. [d]5% $Pd(PCy_3)_2$.

Scheme 50. Catalytic Suzuki-Miyaura Reactions of Sterically-Distinct Boronic Acids

A competition of sterically-distinct arylboronic acids was proposed to alleviate the shortcomings of the electronic competition experiments because the electronic properties of sterically-distinct constitutional isomers is expected to be similar. Thus, we conducted coupling reactions of iodo-, bromo-, and chlorobenzene with 3,4-dimethylphenylboronic acid and 2,4-dimethylphenylboronic acid catalyzed by $Pd(PCy_3)_2$. These reactions gave similar biaryl product distributions (Scheme 50); in all cases 2,4-dimethylbiphenyl was

the major product, and a similar selectivity was observed from reactions conducted with either weak or strong base. The lack of pH dependence for this pair of arylboron reagents is attributed to the similar electronic properties of the two substrates resulting in similar populations of the boronic acid and trihydroxyborate forms.

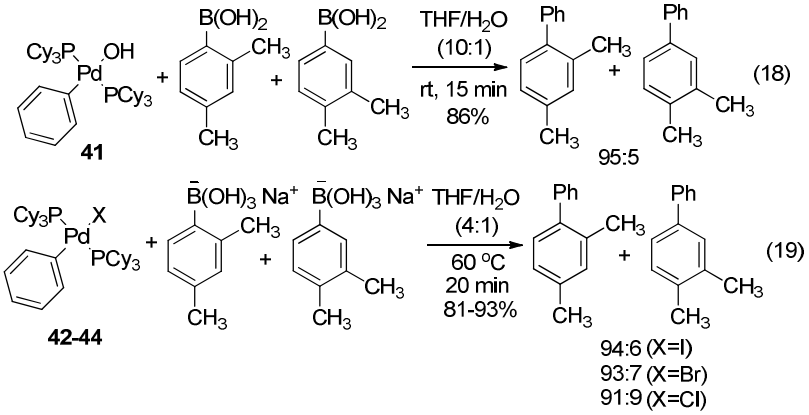

The reaction of palladium hydroxide **41** with the same arylboronic acids (Eq 18) formed a distribution of biaryls similar to those observed in the catalytic reactions. The reactions of the preformed sodium trihydroxyborates with palladium halide complexes (Eq 19) also formed a ratio of biaryl products that was indistinguishable from the corresponding catalytic reactions.

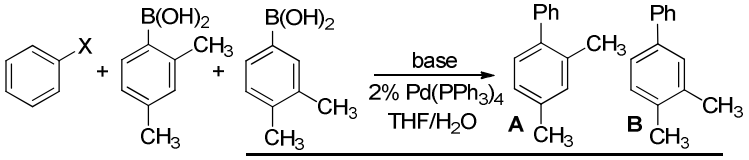

	X=	Base	Temp.	Yield[a]	A:B
1.	I	K_2CO_3[b]	60 °C	98%	93:7
2.	Br	K_2CO_3[b]	60 °C	88%	93:7

[a]Determined by GC versus *n*-tetradecane as internal standard. [b]2.5 equiv.

Scheme 51. Catalytic Suzuki-Miyaura Reactions Catalyzed by $Pd(PPh_3)_4$

Coupling reactions of iodo- and bromobenzene with 3,4-dimethylphenylboronic acid and 2,4-dimethylphenylboronic acid catalyzed by $Pd(PPh_3)_4$ were also examined. These reactions also gave similar biaryl product distributions in the presence of the weak base potassium carbonate in aqueous THF mixtures (Scheme 51); in all cases 2,4-dimethylbiphenyl was the major product.

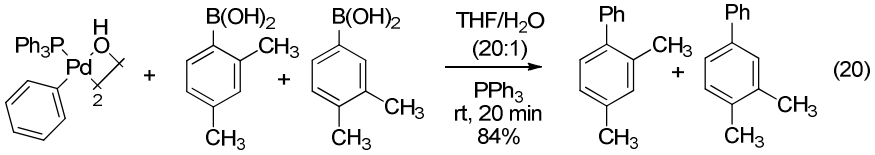

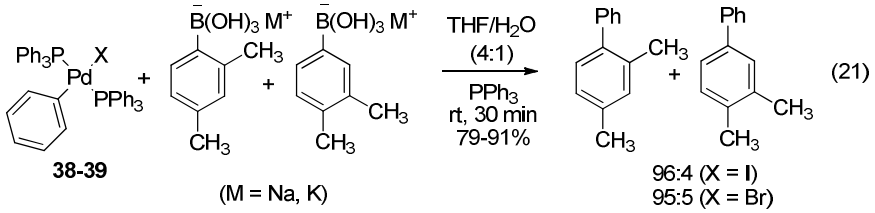

Similar to reactions of complexes ligated by PCy_3, the reaction of palladium hydroxide **37** with the same arylboronic acids (Eq 20) formed a distribution of biaryls similar to those observed in the catalytic reactions. The reactions of the preformed sodium trihydroxyborates with palladium halide complexes (Eq 21) also formed a ratio of biaryl products that was indistinguishable from the corresponding catalytic reactions. Because the distribution of biaryl products in the competition experiments involving electronically-distinct boronic acids have been shown to be sensitive to the pH of the medium or even the identity of the halide (Scheme 49 and Scheme 50), stoichiometric transmetallation reactions that proceed through different intermediates would be expected to form dissimilar product distributions. However, the reactions of palladium halide complexes with trihydroxyborates and the reactions of palladium hydroxide complexes

with boronic acids all formed product distributions that were similar to the corresponding catalytic reactions. We conclude that these similarities signify that the two stoichiometric reactions proceed through a common intermediate. The reaction of hydroxo complexes with boronic acid have been shown to occur much faster than reaction of halide complexes with trihydroxyborate (vide supra). Thus, the common intermediate among these competition reactions could be the palladium hydroxide complex. Additional experiments to probe this mechanistic proposal are discussed in the following sections.

5.2.6 Kinetic Studies of Reactions of Palladium Halide Complexes and Trihydroxyborates

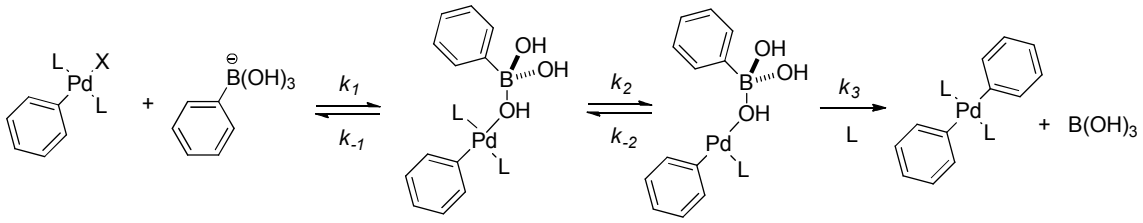

$$rate = k_{obs}\,[L_2Pd(Ar)(X)]$$

$$k_{obs} = K_1K_2k_3 \cdot \frac{[Ar\text{-}\overset{\ominus}{B}(OH)_3]}{[X^-]\,[L]}$$

Scheme 52. Possible Mechanism for Transmetallation

A mechanism for transmetallation of an aryltrihydroxyborate with a palladium halide complex that has been proposed in computational studies is shown in Scheme 52.[9,35] The mechanism proceeds by nucleophilic displacement of halide by borate followed by dissociation of phosphine, and finally β-elimination transfers the organic ligand to palladium. If β-elimination is the first irreversible step of this sequence, the rate of the reaction should occur with a first-order dependence on the concentration of palladium complex and trihydroxyborate and with an inverse dependence on the concentration of

halide and ligand. To investigate this proposed mechanism empirically, we conducted kinetic studies of the reactions of isolated palladium halide complex **39** with aryltrihydroxyborates.

The dependence of the rate of reaction for the combination of halide complex **39** and potassium *p*-tolyltrihydroxyborate on the concentration of borate, ligand, and added halide are shown in Figures 41-43. The rate of this reaction occurs with a first-order dependence on the concentration of trihydroxyborate, an inverse dependence on the concentration of free phosphine, and an apparent zeroth-order dependence on the concentration of added bromide.

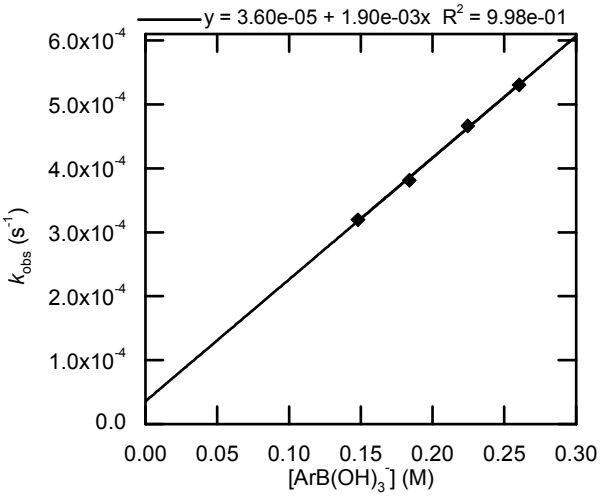

Figure 41. Dependence of k_{obs} on the concentration of potassium *p*-tolyltrihydroxyborate (0.15-0.25 M) for the reaction of **39** (0.030 M) and potassium *p*-tolyltrihydroxyborate in the presence of PPh_3 (0.30 M) and 18-crown-6 in THF/H_2O (50:1) at 10 °C as monitored by ^{31}P NMR spectroscopy.

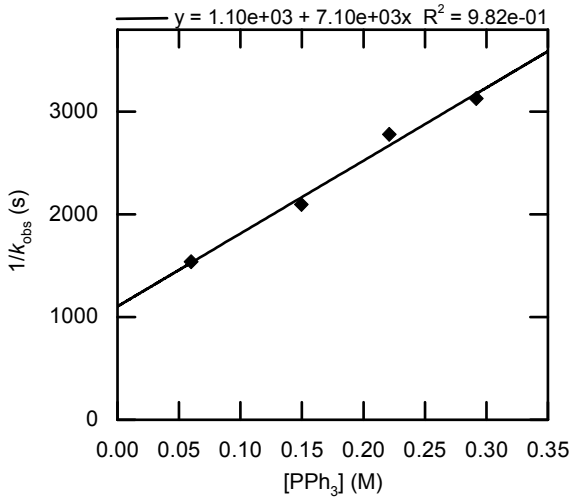

Figure 42. Dependence of k_{obs} on the concentration of PPh_3 (0.06-0.30 M) for the reaction of **39** (0.030 M) and potassium *p*-tolyltrihydroxyborate (0.15 M) in the presence of 18-crown-6 in THF/H_2O (50:1) at 10 °C as monitored by ^{31}P NMR spectroscopy.

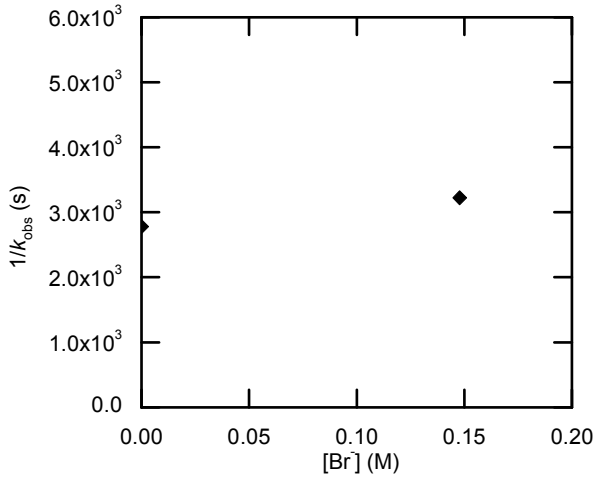

Figure 43. Dependence of k_{obs} on the concentration of $N(heptyl)_4Br$ (0-0.15 M) for the reaction of **39** (0.030 M) and potassium *p*-tolyltrihydroxyborate (0.15 M) in the presence of PPh_3 (0.22 M) and 18-crown-6 in THF/H_2O (50:1) at 10 °C as monitored by ^{31}P NMR spectroscopy.

If reversible displacement of halide on complex **39** by borate preceded β-elimination of the aryl group, the reaction should display an inverse dependence on the concentration of added halide. Because a dependence on the concentration of added halide is not

observed but an inverse dependence on the concentration of phosphine is observed, an alternative mechanism for transmetallation must be operative during the reaction of a palladium halide complex and trihydroxyborate other than the mechanism shown in Scheme 49. It is possible that halide salt could be tight ion paired in these aqueous THF mixtures, which could lead to slow equilibration. However, this possibility seems unlikely considering the fast equilibrium observed for interchange of palladium halide and hydroxide complexes under similar conditions (see Section 5.2.2). An alternative mechanism for the transmetallation during reactions of trihydroxyborates with palladium halide complexes is discussed in Section 5.2.7.

5.2.7 Alternative Mechanism of Transmetallation of Trihydroxyborates Deduced from Kinetic Studies

The reaction of halide complex **43** (0.026 M) with potassium *p*-tolyltrihydroxyborate (0.13 M) in the presence of PCy_3 (0.052 M) and 18-crown-6 in THF/H_2O at 20 °C was monitored by ^{31}P NMR spectroscopy. This reaction is slow at room temperature, and formation of hydroxo complex **41** was observed from the combination of halide complex **43** and trihydroxyborates (Fig 44). The relative population of the halide and hydroxide complexes (11:1) was determined by the integrations of their respective ^{31}P NMR resonances. We hypothesize that hydroxide dissociates from the trihydroxyborate and exchanges with the halide in complex **43** to generate the hydroxo complex **41**.

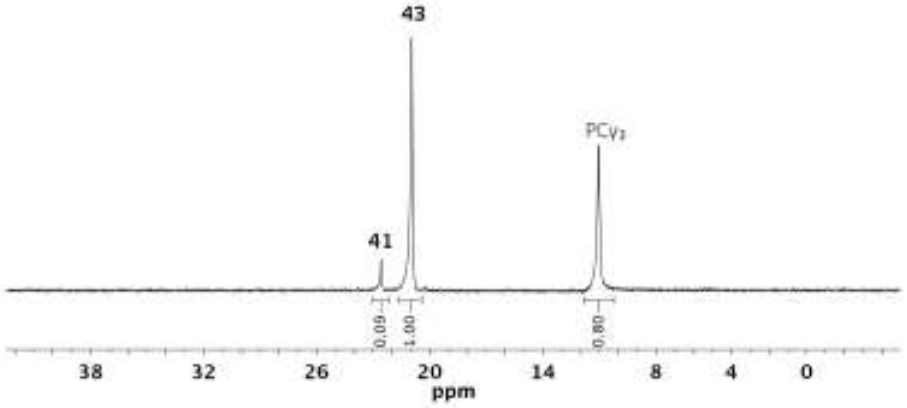

Figure 44. ^{31}P NMR spectrum for the reaction of halide complex **43** (0.026 M) with potassium *p*-tolyltrihydroxyborate (0.13 M) in the presence of PCy_3 (0.052 M) and 18-crown-6 in THF/H_2O at 20 °C.

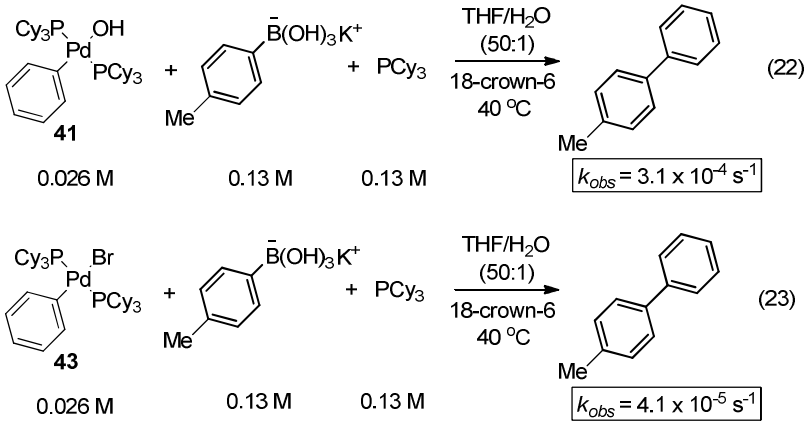

Because hydroxide **41** and halide **43** both exist in solution from the combination of **43** and trihydroxyborate in aqueous THF, we examined the rate of reaction of hydroxide **41** with trihydroxyborate to determine the rate of this reaction compared to that of halide complex **43** and trihydroxyborate under the same conditions. The reaction of hydroxide **41** (0.026 M) with potassium *p*-tolyltrihydroxyborate (0.13 M) in the presence of PCy_3 (0.13 M) was monitored by ^{31}P NMR spectroscopy at 40 ^{o}C and occurred with an observed rate constant of 3.1 x 10^{-4} s^{-1} (Eq 22). The reaction of halide **43** (0.026 M) with potassium *p*-tolyltrihydroxyborate (0.13 M) in the presence of PCy_3 (0.13 M) was also

monitored by ^{31}P NMR spectroscopy at 40 ^{o}C and occurred with an observed rate constant of 4.1 x 10^{-5} s^{-1} (Eq 23). The later reaction was slower than reaction of hydroxide **41** with trihydroxyborate by a factor of ca. 8, indicating that the hydroxo pathway for transmetallation (Path B) could still be faster than Path A under catalytic conditions utilizing strong base that converts boronic acid completely to trihydroxyborate.

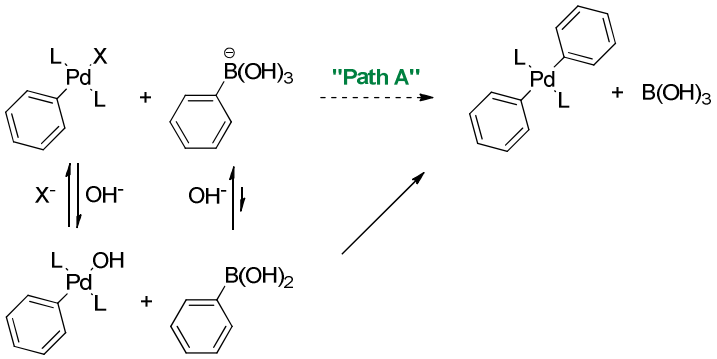

Scheme 53. Alternative Mechanism for Transmetallation

Additionally, the kinetic studies described in this section also suggest an alternative mechanism for transmetallation during the reaction of a palladium halide complex with trihydroxyborate. The Path A mechanism of transmetallation could potentially proceed through a Path B type mechanism shown in Scheme 53 because: palladium hydroxide is generated reversibly from the combination of palladium halide and trihydroxyborate, hydroxide can dissociate from trihydroxyborate to generate a low concentration of free boronic acid, the rate constant for the reaction of palladium hydroxide with boronic acid was shown to be orders of magnitude larger than for the reaction of palladium halide with trihydroxyborate, and steric competition studies suggest that both classes of stoichiometric reactions proceed through a common intermediate.

5.2.8 Kinetic Studies of Reactions of Palladium Hydroxide Complexes and Boronic Acids

Kinetic studies of the reaction of hydroxo complex **37** with arylboronic acid were also conducted to explore potential mechanisms of transfer of the organic ligand from boron to palladium. In all cases, the decay of dimeric **37** occurs by a first-order exponential decay, not by an half-order exponential decay. The dependence of k_{obs} on the concentration of free phosphine or boronic acid, as monitored by ^{31}P NMR spectroscopy, is shown in Eq 24 and Eq 25. The reaction of hydroxide **37** with *p*-tolylboronic acid and PPh_3 in THF/H_2O (50:1) at -40 °C appears to occur with a first-order dependence on the concentration of added ligand and a first-order dependence on the concentration of boronic acid. The reaction of **37** with boronic acid at -40 °C initially forms an unknown palladium complex (δ 20.1 ppm), postulated to be a palladium boronate. The first-order dependence of this reaction on free phosphine may arise from initial coordination of phosphine that breaks a bridging hydroxide ligand in the dimeric complex **37** prior to reaction with boronic acid.

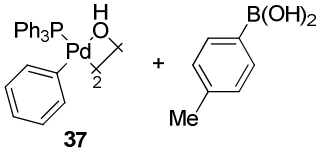

[PPh_3] (M)	k_{obs} (s^{-1})
0.15	2.4 x 10^{-3}
0.30	5.9 x 10^{-3}

(24)

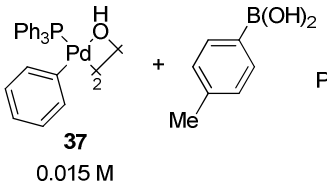

[Ar-$B(OH)_2$] (M)	k_{obs} (s^{-1})
0.09	1.1 x 10^{-3}
0.15	2.4 x 10^{-3}

(25)

The decay of the intermediate complex (δ 20.1 ppm), formed by initial reaction of hydroxide **37** with *p*-tolylboronic acid at -40 °C, was monitored at -15 °C by ^{31}P NMR

spectroscopy (Fig 45). The disappearance of the intermediate complex occurred by a distinctive sigmoidal decay, indicative of an autocatalytic process. This decay was slower in the presence of higher concentrations of free phosphine. If the intermediate is a palladium-boronate, β-elimination from this species could occur by initial reversible dissociation of phosphine from palladium. If this mechanism is operative, the observed autocatalytic decay of the intermediate may be due to a decrease in the concentration of free phosphine over time due to scavenging by $Pd^0(PPh_3)_2$, followed by precipitation of $Pd(PPh_3)_4$ from solution.[36] Kinetic experiments conducted with large excess of phosphine that would quench the autocatalysis are needed to gain quantitative data for the dependence of the rate of decay of the intermediate on the concentration of phosphine. Studies aimed at identification of the intermediate complex are described in Section 5.2.9.

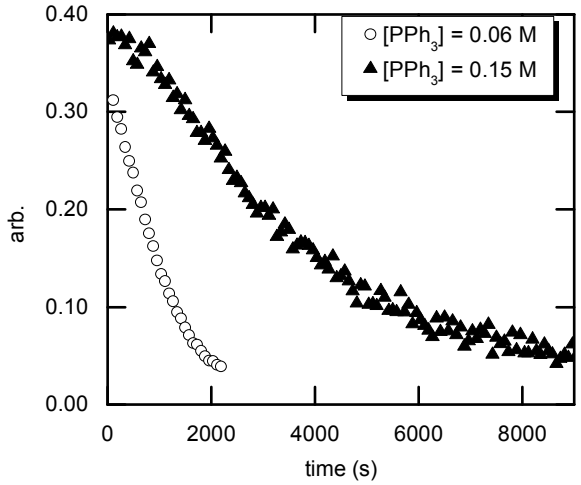

Figure 45. Decay of intermediate complex (δ 20.1 ppm), formed from initial reaction of **37** (0.015 M) with *p*-tolylboronic acid (0.15 M) at in THF/H_2O (50:1) at -40 °C, at -15 °C in the presence of PPh_3 (0.06-0.15 M) as monitored by ^{31}P NMR spectroscopy.

5.2.9 Preparation of Proposed Transmetallation Intermediates

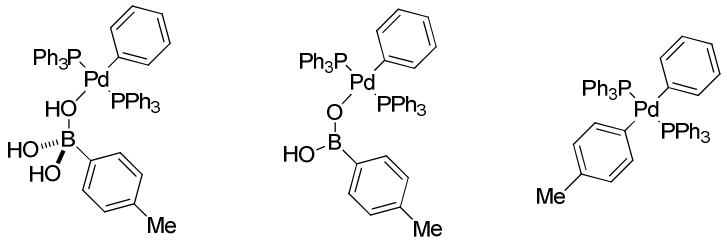

Figure 46. Possible structures of the initial complex (δ 20.1 ppm by ^{31}P NMR spectroscopy) formed upon reaction of palladium hydroxide **37** with *p*-tolylboronic acid at -40 °C.

The reaction of hydroxide **37** with *p*-tolylboronic acid could generate one of several stable adducts at low temperature that corresponds to the intermediate complex observed by ^{31}P NMR spectroscopy (see Section 5.2.8). Potential structures of the intermediate are shown in Figure 46. Attempts to identify the structure of the intermediate complex by independent synthesis were conducted. The reaction of iodide complex **45** with sodium *p*-fluorophenylborate in the presence of PPh_3 and excess aryl halide formed a single product as observed by ^{31}P NMR spectroscopy (Eq 26).[37] After isolation of the resulting palladium complex, the structure was deduced from NMR spectroscopic characterization and confirmed by single crystal X-ray diffraction (Fig 47). The product of this reaction was not the desired palladium boronate intermediate that is proposed as the initial product of the transmetallation sequence, but a stable *trans*-bis-arylpalladium complex.[38] The ^{31}P NMR chemical shift of complex **46** (δ 26 ppm) is significantly different than the observed intermediate (δ 20.1 ppm) formed upon reaction of hydroxide **37** with boronic acid at -40 °C. The preparation of a stable palladium boronate complex remains elusive, but the isolation of **46** definitively excludes one possible structure of the intermediate

complex formed from the reaction of palladium hydroxide and boronic acid at low temperature.

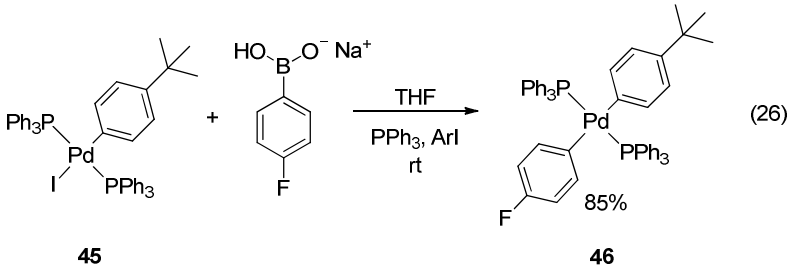

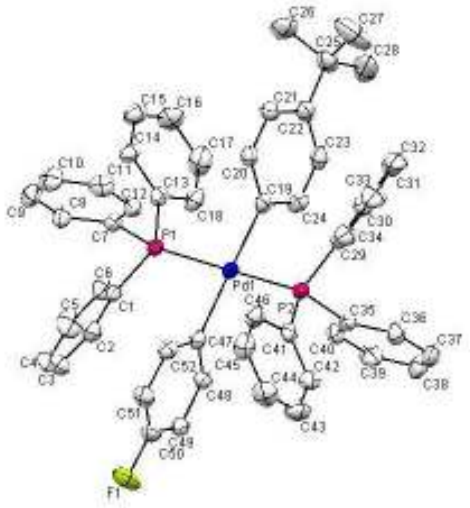

Figure 47. ORTEP diagram of *trans*-$(Ph_3P)_2Pd(C_6H_4$-*p*-F$)(C_6H_4$-*p*-^{t}Bu) (**46**). Thermal ellipsoids are shown at 50% probability.

5.3 Conclusions

In conclusion, we have shown that the reactions of isolated palladium hydroxides with boronic acids and the reactions of palladium iodides with aryltrihydroxyborates both form biaryl products rapidly in the absence of additives. Between these two classes of reactions, transmetallation between an arylpalladium hydroxo complex and a boronic acid would occur faster within the catalytic cycle because the populations of palladium halide and palladium hydroxo complex are similar to each other, the populations of

boronic acid and trihydroxyborate are similar to each other in the presence of water and bases of the strength of carbonates, but the rate of reaction of hydroxo complex with boronic acid is several orders of magnitude faster than the reaction of halide complexes with trihydroxyborate. The fast reaction of hydroxo complex **37** with arylboronic esters suggests that Suzuki-Miyaura reactions with these substrates also proceed by reaction of the neutral arylboron species with a palladium hydroxo complex.

These results provide the first quantitative assessment of the rates of the two pathways and populations of the reactants in these two pathways, but our conclusions must be made with several caveats. First, the data we present here cannot be extrapolated to all metal-ligand systems. Second, reactions with stronger bases will contain more trihydroxyborate and if the base is sufficiently strong, then one might expect the borate pathway (Path A) to become competitive with the hydroxo pathway (Path B). Regardless, the majority of catalytic Suzuki-Miyaura reactions are conducted with relatively weak bases such as carbonate or phosphate that lead to considerable concentrations of free boronic acid. Third, Lloyd-Jones et al. have recently reported that Suzuki-Miyaura reactions of trifluoroborates occur through the free boronic acid after hydrolysis.[31] Thus, the mechanism for transmetallation in these systems could also proceed by reaction of a palladium hydroxo complex with boronic acid, but we have not yet assessed the rates of reaction under these conditions.

Finally, our data do not reveal the intimate mechanism for transfer of the organic moiety from boron to palladium. Kinetic data and competitions studies of sterically-distinct organoboron compounds suggest the mechanism of the reaction of palladium

halide complexes with trihydroxyborates (Path A) could proceed through the intermediacy of palladium hydroxide complexes and neutral boronic acid (Path B) in aqueous solvent mixtures. The characterization of a palladium-boronate intermediate, however, remains elusive. Nevertheless, we hope these data will provide an anchor point to guide further mechanistic and computational studies.

5.4 Experimental

General Methods. All manipulations were conducted in an inert atmosphere dry box or using standard Schlenk techniques unless otherwise specified. ^{1}H spectra were recorded on a 400 MHz spectrometer; ^{13}C spectra were recorded at 125 MHz with external $CDCl_3$ as a reference; $^{31}P\{^{1}H\}$ NMR spectra were recorded at 160 or 200 MHz with external H_3PO_4 as a reference; $^{19}F\{^{1}H\}$ NMR spectra were recorded at 375 MHz with external $CFCl_3$ as a reference; $^{11}B\{^{1}H\}$ NMR spectra were recorded at 130 MHz with external $BF_3{\cdot}Et_2O$ as a reference. The complexes $[(Ph_3P)Pd(Ph)(\mu\text{-}OH)]_2$,[39] $(Cy_3P)_2Pd(Ph)(OH)$,[21-22] $(Cy_3P)_2Pd(Ph)(I)$,[25] $(Cy_3P)_2Pd(Ph)(Br)$,[23] $(Cy_3P)_2Pd(Ph)(Cl)$,[24] $(Ph_3P)_2Pd(C_6H_4\text{-}p\text{-}^{t}Bu)(I)$,[40] $(Ph_3P)_2Pd(Ph)(I)$,[41] and $(Ph_3P)_2Pd(Ph)(Br)$[41] were prepared by published procedures. Tetrahydrofuran and pentane used for the preparation of palladium complexes were dried with a solvent purification system by percolation through neutral alumina under positive pressure of argon. All other reagents and solvents were obtained from commercial sources and used without further purification.

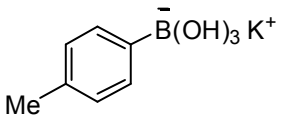

Potassium *p*-tolyltrihydroxyborate. Powdered potassium hydroxide (56 mg, 1.0 mmol) and *p*-tolylboronic acid (136 mg, 1.00 mmol) were weighed into a vial, and THF (5 mL) was added. The mixture was sonicated for 20 min. Upon reduction of the solvent volume to ~1 mL by evaporation under vacuum a white solid precipitated. Hexane (15 mL) was added, and after stirring for 5 min the white solid was filtered, washed with pentane (2x2 mL) and dried to afford 160 mg of product (83%). ^{1}H NMR (D_2O, 400 MHz) δ 7.28 (d, J = 7.2 Hz, 2H), 6.96 (d, J = 7.6 Hz, 2H), 2.10 (s, 3H); ^{13}C NMR (D_2O, 125 MHz) δ 149.73 (br), 138.43, 134.20, 130.50, 22.78; ^{11}B{^{1}H} NMR (D_2O, 130 MHz) δ 4.8; Anal. Calc'd for $C_7H_{10}BKO_3$: C, 43.77; H, 5.25. Found: C, 43.74; H, 4.95.

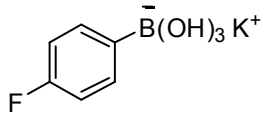

Potassium 4-fluorophenyltrihydroxyborate. 4-fluorophenylboronic anhydride (122 mg, 0.333 mmol) and powdered potassium hydroxide (56 mg, 1.0 mmol) were weighed into a vial. Water (18 μL) and THF (5 mL) were added, and the mixture was sonicated for 20 min. Upon reduction of the solvent volume to ~2 mL by evaporation under vacuum a white solid precipitated. Hexane (15 mL) was added, and after stirring for 30 min the white solid was filtered, washed with pentane (2x2 mL) and dried to afford 139 mg of product (71%). ^{1}H NMR (D_2O, 400 MHz) δ 7.38 (t, J = 6.4 Hz, 2H), 6.84 (t, J = 8.8 Hz, 2H); ^{13}C NMR (D_2O, 125 MHz) δ 164.46 (d, J = 240 Hz), 147.53 (br), 135.70, 116.21 (d, J = 18.6 Hz); ^{19}F{^{1}H} NMR (D_2O, 375 MHz) δ -117.95; ^{11}B{^{1}H} NMR (D_2O,

130 MHz) δ 6.2; Anal. Calc'd for $C_6H_7BFKO_3$: C, 36.76; H, 3.60. Found: C, 36.62; H, 3.41.

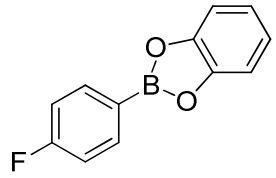

4-Fluorophenylboronic acid catechol ester. 4-fluorophenylboronic anhydride (185 mg, 0.506 mmol) and 1,2-dihydroxybenzene (167 mg, 1.50 mmol) were weighed into a flask. Water (20 μL) and benzene (5 mL) were added, and the mixture was refluxed with a Dean-Stark trap for 1 h. The solvent was evaporated to dryness. The residue was dissolved in hexane (10 mL), filtered through a plug of Celite, and the filtrate was evaporated under vacuum to dryness. The residue was dissolved in hot hexane (2 mL) and then cooled to -20 °C for 3 h. The resulting crystalline precipitate was filtered, washed with cold pentane (2x2 mL) and dried to afford 212 mg (65%) of product as colorless needles. ^{1}H NMR ($CDCl_3$, 400 MHz) δ 8.09 (dd, *J* = 8.4, 6.0 Hz, 2H), 7.31 (dd, *J* = 5.7, 3.6 Hz, 2H), 7.19 (t, *J* = 8.4 Hz, 2H), 7.14 (dd, *J* = 5.6, 3.6 Hz, 2H); ^{13}C NMR ($CDCl_3$, 125 MHz) δ 165.72 (d, *J* = 253 Hz), (C-B is broad, not observed), 148.45, 137.33 (d, *J* = 8.8 Hz), 122.82, 115.57 (d, *J* = 20.5 Hz), 112.54; ^{19}F{^{1}H} NMR ($CDCl_3$, 375 MHz) δ -106.51; ^{11}B{^{1}H} NMR ($CDCl_3$, 130 MHz) δ 31.6; Anal. Calc'd for $C_{12}H_8BFO_2$: C, 67.35; H, 3.77. Found: C, 67.48; H, 3.70.

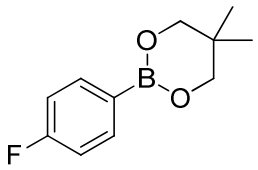

4-Fluorophenylboronic acid neopentyl glycol ester. 4-fluorophenylboronic anhydride (183 mg, 0.500 mmol) and neopentyl glycol (156 mg, 1.50 mmol) were weighed into a flask. Water (20 μL) and benzene (5 mL) were added, and the mixture was refluxed with a Dean-Stark trap for 1 h. Solvent was concentrated to dryness affording the product as a colorless solid (312 mg) in quantitative yield. ^{1}H and ^{13}C NMR chemical shifts matched literature values.[42]

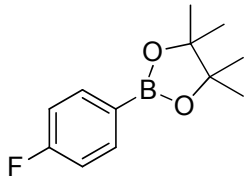

4-Fluorophenylboronic acid pinacol ester. 4-fluorophenylboronic anhydride (200 mg, 0.547 mmol) and pinacol (194 mg, 1.64 mmol) were weighed into a flask. Water (20 μL) and benzene (5 mL) were added, and the mixture was refluxed with a Dean-Stark trap for 1 h. The solution was passed through a silica plug and washed with 50 mL of hexane/ethyl acetate (3:1). The filtrate was evaporated affording 255 mg (70%) of product as a pale tan liquid. ^{1}H and ^{13}C NMR chemical shifts matched literature values.[43]

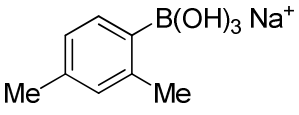

Sodium 2,4-dimethylphenyltrihydroxyborate.[26] 2,4-dimethylphenylboronic acid (250 mg, 1.67 mmol) was dissolved in hot benzene (15 mL). After cooling to near room

temperature, sodium hydroxide solution (0.15 mL, 12.5 M) was added with vigorously stirring. After 30 min, solvent was evaporated. Hexane (15 mL) was added to the residue and stirred. After 5 min, the white solid was filtered, washed with pentane (2x2 mL) and dried to afford 312 mg of product (98%). ^{1}H NMR (D_2O, 400 MHz) δ 7.24 (d, J = 7.2 Hz, 1H), 6.80 (s, 1H), 6.76 (d, J = 7.6 Hz, 1H), 2.23 (s, 3H), 2.05 (s, 3H); ^{13}C NMR (D_2O, 125 MHz) δ 148.18 (br), 144.13, 138.32, 134.76, 132.87, 127.38, 24.29, 22.55; ^{11}B{^{1}H} NMR (D_2O, 130 MHz) δ 3.6; Anal. Calc'd for $C_8H_{12}BNaO_3$: C, 50.58; H, 6.37. Found: C, 50.88; H, 6.39.

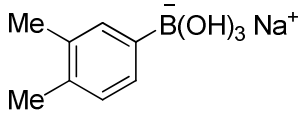

Sodium 2,3-dimethylphenyltrihydroxyborate.[26] 2,3-dimethylphenylboronic acid (250 mg, 1.67 mmol) was dissolved in hot toluene (10 mL). After cooling to near room temperature, sodium hydroxide solution (0.15 mL, 12.5 M) was added with vigorously stirring. After 30 min, hexane (15 mL) was added and stirring was continued. After 1 h, the white solid was filtered, washed with pentane (2x2 mL) and dried to afford 316 mg of product (99%). ^{1}H NMR (D_2O, 400 MHz) δ 7.17 (s, 1H), 7.11 (d, J = 7.2 Hz, 1H), 6.91 (d, J = 7.2 Hz, 1H), 2.06 (s, 3H), 2.03 (s, 3H); ^{13}C NMR (D_2O, 125 MHz) δ 152.51 (br), 137.84, 136.50, 135.26, 131.49, 131.03, 21.46, 21.02; ^{11}B{^{1}H} NMR (D_2O, 130 MHz) δ 3.5; Anal. Calc'd for $C_8H_{12}BNaO_3$: C, 50.58; H, 6.37. Found: C, 50.68; H, 6.35.

Preparation of *trans*-$(Ph_3P)_2Pd(C_6H_4$-*p*-F)(C_6H_4-*p*-^{t}Bu) (46). 4-fluorophenylboronic anhydride (1.1 g, 3.0 mmol) was dissolved in THF (20 mL) and H_2O

(0.16 mL). The solution was slowly transferred to a flask containing stirring suspension of washed sodium hydride (0.22 g, 9.0 mmol) in THF (20 mL). After 20 min, the resulting borate solution was transferred to a second flask containing $(Ph_3P)_2Pd(C_6H_4$-*p*-$^tBu)(I)$ (0.40 g, 0.45 mmol), PPh_3 (0.12 g, 0.45 mmol), and 4-*tert*-butyliodobenzene (0.59 g, 0.23 mmol) in THF (25 mL). After stirring for 1.5 h at room temperature, an aliquot was analyzed by ^{31}P NMR spectroscopy, which indicated that consumption of the starting complex was complete. Solvent was evaporated under vacuum to dryness. The residue was then triturated with a 1:1 mixture of DMF/MeOH (2x15 mL) then with MeOH, filtered and dried under vacuum affording 0.35 g (85%) of product as a white powder. Recrystallization of the product from THF/pentane at 0 °C afforded colorless crystals suitable for X-ray analysis. ^1H NMR (THF-d_8, 400 MHz) δ 7.23 (m, 18H), 6.84 (d, J = 7.2 Hz, 2H), 6.75 (t, J = 7.2 Hz, 2H), 6.39 (d, J = Hz, 2H), 6.00 (t, J = 8.8 Hz, 2H), 1.11 (s, 9H); ^{13}C NMR (THF-d_8, -30 °C, 125 MHz) δ 161.36 (dt, J = 88 Hz, 10.8 Hz), 160.58 (d, J = 237 Hz), 143.86, 141.14, 135.20, 133.18 (t, J = 22.5 Hz), 129.98, 128.39, 123.99 (d, J = 5.9 Hz), 112.91 (t, J = 16.6 Hz), 34.29, 32.03 (t, J = 18.5 Hz); $^{19}F\{^1H\}$ NMR (THF-d_8, 375 MHz) δ -126.51; $^{31}P\{^1H\}$ NMR (THF-d_8, 160 MHz) δ 26.17.

Reaction of $[(Ph_3P)Pd(Ph)(\mu\text{-}OH)]_2$ (37) with *p*-tolylboronic acid (Eq 8). A solution of p-tolylboronic acid (10 mg, 0.075 mmol) in THF/H_2O (0.25 mL/10 μL) was added by to a vial containing **37** (7.0 mg, 7.6 μmol), PPh_3 (12 mg, 0.045 mmol), and *n*-tetradecane (5.0 μL, 0.019 mmol, internal standard) in THF (0.25 mL). The resulting solution was stirred at room temperature. Aliquots of the reaction mixture (50 μL) were

diluted in ethyl acetate (0.75 mL), passed through a silica plug, and the yield of 4-methylbiphenyl was determined by gas chromatography.

Reaction of $(Ph_3P)_2Pd(Ph)(I)$ (38) with potassium *p*-tolyltrihydroxyborate (Eq 9). A solution of potassium *p*-tolyltrihydroxyborate (15 mg, 0.078 mmol) and 18-crown-6 (20 mg, 0.075 mmol) in THF/H_2O (0.25 mL/10 μL) was added to a vial containing **38** (13 mg, 0.015 mmol), PPh_3 (8 mg, 0.03 mmol), and *n*-tetradecane (5.0 μL, 0.019 mmol, internal standard) in THF (0.25 mL). The resulting solution was stirred at room temperature. Aliquots of the reaction mixture (50 μL) were diluted in ethyl acetate (0.75 mL), passed through a silica plug, and the yield of 4-methylbiphenyl was determined by gas chromatography.

Reaction of iodobenzene with *p*-tolylboronic acid (Eq 10). Iodobenzene (20 mg, 0.10 mmol), *p*-tolylboronic acid (16 mg, 0.12 mmol), potassium carbonate (35 mg, 0.25 mmol), and $Pd(PPh_3)_4$ (1 mg, 0.001 mmol) were weighed into a small vial. THF (0.50 mL), and *n*-tetradecane (15 μL, 0.076 mmol, internal standard) were added, and the vial was sealed with a septum cap. Water (0.25 mL) was added by syringe, and the mixture was stirred vigorously at 80 ^{o}C. Aliquots of the reaction mixture (20 μL) were diluted in ethyl acetate (0.75 mL), passed through a silica plug, and the yield of 4-methylbiphenyl was determined by gas chromatography.

Reaction of $(Cy_3P)_2Pd(Ph)(OH)$ (41) with *p*-tolylboronic acid (Eq 11). 41 (10 mg, 0.013 mmol) was weighed into a small vial. *n*-tetradecane (5.0 mL, 0.019 mmol, internal standard) and THF (0.5 mL) were added, and the mixture was heated briefly to

dissolution then cooled to room temperature. The palladium solution was transferred to a second vial equipped with a magnetic stir bar, containing *p*-tolylboronic acid (9 mg, 0.07 mmol) in THF (0.5 mL). The mixture was stirred at room temperature. Aliquots of the reaction mixture (50 μL) were diluted in ethyl acetate (0.75 mL), passed through a silica plug, and the yield of 4-methylbiphenyl was determined by gas chromatography.

Reaction of $(Cy_3P)_2Pd(Ph)(I)$ (42) with potassium *p*-tolyltrihydroxyborate (Eq 12). A solution of potassium *p*-tolyltrihydroxyborate (13 mg, 0.068 mmol) and 18-crown-6 (17 mg, 0.064 mmol) in THF/H_2O (0. 5 mL/20 μL) was added to a vial containing **42** (11 mg, 0.013 mmol) and *n*-tetradecane (5.0 μL, 0.019 mmol, internal standard) in THF (0.5 mL). The resulting mixture was stirred at room temperature. Aliquots of the reaction mixture (50 μL) were diluted in ethyl acetate (0.75 mL), passed through a silica plug, and the yield of 4-methylbiphenyl was determined by gas chromatography.

Reaction of iodobenzene with *p*-tolylboronic acid (Eq 13). Iodobenzene (20 mg, 0.10 mmol), *p*-tolylboronic acid (16 mg, 0.12 mmol), potassium carbonate (35 mg, 0.25 mmol), and $Pd(PCy_3)_2$ (2 mg, 0.002 mmol) were weighed into a small vial. THF (0.50 mL), and *n*-tetradecane (15 μL, 0.076 mmol, internal standard) were added, and the vial was sealed with a septum cap. Water (0.25 mL) was added by syringe, and the mixture was stirred vigorously at 80 ^{o}C. Aliquots of the reaction mixture (20 μL) were diluted in ethyl acetate (0.75 mL), passed through a silica plug, and the yield of 4-methylbiphenyl was determined by gas chromatography.

Representative procedure for determination of *K* for reaction of 4-fluorophenylboronic acid with potassium carbonate (Eq 14). A stock solution of 4-fluorophenylboronic anhydride (0.020 M) in a 50:50 acetone/H_2O mixture was prepared. A portion of the resulting solution of 4-fluorophenylboronic acid (0.50 mL, 0.030 mmol) was added to a small vial, followed by addition of aqueous K_2CO_3 (15 μL, 75 μmol, 5.0 M) by microliter syringe. The mixture was transferred to an NMR tube. The ratio of boronic acid and trihydroxyborate was calculated from the observed time-averaged ^{11}B and ^{19}F NMR chemical shifts at 20 ^oC ($^{19}F\{^1H\}$ NMR (375 MHz) δ -116.2; $^{11}B\{^1H\}$ NMR (130 MHz) δ 13.8), relative to pure 4-fluorophenylboronic acid ($^{19}F\{^1H\}$ NMR (375 MHz) δ -110.9; $^{11}B\{^1H\}$ NMR (130 MHz) δ 28.7) and potassium 4-fluorophenyltrihydroxyborate ($^{19}F\{^1H\}$ NMR (375 MHz) δ -119.7; $^{11}B\{^1H\}$ NMR (130 MHz) δ 3.5) at the same concentration and solvent ratio.

Representative procedure for determination of *K* for reaction of $[(Ph_3P-)Pd(Ph)(\mu\text{-}OH)]_2$ (37) with halide salt (Eq 15). A stock solution of **37** (40 mg, 0.043 mmol) and PPh_3 (115 mg, 0.438 mmol) in THF (2.0 mL) was prepared. Separately, a stock solution of $N(butyl)_4I$ (32 mg, 0.087 mmol) in THF/H_2O (25:1, 1.04 mL) was prepared. The palladium solution (0.50 mL) and halide solution (0.52 mL) were combined in a small vial then transferred to an NMR tube and sealed with a septum. The relative ratios of **37**, $(Ph_3P)_2Pd(Ph)(OH)$, and $(PPh_3)_2Pd(Ph)(I)$ (**38**) were subsequently determined by ^{31}P NMR spectroscopy at 20 ^oC.

Representative procedure for determination of *K* for reaction of $(Cy_3P-)_2Pd(Ph)(OH)$ (41) with halide salt (Eq 16 and 17). A stock solution of **41** (40 mg, 0.052 mmol) in THF (2.0 mL) was prepared. Separately, a stock solution of $N(butyl)_4I$ (19 mg, 0.051 mmol) in THF/H_2O (25:1, 2.08 mL) was prepared. The palladium solution (0.50 mL) and halide solution (0.52 mL) were combined in a small vial then transferred to an NMR tube and sealed with a septum. The relative ratios of **41** and $(Cy_3P)_2Pd(Ph)(I)$ (**42**) were subsequently determined by ^{31}P NMR spectroscopy at 20 ^{o}C.

Procedure for kinetic experiments: reaction of $[(Ph_3P)Pd(Ph)(\mu\text{-}OH)]_2$ (37) with *p*-tolylboronic acid (Fig 37). A stock solution of **37** (14 mg, 0.015 mmol) and PPh_3 (40 mg, 0.15 mmol) in THF (0.5 mL) was prepared. The solution containing palladium complex and ligand (0.25 mL) was transferred to an NMR tube. A sealed capillary containing a 1.0 M solution of PBu_4Br in DMF was also placed in the NMR tube as a ^{31}P NMR external reference. The NMR tube was sealed with a septum. A stock solution of *p*-tolylboronic acid (20 mg, 0.15 mmol) in THF/H_2O (25:1, 0.52 mL) was prepared. The NMR tube was cooled to -50 ^{o}C, and the solution of boronic acid (0.26 mL) was added by syringe. The resulting solution was placed in the NMR probe cooled to -40 ^{o}C. ^{31}P NMR spectra were acquired at fixed time intervals throughout the length of experiment with the aid of an automated data collection program.

Representative procedure for kinetic experiments: reaction of $(Ph_3P)_2Pd(Ph)(Br)$ (39) with potassium *p*-tolyltrihydroxyborate (Fig 37 and Fig 38). A stock solution of **39** (12 mg, 0.015 mmol) and PPh_3 (4 mg, 0.015 mmol) in THF (0.5 mL) was prepared.

The solution containing palladium complex and ligand (0.25 mL) was transferred to an NMR tube. A sealed capillary containing a 1.0 M solution of PBu_4Br in DMF was also placed in the NMR tube as a ^{31}P NMR external reference. The NMR tube was sealed with a septum. A stock solution of potassium *p*-tolyltrihydroxyborate (14 mg, 0.073 mmol) and 18-crown-6 (20 mg, 0.075 mmol) in THF/H_2O (25:1, 0.52 mL) was prepared. The NMR tube was cooled to -50 ^oC, and the solution of borate (0.26 mL) was added by syringe. The resulting solution was placed in the NMR probe cooled to -30 ^oC. ^{31}P NMR spectra were acquired at fixed time intervals throughout the length of experiment with the aid of an automated data collection program.

Procedure for kinetic experiments: reaction of $(Cy_3P)_2Pd(Ph)(OH)$ (41) with *p*-tolylboronic acid (Fig 39). A stock solution of **41** (20 mg, 0.026 mmol) and PCy_3 (22 mg, 0.080 mmol) in THF (0.5 mL) was prepared. The solution containing palladium complex and ligand (0.25 mL) was transferred to an NMR tube. A sealed capillary containing a 1.0 M solution of PBu_4Br in DMF was also placed in the NMR tube as a ^{31}P NMR external reference. The NMR tube was sealed with a septum. A stock solution of *p*-tolylboronic acid (18 mg, 0.13 mmol) in THF/H_2O (25:1, 0.52 mL) was prepared. The NMR tube was cooled to -35 ^oC, and the solution of boronic acid (0.26 mL) was added by syringe. The resulting solution was placed in the NMR probe cooled to -20 ^oC. ^{31}P NMR spectra were acquired at fixed time intervals throughout the length of experiment with the aid of an automated data collection program.

Representative procedure for the kinetic experiment: reaction of $(Cy_3P-)_2Pd(Ph)(Br)$ (43) with potassium *p*-tolyltrihydroxyborate (Fig 39 and Fig 40). A stock solution of **43** (22 mg, 0.026 mmol) and PCy_3 (22 mg, 0.080 mmol) in THF (0.5 mL) was prepared. The solution containing palladium complex and ligand (0.25 mL) was transferred to an NMR tube. A sealed capillary containing a 1.0 M solution of PBu_4Br in DMF was also placed in the NMR tube as a ^{31}P NMR external reference. The NMR tube was sealed with a septum. A stock solution of potassium *p*-tolyltrihydroxyborate (25 mg, 0.13 mmol) and 18-crown-6 (34 mg, 0.13 mmol) in THF/H_2O (25:1, 0.52 mL) was prepared. The NMR tube was cooled to -35 ^oC, and the solution of trihydroxyborate (0.26 mL) was added by syringe. The resulting mixture was placed in the NMR probe that was cooled to -20 ^oC. ^{31}P NMR spectra were acquired at fixed time intervals throughout the length of experiment with the aid of an automated data collection program.

Representative procedure for the reaction of $[(Ph_3P)Pd(Ph)(\mu\text{-}OH)]_2$ (37) with 4-fluorophenylboronic acid esters (Scheme 48). A stock solution of **37** (14 mg, 0.015 mmol) and PPh_3 (40 mg, 0.15 mmol) in THF (0.5 mL) was prepared. The solution containing palladium complex and ligand (0.25 mL) was transferred to an NMR tube. A stock solution of 4-fluorophenylboronic acid neopentyl glycol ester (32 mg, 0.15 mmol) in THF/H_2O (25:1, 0.52 mL) was prepared. The NMR tube was cooled to -78 ^oC, and the solution of boronic ester (0.26 mL) was added by syringe. The resulting solution was placed in the NMR probe chilled to -55 ^oC. ^{31}P NMR spectra were acquired at fixed time

intervals throughout the length of experiment with the aid of an automated data collection program.

Catalytic reaction of iodobenzene with 4-(trifluoromethyl)phenylboronic acid and 4-methoxyphenylboronic acid (Scheme 49, entry 1). Iodobenzene (20 mg, 0.10 mmol), 4-(trifluoromethyl)phenylboronic acid (95 mg, 0.50 mmol), 4-(methoxy)phenylboronic acid (76 mg, 0.50 mmol), potassium carbonate (35 mg, 0.25 mmol), and $Pd(PCy_3)_2$ (2 mg, 0.002 mmol) were weighed into a small vial. THF (1 mL), and *n*-tetradecane (15 μL, 0.076 mmol, internal standard) were added, and the vial was sealed with a septum cap. Water (0.2 mL) was added by syringe, and the mixture was stirred vigorously at 60 ^{o}C. Aliquots of the reaction mixture (20 μL) were diluted in ethyl acetate (0.75 mL), passed through a silica plug, and the yield of 4-methylbiphenyl was determined by gas chromatography.

Representative procedure for the catalytic reaction of iodobenzene with 4-(trifluoromethyl)phenylboronic acid and 4-methoxyphenylboronic acid (Scheme 49, entry 2 and entry 3). Iodobenzene (20 mg, 0.10 mmol), 4-(trifluoromethyl)phenylboronic acid (95 mg, 0.50 mmol), 4-(methoxy)phenylboronic acid (76 mg, 0.50 mmol), potassium hydroxide (28 mg, 0.50 mmol), and $Pd(PCy_3)_2$ (2 mg, 0.002 mmol) were weighed into a small vial. THF (1 mL), and *n*-tetradecane (15 μL, 0.076 mmol, internal standard) were added, and the vial was sealed with a septum cap. Water (0.2 mL) was added by syringe, and the mixture was stirred vigorously at 60 ^{o}C. Aliquots of the reaction mixture (20 μL) were diluted in ethyl acetate (0.75 mL), passed

through a silica plug, and the yield of 4-methylbiphenyl was determined by gas chromatography.

Catalytic reaction of iodobenzene with 2,3-dimethylphenylboronic acid and 2,4-dimethylphenylboronic acid (Scheme 50, entry 1). Iodobenzene (20 mg, 0.10 mmol), 2,4-dimethylphenylboronic acid (75 mg, 0.50 mmol), 2,3-dimethylphenylboronic acid (75 mg, 0.50 mmol), potassium carbonate (35 mg, 0.25 mmol), and $Pd(PCy_3)_2$ (2 mg, 0.002 mmol) were weighed into a small vial. THF (1.0 mL) and *n*-tetradecane (15 μL, 0.076 mmol, internal standard) were added, and the vial was sealed with a septum cap. Water (0.2 mL) was added by syringe and the mixture was stirred vigorously at 60 ^{o}C. Aliquots of the reaction mixture (50 μL) were diluted in ethyl acetate (1 mL), passed through a silica plug, and the distribution of biaryl products was determined by gas chromatography.

Catalytic reaction of bromobenzene with 2,3-dimethylphenylboronic acid and 2,4-dimethylphenylboronic acid (Scheme 50, entry 2). Bromobenzene (16 mg, 0.10 mmol), 2,4-dimethylphenylboronic acid (75 mg, 0.50 mmol), 2,3-dimethylphenylboronic acid (75 mg, 0.50 mmol), potassium carbonate (35 mg, 0.25 mmol), and $Pd(PCy_3)_2$ (2 mg, 0.002 mmol) were weighed into a small vial. THF (1.0 mL) and *n*-tetradecane (15 μL, 0.076 mmol, internal standard) were added, and the vial was sealed with a septum cap. Water (0.2 mL) was added by syringe and the mixture was stirred vigorously at 60 ^{o}C. Aliquots of the reaction mixture (50 μL) were diluted in ethyl acetate (1 mL), passed

through a silica plug, and the distribution of biaryl products was determined by gas chromatography.

Catalytic reaction of chlorobenzene with 2,3-dimethylphenylboronic acid and 2,4-dimethylphenylboronic acid (Scheme 50, entry 3). Chlorobenzene (11 mg, 0.10 mmol), 2,4-dimethylphenylboronic acid (75 mg, 0.50 mmol), 2,3-dimethylphenylboronic acid (75 mg, 0.50 mmol), potassium carbonate (35 mg, 0.25 mmol), and $Pd(PCy_3)_2$ (4.5 mg, 5.2 μmol) were weighed into a small vial. THF (1.0 mL) and *n*-tetradecane (15 μL, 0.076 mmol, internal standard) were added, and the vial was sealed with a septum cap. Water (0.2 mL) was added by syringe and the mixture was stirred vigorously at 90 ^{o}C. Aliquots of the reaction mixture (50 μL) were diluted in ethyl acetate (1 mL), passed through a silica plug, and the distribution of biaryl products was determined by gas chromatography.

Catalytic reaction of iodobenzene with 2,3-dimethylphenylboronic acid and 2,4-dimethylphenylboronic acid (Scheme 50, entry 4). Iodobenzene (20 mg, 0.10 mmol), 2,4-dimethylphenylboronic acid (75 mg, 0.50 mmol), 2,3-dimethylphenylboronic acid (75 mg, 0.50 mmol), potassium hydroxide (90 mg, 1.6 mmol), and $Pd(PCy_3)_2$ (2 mg, 0.002 mmol) were weighed into a small vial. THF (1.0 mL) and *n*-tetradecane (15 μL, 0.076 mmol, internal standard) were added, and the vial was sealed with a septum cap. Water (0.2 mL) was added by syringe and the mixture was stirred vigorously at room temperature. Aliquots of the reaction mixture (50 μL) were diluted in ethyl acetate (1

mL), passed through a silica plug, and the distribution of biaryl products was determined by gas chromatography.

Reaction of $(Cy_3P)_2Pd(Ph)(OH)$ (41) with 2,3-dimethylphenylboronic acid and 2,4-dimethylphenylboronic acid (Eq 18). $(Cy_3P)_2Pd(Ph)(OH)$ (**41**) (10 mg, 0.013 mmol) was weighed into a small vial. THF (0.5 mL) and *n*-tetradecane (5.0 μL, 0.019 mmol, internal standard) were added and the solution was heated briefly to dissolution then cooled back to room temperature. A solution of 2,4-dimethylphenylboronic acid (10 mg, 0.067 mmol) and 2,3-dimethylphenylboronic acid (10 mg, 0.067 mmol) in THF (0.5 mL) and water (0.1 mL) was also prepared. The solutions were combined, and the mixture stirred at room temperature. Aliquots of the reaction mixture (0.1 mL) were diluted in ethyl acetate (1 mL), passed through a silica plug, and the distribution of biaryl products was determined by gas chromatography.

Representative procedure for the reaction of $(Cy_3P)_2Pd(Ph)(X)$ (X = I, Br, Cl) with dimethylphenyltrihydroxyborates (Eq 19). $(Cy_3P)_2Pd(Ph)(I)$ (**42**) (15 mg, 0.017 mmol) was weighed into a small vial. THF (0.6 mL) and *n*-tetradecane (5.0 μL, 0.019 mmol, internal standard) were added, and the vial was sealed with a septum cap. Sodium 2,4-dimethylphenyltrihydroxyborate (16 mg, 0.085 mmol) and sodium 2,3-dimethylphenyltrihydroxyborate (16 mg, 0.085 mmol) were weighed into a separate vial and dissolved in THF (0.6 mL) and water (0.3mL). The borate solution was added by syringe to the first vial and the mixture stirred vigorously at 60 ^{o}C. Aliquots of the

reaction mixture (0.1 mL) were diluted in ethyl acetate (1 mL), passed through a silica plug, and the distribution of biaryl products was determined by gas chromatography.

Catalytic reaction of iodobenzene with 2,3-dimethylphenylboronic acid and 2,4-dimethylphenylboronic acid (Scheme 51, entry 1). Iodobenzene (20 mg, 0.10 mmol), 2,4-dimethylphenylboronic acid (75 mg, 0.50 mmol), 2,3-dimethylphenylboronic acid (75 mg, 0.50 mmol), potassium carbonate (35 mg, 0.25 mmol), and $Pd(PCy_3)_2$ (2 mg, 0.002 mmol) were weighed into a small vial. THF (1.0 mL) and *n*-tetradecane (15 μL, 0.076 mmol, internal standard) were added, and the vial was sealed with a septum cap. Water (0.2 mL) was added by syringe and the mixture was stirred vigorously at 60 ^{o}C. Aliquots of the reaction mixture (50 μL) were diluted in ethyl acetate (1 mL), passed through a silica plug, and the distribution of biaryl products was determined by gas chromatography.

Catalytic reaction of bromobenzene with 2,3-dimethylphenylboronic acid and 2,4-dimethylphenylboronic acid (Scheme 51, entry 2). Bromobenzene (16 mg, 0.10 mmol), 2,4-dimethylphenylboronic acid (75 mg, 0.50 mmol), 2,3-dimethylphenylboronic acid (75 mg, 0.50 mmol), potassium carbonate (35 mg, 0.25 mmol), and $Pd(PPh_3)_4$ (2 mg, 0.002 mmol) were weighed into a small vial. THF (1.0 mL) and *n*-tetradecane (15 μL, 0.076 mmol, internal standard) were added, and the vial was sealed with a septum cap. Water (0.2 mL) was added by syringe and the mixture was stirred vigorously at 60 ^{o}C. Aliquots of the reaction mixture (50 μL) were diluted in ethyl acetate (1 mL), passed

through a silica plug, and the distribution of biaryl products was determined by gas chromatography.

Reaction of $[(Ph_3P)Pd(Ph)(\mu\text{-}OH)]_2$ (37) with 2,3-dimethylphenylboronic acid and 2,4-dimethylphenylboronic acid (Eq 20). 37 (6 mg, 0.007 mmol) and *n*-tetradecane (5.0 mL, 0.019 mmol, internal standard) were dissolved in THF (0.5 mL). In a separate vial, 2,4-dimethylphenylboronic acid (10 mg, 0.067 mmol) and 2,3-dimethylphenylboronic acid (10 mg, 0.067 mmol) were dissolved in THF (0.5 mL) and H_2O (50 mL). The two solutions were combined and stirred at room temperature. Aliquots of the reaction mixture (0.1 mL) were diluted in ethyl acetate (1 mL), passed through a silica plug, and the distribution of biaryl products was determined by gas chromatography.

Representative procedure for the reaction of $(Ph_3P)_2Pd(Ph)(X)$ (X = I, Br) with trihydroxyborates (Eq 21). $(Ph_3P)_2Pd(Ph)(I)$ (**38**) (11 mg, 0.013 mmol), PPh_3 (5 mg, 0.04 mmol), and *n*-tetradecane (5.0 μL, 0.019 mmol, internal standard) were dissolved in THF (0.5 mL). In a separate vial, sodium 2,4-dimethylphenyltrihydroxyborate (12 mg, 0.063 mmol) and sodium 2,3-dimethylphenyltrihydroxyborate (12 mg, 0.063 mmol) were dissolved in THF (0.5 mL) and water (0.25 mL). The two solutions were combined and stirred vigorously at room temperature. Aliquots of the reaction mixture (0.1 mL) were diluted in ethyl acetate (1 mL), passed through a silica plug, and the distribution of biaryl products was determined by gas chromatography.

Representative procedure for the kinetic experiments: reaction of $(Ph_3P)_2Pd(Ph)(Br)$ (39) with potassium *p*-tolyltrihydroxyborate (Fig 41, Fig 42, and Fig 43). A solution was prepared by gently heating a mixture of **39** (12 mg, 0.015 mmol), PPh_3 (39 mg, 0.15 mmol) in THF (0.5 mL) and H_2O (10 μL) in a sealed vial. The resulting solution was transferred by syringe to a sealed, chilled (0 °C) vial containing potassium *p*-tolyltrihydroxyborate (14 mg, 0.073 mmol) and 18-crown-6 (20 mg, 0.075 mmoL). The mixture was quickly sonicated to dissolution of the borate, then transferred by syringe to a sealed, chilled (0 °C) NMR tube equipped with a septum cap. The NMR tube contained a sealed capillary containing a 1.0 M solution of P(*o*-tol)$_3$ in toluene as a ^{31}P NMR external reference. The resulting solution was placed in the NMR probe cooled to 10 ^{o}C. ^{31}P NMR spectra were acquired at fixed time intervals throughout the length of experiment with the aid of an automated data collection program.

Procedure for the reaction of $(Cy_3P)_2Pd(Ph)(Br)$ (43) with potassium *p*-tolyltrihydroxyborate (Fig 44). 43 (11 mg, 0.013 mmol) and PCy_3 (7 mg, 0.03 mmol) were dissolved in THF (0.25 mL) with gentle heating and cooled back to room temperature upon dissolution. In a separate vial, potassium *p*-tolyltrihydroxyborate (13 mg, 0.068 mmol) and 18-crown-6 (17 mg, 0.065 mmol) were dissolved in THF (0.25 mL) and H_2O (10 μL). The solutions were combined and transferred to an NMR tube. The ratios of **43**, **41**, and PCy_3 were determined from the integral values obtained by ^{31}P NMR spectroscopy.

Representative procedure for the kinetic experiments: reaction of $(Cy_3P-)_2Pd(Ph)(OH)$ (41) with potassium *p*-tolyltrihydroxyborate (Eq 22 and Eq 23). 41 (10 mg, 0.013 mmol) and PCy_3 (18 mg, 0.064 mmol) were dissolved in THF (0.25 mL) with gentle heating and cooled back to room temperature upon dissolution. In a separate vial, potassium *p*-tolyltrihydroxyborate (13 mg, 0.068 mmol) and 18-crown-6 (17 mg, 0.065 mmol) were dissolved in THF (0.25 mL) and H_2O (10 μL). The solutions were combined and transferred to an NMR tube, which was sealed with a septum. A sealed capillary containing a 1.0 M solution of PBu_4Br in DMF was also placed in the NMR tube as a ^{31}P NMR external reference. Prior to inserting the sample, the NMR probe was heated to 40 ^oC using ethylene glycol as a temperature standard. ^{31}P NMR spectra were acquired at fixed time intervals throughout the length of experiment with the aid of an automated data collection program.

Representative procedure for kinetic experiments: reaction of $[(Ph_3P)Pd(Ph)(\mu-OH)]_2$ (37) with *p*-tolylboronic acid (Eq 24 and Eq 25). A stock solution of **37** (14 mg, 0.015 mmol) and PPh_3 (78 mg, 0.30 mmol) in THF (0.5 mL) was prepared. The solution containing palladium complex and ligand (0.25 mL) was transferred to an NMR tube. A sealed capillary containing a 1.0 M solution of PBu_4Br in DMF was also placed in the NMR tube as a ^{31}P NMR external reference. The NMR tube was sealed with a septum. A stock solution of *p*-tolylboronic acid (20 mg, 0.15 mmol) in THF/H_2O (25:1, 0.52 mL) was prepared. The NMR tube was cooled to -50 ^oC, and the solution of boronic acid (0.26 mL) was added by syringe. The resulting solution was placed in the NMR probe

cooled to -40 ^{o}C. ^{31}P NMR spectra were acquired at fixed time intervals throughout the length of experiment with the aid of an automated data collection program.

Representative procedure for kinetic experiments: decay of the intermediate complex (δ 20.1 ppm) (Fig 45). A stock solution of **37** (14 mg, 0.015 mmol) and PPh_3 (40 mg, 0.15 mmol) in THF (0.5 mL) was prepared. The solution containing palladium complex and ligand (0.25 mL) was transferred to an NMR tube. A sealed capillary containing a 1.0 M solution of PBu_4Br in DMF was also placed in the NMR tube as a ^{31}P NMR external reference. The NMR tube was sealed with a septum. A stock solution of *p*-tolylboronic acid (20 mg, 0.15 mmol) in THF/H_2O (25:1, 0.52 mL) was prepared. The NMR tube was cooled to -50 ^{o}C, and the solution of boronic acid (0.26 mL) was added by syringe. The resulting solution was placed in the NMR probe cooled to -40 ^{o}C. After the disappearance of **37** was observed by ^{31}P NMR spectroscopy, the sample was placed back into a -50 °C cold bath, and the temperature of the NMR probe was adjusted to -15 °C. The sample was placed back into the NMR probe and ^{31}P NMR spectra were acquired at fixed time intervals throughout the length of experiment with the aid of an automated data collection program.

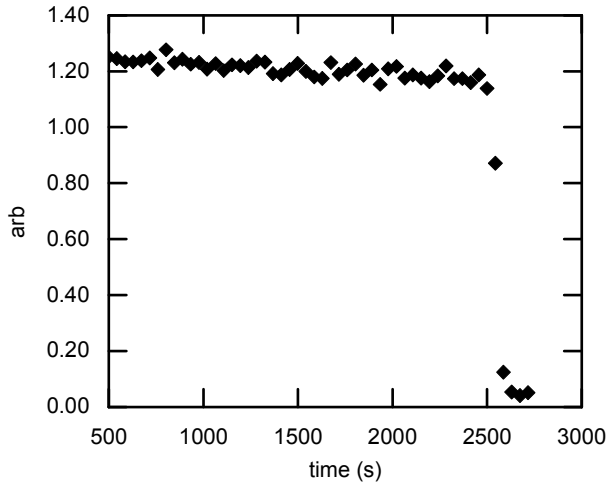

Figure 48. Decay of **46** (0.034 M) in THF at 25 °C as monitored by ^{31}P NMR spectroscopy.

Reduction elimination of biaryl from *trans*-$(Ph_3P)_2Pd(C_6H_4$-*p*-F)$(C_6H_4$-*p*-^{t}Bu) (46) (Fig 48). A solution of **46** was prepared by addition of chilled THF (0.5 mL) to a chilled vial containing **46** (15 mg, 0.017 mmol). *n*-tetradecane (5.0 mL, 0.019 mmol) was added as an internal standard for GC analysis. Sonication of the cold suspension afforded a colorless solution that was transferred by syringe to a sealed NMR tube containing a capillary of 1.0 M H_3PO_4 as an external standard. The resulting solution was placed in the NMR probe at 25 ^oC. ^{31}P NMR spectra were acquired at fixed time intervals throughout the length of experiment with the aid of an automated data collection program. After complete conversion of **46** was observed, the yield of 4-fluoro-4'-(*tert*-butyl)-biphenyl (99%) was determined by GC analysis.

Table 28. Crystal data and structure refinement for *trans*-$(Ph_3P)_2Pd(C_6H_4$-*p*-F)$(C_6H_4$-*p*-^{t}Bu) (**46**).

Identification code	ba16gasx	
Empirical formula	C52 H47 F P2 Pd	
Formula weight	859.24	
Temperature	193(2) K	
Wavelength	0.71073 Å	
Crystal system	Monoclinic	
Space group	P2(1)/c	
Unit cell dimensions	a = 11.7326(5) Å	a= 90°.
	b = 38.9611(17) Å	b= 95.203(2)°.
	c = 9.1732(4) Å	g = 90°.
Volume	4175.9(3) Å^3	
Z	4	
Density (calculated)	1.367 Mg/m^3	
Absorption coefficient	0.561 mm^{-1}	
F(000)	1776	
Crystal size	0.342 x 0.227 x 0.112 mm^3	
Theta range for data collection	1.74 to 25.38°.	
Index ranges	-14<=h<=14, -46<=k<=46, -11<=l<=11	
Reflections collected	57966	
Independent reflections	7647 [R(int) = 0.0746]	
Completeness to theta = 25.38°	99.8 %	
Absorption correction	Integration	
Max. and min. transmission	0.9652 and 0.8680	
Refinement method	Full-matrix least-squares on F^2	
Data / restraints / parameters	7647 / 0 / 508	
Goodness-of-fit on F^2	1.052	
Final R indices [I>2sigma(I)]	R1 = 0.0375, wR2 = 0.0730	
R indices (all data)	R1 = 0.0617, wR2 = 0.0799	
Largest diff. peak and hole	0.383 and -0.415 e.Å^{-3}	

Table 29. Atomic coordinates (x 10^4) and equivalent isotropic displacement parameters (Å^{2}x 10^3) for *trans*-$(Ph_3P)_2Pd(C_6H_4$-*p*-F)$(C_6H_4$-*p*-^{t}Bu) (**46**). U(eq) is defined as one third of the trace of the orthogonalized U^{ij} tensor.

	x	y	z	U(eq)
Pd(1)	984(1)	1336(1)	1360(1)	21(1)
P(1)	2931(1)	1394(1)	1181(1)	22(1)
P(2)	-952(1)	1342(1)	1670(1)	23(1)
F(1)	378(2)	2184(1)	-4437(2)	51(1)
C(1)	3547(3)	1432(1)	-585(3)	25(1)
C(2)	3278(3)	1712(1)	-1476(4)	35(1)
C(3)	3762(3)	1754(1)	-2771(4)	43(1)
C(4)	4531(3)	1516(1)	-3215(4)	46(1)
C(5)	4805(3)	1237(1)	-2353(4)	49(1)
C(6)	4324(3)	1194(1)	-1034(4)	35(1)
C(7)	3389(3)	1797(1)	2069(3)	24(1)
C(8)	4449(3)	1944(1)	1851(4)	35(1)
C(9)	4811(3)	2237(1)	2600(4)	42(1)
C(10)	4131(3)	2389(1)	3572(4)	43(1)
C(11)	3078(3)	2249(1)	3778(4)	37(1)
C(12)	2709(3)	1956(1)	3026(3)	28(1)
C(13)	3850(2)	1070(1)	2132(3)	25(1)
C(14)	4759(3)	1149(1)	3143(3)	31(1)
C(15)	5398(3)	894(1)	3881(4)	39(1)
C(16)	5130(3)	556(1)	3617(4)	46(1)
C(17)	4241(3)	471(1)	2603(4)	47(1)
C(18)	3603(3)	725(1)	1871(4)	35(1)
C(19)	1323(2)	998(1)	3096(3)	25(1)

Table 29 (cont.)

C(20)	1826(3)	1099(1)	4465(3)	28(1)
C(21)	2086(3)	870(1)	5603(4)	32(1)
C(22)	1875(3)	520(1)	5445(4)	31(1)
C(23)	1388(3)	414(1)	4088(4)	34(1)
C(24)	1118(3)	646(1)	2952(4)	33(1)
C(25)	2181(3)	276(1)	6731(4)	40(1)
C(26)	3462(3)	297(1)	7193(4)	51(1)
C(27)	1528(4)	385(1)	8028(5)	83(2)
C(28)	1890(4)	-96(1)	6347(5)	66(1)
C(29)	-1456(3)	1297(1)	3512(3)	27(1)
C(30)	-1208(3)	997(1)	4287(3)	33(1)
C(31)	-1533(3)	950(1)	5679(4)	39(1)
C(32)	-2112(3)	1207(1)	6335(4)	41(1)
C(33)	-2379(3)	1505(1)	5586(4)	44(1)
C(34)	-2062(3)	1554(1)	4181(4)	36(1)
C(35)	-1662(2)	977(1)	701(3)	24(1)
C(36)	-2803(3)	896(1)	861(4)	34(1)
C(37)	-3294(3)	610(1)	163(4)	44(1)
C(38)	-2666(3)	406(1)	-683(4)	44(1)
C(39)	-1540(3)	481(1)	-828(4)	38(1)
C(40)	-1036(3)	768(1)	-137(3)	29(1)
C(41)	-1712(3)	1726(1)	978(3)	26(1)
C(42)	-2589(3)	1724(1)	-137(3)	32(1)
C(43)	-3109(3)	2030(1)	-621(4)	42(1)
C(44)	-2757(3)	2337(1)	13(4)	45(1)
C(45)	-1888(3)	2344(1)	1123(4)	40(1)
C(46)	-1359(3)	2040(1)	1589(4)	33(1)
C(47)	690(2)	1638(1)	-508(3)	24(1)

Table 29 (cont.)

C(48)	571(3)	1477(1)	-1869(3)	28(1)
C(49)	452(3)	1655(1)	-3190(3)	30(1)
C(50)	464(3)	2004(1)	-3132(4)	33(1)
C(51)	561(3)	2183(1)	-1847(4)	34(1)
C(52)	672(3)	1998(1)	-545(3)	29(1)

Table 30. Bond lengths [Å] and angles [°] for *trans*-$(Ph_3P)_2Pd(C_6H_4$-*p*-F)$(C_6H_4$-*p*-^{t}Bu) (**46**).

Pd(1)-C(19)	2.076(3)
Pd(1)-C(47)	2.082(3)
Pd(1)-P(2)	2.3147(8)
Pd(1)-P(1)	2.3158(8)
P(1)-C(7)	1.825(3)
P(1)-C(13)	1.832(3)
P(1)-C(1)	1.839(3)
P(2)-C(41)	1.828(3)
P(2)-C(35)	1.834(3)
P(2)-C(29)	1.848(3)
F(1)-C(50)	1.382(4)
C(1)-C(2)	1.381(4)
C(1)-C(6)	1.390(4)
C(2)-C(3)	1.372(5)
C(2)-H(2A)	0.9500
C(3)-C(4)	1.380(5)
C(3)-H(3A)	0.9500
C(4)-C(5)	1.365(5)
C(4)-H(4A)	0.9500
C(5)-C(6)	1.391(5)
C(5)-H(5A)	0.9500
C(6)-H(6A)	0.9500
C(7)-C(12)	1.385(4)
C(7)-C(8)	1.400(4)
C(8)-C(9)	1.378(5)
C(8)-H(8A)	0.9500

Table 30 (cont.)

C(9)-C(10)	1.383(5)
C(9)-H(9A)	0.9500
C(10)-C(11)	1.379(5)
C(10)-H(10A)	0.9500
C(11)-C(12)	1.385(4)
C(11)-H(11A)	0.9500
C(12)-H(12A)	0.9500
C(13)-C(14)	1.383(4)
C(13)-C(18)	1.389(4)
C(14)-C(15)	1.384(4)
C(14)-H(14A)	0.9500
C(15)-C(16)	1.370(5)
C(15)-H(15A)	0.9500
C(16)-C(17)	1.374(5)
C(16)-H(16A)	0.9500
C(17)-C(18)	1.378(5)
C(17)-H(17A)	0.9500
C(18)-H(18A)	0.9500
C(19)-C(20)	1.394(4)
C(19)-C(24)	1.397(4)
C(20)-C(21)	1.385(4)
C(20)-H(20A)	0.9500
C(21)-C(22)	1.392(4)
C(21)-H(21A)	0.9500
C(22)-C(23)	1.384(5)
C(22)-C(25)	1.531(4)
C(23)-C(24)	1.393(4)
C(23)-H(23A)	0.9500

Table 30 (cont.)

C(24)-H(24A)	0.9500
C(25)-C(28)	1.524(5)
C(25)-C(26)	1.526(5)
C(25)-C(27)	1.531(5)
C(26)-H(26A)	0.9800
C(26)-H(26B)	0.9800
C(26)-H(26C)	0.9800
C(27)-H(27A)	0.9800
C(27)-H(27B)	0.9800
C(27)-H(27C)	0.9800
C(28)-H(28A)	0.9800
C(28)-H(28B)	0.9800
C(28)-H(28C)	0.9800
C(29)-C(30)	1.386(4)
C(29)-C(34)	1.400(4)
C(30)-C(31)	1.378(4)
C(30)-H(30A)	0.9500
C(31)-C(32)	1.379(5)
C(31)-H(31A)	0.9500
C(32)-C(33)	1.371(5)
C(32)-H(32A)	0.9500
C(33)-C(34)	1.387(5)
C(33)-H(33A)	0.9500
C(34)-H(34A)	0.9500
C(35)-C(40)	1.377(4)
C(35)-C(36)	1.396(4)
C(36)-C(37)	1.385(5)
C(36)-H(36A)	0.9500

Table 30 (cont.)

C(37)-C(38)	1.370(5)
C(37)-H(37A)	0.9500
C(38)-C(39)	1.371(5)
C(38)-H(38A)	0.9500
C(39)-C(40)	1.392(4)
C(39)-H(39A)	0.9500
C(40)-H(40A)	0.9500
C(41)-C(42)	1.384(4)
C(41)-C(46)	1.393(4)
C(42)-C(43)	1.392(4)
C(42)-H(42A)	0.9500
C(43)-C(44)	1.377(5)
C(43)-H(43A)	0.9500
C(44)-C(45)	1.375(5)
C(44)-H(44A)	0.9500
C(45)-C(46)	1.385(4)
C(45)-H(45A)	0.9500
C(46)-H(46A)	0.9500
C(47)-C(48)	1.393(4)
C(47)-C(52)	1.400(4)
C(48)-C(49)	1.393(4)
C(48)-H(48A)	0.9500
C(49)-C(50)	1.363(4)
C(49)-H(49A)	0.9500
C(50)-C(51)	1.365(5)
C(51)-C(52)	1.393(4)
C(51)-H(51A)	0.9500
C(52)-H(52A)	0.9500

Table 30 (cont.)

C(19)-Pd(1)-C(47)	174.66(12)
C(19)-Pd(1)-P(2)	91.93(8)
C(47)-Pd(1)-P(2)	90.28(8)
C(19)-Pd(1)-P(1)	89.71(8)
C(47)-Pd(1)-P(1)	88.66(8)
P(2)-Pd(1)-P(1)	173.15(3)
C(7)-P(1)-C(13)	104.10(14)
C(7)-P(1)-C(1)	101.59(14)
C(13)-P(1)-C(1)	102.35(14)
C(7)-P(1)-Pd(1)	107.78(10)
C(13)-P(1)-Pd(1)	116.10(10)
C(1)-P(1)-Pd(1)	122.65(10)
C(41)-P(2)-C(35)	106.29(13)
C(41)-P(2)-C(29)	101.96(14)
C(35)-P(2)-C(29)	101.67(14)
C(41)-P(2)-Pd(1)	114.71(10)
C(35)-P(2)-Pd(1)	109.93(10)
C(29)-P(2)-Pd(1)	120.69(10)
C(2)-C(1)-C(6)	118.3(3)
C(2)-C(1)-P(1)	119.8(2)
C(6)-C(1)-P(1)	121.9(2)
C(3)-C(2)-C(1)	121.0(3)
C(3)-C(2)-H(2A)	119.5
C(1)-C(2)-H(2A)	119.5
C(2)-C(3)-C(4)	120.6(4)
C(2)-C(3)-H(3A)	119.7
C(4)-C(3)-H(3A)	119.7

Table 30 (cont.)

C(5)-C(4)-C(3)	119.3(3)
C(5)-C(4)-H(4A)	120.3
C(3)-C(4)-H(4A)	120.3
C(4)-C(5)-C(6)	120.5(4)
C(4)-C(5)-H(5A)	119.8
C(6)-C(5)-H(5A)	119.8
C(1)-C(6)-C(5)	120.4(3)
C(1)-C(6)-H(6A)	119.8
C(5)-C(6)-H(6A)	119.8
C(12)-C(7)-C(8)	118.5(3)
C(12)-C(7)-P(1)	120.2(2)
C(8)-C(7)-P(1)	121.2(2)
C(9)-C(8)-C(7)	120.4(3)
C(9)-C(8)-H(8A)	119.8
C(7)-C(8)-H(8A)	119.8
C(8)-C(9)-C(10)	120.4(3)
C(8)-C(9)-H(9A)	119.8
C(10)-C(9)-H(9A)	119.8
C(11)-C(10)-C(9)	119.7(3)
C(11)-C(10)-H(10A)	120.1
C(9)-C(10)-H(10A)	120.1
C(10)-C(11)-C(12)	120.1(3)
C(10)-C(11)-H(11A)	119.9
C(12)-C(11)-H(11A)	119.9
C(7)-C(12)-C(11)	120.8(3)
C(7)-C(12)-H(12A)	119.6
C(11)-C(12)-H(12A)	119.6
C(14)-C(13)-C(18)	117.9(3)

Table 30 (cont.)

C(14)-C(13)-P(1)	123.3(2)
C(18)-C(13)-P(1)	118.7(2)
C(15)-C(14)-C(13)	121.2(3)
C(15)-C(14)-H(14A)	119.4
C(13)-C(14)-H(14A)	119.4
C(16)-C(15)-C(14)	119.8(3)
C(16)-C(15)-H(15A)	120.1
C(14)-C(15)-H(15A)	120.1
C(15)-C(16)-C(17)	120.0(3)
C(15)-C(16)-H(16A)	120.0
C(17)-C(16)-H(16A)	120.0
C(16)-C(17)-C(18)	120.1(3)
C(16)-C(17)-H(17A)	120.0
C(18)-C(17)-H(17A)	120.0
C(17)-C(18)-C(13)	121.0(3)
C(17)-C(18)-H(18A)	119.5
C(13)-C(18)-H(18A)	119.5
C(20)-C(19)-C(24)	114.5(3)
C(20)-C(19)-Pd(1)	123.3(2)
C(24)-C(19)-Pd(1)	122.0(2)
C(21)-C(20)-C(19)	123.0(3)
C(21)-C(20)-H(20A)	118.5
C(19)-C(20)-H(20A)	118.5
C(20)-C(21)-C(22)	121.8(3)
C(20)-C(21)-H(21A)	119.1
C(22)-C(21)-H(21A)	119.1
C(23)-C(22)-C(21)	116.1(3)
C(23)-C(22)-C(25)	123.9(3)

Table 30 (cont.)

C(21)-C(22)-C(25)	120.0(3)
C(22)-C(23)-C(24)	121.8(3)
C(22)-C(23)-H(23A)	119.1
C(24)-C(23)-H(23A)	119.1
C(23)-C(24)-C(19)	122.8(3)
C(23)-C(24)-H(24A)	118.6
C(19)-C(24)-H(24A)	118.6
C(28)-C(25)-C(26)	108.0(3)
C(28)-C(25)-C(22)	112.3(3)
C(26)-C(25)-C(22)	109.7(3)
C(28)-C(25)-C(27)	108.9(3)
C(26)-C(25)-C(27)	108.6(4)
C(22)-C(25)-C(27)	109.2(3)
C(25)-C(26)-H(26A)	109.5
C(25)-C(26)-H(26B)	109.5
H(26A)-C(26)-H(26B)	109.5
C(25)-C(26)-H(26C)	109.5
H(26A)-C(26)-H(26C)	109.5
H(26B)-C(26)-H(26C)	109.5
C(25)-C(27)-H(27A)	109.5
C(25)-C(27)-H(27B)	109.5
H(27A)-C(27)-H(27B)	109.5
C(25)-C(27)-H(27C)	109.5
H(27A)-C(27)-H(27C)	109.5
H(27B)-C(27)-H(27C)	109.5
C(25)-C(28)-H(28A)	109.5
C(25)-C(28)-H(28B)	109.5
H(28A)-C(28)-H(28B)	109.5

Table 30 (cont.)

C(25)-C(28)-H(28C)	109.5
H(28A)-C(28)-H(28C)	109.5
H(28B)-C(28)-H(28C)	109.5
C(30)-C(29)-C(34)	117.9(3)
C(30)-C(29)-P(2)	118.6(2)
C(34)-C(29)-P(2)	123.5(3)
C(31)-C(30)-C(29)	121.7(3)
C(31)-C(30)-H(30A)	119.2
C(29)-C(30)-H(30A)	119.2
C(30)-C(31)-C(32)	119.8(3)
C(30)-C(31)-H(31A)	120.1
C(32)-C(31)-H(31A)	120.1
C(33)-C(32)-C(31)	119.7(3)
C(33)-C(32)-H(32A)	120.2
C(31)-C(32)-H(32A)	120.2
C(32)-C(33)-C(34)	120.9(3)
C(32)-C(33)-H(33A)	119.6
C(34)-C(33)-H(33A)	119.6
C(33)-C(34)-C(29)	120.0(3)
C(33)-C(34)-H(34A)	120.0
C(29)-C(34)-H(34A)	120.0
C(40)-C(35)-C(36)	119.3(3)
C(40)-C(35)-P(2)	119.1(2)
C(36)-C(35)-P(2)	121.5(2)
C(37)-C(36)-C(35)	119.8(3)
C(37)-C(36)-H(36A)	120.1
C(35)-C(36)-H(36A)	120.1
C(38)-C(37)-C(36)	120.3(3)

Table 30 (cont.)

C(38)-C(37)-H(37A)	119.8
C(36)-C(37)-H(37A)	119.8
C(37)-C(38)-C(39)	120.3(3)
C(37)-C(38)-H(38A)	119.8
C(39)-C(38)-H(38A)	119.8
C(38)-C(39)-C(40)	120.0(3)
C(38)-C(39)-H(39A)	120.0
C(40)-C(39)-H(39A)	120.0
C(35)-C(40)-C(39)	120.3(3)
C(35)-C(40)-H(40A)	119.9
C(39)-C(40)-H(40A)	119.9
C(42)-C(41)-C(46)	118.5(3)
C(42)-C(41)-P(2)	123.9(2)
C(46)-C(41)-P(2)	117.6(2)
C(41)-C(42)-C(43)	120.3(3)
C(41)-C(42)-H(42A)	119.8
C(43)-C(42)-H(42A)	119.8
C(44)-C(43)-C(42)	120.2(3)
C(44)-C(43)-H(43A)	119.9
C(42)-C(43)-H(43A)	119.9
C(45)-C(44)-C(43)	120.2(3)
C(45)-C(44)-H(44A)	119.9
C(43)-C(44)-H(44A)	119.9
C(44)-C(45)-C(46)	119.6(3)
C(44)-C(45)-H(45A)	120.2
C(46)-C(45)-H(45A)	120.2
C(45)-C(46)-C(41)	121.2(3)
C(45)-C(46)-H(46A)	119.4

Table 30 (cont.)

C(41)-C(46)-H(46A)	119.4
C(48)-C(47)-C(52)	115.5(3)
C(48)-C(47)-Pd(1)	118.5(2)
C(52)-C(47)-Pd(1)	125.9(2)
C(49)-C(48)-C(47)	123.3(3)
C(49)-C(48)-H(48A)	118.4
C(47)-C(48)-H(48A)	118.4
C(50)-C(49)-C(48)	117.6(3)
C(50)-C(49)-H(49A)	121.2
C(48)-C(49)-H(49A)	121.2
C(49)-C(50)-C(51)	123.0(3)
C(49)-C(50)-F(1)	118.2(3)
C(51)-C(50)-F(1)	118.9(3)
C(50)-C(51)-C(52)	118.0(3)
C(50)-C(51)-H(51A)	121.0
C(52)-C(51)-H(51A)	121.0
C(51)-C(52)-C(47)	122.7(3)
C(51)-C(52)-H(52A)	118.7
C(47)-C(52)-H(52A)	118.7

Symmetry transformations used to generate equivalent atoms:

Table 31. Anisotropic displacement parameters ($Å^2 x\ 10^3$) for *trans*-$(Ph_3P)_2Pd(C_6H_4$-*p*-F)(C_6H_4-*p*-^{t}Bu) (**46**). The anisotropic displacement factor exponent takes the form: $-2p^2[h^2 a^{*2} U^{11} + ... + 2 h k a^* b^* U^{12}]$

	U^{11}	U^{22}	U^{33}	U^{23}	U^{13}	U^{12}
Pd(1)	16(1)	23(1)	24(1)	1(1)	0(1)	1(1)
P(1)	18(1)	25(1)	24(1)	-1(1)	1(1)	0(1)
P(2)	17(1)	28(1)	23(1)	1(1)	1(1)	1(1)
F(1)	66(2)	52(1)	35(1)	20(1)	4(1)	7(1)
C(1)	17(2)	35(2)	24(2)	-4(1)	1(1)	-5(1)
C(2)	29(2)	44(2)	33(2)	3(2)	3(2)	-1(2)
C(3)	42(2)	59(3)	29(2)	10(2)	3(2)	-10(2)
C(4)	49(3)	68(3)	23(2)	-8(2)	12(2)	-18(2)
C(5)	44(2)	58(3)	48(3)	-16(2)	20(2)	2(2)
C(6)	32(2)	41(2)	33(2)	-6(2)	7(2)	-1(2)
C(7)	23(2)	26(2)	24(2)	1(1)	-1(1)	-3(1)
C(8)	31(2)	39(2)	35(2)	-6(2)	8(2)	-8(2)
C(9)	42(2)	42(2)	42(2)	-5(2)	0(2)	-17(2)
C(10)	56(3)	30(2)	41(2)	-8(2)	-4(2)	-6(2)
C(11)	42(2)	32(2)	35(2)	-6(2)	1(2)	7(2)
C(12)	26(2)	28(2)	29(2)	1(1)	3(1)	2(1)
C(13)	18(2)	31(2)	26(2)	-4(1)	6(1)	3(1)
C(14)	23(2)	39(2)	30(2)	-2(2)	2(1)	3(1)
C(15)	27(2)	54(2)	36(2)	-1(2)	-3(2)	7(2)
C(16)	33(2)	50(2)	55(3)	11(2)	-1(2)	16(2)
C(17)	38(2)	30(2)	73(3)	1(2)	2(2)	4(2)
C(18)	25(2)	33(2)	46(2)	-5(2)	-1(2)	1(2)
C(19)	14(2)	32(2)	30(2)	5(1)	5(1)	3(1)

Table 31 (cont.)

C(20)	25(2)	24(2)	35(2)	3(1)	5(2)	-2(1)
C(21)	31(2)	39(2)	27(2)	5(2)	2(2)	3(2)
C(22)	21(2)	33(2)	38(2)	10(2)	5(2)	5(1)
C(23)	27(2)	22(2)	52(2)	4(2)	3(2)	-1(1)
C(24)	26(2)	38(2)	34(2)	-1(2)	-4(2)	1(2)
C(25)	34(2)	40(2)	46(2)	19(2)	6(2)	8(2)
C(26)	48(3)	42(2)	60(3)	15(2)	-15(2)	6(2)
C(27)	96(4)	91(4)	68(3)	46(3)	41(3)	44(3)
C(28)	53(3)	46(3)	93(4)	37(2)	-21(2)	-8(2)
C(29)	17(2)	38(2)	25(2)	-2(2)	-1(1)	-3(1)
C(30)	27(2)	45(2)	28(2)	2(2)	5(2)	2(2)
C(31)	31(2)	56(2)	29(2)	9(2)	1(2)	-5(2)
C(32)	37(2)	65(3)	22(2)	-5(2)	5(2)	-6(2)
C(33)	41(2)	56(2)	35(2)	-14(2)	12(2)	1(2)
C(34)	32(2)	42(2)	32(2)	-3(2)	4(2)	1(2)
C(35)	21(2)	28(2)	23(2)	4(1)	-1(1)	1(1)
C(36)	24(2)	37(2)	41(2)	2(2)	7(2)	1(2)
C(37)	26(2)	45(2)	58(3)	7(2)	-3(2)	-12(2)
C(38)	45(2)	38(2)	45(2)	-2(2)	-9(2)	-17(2)
C(39)	51(2)	33(2)	30(2)	-6(2)	5(2)	-5(2)
C(40)	27(2)	35(2)	27(2)	1(1)	6(1)	-3(1)
C(41)	20(2)	31(2)	27(2)	3(1)	8(1)	3(1)
C(42)	32(2)	37(2)	25(2)	0(2)	0(2)	5(2)
C(43)	38(2)	49(2)	38(2)	6(2)	-5(2)	10(2)
C(44)	40(2)	37(2)	58(3)	11(2)	5(2)	15(2)
C(45)	33(2)	32(2)	57(2)	-1(2)	8(2)	1(2)
C(46)	23(2)	34(2)	43(2)	1(2)	-1(2)	3(1)
C(47)	17(2)	26(2)	31(2)	-1(1)	2(1)	1(1)

Table 31 (cont.)

C(48)	27(2)	27(2)	30(2)	2(1)	-1(1)	-1(1)
C(49)	28(2)	36(2)	25(2)	-1(2)	0(1)	-1(1)
C(50)	29(2)	38(2)	30(2)	12(2)	0(2)	3(2)
C(51)	35(2)	24(2)	42(2)	7(2)	2(2)	3(1)
C(52)	24(2)	32(2)	30(2)	-2(1)	0(1)	2(1)

Table 32. Hydrogen coordinates (x 10^4) and isotropic displacement parameters (Å^{2}x 10^3) for *trans*-$(Ph_3P)_2Pd(C_6H_4$-*p*-F)(C_6H_4-*p*-^{t}Bu) (**46**).

	x	y	z	U(eq)
H(2A)	2749	1878	-1187	42
H(3A)	3566	1948	-3367	52
H(4A)	4865	1546	-4111	55
H(5A)	5328	1071	-2656	59
H(6A)	4528	1000	-436	42
H(8A)	4921	1842	1184	42
H(9A)	5532	2335	2447	51
H(10A)	4388	2589	4095	51
H(11A)	2606	2354	4438	44
H(12A)	1979	1862	3167	33
H(14A)	4947	1383	3334	37
H(15A)	6022	953	4568	47
H(16A)	5558	381	4136	56
H(17A)	4066	236	2406	57
H(18A)	2986	664	1177	42
H(20A)	1997	1335	4625	33
H(21A)	2417	955	6516	39
H(23A)	1233	177	3926	41
H(24A)	780	561	2043	40
H(26A)	3891	240	6357	77
H(26B)	3660	135	7991	77
H(26C)	3658	531	7527	77
H(27A)	703	364	7758	124
H(27B)	1714	624	8286	124

Table 32 (cont.)

H(27C)	1749	236	8868	124
H(28A)	2266	-163	5479	98
H(28B)	1059	-120	6143	98
H(28C)	2157	-244	7171	98
H(30A)	-804	819	3848	40
H(31A)	-1359	742	6185	46
H(32A)	-2326	1178	7302	50
H(33A)	-2787	1681	6036	52
H(34A)	-2255	1761	3673	43
H(36A)	-3241	1036	1447	40
H(37A)	-4071	554	270	52
H(38A)	-3012	212	-1170	52
H(39A)	-1104	336	-1401	45
H(40A)	-257	820	-244	35
H(42A)	-2838	1513	-575	38
H(43A)	-3708	2026	-1390	51
H(44A)	-3116	2545	-319	54
H(45A)	-1652	2555	1569	48
H(46A)	-745	2046	2339	40
H(48A)	572	1233	-1896	33
H(49A)	364	1537	-4100	36
H(51A)	552	2427	-1842	40
H(52A)	737	2120	355	35

5.5 References

(1) King, A. O.; Yasuda, N. In *Organometallics in Process Chemistry*; Springer Berlin / Heidelberg: 2004; Vol. 6, p 205-245.
(2) Nicolaou, K. C.; Bulger, P. G.; Sarlah, D. *Angew. Chem. Int. Ed.* **2005**, *44*, 4442-4489.
(3) Tsukano, C.; Sasaki, M. *J. Am. Chem. Soc.* **2003**, *125*, 14294-14295.
(4) Tsukano, C.; Ebine, M.; Sasaki, M. *J. Am. Chem. Soc.* **2005**, *127*, 4326-4335.
(5) Yoshida, K.; Hayashi, T. In *Boronic Acids*; Wiley-VCH Verlag GmbH & Co. KGaA: 2006, p 171-203.
(6) Zhao, P.; Incarvito, C. D.; Hartwig, J. F. *J. Am. Chem. Soc.* **2007**, *129*, 1876-1877.
(7) Chan, D. M. T.; Lam, P. Y. S. In *Boronic Acids*; Wiley-VCH Verlag GmbH & Co. KGaA: 2006, p 205-240.
(8) Miyaura, N. *J. Organomet. Chem.* **2002**, *653*, 54-57.
(9) Braga, A. A. C.; Morgen, N. H.; Ujaque, G.; Maseras, F. *J. Am. Chem. Soc.* **2005**, *127*, 9298-9307.
(10) Braga, A. A. C.; Morgon, N. H.; Ujaque, G.; Lledos, A.; Maseras, F. *J. Organomet. Chem.* **2006**, *691*, 4459–4466.
(11) Smith, G. B.; Dezeny, G. C.; Hughes, D. L.; King, A. O.; Verhoeven, T. R. *J. Org. Chem.* **1994**, *59*, 8151-8156.
(12) Aliprantis, A. O.; Canary, J. W. *J. Am. Chem. Soc.* **1994**, *116*, 6985-6986.
(13) Matos, K.; Soderquist, J. A. *J. Org. Chem.* **1998**, *63*, 461-470.
(14) Nunes, C. M.; Monteiro, A. L. *J. Braz. Chem. Soc.* **2007**, *18*, 1443-1447.
(15) Goossen, L. J.; Koley, D.; Hermann, H. L.; Thiel, W. *J. Am. Chem. Soc.* **2005**, *127*, 11102-11114.
(16) Goossen, L. J.; Koley, D.; Hermann, H. L.; Thiel, W. *Organometallics* **2006**, *25*, 54-67.
(17) Suzaki, Y.; Osakada, K. *Organometallics* **2006**, *25*, 3251-3258.
(18) Siegmann, K.; Pregosin, P. S.; Venanzi, L. M. *Organometallics* **1989**, *8*, 2659-2664.
(19) Moriya, T.; Miyaura, N.; Suzuki, A. *Synlett* **1994**, 149-151.
(20) Kakino, R.; Shimizu, I.; Yamamoto, A. *Bull. Chem. Soc. Jpn.* **2001**, *74* 371–376.
(21) Grushin, V. V.; Alper, H. *Organometallics* **1993**, *12*, 1890-1901.
(22) Grushin, V. V.; Alper, H. *Organometallics* **1996**, *15*, 5242-5245.
(23) Stambuli, J. P.; Incarvito, C. D.; Bühl, M.; Hartwig, J. F. *J. Am. Chem. Soc.* **2004**, *126*, 1184-1194.
(24) Huser, M.; Youinou, M. T.; Osborn, J. A. *Angew. Chem.* **1989**, *101*, 1427-1430.
(25) Ozawa, F.; Kawasaki, N.; Okamoto, H.; Yamamoto, T.; Yamamoto, A. *Organometallics* **1987**, *6*, 1640-1651.
(26) Cammidge, A. N.; Goddard, V. H. M.; Gopee, H.; Harrison, N. L.; Hughes, D. L.; Schubert, C. J.; Benjamin M. Sutton; Watts, G. L.; Whitehead, A. J. *Org. Lett.* **2006**, *8*, 4071-4074.

(27) Yields for organic products were determined by GC analysis versus *n*-tetradecane as internal standard.
(28) A similar reaction was reported previously with no experimental details in reviews by Suzuki and Miyaura. See Ref 29 and 30.
(29) Miyaura, N.; Suzuki, A. *Chem. Rev.* **1995**, *95*, 2457-2483.
(30) Miyaura, N. In *Cross-Coupling Reactions*; Miyaura, N., Ed.; Springer Berlin / Heidelberg: 2002; Vol. 219, p 11-59.
(31) Butters, M.; Harvey, J.; Jover, J.; Lennox, A.; Lloyd-Jones, G.; Murray, P. *Angew. Chem. Int. Ed.* **2010**, *49*, 5156-5160.
(32) Aqueous THF mixtures are biphasic in the presence of inorganic base, whereas aqueous acetone mixtures remain homogeneous.
(33) The decay of **41** was concurrent with the appearance of an intermediate at a nearly overlapping chemical shift, which caused the kinetic curve to level off at a positive integration rather than decaying to zero. However, the rate constant obtained from the fit of this exponential decay can only be larger than the actual value, and the ratio of the two rate constants can only be smaller than the actual value because this is the faster of the two reactions.
(34) Carrow, B. P.; Hartwig, J. F. *J. Am. Chem. Soc.* **2010**, *132*, 79-81.
(35) Jover, J.; Fey, N.; Purdie, M.; Lloyd-Jones, G. C.; Harvey, J. N. *J. Mol. Catal. A.: Chem.* **2010**, *324*, 39-47.
(36) Precipitation of $Pd(PPh_3)_4$ is observed during reactions conducted in aqueous THF mixtures.
(37) The borate was generated in situ by the reaction of NaH with *p*-fluorophenylboronic acid.
(38) see Experimetnal Section for a kinetic study of reductive elimination from complex **46**.
(39) Driver, M. S.; Hartwig, J. F. *Organometallics* **1997**, *16*, 5706-5715.
(40) Roy, A. H.; Hartwig, J. F. *Organometallics* **2004**, *23*, 1533-1541.
(41) Fitton, P.; Johnson, M. P.; McKeon, J. E. *Chem. Comm.* **1968**, 6-7.
(42) Wilson, D. A.; Wilson, C. J.; Moldoveanu, C.; Resmerita, A.-M.; Corcoran, P.; Hoang, L. M.; Rosen, B. M.; Percec, V. *J. Am. Chem. Soc.* **2010**, *132*, 1800-1801.
(43) Mo, F.; Jiang, Y.; Qiu, D.; Zhang, Y.; Wang, J. *Angew. Chem. Int. Ed.* **2010**, *49*, 1846-1849.